

Supporting Information

**Dual Nickel- and Photoredox-Catalyzed Enantioselective
Desymmetrization of Cyclic *meso*-Anhydrides**

Erin E. Stache, Tomislav Rovis, and Abigail G. Doyle**

anie_201700097_sm_miscellaneous_information.pdf

Table of Contents

I.	General Information.....	S3
II.	Selected Optimization Studies.....	S5
III.	Isolated Yields and Product Characterization.....	S9
IV.	Trifluoroborate Preparation and Characterization.....	S42
V.	Epimerization Studies.....	S47
VI.	Oxidative Addition Studies.....	S48
VII.	Evaluation of Racemic Background Reaction.....	S54
VIII.	Effect of Trifluoroborate Purity.....	S57
IX.	Derivatization Studies.....	S58
X.	Determination of Absolute Stereochemistry.....	S67
XI.	NMR Spectra.....	S68
XII.	Crystallographic Data.....	S149

I. General Information

General Procedures. Unless otherwise noted, reactions were performed under a nitrogen atmosphere with the exclusion of moisture. N₂-flushed stainless steel needles and plastic syringes were used to transfer air- and moisture-sensitive reagents. Reactions were monitored by thin-layer chromatography (TLC) on EMD Silica Gel 60 F254 plates, visualizing with UV light (254 nm) or KMnO₄ stain. Solvent was freshly distilled/degassed prior to use unless otherwise noted. Organic solutions were concentrated under reduced pressure using a rotary evaporator (25 °C, <50 torr). Automated column chromatography was performed using pre-packed silica gel cartridges on a Biotage SP4 (40-53 μm, 60 Å).

Materials. Commercial reagents were purchased from Sigma-Aldrich, Alfa Aesar, Acros, Strem, TCI, Boron Molecular, Frontier Scientific or Oakwood and used as received with the following exceptions. Diethyl ether (Et₂O), tetrahydrofuran (THF), dichloromethane (CH₂Cl₂), toluene (PhCH₃) and 1,4-dioxane were dried by passing through activated alumina columns and stored over molecular sieves in a N₂-filled glovebox; *N,N*-dimethylformamide (DMF) was dried by passing through a column of activated molecular sieves. Ni(cod)₂ was purchased from Strem and (-)-2,2'-Isopropylidenebis-(4*S*)-4-phenyl-2-oxazoline (**L1**) was purchased from Sigma-Aldrich and both stored at -40 °C in a N₂-filled glovebox. Nickel (II) chloride dimethoxymethane (Strem) was stored at room temperature in a N₂-filled glovebox. Anhydride **1** was used without further purification. Anhydrides **4-A**¹, **5-A**, **6-A**, **7-A**, and **10-A** were treated with trifluoroacetic acid in CH₂Cl₂ to ensure purity of the anhydride.² Anhydrides **8-A** and **9-A** were synthesized according to literature procedures.² Benzyl trifluoroborate was purchased from Boron Molecular and used without further purification. All other trifluoroborates were synthesized according to literature procedures.³

Instrumentation. Proton nuclear magnetic resonance (¹H NMR) spectra were recorded on a Bruker 500 MHz or NB 300 MHz AVANCE spectrometer. Proton chemical shifts are reported in parts per million downfield from tetramethylsilane and are referenced to residual protium in the NMR solvent (CHCl₃ = δ 7.26 ppm or (CD₃)₂CO = 2.05). Carbon nuclear magnetic resonance (¹³C NMR) were recorded on a Bruker 500 AVANCE spectrometer (125 MHz). Chemical shifts for carbon are reported in parts per million downfield from tetramethylsilane and are referenced to the carbon resonances of the solvent residual peak (CDCl₃ = δ 77.16 ppm or ((CD₃)₂CO = 206.26 ppm and 29.840 ppm). Fluorine nuclear magnetic resonance (¹⁹F NMR) were reported on a Bruker NB 300 AVANCE (282 MHz) spectrometer. Boron nuclear magnetic resonance (¹¹B NMR) were reported on a Bruker NB 300 AVANCE (96 MHz) spectrometer. NMR data are represented as follows: chemical shift (δ ppm), multiplicity (s = singlet, d = doublet, t = triplet, q = quartet, m = multiplet), coupling constant in Hertz (Hz), integration. High-resolution mass spectrometry was performed on an Agilent 6220 LC/MS using electrospray ionization time-of-flight (ESI-TOF). FT-IR spectra were recorded on a Perkin- Elmer Paragon 500 and are reported in terms of frequency of absorption (cm⁻¹). Reversed-phase liquid chromatography/mass

¹ Anhydride designation corresponds to keto acid product number (#-A).

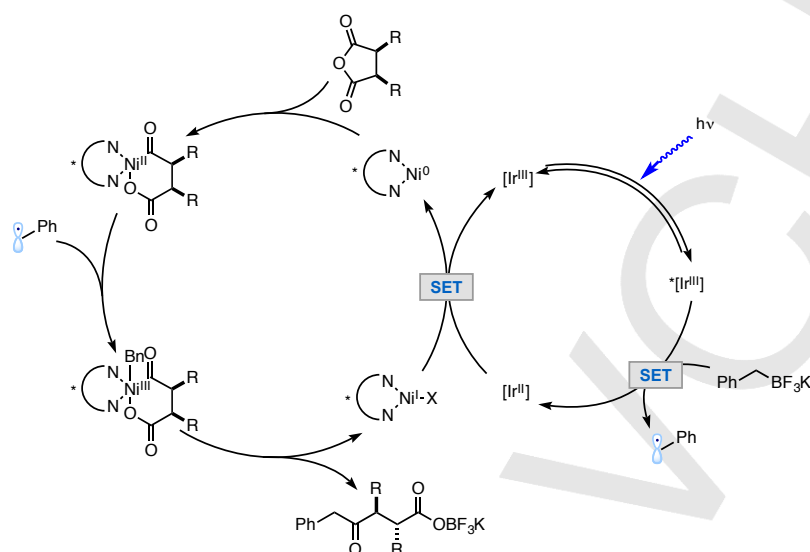
² E. A. Bercot, T. Rovis, *J. Am. Chem. Soc.* **2005**, *127*, 248-254.

³ Trifluoroborate designation corresponds to keto-acid product number (#-B).

spectrometry (LC/MS) was performed on an Agilent 1260 Infinity analytical LC and Agilent 6120 Quadrupole LC/MS system using electrospray ionization/atmospheric-pressure chemical ionization (ESI/APCI) and UV detection at 254 nm and 280 nm. Ultraviolet-visible absorption spectra were collected on an Agilent Cary 60 Spectrophotometer using 10 mm quartz cuvettes. High-performance liquid chromatography (HPLC) was performed on an Agilent 1200 series instrument with a binary pump and a diode array detector, using Chiralcel OD-H (25 cm x 0.46 cm), Chiralcel OJ-H (25 cm x 0.46 cm), Chiralpak AS-H (25 cm x 0.46 cm), Chiralpak AD-H (25 cm x 0.46 cm), Chiralpak IC (25 cm x 0.46 cm) and Chiralpak ID (25 cm x 0.46 cm). Optical rotations were taken with a Jasco P-1010 polarimeter Na/Hal lamp with a 0.5 dm/1 mL cell in spectral grade CHCl₃ or acetone.

Light Sources. Screening scale reactions (0.025-0.1 mmol) were carried out using 12-inch Sapphire Flex LED Strips (5050, High Density, 12V DC Power Leads, Waterproof, Black backing) purchased from Creative Lightings. The strips were wrapped on the inside of a Pyrex crystallizing dish. Scale up reactions (0.25 mmol) were carried out using Blue Kessil H150 LED Grow Lights. Larger scale up reactions (0.5 mmol) were carried out using the Merck Photoreactor (450 nm light).

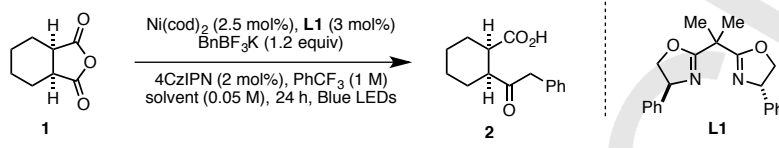
II. Selected Optimization Studies



Scheme S1. Proposed catalytic cycle for nickel-photoredox catalyzed desymmetrization (using photocatalyst **3**). Upon irradiation with light, a photocatalyst excited state is produced, which can undergo a single electron transfer with benzyl trifluoroborate to afford the oxidized benzylic radical, and reduced ground state photocatalyst. At the same time the nickel catalytic cycle is initiated by oxidative addition of Ni(0) into a cyclic anhydride. This oxidative addition adduct is intercepted by the benzylic radical to afford an electron deficient Ni(III) species. Upon reductive elimination, the desired keto-carboxylate product is released. Another single electron transfer from the reduced photocatalyst to Ni(I) closes both catalytic cycles.

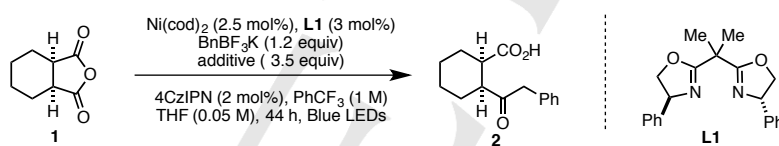
General procedure for screening: Cyclohexanecarboxylic anhydride **1** (0.025 mmol-0.1 mmol) and benzyl trifluoroborate **2-B** (1.2 equiv) were weighed into a 1-dram vial or 13 x 100 mm reaction tube and equipped with a stir bar. The reaction tube was then brought into an N₂-filled glovebox. Then a pre-stirred dissolved solution in THF of Ni(cod)₂ and ligand were added. The mixture was allowed to stir for ~5 minutes at room temperature, at which point the reaction mixture became homogenous. A solution of photocatalyst in solvent was added, and the reaction tube sealed with a septa cap. The vial was wrapped with electrical tape, and then removed from the glovebox, where it was immediately irradiated with blue LED's. A fan was used to keep the reaction cool. After the reaction was complete, the reaction tube was removed from the light source where benzoic acid (1 equiv) was added as an external standard. The solvent was then removed. The residue was dissolved in equal volumes 1 M HCl and diethyl ether. A small aliquot was removed, dried over Na₂SO₄ and concentrated to determine yield by ¹H NMR. The remaining organic layer was then extracted with sat. aq. Na₂CO₃ (2 x 1 mL). The combined aqueous layers were acidified with conc. HCl until ~pH 2. The aqueous layer was extracted with diethyl ether (2 x 5 mL). The combined organic layers were then dried over Na₂SO₄, filtered and concentrated. The crude acid was analyzed by HPLC analysis on a chiral stationary phase. The product was converted to the methyl ester (when necessary) by dissolving the product in a 1:1 mixture of CH₂Cl₂/MeOH (~0.04 M). The reaction was cooled to 0 °C, at which point TMSCHN₂ (2.0 M in hexanes) was added dropwise until a light yellow color persisted. The reaction was stirred for 1 h at 0 °C. The reaction was quenched by adding an excess of acetic

acid, until the yellow color disappeared. The solvent was removed, and the residue was taken up in diethyl ether and 1 M HCl. The organic layer was subsequently washed with sat. aq. Na₂CO₃, then dried over Na₂SO₄, filtered and concentrated. The methyl ester was then analyzed by HPLC on a chiral stationary phase. In cases where diastereoselectivity was determined by ¹H NMR, the methyl ester protons or benzylic protons were used as the diagnostic peaks.



entry	solvent	% yield ^[a]	%ee ^[b]
1	PhCF ₃	57%	nd
2	Et ₂ O	75%	41%
3	PhCH ₃	62%	52%
4	DMF	<10%	nd
5	DMA	<10%	nd
6	dioxane	82%	48%
7	acetone	<10%	nd
8	CH ₃ CN	<10%	nd

Table S1. Solvent screen. [a] determined by LC/MS with benzoic acid as an external standard, 0.025 mmol scale. [b] determined by HPLC analysis on a chiral stationary phase on the methyl ester.



entry	additive	% yield ^a	%ee ^b
1	none	60%	39%
2	2,6-lutidine	47%	24%
3	Li ₃ PO ₄	60%	24%
4	Li ₂ CO ₃	66%	33%
5	NaOBz	41%	nd

Table S2. Additive screen. [a] determined by LC/MS with benzoic acid as a standard, 0.025 mmol scale. [b] determined by HPLC analysis on a chiral stationary phase on the methyl ester. Interestingly, all additives had a negative impact on yield and/or enantioselectivity. It is likely that the carboxylate product can sequester BF₃.

entry	photocatalyst loading	% yield ^a	% ee ^b
1	1 mol%	27%	94%
2	2 mol%	53%	92%
3	4 mol%	56%	71%

Table S3. Photocatalyst loading screen. [a] determined by LC/MS with benzoic acid as a standard, 0.025 mmol scale. [b] determined by HPLC analysis on a chiral stationary phase on the methyl ester.

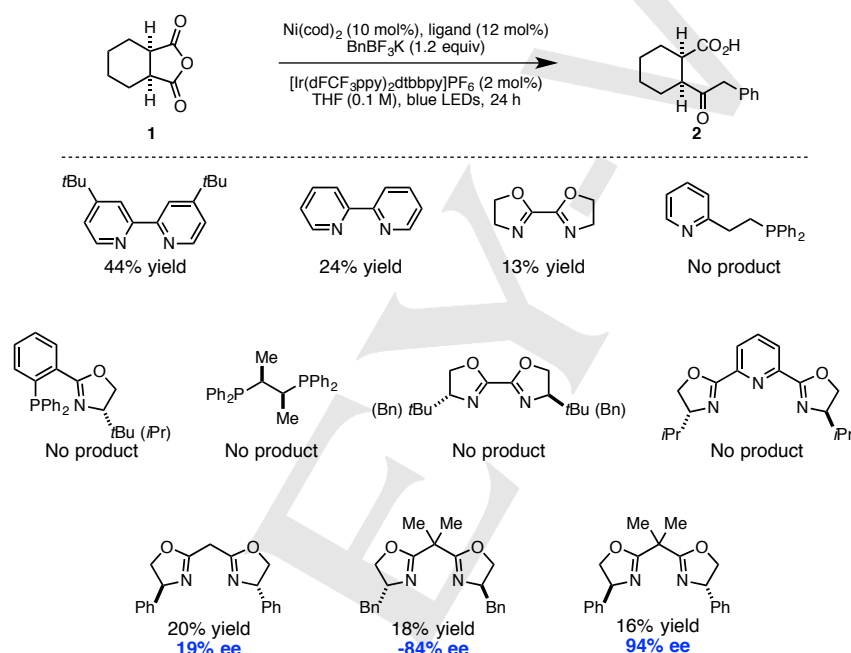


Figure S1. Initial (chiral) ligand screen. Bipyridine and bis-oxazoline (BiOx) ligands proved the most privileged ligand class in early reaction screening. Interestingly, PyPhos, a very effective ligand in the first example of nickel catalyzed anhydride openings⁴ was completely ineffective under the reaction conditions. Additionally, PHOX ligands, providing the highest levels of enantioselectivity in the same report were also completely ineffective in providing product. (*S,S*)-Chiraphos, substituted BiOx and PyBox ligands were also ineffective in the reaction. Box ligands proved the most privileged in terms of reactivity and selectivity in the asymmetric reaction.

⁴ E. A. Bercot, T. Rovis, *J. Am. Chem. Soc.* **2002**, *124*, 174-175.

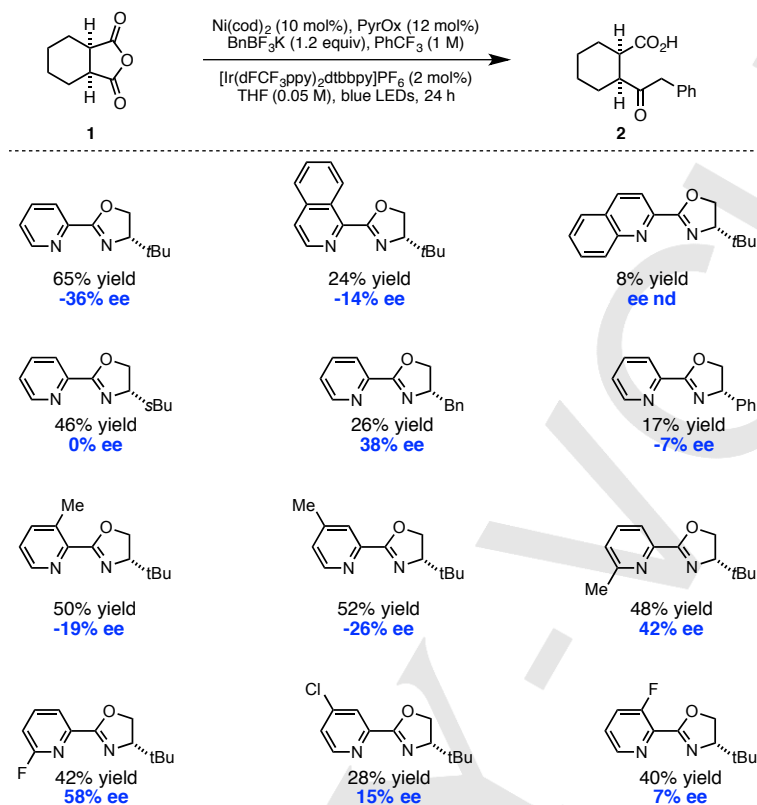


Figure S2. Screen with PyrOx ligand class. After initial optimization, the PyrOx class of ligands was also screened, providing product in good yields and modest selectivity, although ultimately ineffective at inducing high levels of asymmetry. An interesting effect was observed with 6-substituted and Cl- and F- substituted PyrOx scaffolds. Despite all ligands being of the same enantiomer, the opposite enantiomer of product was formed in the latter cases. Further investigation into this effect is underway.

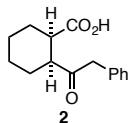
III. Isolated Yields and Product Characterization

General procedure **A** for anhydride opening: Cyclohexanecarboxylic anhydride **1** (38.5 mg, 0.25 mmol) and benzyl trifluoroborate (59.4 mg, 0.30 mmol) were weighed into a 16 x 100 mm threaded reaction tube, equipped with a teflon coated stirbar. The reaction tube was then brought into an N₂-filled glovebox and 1.0 mL dioxane was added. Then a pre-stirred dissolved solution of Ni(cod)₂ (3.4 mg, 0.0125 mmol) and (-)-2,2'-Isopropylidenebis-(4*S*)-4-phenyl-2-oxazoline (**L1**) (5.0 mg, 0.0150 mmol) in 3.0 mL of dioxane was added. The mixture was allowed to stir for ~5 minutes at room temperature, at which point the reaction mixture became homogenous. A solution of 4CzIPN (3.9 mg, 0.005 mmol) in 1.0 mL dioxane was added, and the reaction tube sealed with a septa cap. The vial was wrapped with electrical tape, and then removed from the glovebox, where it was immediately irradiated with a 34W blue LED lamp, ~3 cm from the light source. A fan was used to keep the reaction cool. After 24 h, the reaction tube was removed from the light source, and the solvent was removed. The residue was dissolved in 1 M HCl (20 mL) and diethyl ether (25 mL). The aqueous layer was extracted once with additional diethyl ether (10 mL). The combined ether layers were then extracted with sat. aq. Na₂CO₃ (4 x 15 mL). The combined aqueous layers were acidified with conc. HCl until ~pH 2. The aqueous layer was extracted with diethyl ether (3 x 20 mL). The combined organic layers were washed with brine (30 mL) and then dried over Na₂SO₄, filtered and concentrated. The crude product was purified over silica gel using CH₂Cl₂ -> 5% MeOH in CH₂Cl₂. The product was converted to the methyl ester (when necessary) by dissolving the product in a 1:1 mixture of CH₂Cl₂/MeOH (~0.04 M). The reaction was cooled to 0 °C, at which point TMSCHN₂ (2.0 M in hexanes) was added dropwise until a light yellow color persisted. The reaction was stirred for 1 h at 0 °C. The reaction was quenched by adding an excess of acetic acid, until the yellow color disappeared. The solvent was removed, and the residue was taken up in diethyl ether and 1 M HCl. The organic layer was subsequently washed with sat. aq. Na₂CO₃ and brine, then dried over Na₂SO₄, filtered and concentrated. The crude product may be run through a silica plug if additional purification was necessary.

General procedure **B** for anhydride opening: Cyclohexanecarboxylic anhydride **1** (38.5 mg, 0.25 mmol) and benzyl trifluoroborate (59.4 mg, 0.30 mmol) were weighed into a 16 x 100 mm threaded reaction tube, equipped with a teflon coated stirbar. The reaction tube was then brought into an N₂-filled glovebox and 1.0 mL Et₂O was added. Then a pre-stirred dissolved solution of Ni(cod)₂ (3.4 mg, 0.0125 mmol) and (-)-2,2'-Isopropylidenebis-(4*S*)-4-phenyl-2-oxazoline (**L1**) (5.0 mg, 0.0150 mmol) in 0.5 mL of THF was added. The mixture was allowed to stir for ~5 minutes at room temperature, at which point the reaction mixture became homogenous. 4CzIPN (3.9 mg, 0.005 mmol) was added in 4.0 mL Et₂O and the reaction tube sealed with a septa cap. The vial was wrapped with electrical tape, and then removed from the glovebox, where it was immediately irradiated with a 34W blue LED lamp, ~3 cm from the light source. A fan was used to keep the reaction cool. After 24 h, the reaction tube was removed from the light source. The reaction was partitioned in 1 M HCl (20 mL) and diethyl ether (25 mL). The aqueous layer was extracted with additional diethyl ether (1 x 10 mL). The combined ether layers were then extracted with sat. aq. Na₂CO₃ (4 x 15 mL). The combined aqueous layers were acidified with conc. HCl until ~pH 2. The aqueous layer was extracted with diethyl ether (3 x 20 mL). The combined organic layers were washed with brine (30 mL) and then dried over Na₂SO₄, filtered

and concentrated. The crude product was purified over silica gel using $\text{CH}_2\text{Cl}_2 \rightarrow 5\% \text{ MeOH}$ in CH_2Cl_2 .

Characterization of new compounds:



According to general procedure **A**, **1** (38.5 mg, 0.25 mmol) and benzyl trifluoroborate (59.4 mg, 0.3 mmol) afforded the product as a pale yellow oil (47.3 mg, 77% yield, 91% ee, 24:1 dr). Run 2 afforded 77% yield, 90% ee, 19:1 dr. NMR data based on methyl ester.

^1H NMR (501 MHz, CDCl_3): δ 7.32 (t, $J = 7.4$ Hz, 2H), 7.24 (d, $J = 6.1$ Hz, 1H), 7.19 (d, $J = 6.8$ Hz, 2H), 3.80 (s, 2H), 3.60 (s, 3H), 2.92-2.91 (m, 1H), 2.79 (dt, $J = 8.9, 4.5$ Hz, 1H), 2.15 – 1.94 (m, 1H), 1.83 (ddt, $J = 13.2, 8.6, 4.4$ Hz, 1H), 1.76 (ddt, $J = 12.7, 8.0, 4.1$ Hz, 1H), 1.64 – 1.52 (m, 1H), 1.49 – 1.33 (m, 4H).

^{13}C NMR (126 MHz, CDCl_3): δ 209.39, 174.51, 134.58, 129.67, 128.65, 126.92, 51.74, 48.92, 47.55, 42.83, 26.26, 26.07, 24.00, 23.64.

HRMS: (ESI-TOF) calculated for $[\text{C}_{15}\text{H}_{18}\text{O}_3 + \text{Na}]^+$: 269.1148, found: 269.1144.

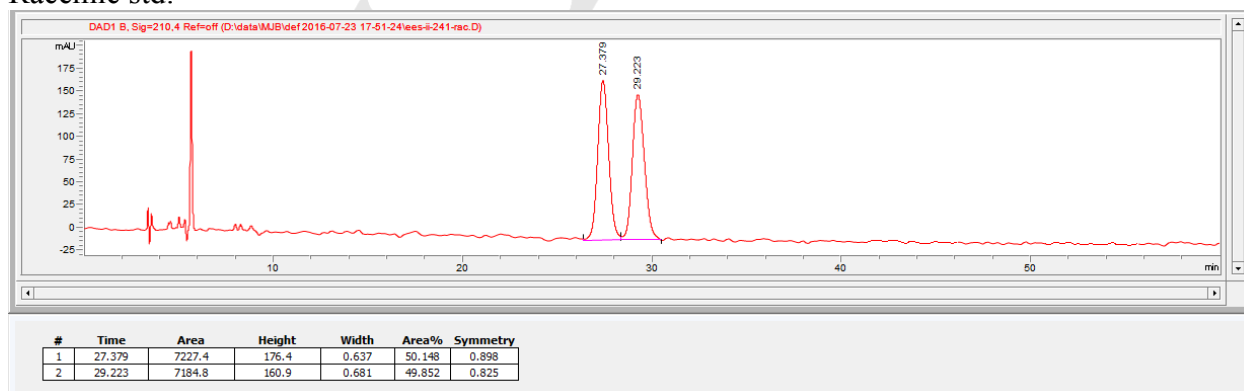
IR (ATR, cm^{-1}): 3029, 2932, 1699, 1453, 1259, 1217, 733, 699.

Optical Rotation: $[\alpha]_{\text{D}}^{26} -57.4$ (c 0.72, CHCl_3).

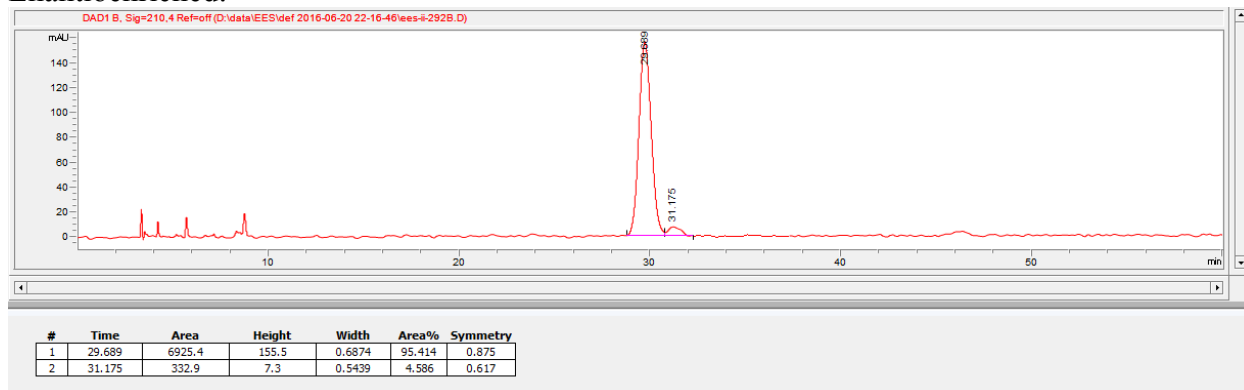
HPLC: ChiralPak[®] IC, 5% IPA (1% TFA) in Hexanes, 60 min run, 1 mL/min.

HPLC (methyl ester): Chiralcel[®] OJ-H, 5% IPA in Hexanes, 3 min run, 1 mL/min. Optimization screening was performed using this method.

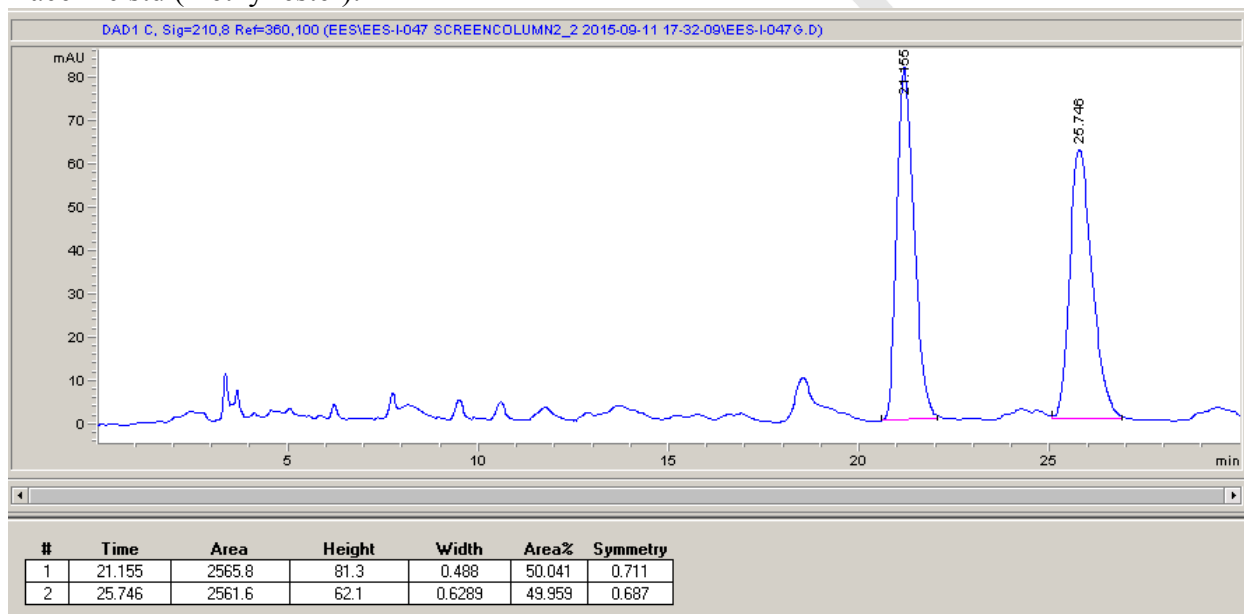
Racemic std:



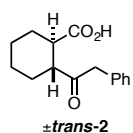
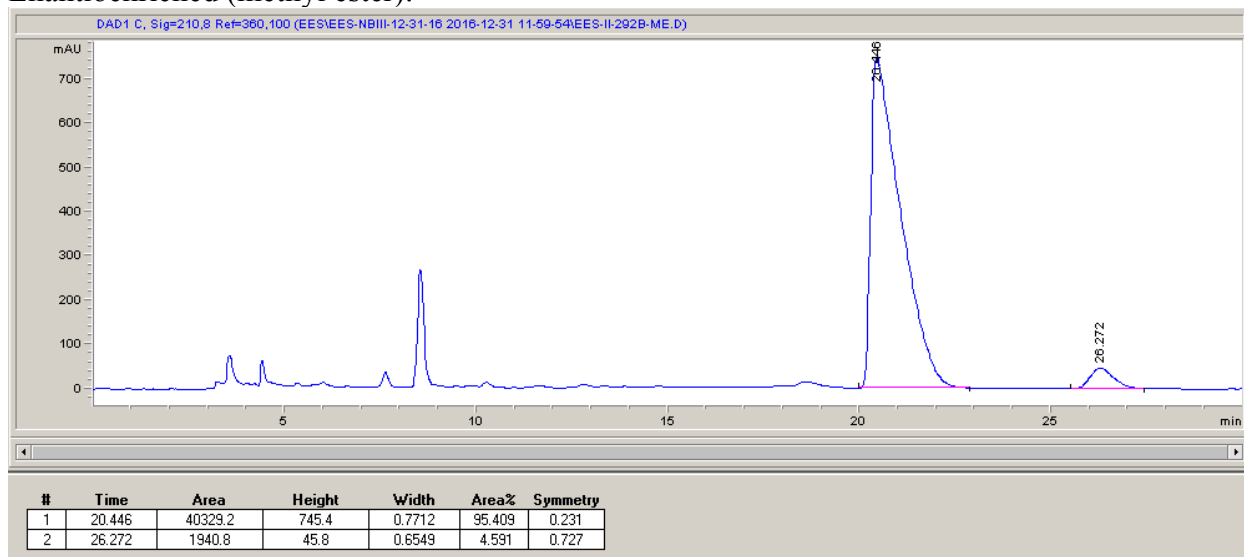
Enantioenriched:



Racemic std (methyl ester):



Enantioenriched (methyl ester):



According to general procedure A, anhydride *trans*-1 (38.5 mg, 0.25 mmol) and benzyl trifluoroborate (59.4 mg, 0.3 mmol) afforded the product as a pale yellow oil (51.3 mg, 83% yield, -2% ee, 19:1 dr). Run 2 afforded 79% yield, -2% ee, 15.7:1 dr. All characterization performed on the acid.

$^1\text{H NMR}$ (501 MHz, CDCl_3): δ 7.35 – 7.28 (m, 2H), 7.27 – 7.22 (m, 1H), 7.22 – 7.12 (m, 2H), 3.82 (ABq, $J = 15.0$ Hz, $\Delta\nu = 26.5$ Hz, 2H), 2.80 (td, $J = 11.1, 3.5$ Hz, 1H), 2.73 (td, $J = 11.2, 3.7$ Hz, 1H), 2.23 – 2.08 (m, 1H), 2.02 – 1.89 (m, 1H), 1.87 – 1.72 (m, 2H), 1.42 – 1.04 (m, 4H).

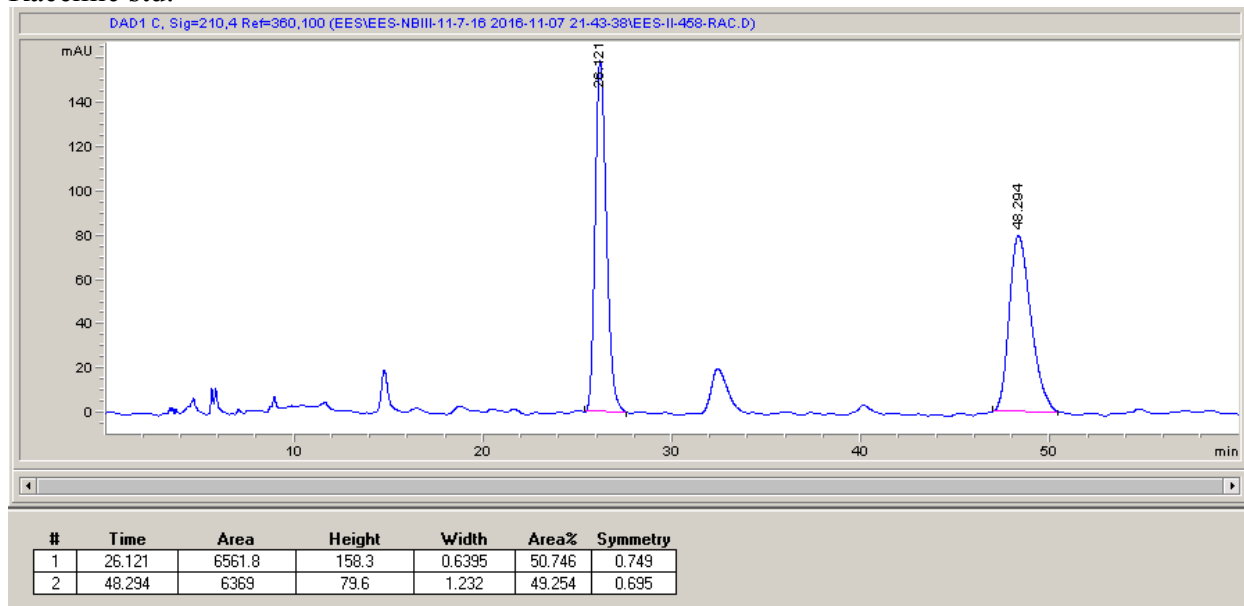
$^{13}\text{C NMR}$ (126 MHz, CDCl_3): δ 210.58, 180.92, 134.17, 129.83, 128.64, 127.01, 50.85, 48.75, 44.25, 28.92, 28.75, 25.54, 25.45.

HRMS: (ESI-TOF) calculated for $([\text{C}_{15}\text{H}_{19}\text{O}_3 + \text{Na}]^+)$: 269.1148, found: 269.1146.

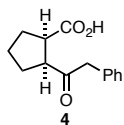
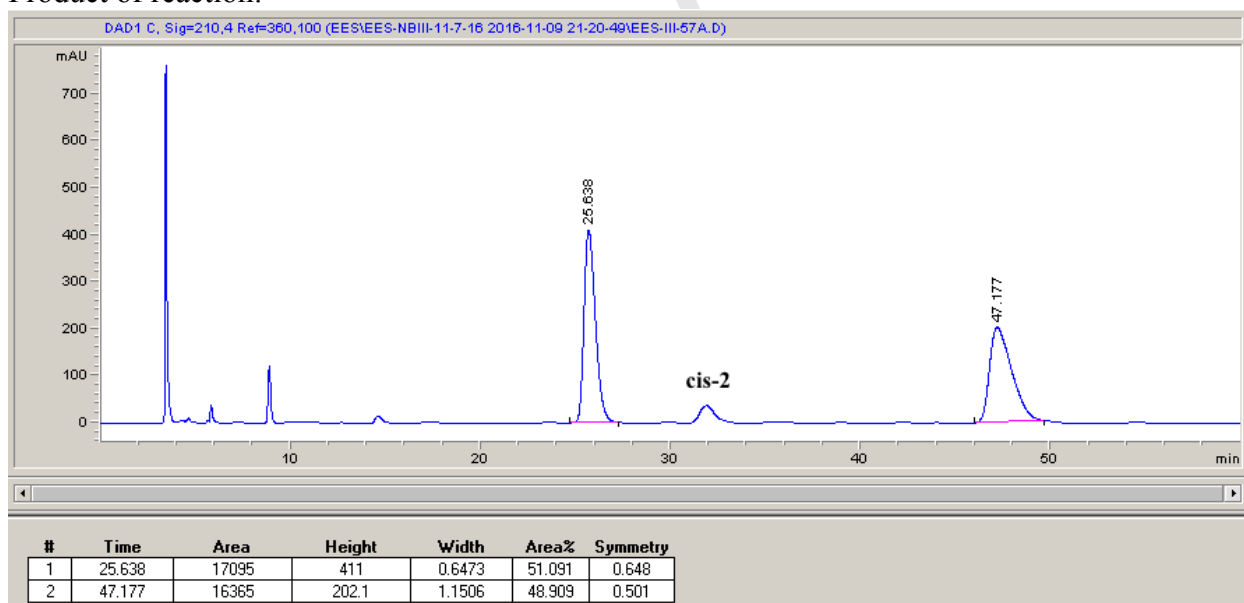
IR (ATR, cm^{-1}): 3029, 2936, 2859, 1734, 1702, 1495, 1451, 1367, 1264, 1216, 732, 701.

HPLC: ChiralPak[®] IC, 5% IPA in Hexanes, 60 min run, 1 mL/min.

Racemic std:



Product of reaction:



According to general procedure A, anhydride **4-A** (35.0 mg, 0.25 mmol) and benzyl trifluoroborate (59.4 mg, 0.3 mmol) afforded the product as a pale yellow oil (47.8 mg, 82% yield, 70% ee, 24:1 dr). Run 2 afforded 85% yield, 69% ee, 19:1 dr. NMR data based on methyl ester.

^1H NMR (501 MHz, CDCl_3): δ 7.33 (t, $J = 7.4$ Hz, 2H), 7.30 – 7.23 (m, 1H), 7.20 (d, $J = 7.5$ Hz, 2H), 3.77 (m, 2H), 3.59 (s, 3H), 3.27 (q, $J = 7.7$ Hz, 1H), 2.98 (q, $J = 7.9$ Hz, 1H), 2.16 – 2.00 (m, 1H), 2.00 – 1.87 (m, 3H), 1.83 (dt, $J = 13.8, 6.9$ Hz, 1H), 1.61 (dt, $J = 12.2, 7.8$ Hz, 1H).

^{13}C NMR (126 MHz, CDCl_3): δ 208.96, 174.64, 134.24, 129.70, 128.71, 127.05, 52.90, 51.77, 49.57, 47.26, 28.74, 28.49, 23.99.

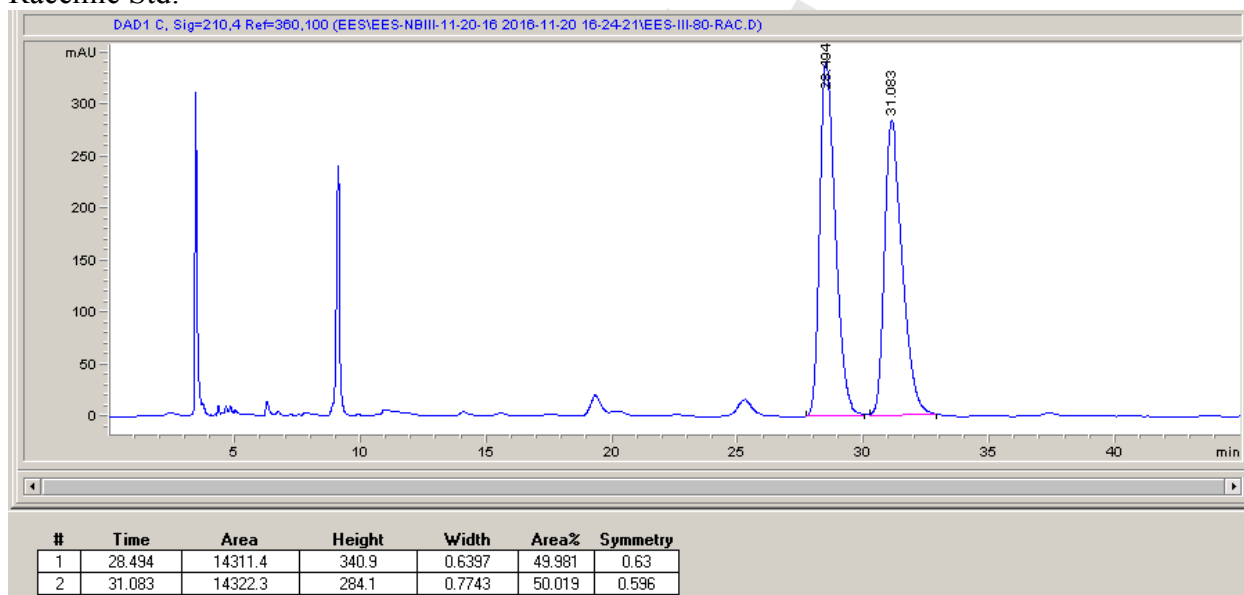
HRMS: (ESI-TOF) calculated for $([\text{C}_{14}\text{H}_{16}\text{O}_3 + \text{Na}]^+)$: 255.0992, found 255.0987.

IR (ATR, cm^{-1}): 3030, 2958, 1702, 1496, 1453, 1413, 1180, 948, 802, 733, 699.

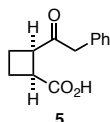
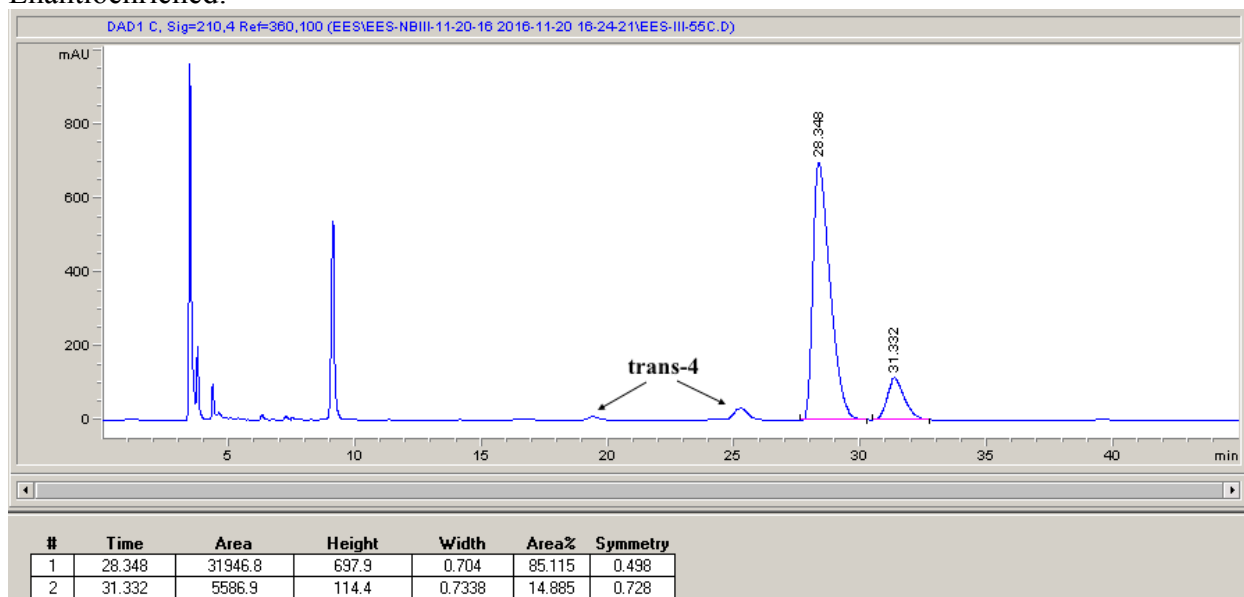
Optical Rotation: $[\alpha]_{\text{D}}^{26} -19.3$ (c 0.71, CHCl_3).

HPLC: ChiralPak[®] IC, 5% IPA in Hexanes, 45 min run, 1 mL/min.

Racemic Std:



Enantioenriched:



(+)-2,2'-Isopropylidenebis-(4*R*)-4-benzyl-2-oxazoline (**L3**) was used as the ligand (5.4 mg, 0.0150 mmol). According to general procedure A, anhydride **5-A** (31.5 mg, 0.25 mmol) and benzyl trifluoroborate (59.4 mg, 0.3 mmol) afforded the product as a pale yellow oil (40.5 mg, 74% yield, 77% ee, >20:1 dr). Run 2 afforded 66% yield, 74% ee, >20:1 dr. Enantioselectivity was determined using the methyl ester. NMR data based on methyl ester.

¹H NMR (501 MHz, CDCl₃): δ 7.35 – 7.29 (m, 2H), 7.28 – 7.23 (m, 1H), 7.19 (dd, *J* = 7.0, 1.6 Hz, 2H), 3.75 – 3.63 (m, 5H), 3.62 – 3.54 (m, 1H), 3.37 – 3.29 (m, 1H), 2.38 – 2.24 (m, 2H), 2.22 – 2.11 (m, 1H), 2.11 – 2.03 (m, 1H).

¹³C NMR (126 MHz, CDCl₃): δ ¹³C NMR (126 MHz, CDCl₃) δ 207.49, 174.15, 134.09, 129.68, 128.77, 127.10, 51.93, 48.56, 46.60, 41.05, 22.19, 21.81.

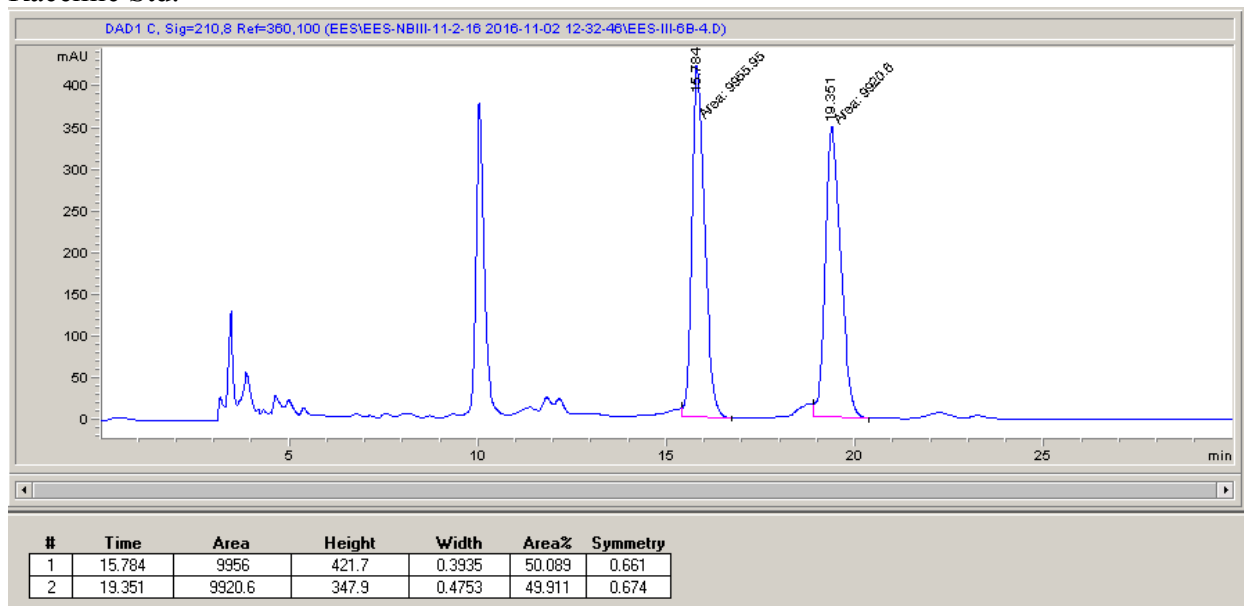
HRMS (acid): (ESI-TOF) calculated for ([C₁₃H₁₄O₃ + Na]⁺): 241.0835, found: 241.0835.

IR (acid, ATR, cm⁻¹): 2951, 1704, 1495, 1454, 1360, 1228, 1030, 923, 700.

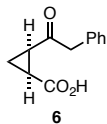
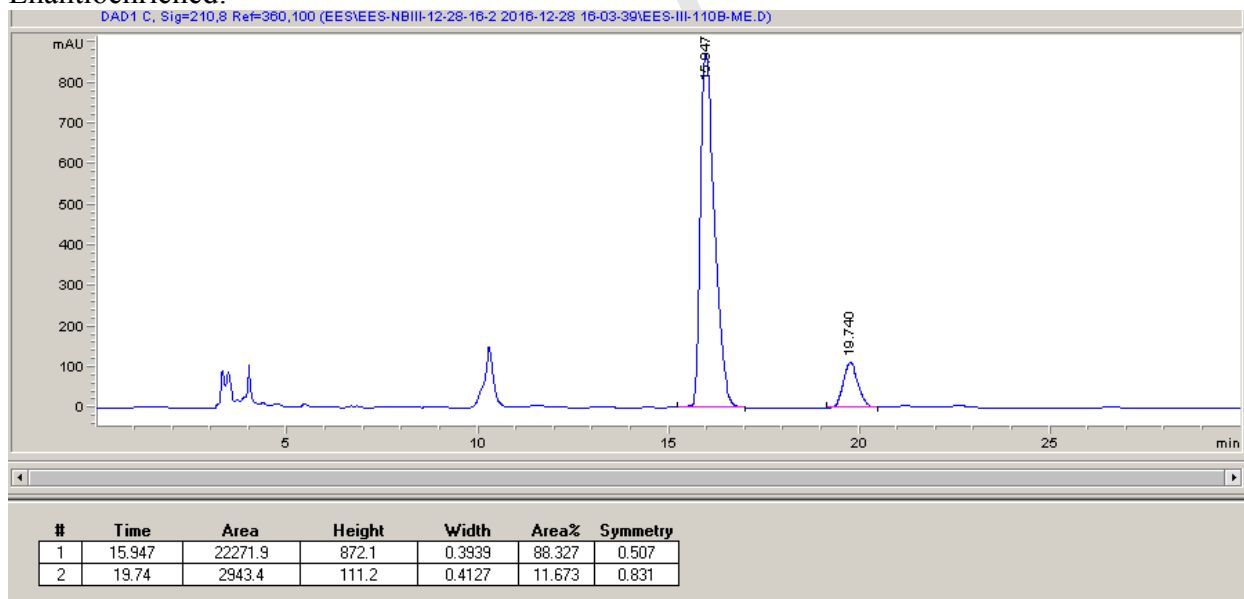
Optical Rotation(acid): [α]_D²⁶ +0.3 (*c* 0.62, CHCl₃).

HPLC (methyl ester): ChiralPak[®] AS-H, 5% IPA in Hexanes, 30 min run, 1 mL/min.

Racemic Std:



Enantioenriched:



(+)-2,2'-Isopropylidenebis-(4*R*)-4-benzyl-2-oxazoline (**L3**) was used as the ligand (5.4 mg, 0.0150 mmol). According to general procedure **A**, anhydride **6-A** (28.0 mg, 0.25 mmol) and benzyl trifluoroborate (59.4 mg, 0.3 mmol) afforded the product as a pale yellow oil (30.9 mg, 61% yield, 65% ee, 24:1 dr). Run 2 afforded 41% yield, 63% ee, 17:1 dr. Enantioselectivity was determined using the methyl ester. NMR data based on methyl ester.

¹H NMR (501 MHz, CDCl₃): δ 7.33 (t, J = 7.3 Hz, 2H), 7.28-7.26 (m, 1H), 7.22 (d, J = 7.0 Hz, 2H), 3.83 (s, 2H), 3.64 (s, 3H), 2.26 (ddd, J = 9.3, 8.2, 6.7 Hz, 1H), 2.06 (td, J = 8.8, 6.8 Hz, 1H), 1.73 (td, J = 6.7, 4.8 Hz, 1H), 1.19 (td, J = 8.3, 4.8 Hz, 1H).

¹³C NMR (126 MHz, CDCl₃): δ 203.41, 170.40, 133.97, 129.75, 128.85, 127.21, 52.28, 50.87, 27.67, 23.82, 12.76.

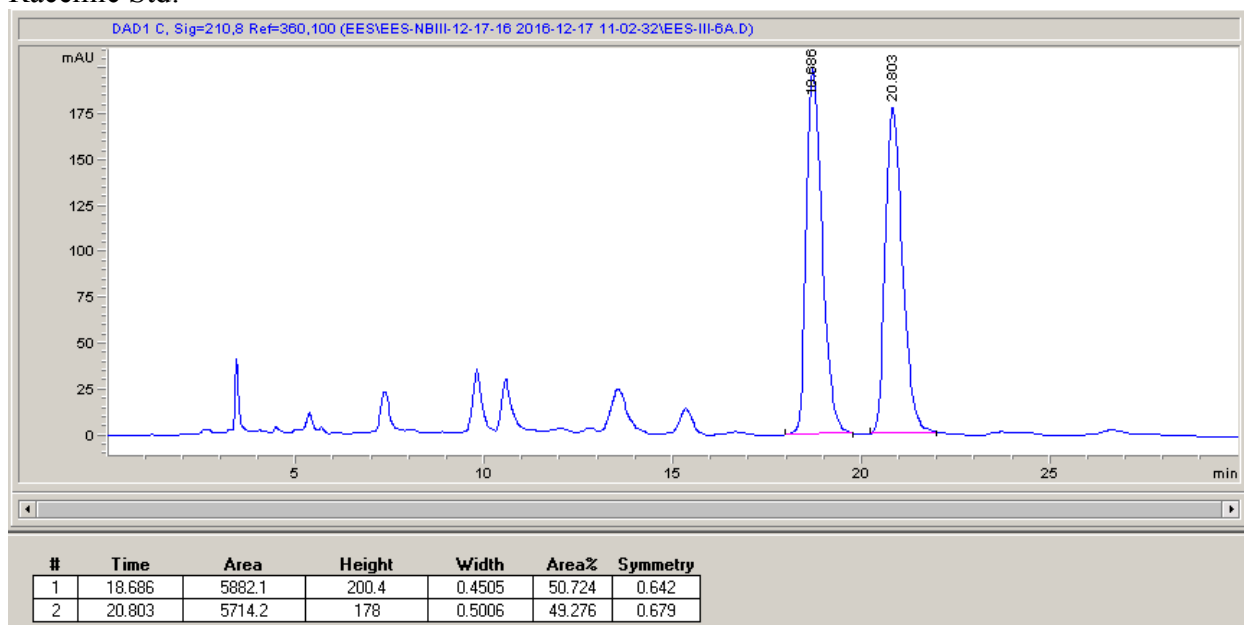
HRMS (acid): (ESI-TOF) calculated for ([C₁₂H₁₃O₃ + H]⁺): 205.0859, found: 205.0858.

IR (acid, ATR, cm⁻¹): 3450, 3026, 2970, 1725, 1496, 1454, 1370, 1228, 1217, 1074, 905, 700.

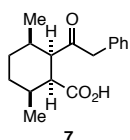
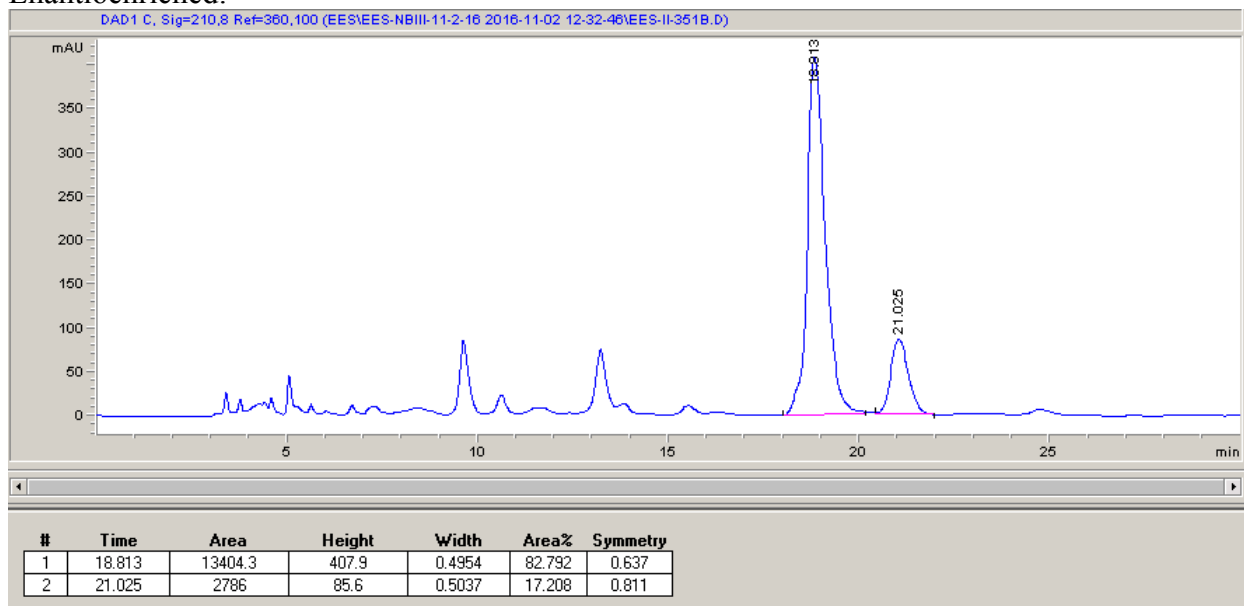
Optical Rotation (acid): $[\alpha]_D^{26}$ +11.3 (c 0.47, CHCl₃).

HPLC (methyl ester): Chiralcel[®] OD-H, 5% IPA in Hexanes, 30 min run, 1 mL/min.

Racemic Std:



Enantioenriched:



(+)-2,2'-Isopropylidenebis-(4*R*)-4-benzyl-2-oxazoline (**L3**) was used as the ligand (5.4 mg, 0.0150 mmol). According to general procedure **A**, anhydride **7-A** (45.6 mg, 0.25 mmol) and benzyl trifluoroborate (59.4 mg, 0.3 mmol) afforded the product as a pale yellow oil (19.0 mg, 28% yield, 37% ee, 8.3:1 dr). Run 2 afforded 40% yield, 35% ee, 9.5:1 dr. NMR data based on methyl ester.

¹H NMR (501 MHz, CDCl₃): δ 7.34 – 7.28 (m, 2H), 7.27 – 7.22 (m, 1H), 7.21 – 7.16 (m, 2H), 3.93, 3.90, 3.78, 3.75 (m, 2H), 3.65 (s, 3H), 2.95 (t, *J* = 5.2 Hz, 1H), 2.86 (t, *J* = 5.3 Hz, 1H), 2.30 – 2.18 (m, 1H), 1.90 – 1.79 (m, 1H), 1.77 – 1.64 (m, 2H), 1.53 – 1.44 (m, 1H), 1.37 (ddt, *J* = 10.0, 6.3, 2.9 Hz, 1H), 1.07 (d, *J* = 7.2 Hz, 3H), 1.01 (d, *J* = 7.0 Hz, 3H).

¹³C NMR (126 MHz, CDCl₃): δ 208.76, 174.24, 134.71, 129.78, 128.67, 126.97, 53.85, 51.35, 49.11, 46.49, 33.20, 30.60, 30.49, 26.78, 18.66, 16.98.

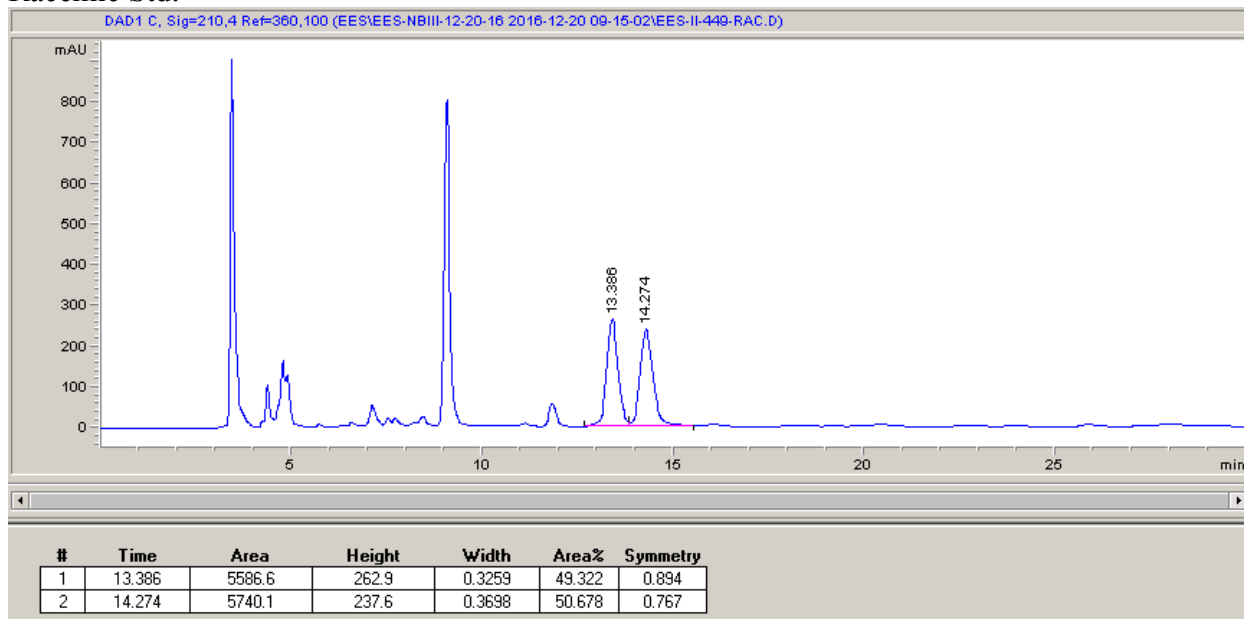
HRMS: (ESI-TOF) calculated for ([C₁₇H₂₂O₃ + Na]⁺): 297.1461, found 297.1455.

IR (ATR, cm⁻¹): 3029, 2925, 1701, 1496, 1453, 1298, 1228, 1057, 925, 803, 742, 699.

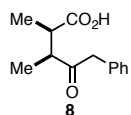
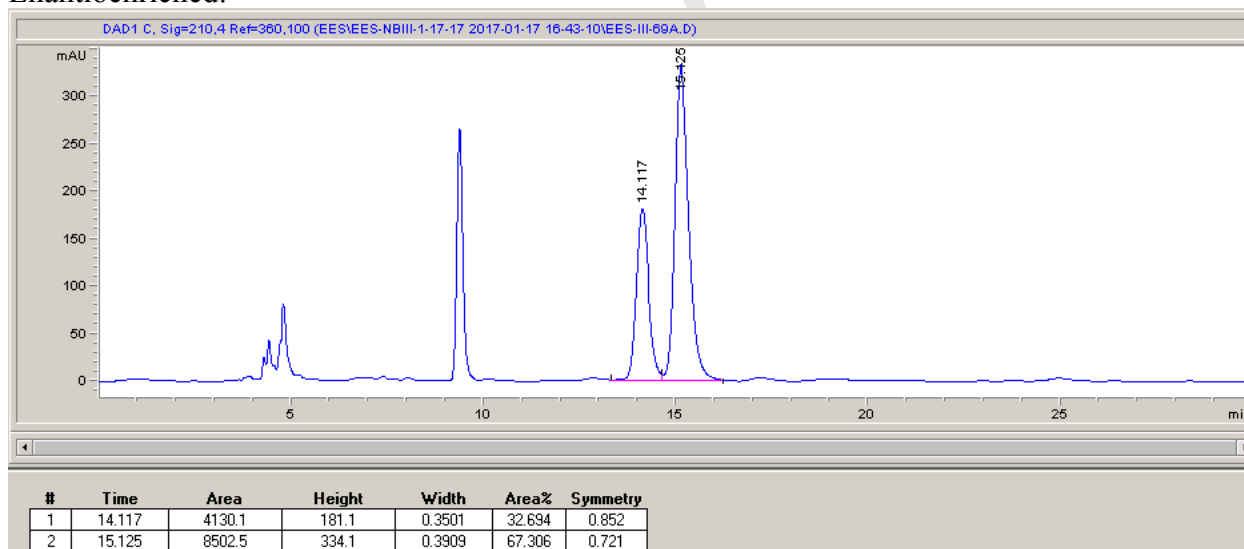
Optical Rotation: [α]_D²⁶ +12.8 (*c* 0.69, CHCl₃).

HPLC: ChiralPak[®] IC, 5% IPA in Hexanes, 60 min run, 1 mL/min.

Racemic Std:



Enantioenriched:



Reaction run for 48 h. According to general procedure **A**, anhydride **8-A** (32.0 mg, 0.25 mmol) and benzyl trifluoroborate (59.4 mg, 0.3 mmol) afforded the product as a pale yellow oil (38.8 mg, 70% yield, 88% ee, 12.3:1 dr). Run 2 afforded 69% yield, 88% ee, 13.4:1 dr. NMR data based on methyl ester.

^1H NMR (501 MHz, CDCl_3): δ 7.38 – 7.29 (m, 2H), 7.29 – 7.23 (m, 1H), 7.23 – 7.12 (m, 2H), 3.76 (s, 2H), 3.66 (s, 3H), 2.96 – 2.87 (m, 1H), 2.80 (qd, $J = 8.6, 6.9$ Hz, 1H), 1.09 (d, $J = 6.9$ Hz, 3H), 1.03 (d, $J = 7.0$ Hz, 3H).

^{13}C NMR (126 MHz, CDCl_3): δ 209.75, 175.73, 133.68, 129.72, 128.83, 127.23, 51.83, 49.59, 48.10, 42.07, 15.57, 15.30.

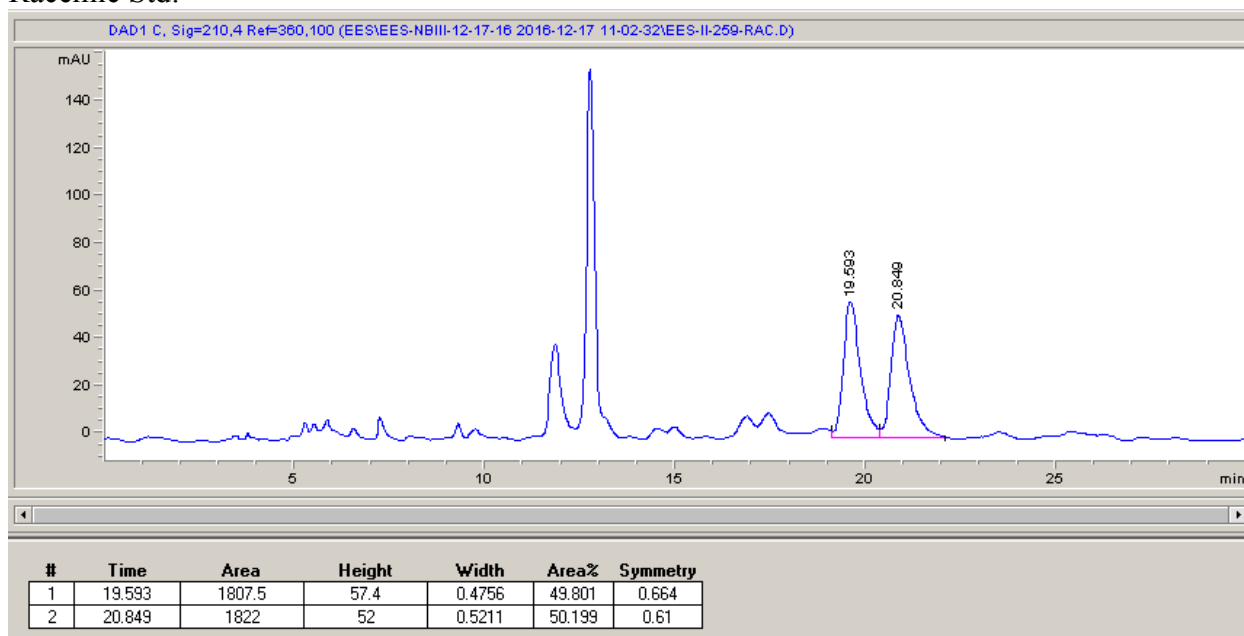
HRMS: (ESI-TOF) calculated for $([\text{C}_{13}\text{H}_{16}\text{O}_3 + \text{Na}]^+)$: 243.0992, found 243.0990.

IR (ATR, cm^{-1}): 3063, 2932, 1699, 1496, 1453, 1381, 1283, 1071, 948, 801, 712, 700.

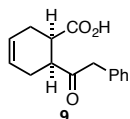
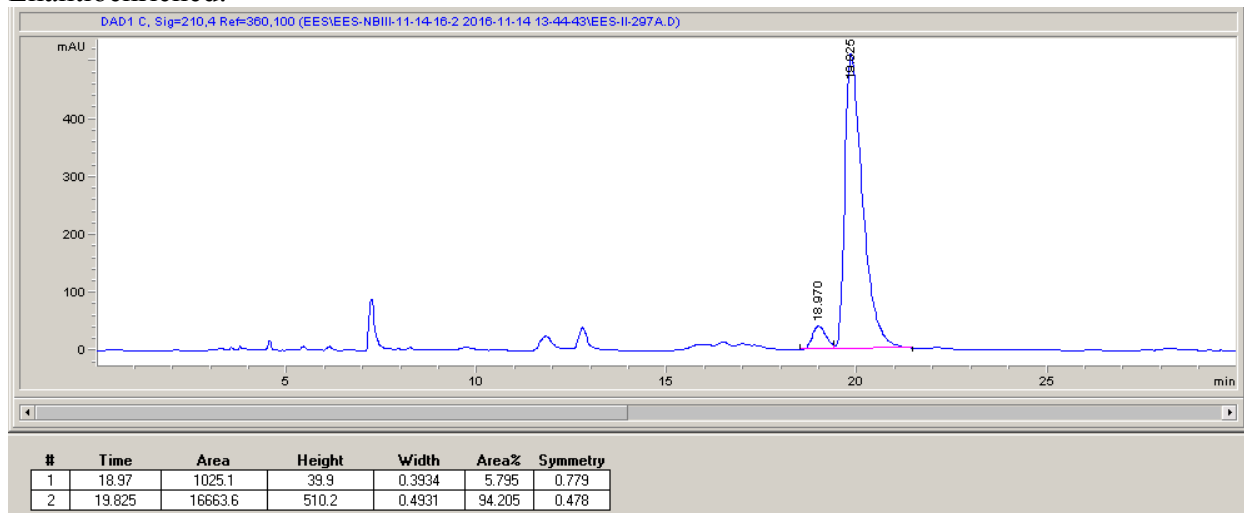
Optical Rotation: $[\alpha]_{\text{D}}^{26} -42.3$ (c 0.65, CHCl_3).

HPLC: ChiralPak[®] IC, 3% IPA in Hexanes, 60 min run, 1 mL/min.

Racemic Std:



Enantioenriched:



According to general procedure A, anhydride **9-A** (38.0 mg, 0.25 mmol) and benzyl trifluoroborate (59.4 mg, 0.3 mmol) afforded the product as a pale yellow oil (40.4 mg, 66% yield, 47% ee, 9.5:1 dr). Run 2 afforded 75% yield, 45% ee, 11.5:1 dr. NMR data based on methyl ester.

^1H NMR (501 MHz, CDCl_3): δ 7.36 – 7.28 (m, 2H), 7.28 – 7.23 (m, 1H), 7.23 – 7.11 (m, 2H), 5.76 – 5.61 (m, 2H), 3.83 (s, 2H), 3.63 (s, 3H), 3.07 (td, $J = 6.2, 3.5$ Hz, 1H), 3.03 (td, $J = 6.8, 3.6$ Hz, 1H), 2.67 – 2.48 (m, 2H), 2.44 – 2.31 (m, 2H).

^{13}C NMR (126 MHz, CDCl_3): δ 208.36, 174.00, 134.40, 129.66, 128.72, 127.02, 125.88, 124.53, 51.19, 47.36, 45.95, 39.65, 26.38, 25.33.

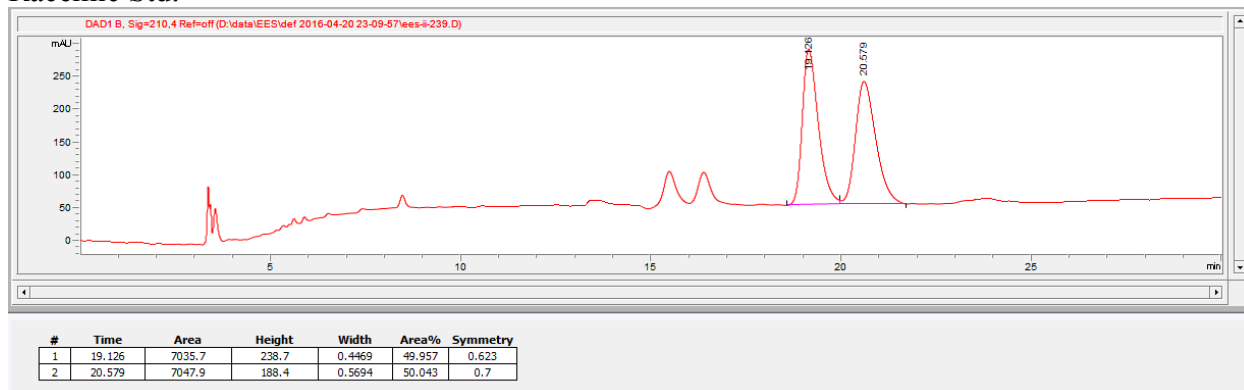
HRMS: (ESI-TOF) calculated for ($[\text{C}_{15}\text{H}_{16}\text{O}_3 + \text{Na}]^+$): 267.0992, found: 267.0984.

IR (ATR, cm^{-1}): 3028, 2923, 1736, 1706, 1496, 1436, 1366, 1229, 1216, 699.

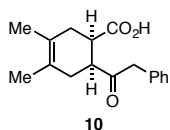
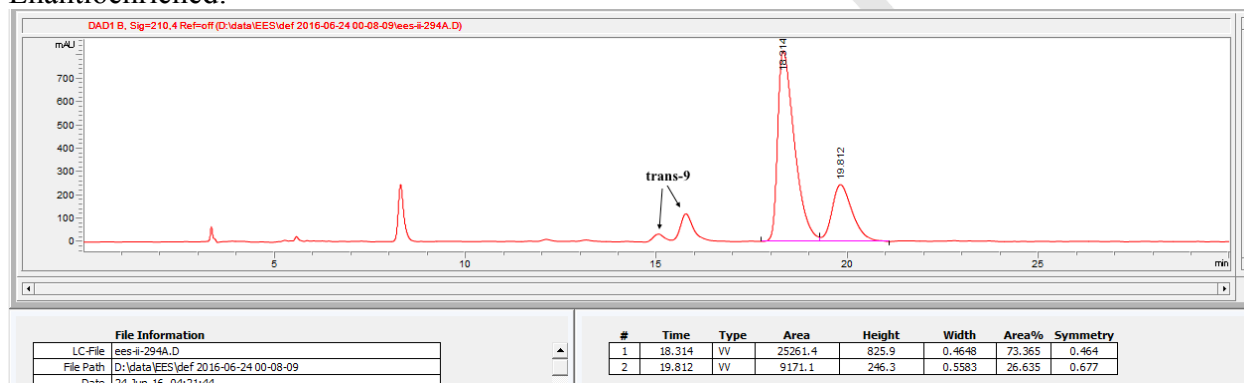
Optical Rotation: $[\alpha]_{\text{D}}^{26} -9.1$ (c 0.76, CHCl_3).

HPLC: ChiralPak[®] ID, 5% IPA (1% TFA) in Hexanes, 30 min run, 1 mL/min.

Racemic Std:



Enantioenriched:



According to general procedure A, anhydride **10-A** (45.1 mg, 0.25 mmol) and benzyl trifluoroborate (59.4 mg, 0.3 mmol) afforded the product as a pale yellow oil (52.4 mg, 77% yield, 87% ee, 18:1 dr). Run 2 afforded 67% yield, 85% ee, 14:1 dr. NMR data based on methyl ester.

^1H NMR (501 MHz, CDCl_3): δ 7.31 (t, $J = 7.4$ Hz, 2H), 7.25 (d, $J = 8.1$ Hz, 1H), 7.18 (d, $J = 7.5$ Hz, 2H), 3.80 (s, 2H), 3.63 (s, 3H), 3.10 – 2.84 (m, 2H), 2.51–2.41 (m, 2H), 2.36 – 2.20 (m, 2H), 1.60 (s, 6H).

^{13}C NMR (126 MHz, CDCl_3): δ 208.50, 174.16, 134.49, 129.61, 128.69, 126.97, 124.74, 123.33, 51.88, 47.37, 46.85, 40.44, 32.31, 31.59, 19.16, 18.98

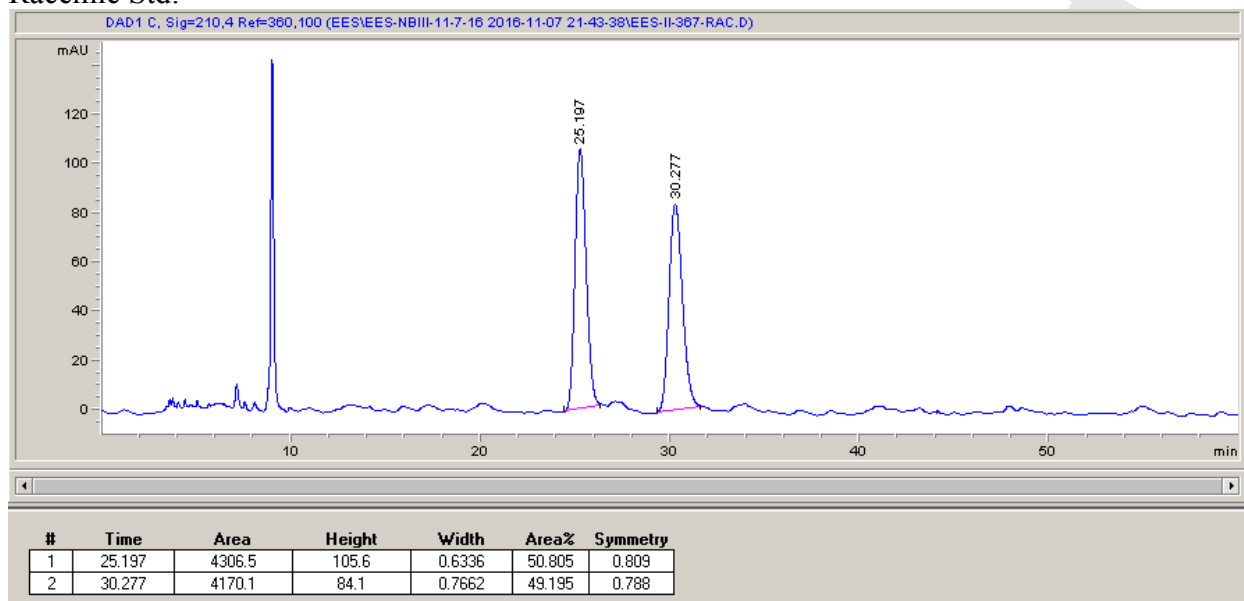
HRMS: (ESI-TOF) calculated for $([\text{C}_{17}\text{H}_{20}\text{O}_3 - \text{H}]^-)$: 271.1340, found: 271.1340.

IR (ATR, cm^{-1}): 3186, 3029, 2920, 1706, 1497, 1454, 1258, 1190, 1085, 798, 701.

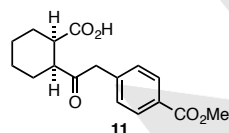
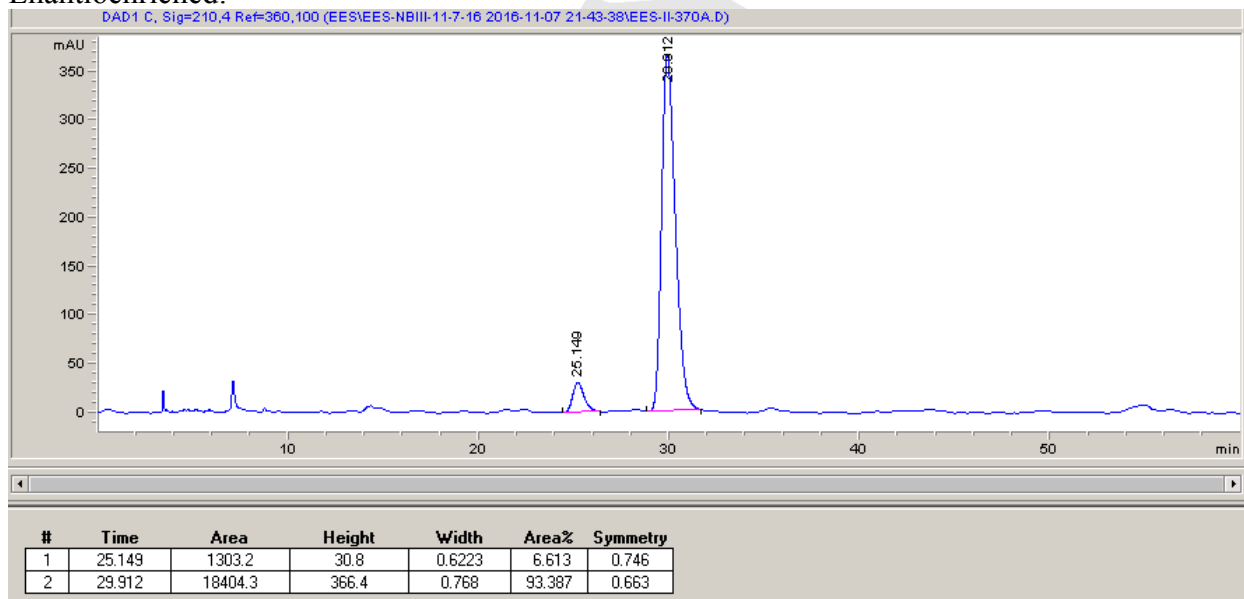
Optical Rotation: $[\alpha]_{\text{D}}^{26} -10.5$ (c 0.81, CHCl_3).

HPLC: ChiralPak[®] IC, 5% IPA in Hexanes, 60 min run, 1 mL/min.

Racemic Std:



Enantioenriched:



According to general procedure **A**, anhydride **1** (38.5 mg, 0.25 mmol) and benzyl trifluoroborate **11-B** (76.8 mg, 0.3 mmol) afforded the product as a pale yellow oil (56.3 mg, 74% yield, 90% ee, 13.3:1 dr). Run 2 afforded 79% yield, 88% ee, 12.7:1 dr. NMR data based on methyl ester. Diastereoselectivity based on ¹H NMR in acetone-d₆.

^1H NMR (501 MHz, CDCl_3): δ 7.99 (d, J = 5.0 Hz, 2H), 7.26 (d, J = 10 Hz, 2H), 3.90 (s, 3H), 3.86 (s, 2H), 3.61 (s, 3H), 2.89 (m, 1H), 2.82 (m, 1H), 2.08 (m, 1H), 2.01 (m, 1H), 1.84 (m, 1H), 1.76 (m, 1H), 1.55 (m, 1H), 1.44 (m, 1H), 1.39 (m, 2H).

^{13}C NMR (126 MHz, CDCl_3): δ 208.55, 174.42, 167.10, 139.87, 129.88, 129.81, 128.81, 52.21, 51.80, 49.19, 47.39, 42.96, 26.29, 25.99, 23.95, 23.61.

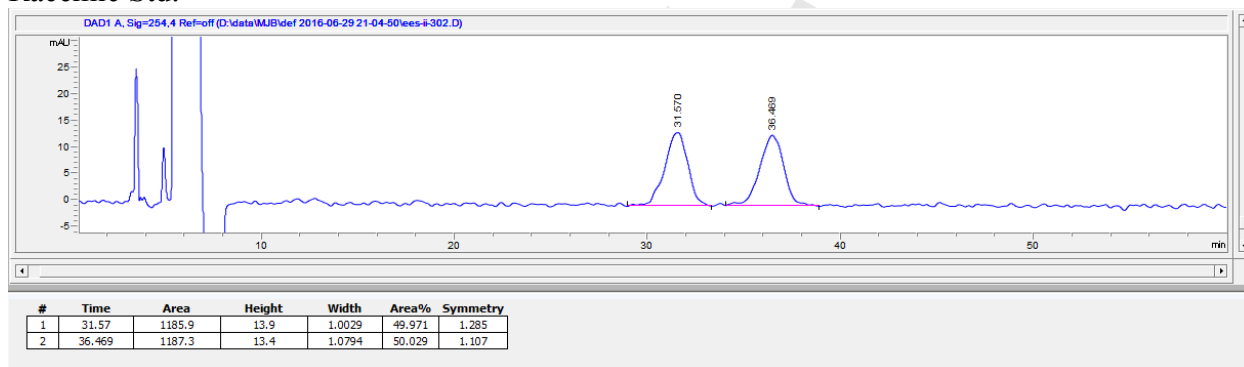
HRMS: (ESI-TOF) calculated for $([\text{C}_{17}\text{H}_{21}\text{O}_5 + \text{H}]^+)$: 305.1384, found 305.1382.

IR (ATR, cm^{-1}): 3006, 2943, 1737, 1722, 1611, 1436, 1368, 1280, 1217 1109, 1021, 757.

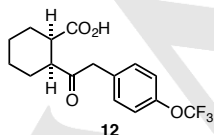
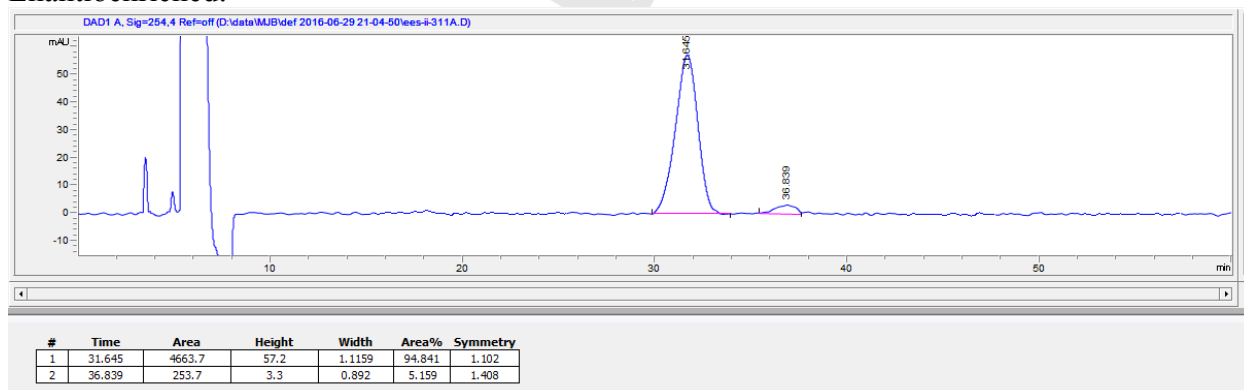
Optical Rotation: $[\alpha]_{\text{D}}^{26}$ -39.1 (c 0.66, CHCl_3).

HPLC: ChiralPak[®] IC, 15% IPA (1% TFA) in Hexanes, 60 min run, 1 mL/min (sample prep in HPLC grade acetone).

Racemic Std:



Enantioenriched:



Reaction run for 46 h. According to general procedure A, anhydride **1** (38.5 mg, 0.25 mmol) and benzyl trifluoroborate **12-B** (84.6 mg, 0.3 mmol) afforded the product as a pale yellow oil (61.0

mg, 74% yield, 81% ee, 12.3:1 dr). Run 2 afforded 70% yield, 81% ee, 11.5:1 dr. NMR data based on methyl ester.

^1H NMR (501 MHz, CDCl_3): δ 7.21 (d, $J = 8.7$ Hz, 2H), 7.18 – 7.14 (m, 2H), 3.87 – 3.77 (m, 2H), 3.61 (s, 3H), 2.94 – 2.78 (m, 2H), 2.16 – 1.97 (m, 2H), 1.92 – 1.71 (m, 2H), 1.63 – 1.35 (m, 4H).

^{13}C NMR (126 MHz, CDCl_3): δ 208.92, 174.48, 148.22, 133.27, 131.12, 121.12, 115.41, 51.81, 49.12, 46.56, 43.02, 26.33, 26.02, 23.98, 23.63.

^{19}F NMR (282 MHz, CDCl_3): δ -57.87

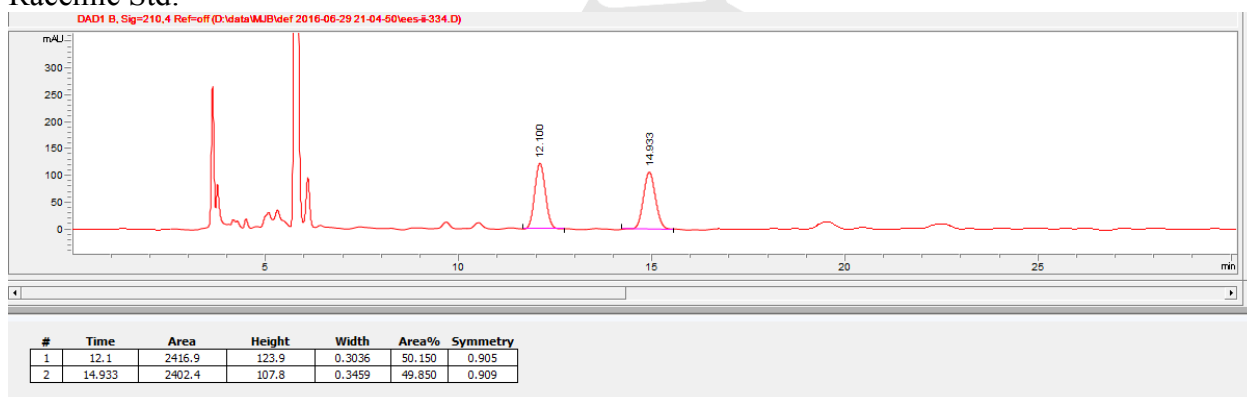
HRMS: (ESI-TOF) calculated for ($[\text{C}_{16}\text{H}_{18}\text{F}_3\text{O}_4 + \text{H}]^+$): 331.1152, found 331.1155.

IR (ATR, cm^{-1}): 2936, 2860, 1736, 1704, 1509 1366, 1254, 1218, 1159, 1019, 811, 736.

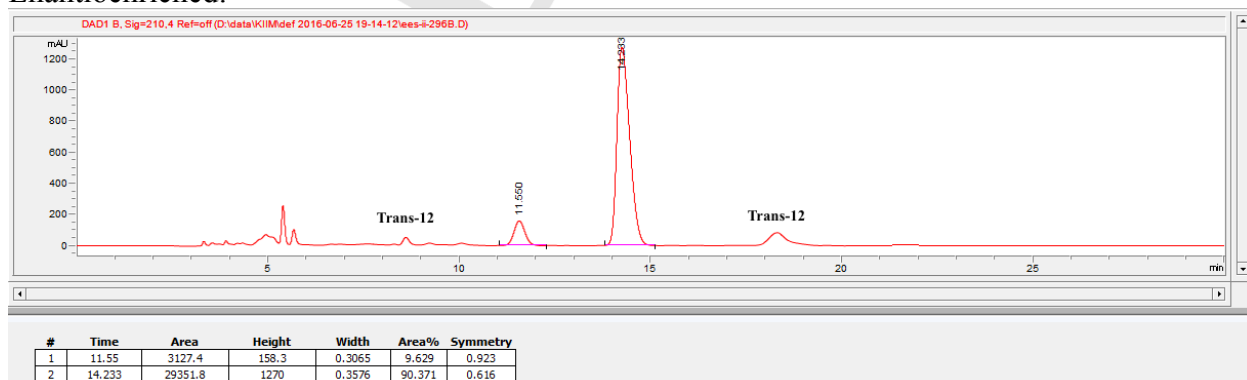
Optical Rotation: $[\alpha]_{\text{D}}^{26}$ -31.6 (c 0.75, CHCl_3).

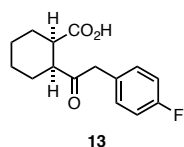
HPLC: ChiralPak[®] IC, 5% IPA (1% TFA) in Hexanes, 30 min run, 1 mL/min.

Racemic Std:



Enantioenriched:





1.5 equiv of trifluoroborate was used. According to general procedure **A**, anhydride **1** (38.5 mg, 0.25 mmol) and 4-fluorobenzyl trifluoroborate **13-B** (79.3 mg, 0.37 mmol) afforded the product as a pale yellow oil (59.4 mg, 90% yield, 88% ee, 15.7:1 dr). Run 2 afforded 89% yield, 88% ee, 15.7:1 dr. NMR data based on methyl ester.

¹H NMR (501 MHz, CDCl₃): δ 7.14 (dd, *J* = 8.4, 5.5 Hz, 2H), 7.00 (t, *J* = 8.7 Hz, 2H), 3.78 (ABq, *J* = 15.0 Hz, Δ*v* = 13.2 Hz, 2H), 3.61 (s, 3H), 2.95 – 2.85 (m, 1H), 2.85 – 2.75 (m, 1H), 2.08 (tq, *J* = 12.4, 4.5 Hz, 1H), 2.01 (ddt, *J* = 14.3, 7.3, 3.7 Hz, 1H), 1.84 (ddt, *J* = 13.0, 8.4, 4.4 Hz, 1H), 1.76 (ddt, *J* = 12.5, 7.7, 4.0 Hz, 1H), 1.56 (dq, *J* = 7.7, 3.6 Hz, 1H), 1.50 – 1.32 (m, 3H).

¹³C NMR (126 MHz, CDCl₃): δ 209.26, 174.50, 162.94, 131.22 (d, *J* = 7.5 Hz), 130.23 (d, *J* = 2.5 Hz), 115.46 (d, *J* = 21.3 Hz), 51.79, 48.99, 46.53, 42.94, 26.29, 26.03, 23.99, 23.63.

¹⁹F NMR (282 MHz, CDCl₃): δ -118.57

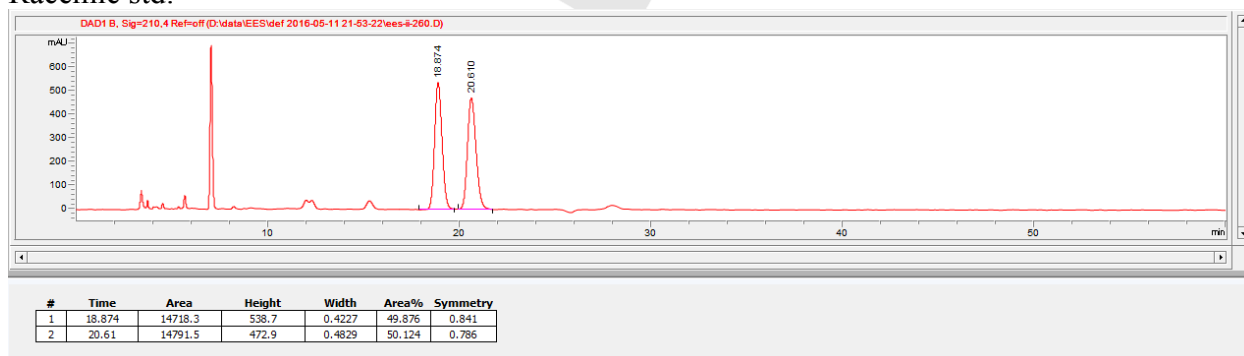
HRMS: (ESI-TOF) calculated for ([C₁₅H₁₈FO₃ + H]⁺): 265.1234, 265.1237.

IR (ATR, cm⁻¹): 2935, 2857, 1703, 1508, 1450, 1366, 1219, 1158, 1016, 823, 792.

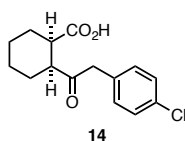
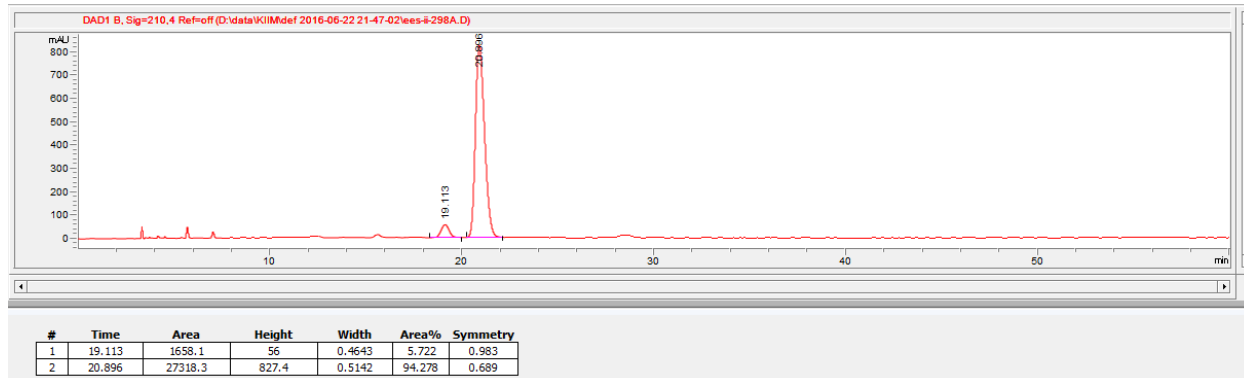
Optical Rotation: [α]_D²⁶ -42.6 (*c* 0.86, CHCl₃).

HPLC: ChiralPak[®] IC, 5% IPA (1% TFA) in Hexanes, 60 min run, 1 mL/min.

Racemic std:



Enantioenriched:



According to general procedure **A**, anhydride **1** (38.5 mg, 0.25 mmol) and benzyl trifluoroborate **14-B** (69.7 mg, 0.3 mmol) afforded the product as a pale yellow oil (45.0 mg, 64% yield, 83% ee, 11.5:1 dr). Run 2 afforded 39% yield, 76% ee, 8.5:1 dr. A third run afforded 56% yield, 78% ee and 9.5:1 dr. NMR data based on methyl ester.

¹H NMR (501 MHz, CDCl₃): δ 7.28 (d, *J* = 8.2 Hz, 2H), 7.12 (d, *J* = 8.2 Hz, 2H), 3.82 – 3.72 (m, 2H), 3.62 (s, 3H), 2.91 – 2.76 (m, 2H), 2.11-1.99 (m, 2H), 1.86-1.74 (m, 2H), 1.61 – 1.34 (m, 4H).

¹³C NMR (126 MHz, CDCl₃): δ 208.92, 174.47, 133.01, 132.85, 131.09, 128.75, 51.81, 49.06, 46.71, 42.97, 26.31, 26.02, 23.98, 23.64.

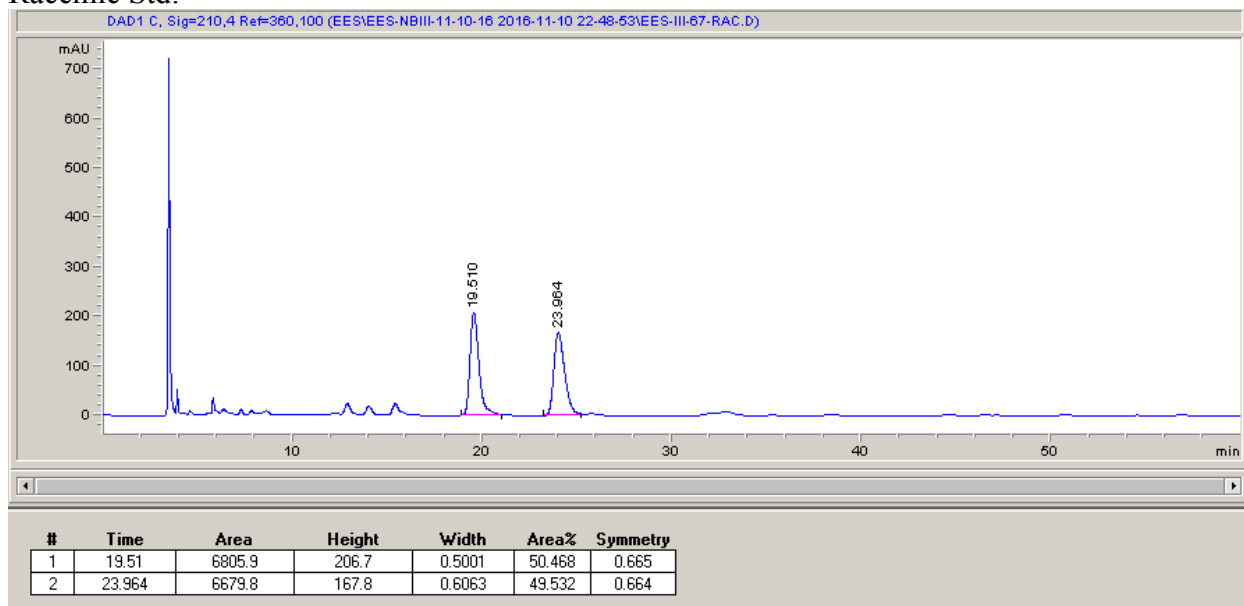
HRMS: 2932, 2857, 1701, 1492, 1449, 1409, 1364, 1219, 1089, 1014, 799, 739.

IR (ATR, cm⁻¹): (ESI-TOF) calculated for ([C₁₅H₁₈ClO₃ + H]⁺): 281.0939, found 281.0933.

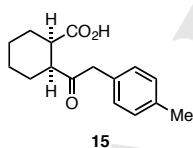
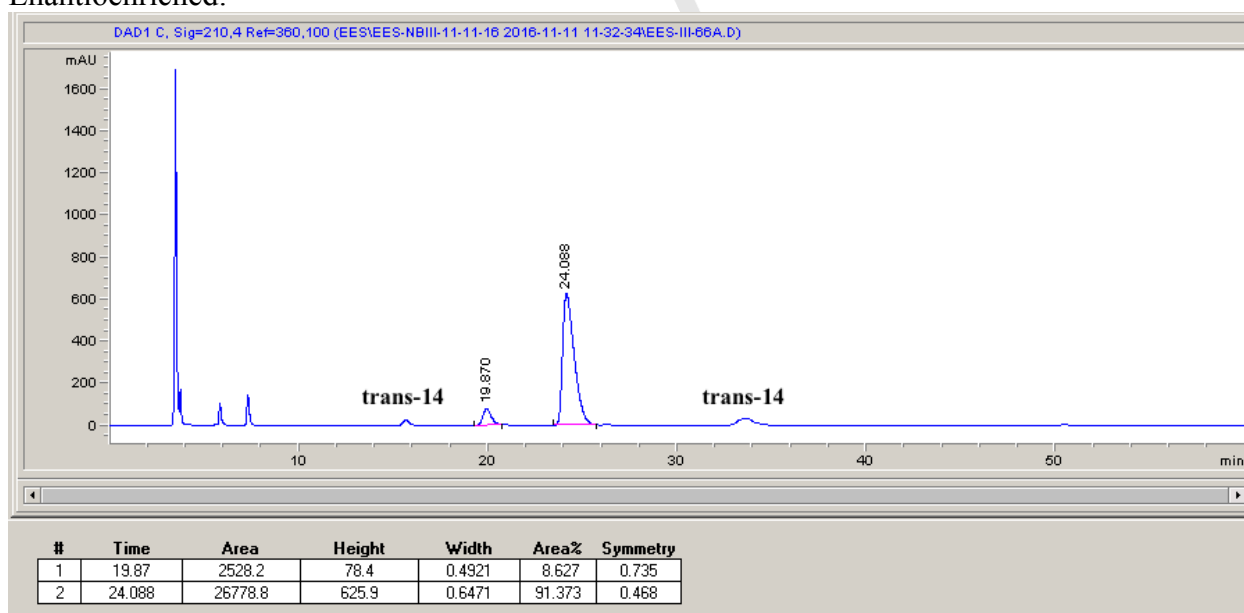
Optical Rotation: [α]_D²⁶ -36.7 (*c* 0.64, CHCl₃).

HPLC: ChiralPak[®] IC, 5% IPA in Hexanes, 60 min run, 1 mL/min.

Racemic Std:



Enantioenriched:



According to general procedure **A**, anhydride **1** (38.5 mg, 0.25 mmol) and benzyl trifluoroborate **15-B** (63.6 mg, 0.3 mmol) afforded the product as a pale yellow oil (55.3 mg, 85% yield, 85% ee, >20:1 dr). Run 2 afforded 85% yield, 85% ee, >20:1 dr. NMR data based on methyl ester.

^1H NMR (501 MHz, CDCl_3): δ 7.12 (d, $J = 7.5$ Hz, 2H), 7.07 (d, $J = 8.1$ Hz, 2H), 3.75 (s, 2H), 3.61 (s, 3H), 2.90 (t, $J = 3.8$ Hz, 1H), 2.82 – 2.74 (m, 1H), 2.32 (s, 3H), 2.12 – 1.98 (m, 2H), 1.85–1.73 (m, 2H), 1.56 (dt, $J = 12.3, 3.4$ Hz, 1H), 1.41 (dddd, $J = 17.7, 15.4, 8.4, 4.3$ Hz, 3H).

^{13}C NMR (126 MHz, CDCl_3): δ 209.59, 174.51, 136.50, 131.49, 129.51, 129.37, 51.72, 48.83, 47.16, 42.79, 26.26, 26.08, 23.99, 23.67, 21.23.

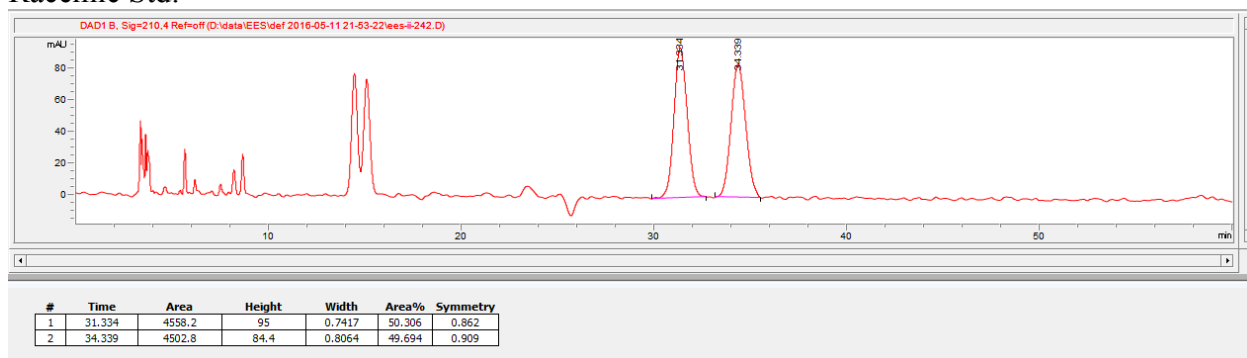
HRMS: (ESI-TOF) calculated for $([\text{C}_{16}\text{H}_{20}\text{O}_3 + \text{Na}]^+)$: 283.1305, found 283.1301.

IR (ATR, cm^{-1}): 2934, 2958, 1737, 1701, 1515, 1450, 1418, 1367, 1264, 1217, 1020, 732, 702.

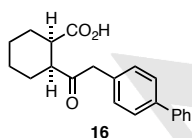
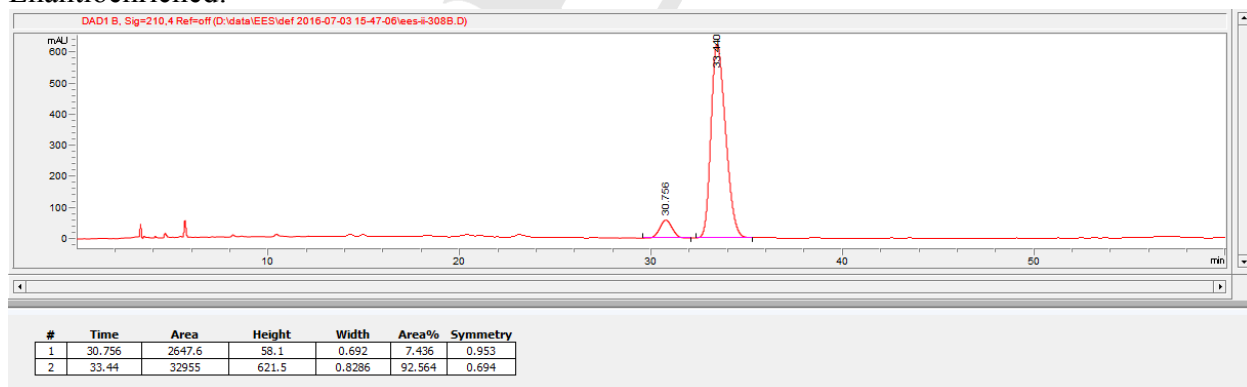
Optical Rotation: $[\alpha]_{\text{D}}^{26}$ -51.7 (c 0.83, CHCl_3).

HPLC: ChiralPak[®] IC, 5% IPA (1% TFA) in Hexanes, 60 min run, 1 mL/min.

Racemic Std:



Enantioenriched:



According to general procedure **A**, anhydride **1** (38.5 mg, 0.25 mmol) and benzyl trifluoroborate **16-B** (82.2 mg, 0.3 mmol) afforded the product as a pale yellow oil (69.4 mg, 86% yield, 84% ee, >20:1 dr). Run 2 afforded 81% yield, 81% ee, >20:1 dr. NMR data based on methyl ester.

^1H NMR (501 MHz, CDCl_3): δ 7.60 – 7.53 (m, 4H), 7.43 (dd, J = 8.4, 7.0 Hz, 2H), 7.36 – 7.31 (m, 1H), 7.29 – 7.24 (m, 2H), 3.85 (s, 2H), 3.62 (s, 3H), 2.94 (d, J = 6.8 Hz, 1H), 2.87 – 2.79 (m, 1H), 2.09 (tdd, J = 13.8, 6.1, 3.6 Hz, 2H), 1.89–1.76 (m, 2H), 1.65 – 1.45 (m, 2H), 1.46 – 1.36 (m, 2H).

^{13}C NMR (126 MHz, CDCl_3): δ 209.39, 174.52, 141.02, 139.87, 133.64, 130.12, 128.87, 127.41, 127.33, 127.20, 51.78, 49.02, 47.16, 42.90, 26.30, 26.10, 24.01, 23.67.

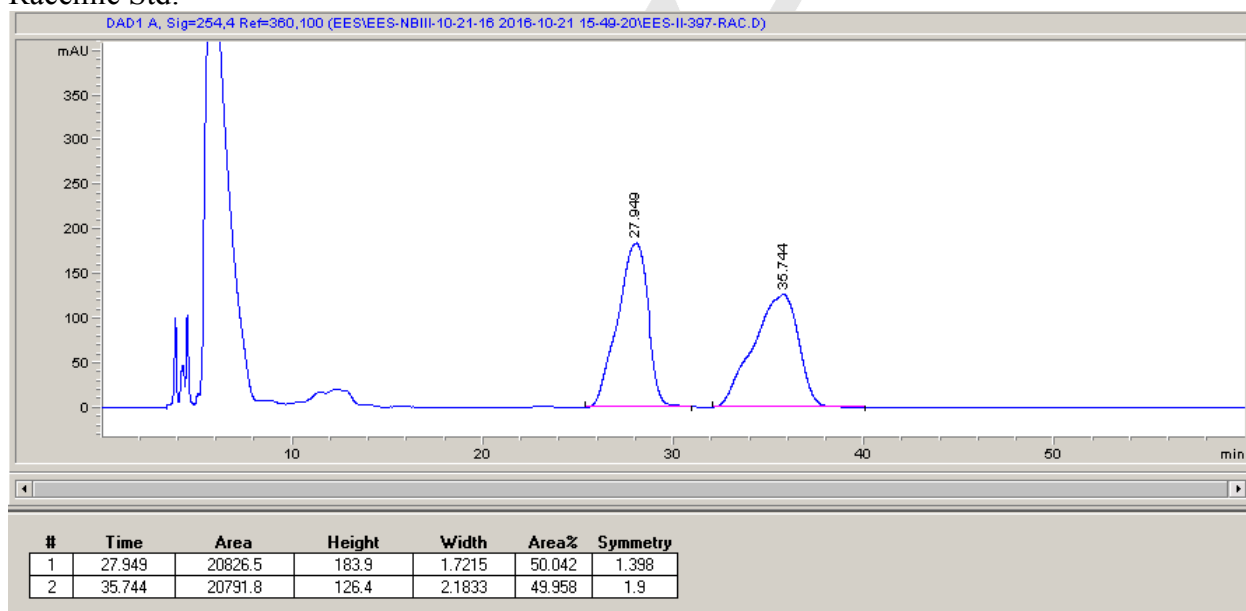
HRMS: (ESI-TOF) calculated for $([\text{C}_{21}\text{H}_{23}\text{O}_3 + \text{H}]^+)$: 323.1642, found 323.1640.

IR (ATR, cm^{-1}): 3229, 2933, 2857, 1701, 1487, 1449, 1207, 1007, 843, 759, 697.

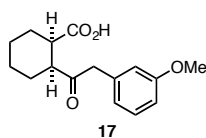
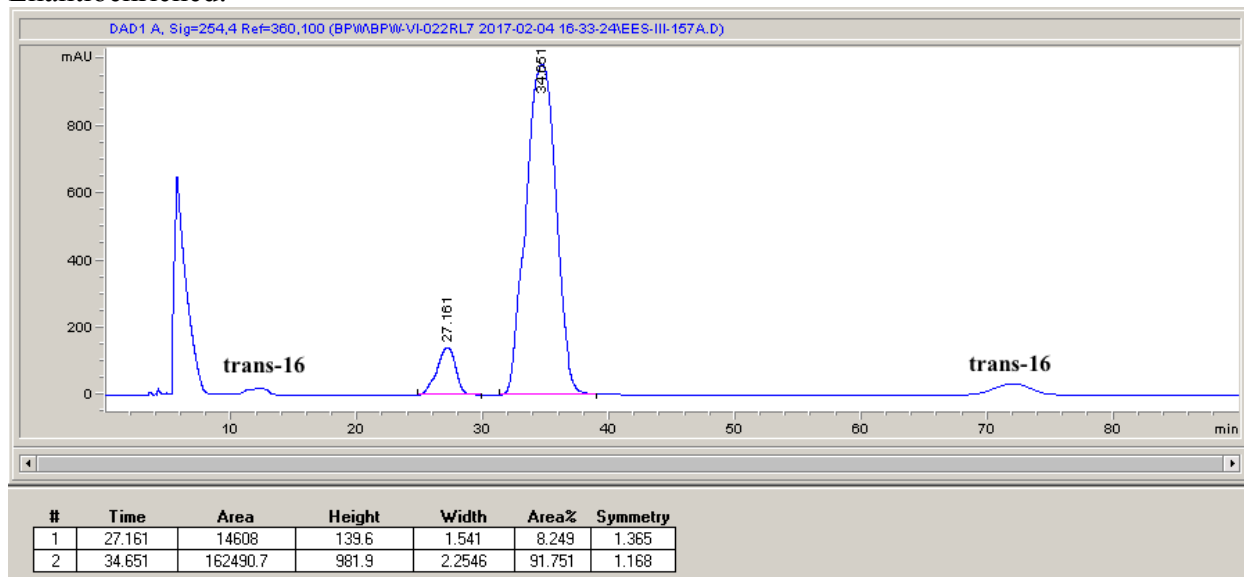
Optical Rotation: $[\alpha]_{\text{D}}^{26}$ -36.1 (c 0.68, CHCl_3).

HPLC: ChiralPak[®] IC, 10% IPA in Hexanes, 60 min run, 1 mL/min (sample prep in HPLC grade acetone).

Racemic Std:



Enantioenriched:



According to general procedure **A**, anhydride **1** (38.5 mg, 0.25 mmol) and benzyl trifluoroborate **17-B** (68.4 mg, 0.3 mmol) afforded the product as a pale yellow oil (60.8 mg, 88% yield, 90% ee, 12:1 dr). Run 2 afforded 83% yield, 88% ee, 10.5:1 dr. NMR data based on methyl ester. Diastereoselectivity based on ^1H NMR in acetone- d_6 .

^1H NMR (501 MHz, CDCl_3): δ 7.23 (t, $J = 7.9$ Hz, 1H), 6.81 – 6.76 (m, 2H), 6.74 (t, $J = 2.1$ Hz, 1H), 3.79 (s, 3H), 3.76 (s, 2H), 3.61 (s, 3H), 2.96 – 2.86 (m, 1H), 2.82 – 2.75 (m, 1H), 2.14 – 1.96 (m, 2H), 1.84–1.73(m, 2H), 1.62 – 1.51 (m, 1H), 1.51 – 1.33 (m, 3H).

^{13}C NMR (126 MHz, CDCl_3): δ 209.29, 174.49, 159.79, 136.04, 129.61, 122.02, 115.29, 112.41, 55.31, 51.72, 48.88, 47.59, 42.80, 26.25, 26.06, 23.96, 23.65.

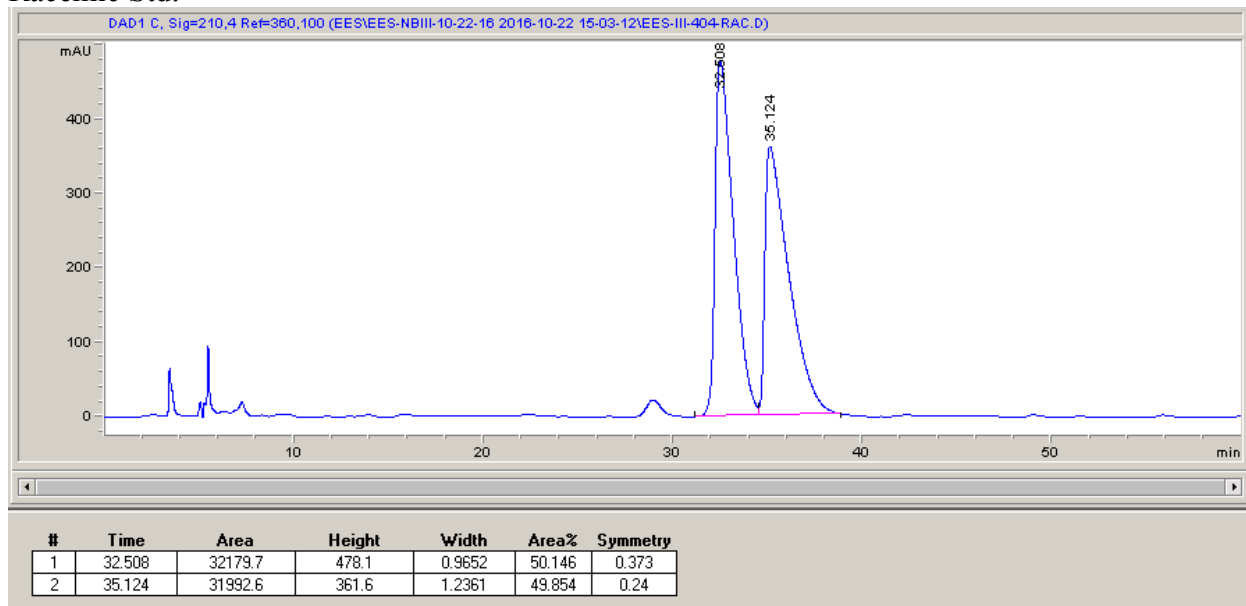
HRMS: (ESI-TOF) calculated for $([\text{C}_{16}\text{H}_{20}\text{O}_4 - \text{H}]^-)$: 275.1289, found: 275.1295.

IR (ATR, cm^{-1}): 3306, 2936, 2857, 1707, 1600, 1490, 1453, 1367, 1257, 1217, 1043, 775, 691.

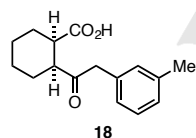
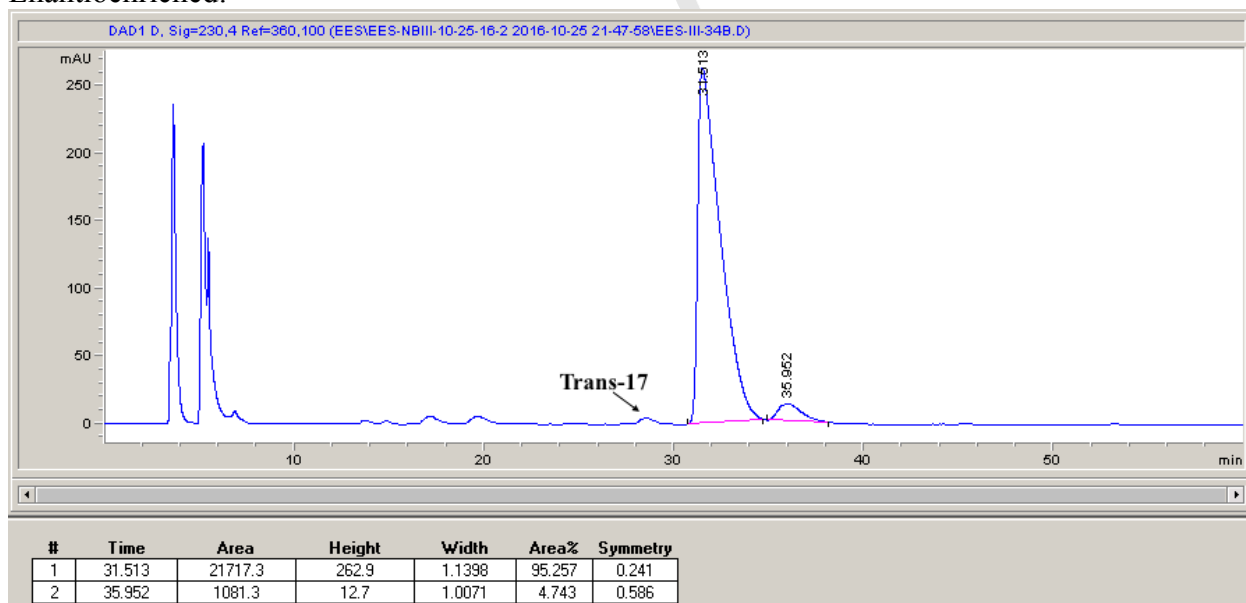
Optical Rotation: $[\alpha]_{\text{D}}^{26} -60.7$ (c 0.78, acetone).

HPLC: ChiralPak[®] ID, 5% IPA in Hexanes, 60 min run, 1 mL/min (sample prep in HPLC grade acetone).

Racemic Std:



Enantioenriched:



According to general procedure **A**, anhydride **1** (38.5 mg, 0.25 mmol) and benzyl trifluoroborate **18-B** (63.6 mg, 0.3 mmol) afforded the product as a pale yellow oil (60.6 mg, 93% yield, 87% ee, 10.3:1 dr). Run 2 afforded 75% yield, 84% ee, 12.6:1 dr. NMR data based on methyl ester.

^1H NMR (501 MHz, CDCl_3): δ 7.20 (t, $J = 7.5$ Hz, 1H), 7.06 (d, $J = 7.6$ Hz, 1H), 7.03 – 6.96 (m, 2H), 3.76 (s, 2H), 3.61 (s, 3H), 2.90 (t, $J = 5.9$ Hz, 1H), 2.83 – 2.74 (m, 1H), 2.33 (s, 3H),

2.13 – 1.99 (m, 2H), 1.85-1.73 (m, 2H), 1.57 (ddd, $J = 16.3, 7.9, 3.8$ Hz, 1H), 1.50 – 1.34 (m, 3H).

^{13}C NMR (126 MHz, CDCl_3): δ 209.52, 174.51, 138.24, 134.44, 130.42, 128.53, 127.69, 126.66, 51.72, 48.90, 47.48, 42.79, 26.27, 26.07, 23.98, 23.66, 21.53.

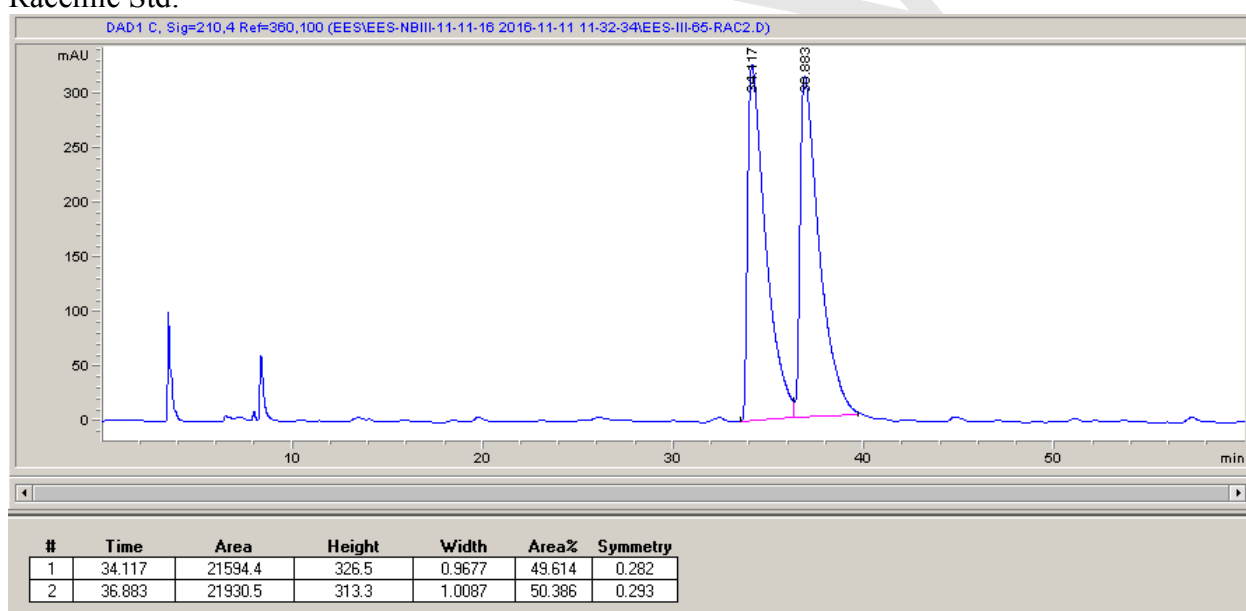
HRMS: (ESI-TOF) calculated for $([\text{C}_{16}\text{H}_{20}\text{O}_3 + \text{Na}]^+)$: 283.1305, found 283.1303.

IR (ATR, cm^{-1}): 3022, 2930, 2856, 1698, 1608, 1489, 1449, 1257, 1219, 914, 771, 703.

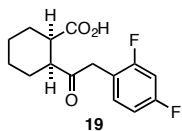
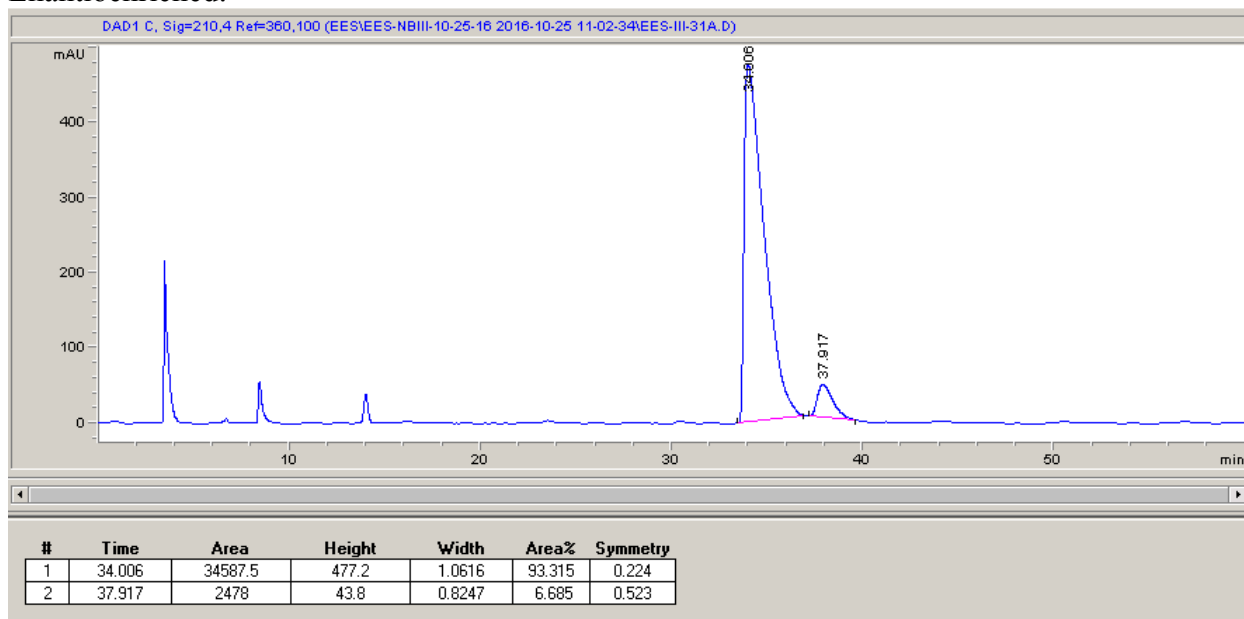
Optical Rotation: $[\alpha]_{\text{D}}^{26} -42.6$ (c 0.60, CHCl_3).

HPLC: ChiralPak[®] ID, 2% IPA in Hexanes, 60 min run, 1 mL/min.

Racemic Std:



Enantioenriched:



According to general procedure **A**, anhydride **1** (38.5 mg, 0.25 mmol) and benzyl trifluoroborate **19-B** (70.2 mg, 0.3 mmol) afforded the product as a pale yellow oil (52.8 mg, 75% yield, 86% ee, 6:1 dr). Run 2 afforded 79% yield, 84% ee, 11.8:1 dr. NMR data based on methyl ester.

¹H NMR (501 MHz, CDCl₃): δ 7.14 (td, $J = 8.4, 6.4$ Hz, 1H), 6.87 – 6.77 (m, 2H), 3.88 – 3.74 (m, 2H), 3.63 (s, 3H), 2.98 – 2.88 (m, 1H), 2.84 (dd, $J = 7.7, 4.3$ Hz, 1H), 2.07 (dddd, $J = 21.3, 14.6, 8.0, 3.7$ Hz, 2H), 1.88 (td, $J = 8.7, 4.2$ Hz, 1H), 1.78 (td, $J = 8.4, 3.9$ Hz, 1H), 1.62 – 1.37 (m, 4H).

¹³C NMR (126 MHz, CDCl₃): Inseparable mixture of diastereomers. See spectrum for details.

¹⁹F NMR (282 MHz, CDCl₃): δ -111.95, -113.27.

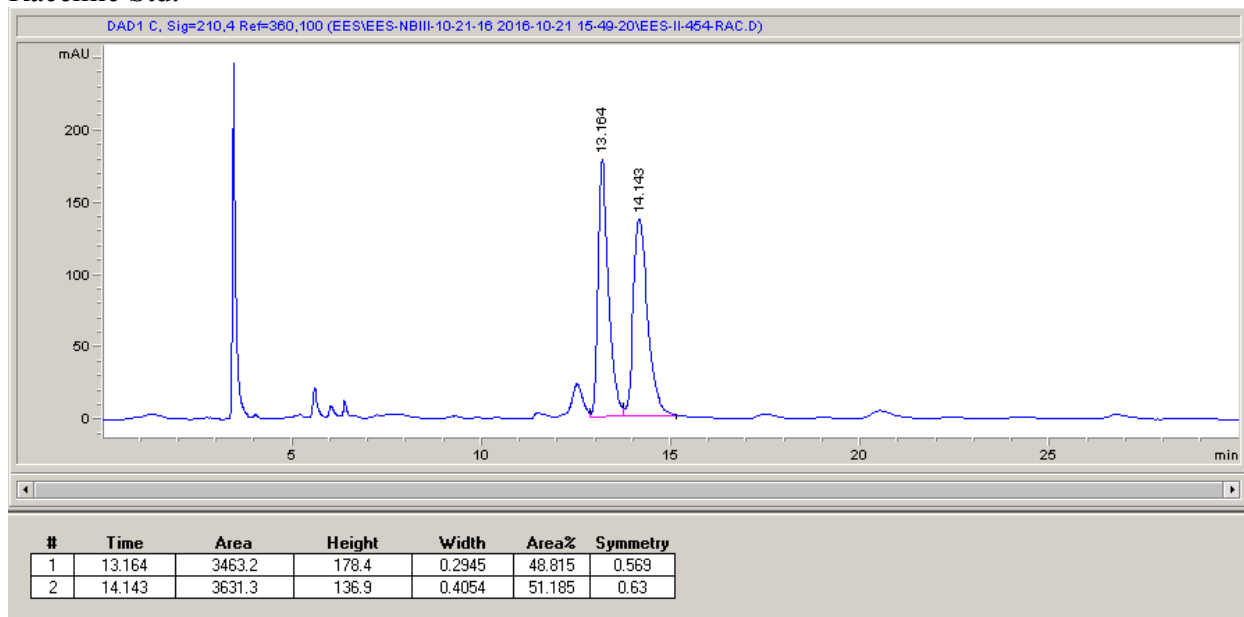
HRMS: (ESI-TOF) calculated for ([C₁₅H₁₆F₂O₃ + Na]⁺): 305.0960, found 305.0955.

IR (ATR, cm⁻¹): 3019, 2970, 1740, 1438, 1368, 1228, 1217, 1091, 901.

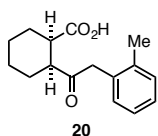
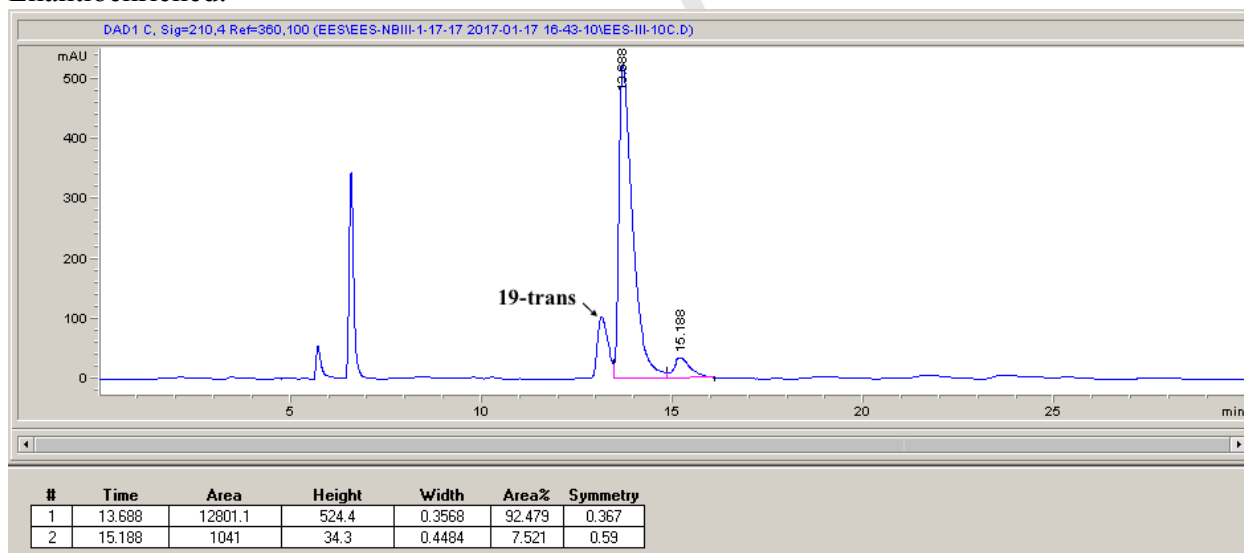
Optical Rotation: $[\alpha]_D^{26}$ -15.5 (c 0.79, acetone).

HPLC: ChiralPak[®] ID, 5% IPA in Hexanes, 30 min run, 1 mL/min.

Racemic Std:



Enantioenriched:



According to general procedure **A**, anhydride **1** (38.5 mg, 0.25 mmol) and *ortho*-methylbenzyl trifluoroborate **20-B** (63.6 mg, 0.3 mmol) afforded the product as a pale yellow oil (51.0 mg, 78% yield, 76% ee, 6.4:1 dr). Run 2 afforded 87% yield, 74% ee, 5.7:1 dr. NMR data based on methyl ester.

^1H NMR (501 MHz, CDCl_3): δ 7.21 – 7.12 (m, 3H), 7.11 – 7.06 (m, 1H), 3.82 (s, 2H), 3.62 (s, 3H), 3.01 – 2.90 (m, 1H), 2.80 – 2.73 (m, 1H), 2.22 (s, 3H), 2.17 – 2.00 (m, 2H), 1.89 – 1.72 (m, 2H), 1.67 – 1.54 (m, 1H), 1.53 – 1.42 (m, 2H), 1.36–1.42 (m, 1H).

^{13}C NMR (126 MHz, CDCl_3): Inseparable mixture of diastereomers. See spectrum for details.

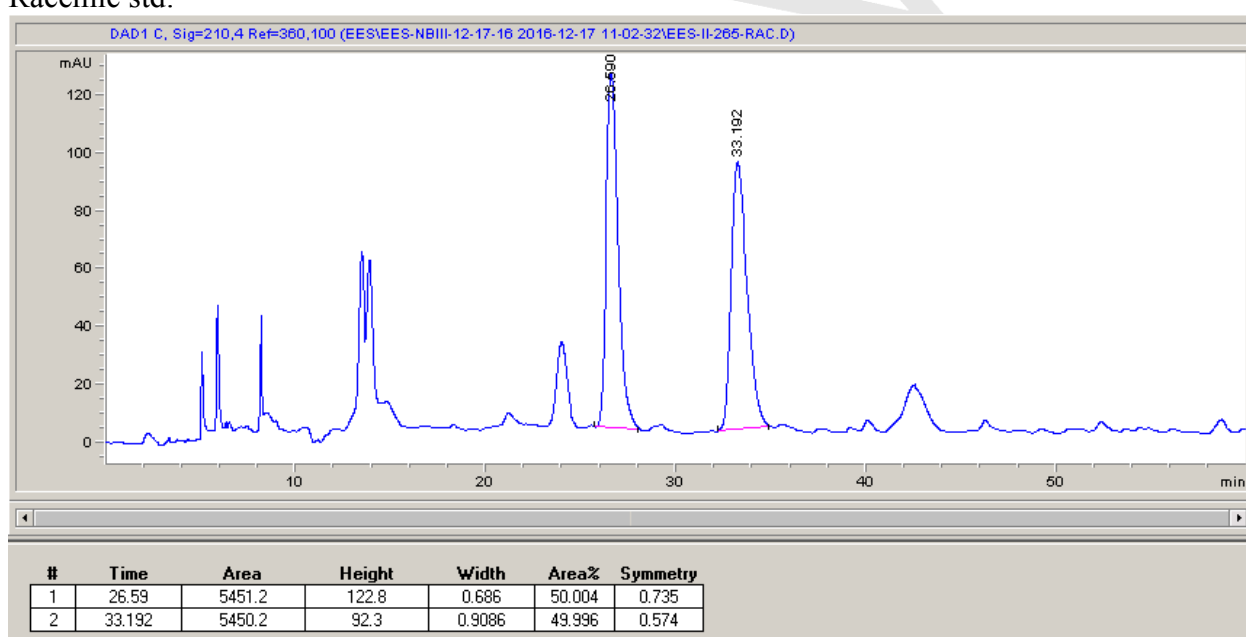
HRMS: (ESI-TOF) calculated for $([\text{C}_{16}\text{H}_{21}\text{O}_3 + \text{Na}]^+)$: 261.1485, found 261.1483.

IR (ATR, cm^{-1}): 3017, 2933, 2858, 1706, 1495, 1449, 1417, 1361, 1219, 1078, 897, 743, 689.

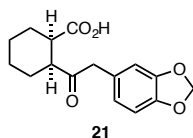
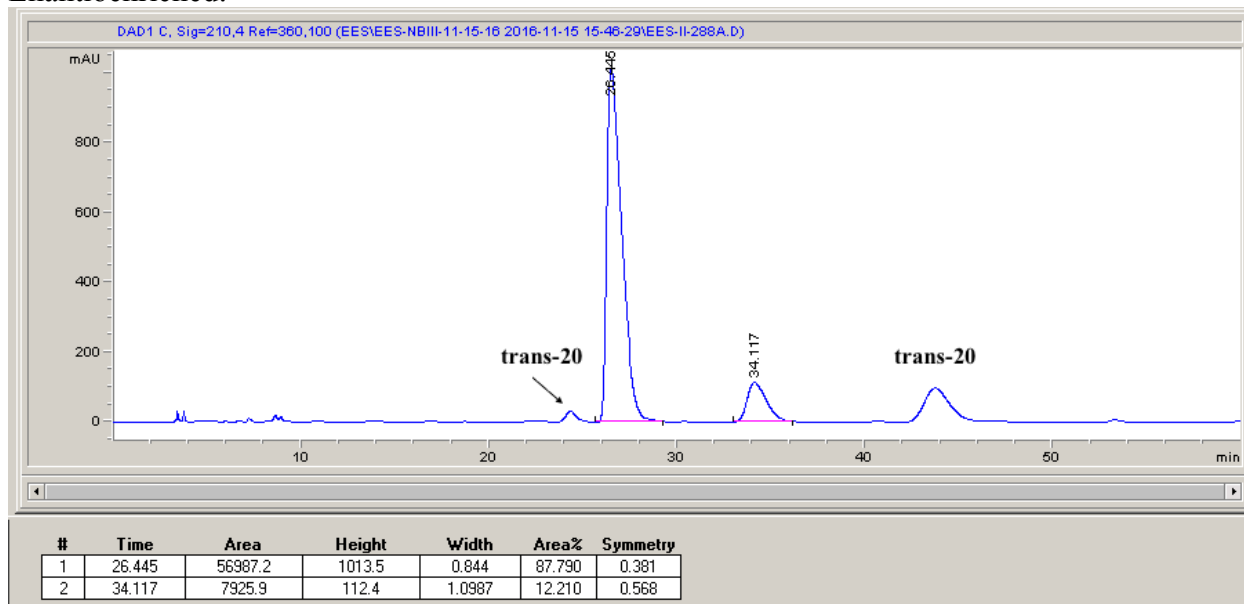
Optical Rotation: $[\alpha]_{\text{D}}^{26}$ -40.0 (c 0.74, CHCl_3).

HPLC: ChiralPak[®] IC, 5% IPA in Hexanes, 60 min run, 1 mL/min.

Racemic std:



Enantioenriched:



According to general procedure **A**, anhydride **1** (38.5 mg, 0.25 mmol) and benzyl trifluoroborate **21-B** (72.6 mg, 0.3 mmol) afforded the product as a pale yellow oil (64.3 mg, 89% yield, 75% ee, >20:1 dr). Run 2 afforded 89% yield, 65% ee, >20:1 dr. NMR data based on methyl ester.

¹H NMR (501 MHz, CDCl₃): δ 6.75 (d, *J* = 7.9 Hz, 1H), 6.68 (d, *J* = 1.7 Hz, 1H), 6.62 (dd, *J* = 7.9, 1.7 Hz, 1H), 5.93 (s, 2H), 3.71 (ABq, *J* = 15.0 Hz, Δ*v* = 13.2 Hz, 2H), 3.62 (s, 3H), 2.89 (q, *J* = 5.5 Hz, 1H), 2.79 (dt, *J* = 8.6, 4.6 Hz, 1H), 2.08 (dtd, *J* = 13.4, 7.9, 3.6 Hz, 1H), 2.01 (ddt, *J* = 14.4, 7.4, 3.8 Hz, 1H), 1.82 (ddt, *J* = 13.3, 8.6, 4.5 Hz, 1H), 1.75 (ddt, *J* = 12.6, 7.9, 4.2 Hz, 1H), 1.61 – 1.50 (m, 1H), 1.52 – 1.33 (m, 3H).

¹³C NMR (126 MHz, CDCl₃): δ 209.56, 174.51, 147.83, 146.58, 128.17, 122.73, 110.12, 108.42, 101.08, 51.77, 48.81, 47.12, 42.88, 26.28, 26.07, 23.98, 23.66.

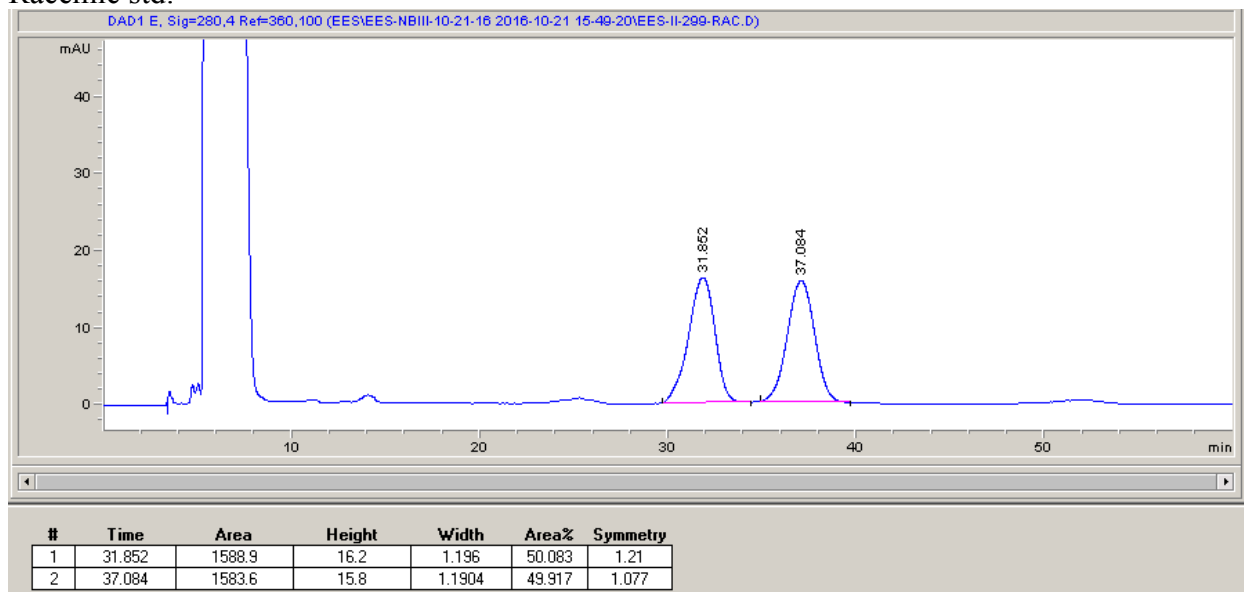
HRMS: (ESI-TOF) calculated for ([C₁₆H₁₈O₅ + Na]⁺): 313.1046, found 313.1044.

IR (ATR, cm⁻¹): 2933, 2858, 1736, 1699, 1503, 1489, 1443, 1364, 1245, 1037, 928, 811, 735.

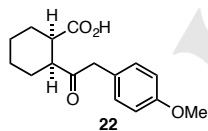
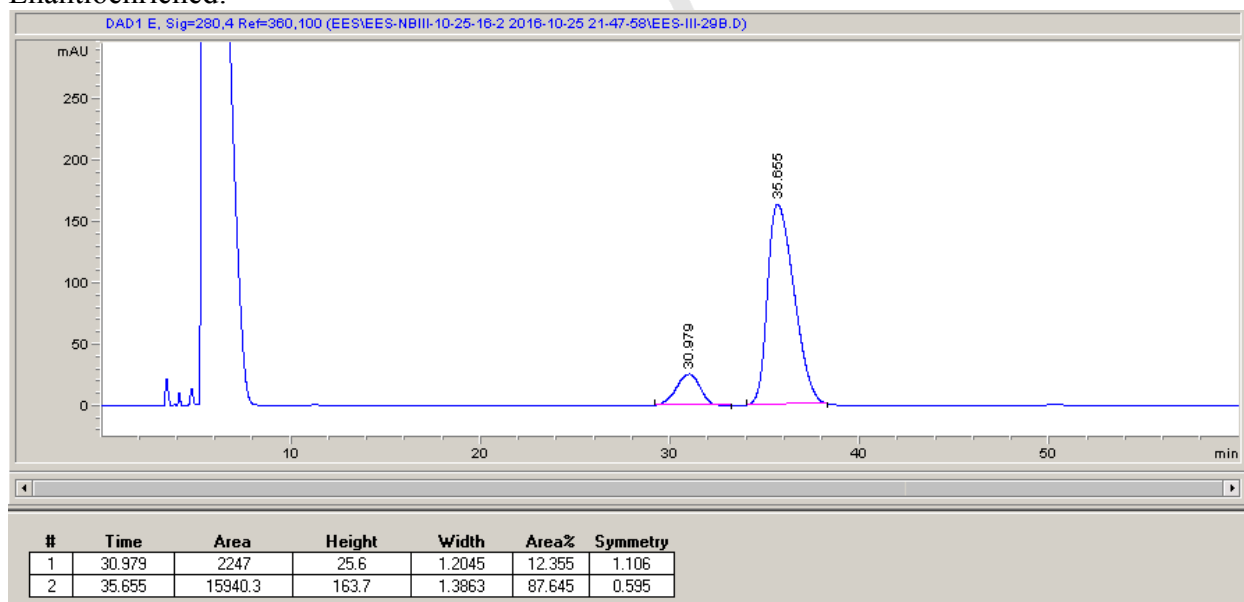
Optical Rotation: [α]_D²⁶ -31.3 (*c* 0.65, CHCl₃).

HPLC: ChiralPak[®] IC, 10% IPA in Hexanes, 60 min run, 1 mL/min (sample prep in HPLC grade acetone).

Racemic std:



Enantioenriched:



According to general procedure **B**, anhydride **1** (38.5 mg, 0.25 mmol) and benzyl trifluoroborate **22-B** (68.4 mg, 0.3 mmol) afforded the product as a pale yellow oil (58.7 mg, 85% yield, 94% ee, >20:1 dr). Run 2 afforded 95% yield, 94% ee, >20:1 dr. NMR data based on methyl ester.

^1H NMR (501 MHz, CDCl_3): δ 7.03 (d, J = 8.1 Hz, 2H), 6.83 – 6.76 (m, 2H), 3.72 (s, 3H), 3.66 (s, 2H), 3.54 (s, 3H), 2.89 – 2.78 (m, 1H), 2.75 – 2.67 (m, 1H), 2.07 – 1.85 (m, 2H), 1.85 – 1.60 (m, 2H), 1.58 – 1.44 (m, 1H), 1.44 – 1.24 (m, 3H).

^{13}C NMR (126 MHz, CDCl_3): δ 209.78, 174.54, 158.59, 130.65, 126.63, 114.11, 55.39, 51.74, 48.79, 46.65, 42.82, 26.27, 26.08, 24.00, 23.66.

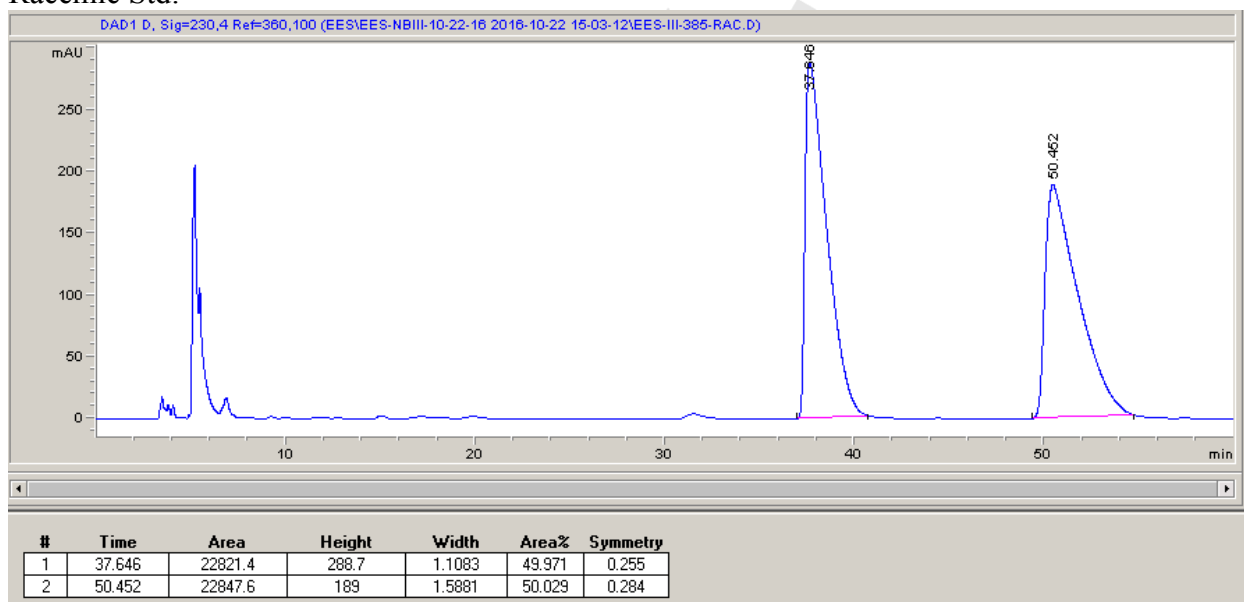
HRMS: (ESI-TOF) calculated for $([\text{C}_{16}\text{H}_{20}\text{O}_4 - \text{H}]^-)$: 275.1289, found: 275.1287.

IR (ATR, cm^{-1}): 2934, 2855, 1736, 1612, 1513, 1450, 1368, 1229, 1217, 1033, 800.

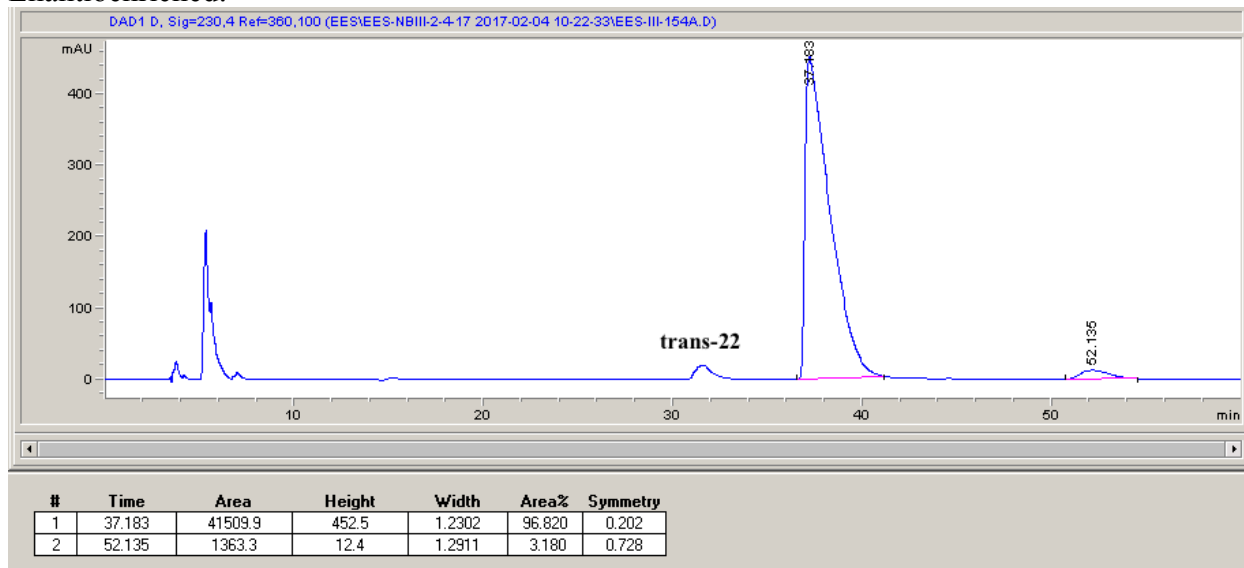
Optical Rotation: $[\alpha]_{\text{D}}^{26}$ -27.5 (c 0.63, CHCl_3).

HPLC: ChiralPak[®] ID, 5% IPA in Hexanes, 60 min run, 1 mL/min (sample prep in HPLC grade acetone).

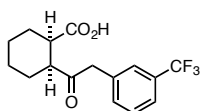
Racemic Std:



Enantioenriched:



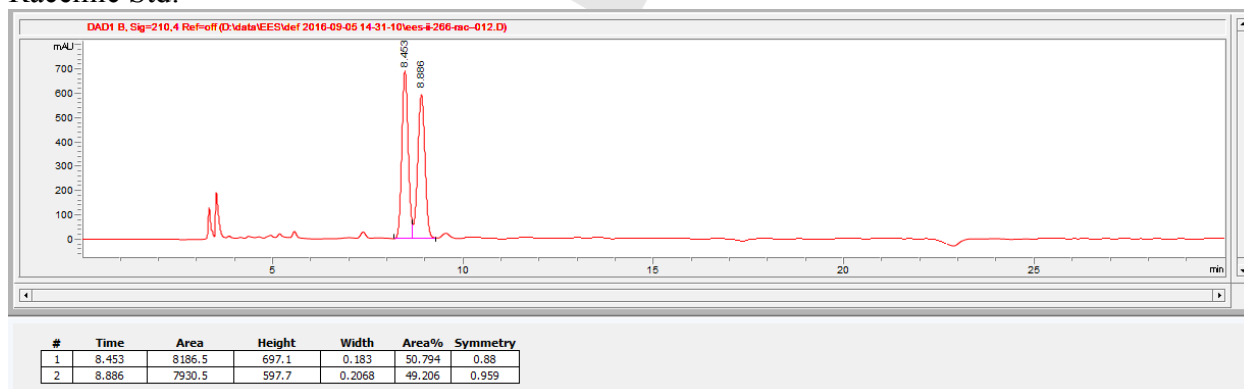
Additional substrates not included in the publication:



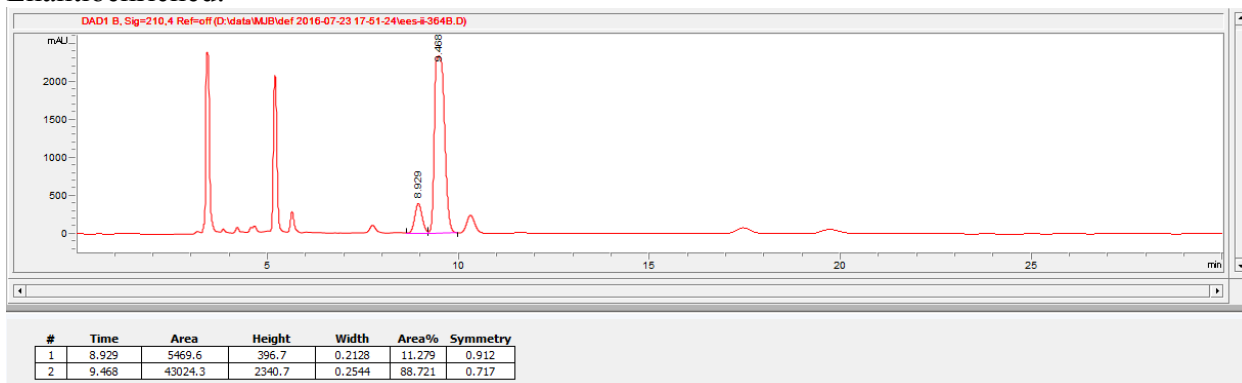
According to general procedure A, anhydride **1** (38.5 mg, 0.25 mmol) and benzyl trifluoroborate **26-B** (79.8 mg, 0.3 mmol) afforded the product as a pale yellow oil (31.6 mg, 40% yield, 75% ee, 7.3:1 dr). Run 2 afforded 37% yield, 77% ee, 7.3:1 dr.

HPLC: ChiralPak[®] IC, 5% IPA in Hexanes, 60 min run, 1 mL/min.

Racemic Std:



Enantioenriched:



IV. Trifluoroborate Preparation and Characterization

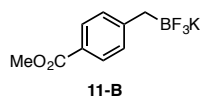
General procedure A for trifluoroborate preparation:⁵ An oven-dried 3-neck round bottom flask fitted with a reflux condenser was charged with magnesium, and the magnesium was activated by stirring under N₂ overnight. Benzyl bromide (3.00 mmol) in diethyl ether (6.5 mL) was added to the magnesium at a rate maintaining a gentle reflux. The suspension was refluxed for a further 3 h, then cooled to room temp. To a separate flame-dried flask was added trimethyl borate (0.502 mL, 4.50 mmol) and THF (6.0 mL) under N₂. The flask was cooled to -78 °C, at which point the Grignard reagent was added dropwise at -78 °C. The reaction was stirred for 1 h at -78 °C, then slowly warmed to room temperature over 1 h. The reaction was then cooled to 0 °C, and MeOH (4.0 mL) was added over 5 min. The flask was opened to air, and a solution of KHF₂ (1.41 g, 18.0 mmol) was added in H₂O (4.0 mL) at 0 °C over 15 min. The reaction was stirred an additional 30 min at 0 °C, then warmed to room temperature and stirred for an additional hour. The solvent was removed, and then the remaining water was removed by azeotrope with toluene. The residue was dried under high vacuum overnight. (*Note: Important to have the residue completely dry, any remaining water made precipitation difficult and could affect purity.) The solid was pulverized with a spatula, then washed in hot acetone and filtered through celite (3 x 30 mL). The filtrate was concentrated, then taken up in a minimal amount of diethyl ether (~10 mL) and CH₂Cl₂ (~5 mL). Hexanes (~200 mL) was added and the product flocculated out of solution. The solid was collected by vacuum filtration, then washed with hexanes (~20 mL) and CH₂Cl₂ (~10 mL) and dried to afford a white powder. Refer to each individual entry for further purification.

General procedure B for trifluoroborate preparation:⁶ A 20 mL reaction vial was charged with benzyl bromide (5.00 mmol), copper iodide (95.2 mg, 0.500 mmol), PPh₃ (170 mg, 0.650 mmol), lithium methoxide (380 mg, 10.0 mmol), and B₂Pin₂ (1.93g, 7.60 mmol) and a stir bar. The reaction vial was fitted with a septa cap and evacuated and backfilled with N₂ five times. DMF (10.0 mL) was added, and the reaction was sealed with electrical tape. The mixture was stirred vigorously at room temperature for 20 h. The reaction vial was uncapped, then filtered through a plug of silica with EtOAc. The solvent was removed, then EtOAc (~20 mL) and MeOH (~30 mL) were added, and the reaction was cooled to 0 °C under air. KHF₂ (2.42 g, 30.0 mmol) in H₂O (6.67 mL) was added over 15 min at 0 °C. The reaction was stirred an additional 30 min at 0 °C, then warmed to room temp and stirred for 1h. The solvent was removed, then pinacol and water were azeotroped with toluene several times. The residue was placed under high vacuum overnight. (*Note: Important to have the residue completely dry, any remaining DMF or water made precipitation difficult and could affect purity.) The solid was pulverized with a spatula, then washed in hot acetone (3 x 35 mL) and filtered through celite. The filtrate was concentrated to ~10 mL acetone, then precipitated with hexanes or pentane (~200 mL). The solid was filtered and dried to afford a white powder. Refer to each individual entry for further purification.

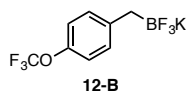
⁵ P. Jain, S. Yi, P. T. Flaherty, *J. Heterocyclic Chem.* **2013**, *50*, E166-E173.

⁶ J. C. Tellis, D. N. Primer, G. A. Molander, *Science* **2014**, *345*, 433-436.

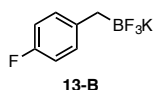
General procedure C for trifluoroborate preparation:⁶ An oven dried flask was charged with benzyl bromide (5.00 mmol), Pd(dba)₂ (86.3 mg, 0.150 mmol), P(*p*-tol)₃ (91.3 mg, 0.300 mmol), KOAc (736 mg, 7.50 mmol), and B₂Pin₂ (1.40 g, 5.50 mmol). The flask was evacuated and backfiled with N₂ (3x). Toluene (31.3 mL) was added, and the suspension was heated to 50 °C for 24h. Upon cooling, the reaction was filtered through a silica plug with EtOAc, then the solvent removed. Then EtOAc (~20 mL) and MeOH (~30 mL) were added, and the reaction was cooled to 0 °C under air. KHF₂ (2.42 g, 30.0 mmol) in H₂O (6.67 mL) was added over 15 min at 0 °C. The reaction was stirred an additional 30 min at 0 °C, then warmed to room temp and stirred for 1h. The solvent was removed, then pinacol and water were azeotroped with toluene several times. The residue was placed under high vacuum overnight. (*Note: Important to have the residue completely dry, any remaining water made precipitation difficult and could affect purity.) The solid was pulverized with a spatula, then washed in hot acetone (3 x 35 mL) and filtered through celite. The filtrate was concentrated to ~10 mL acetone, then precipitated with hexanes or pentane (~200 mL). The solid was filtered and dried to afford a white powder. Refer to each individual entry for further purification.³



According to general procedure C. 825 mg, 64% yield. No further purification necessary. Characterization data matched literature values.⁶



According to general procedure A. 700 mg, 50% yield. No recrystallization performed. Characterization data matched literature values.⁶



According to general procedure A. 317 mg, 49% yield. No further purification necessary.

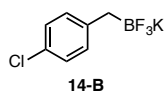
¹H NMR (501 MHz, Acetone-d₆): δ 7.08 (t, *J* = 6.9 Hz, 2H), 6.79 (t, *J* = 8.8 Hz, 2H), 1.61 (bs, 2H).

¹³C NMR (126 MHz, Acetone-d₆): δ 161.29, 159.51, 143.26, 130.63 (d, *J* = 8.2 Hz), 114.13 (d, *J* = 20.6 Hz).

¹¹B NMR (96 MHz, Acetone-d₆): δ 4.34 (q, *J* = 58.6 Hz)

HRMS: (ESI-TOF) calculated for ([C₇H₆BF₄]⁺): 177.0499, found 177.0505.

IR (ATR, cm⁻¹): 3041, 2915, 1600, 1503, 1244, 1217, 1086, 1066, 965, 932, 836, 779, 730, 692.



According to general procedure B. 942 mg, 81% yield. Recrystallized from isopropanol (1x) to afford a white powder.

$^1\text{H NMR}$ (501 MHz, Acetone- d_6): δ 7.07 (d, J = 8.2 Hz, 2H), 7.02 (d, J = 8.5 Hz, 2H), 1.60 (bs, 2H).

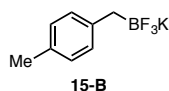
$^{13}\text{C NMR}$ (126 MHz, Acetone- d_6): δ 147.14, 131.31, 128.03, 127.64

$^{19}\text{F NMR}$ (282 MHz, Acetone- d_6): δ -139.16 (q, J = 59.2 Hz)

$^{11}\text{B NMR}$ (96 MHz, Acetone- d_6): δ 4.46 (q, J = 58.6 Hz)

HRMS: (ESI-TOF) calculated for ($[\text{C}_7\text{H}_6\text{BClF}_3]^-$): 193.0203, found 193.0201.

IR (ATR, cm^{-1}): 2895, 1488, 1240, 1092, 1064, 967, 834, 775, 726, 656.



According to general procedure A. 517 mg, 49% yield. No further purification necessary.

$^1\text{H NMR}$ (501 MHz, Acetone- d_6): δ 6.98 (d, J = 7.6 Hz, 2H), 6.85 (d, J = 7.5 Hz, 2H), 2.19 (s, 3H), 1.58 (bs, 2H).

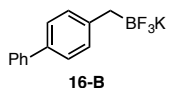
$^{13}\text{C NMR}$ (126 MHz, Acetone- d_6): δ 144.74, 131.53, 129.67, 128.57, 21.03.

$^{19}\text{F NMR}$ (282 MHz, Acetone- d_6): δ -140.78 (q, J = 64.9 Hz)

$^{11}\text{B NMR}$ (96 MHz, Acetone- d_6): δ 4.85 (q, J = 59.5 Hz)

HRMS: (ESI-TOF) calculated for ($[\text{C}_8\text{H}_9\text{BF}_3]^-$): 173.0749, found 173.0750.

IR (ATR, cm^{-1}): 3020, 2901, 1609, 1509, 1364, 1244, 1099, 1065, 949, 774, 731.



According to general procedure B. 703 mg, 51% yield. Recrystallized from EtOH (3x) to afford a white solid with a cotton-like consistency (very small needles).

$^1\text{H NMR}$ (501 MHz, Acetone- d_6): δ 7.58 (d, J = 7.7 Hz, 2H), 7.44 – 7.32 (m, 4H), 7.25 (t, J = 7.4 Hz, 1H), 7.19 (d, J = 7.7 Hz, 2H), 1.68 (s, 2H).

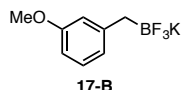
^{13}C NMR (126 MHz, Acetone- d_6): δ 147.84, 142.89, 135.68, 130.24, 129.48, 127.26, 127.05, 126.43.

^{19}F NMR (282 MHz, Acetone- d_6): δ -140.57 (q, J = 64.9 Hz)

^{11}B NMR (96 MHz, Acetone- d_6): δ 4.76 (q, J = 56.6 Hz)

HRMS: (ESI-TOF) calculated for ($[\text{C}_{13}\text{H}_{11}\text{BF}_4]^-$): 235.0906, found 235.0909.

IR (ATR, cm^{-1}): 2970, 1612, 1484, 1368, 1231, 1217, 1097, 958, 940, 762, 739, 698.



According to general procedure B. 875 mg, 77% yield. Recrystallized from EtOH (slightly hazy solution filtered through standard filter paper before crystallizing) (1x) as needles.

^1H NMR (501 MHz, Acetone- d_6): δ 6.93 (t, J = 7.8 Hz, 1H), 6.70 – 6.60 (m, 2H), 6.45 (dd, J = 8.0, 2.6 Hz, 1H), 3.69 (s, 3H), 1.61 (s, 2H).

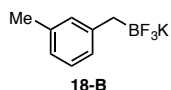
^{13}C NMR (126 MHz, Acetone- d_6): δ 160.01, 149.71, 128.48, 122.41, 115.34, 108.47, 54.99.

^{19}F NMR (282 MHz, Acetone- d_6): δ -140.53 (q, J = 67.7 Hz)

^{11}B NMR (96 MHz, Acetone- d_6): δ 4.39 (q, J = 56.6 Hz)

HRMS: (ESI-TOF) calculated for ($[\text{C}_8\text{H}_9\text{BF}_3\text{O}]^-$): 189.0699, found 189.0701.

IR (ATR, cm^{-1}): 2961, 1607, 1577, 1486, 1242, 1155, 1070, 1049, 974, 958, 773, 720.



According to general procedure B. 721 mg, 68% yield. Recrystallized from EtOH (slightly hazy solution filtered through standard filter paper before crystallizing) (1x) to afford a white solid with a cotton-like consistency.

^1H NMR (501 MHz, Acetone- d_6): δ 7.00 – 6.81 (m, 3H), 6.69 (d, J = 7.2 Hz, 1H), 2.20 (s, 3H), 1.60 (s, 2H).

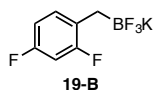
^{13}C NMR (126 MHz, Acetone- d_6): δ 147.83, 136.64, 130.60, 127.79, 126.87, 123.73, 21.65.

^{19}F NMR (282 MHz, Acetone- d_6): δ -140.61 (q, J = 62.0 Hz)

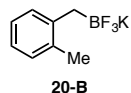
^{11}B NMR (96 MHz, Acetone- d_6): δ 4.50 (q, J = 58.6 Hz)

HRMS: (ESI-TOF) calculated for $[\text{C}_8\text{H}_9\text{BF}_3]^-$: 173.0749, found 173.0759.

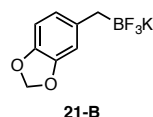
IR (ATR, cm^{-1}): 3015, 2921, 1602, 1364, 1259, 1225, 1064, 950, 776, 716.



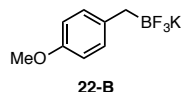
According to general procedure B. 884 mg, 76% yield. Recrystallized from EtOH (slightly hazy solution filtered through standard filter paper before crystallizing) (1x). Characterization data matched literature values.⁶



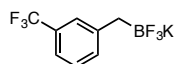
According to general procedure A. 340 mg, 32% yield. No further purification necessary. Characterization data matched literature values.⁶



According to general procedure C. 864 mg, 71% yield. Recrystallized from MeOH (slightly hazy solution filtered through standard filter paper before crystallizing) (1x) as needles. Characterization data matched literature values.⁶ Best if used immediately after purification to avoid decomposition.



According to general procedure B. 482 mg, 42% yield. Recrystallized from EtOH (1x) as plates. Characterization data matched literature values.⁶



^1H NMR (501 MHz, Acetone- d_6): δ 7.42 (s, 1H), 7.35 (d, J = 7.6 Hz, 1H), 7.23 (dd, J = 19.1, 7.7 Hz, 2H), 1.73 (s, 2H).

^{13}C NMR (126 MHz, Acetone- d_6): δ 149.91, 133.50, 128.37, 125.94, 119.56.

^{19}F NMR (282 MHz, Acetone- d_6): δ -62.69, -140.11 (q, J = 56.4 Hz).

^{11}B NMR (96 MHz, Acetone- d_6): δ 4.11 (q, J = 59.5 Hz)

V. Epimerization Studies

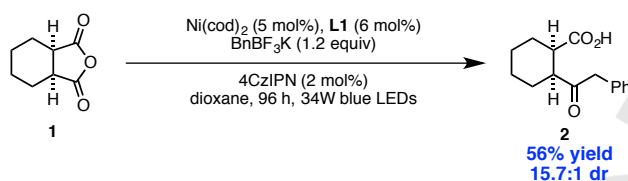


Figure S3. Extended reaction time. Even with extended reaction times, there is no significant additional epimerization observed. This suggests that epimerization is not occurring on the product throughout the course of the reaction.

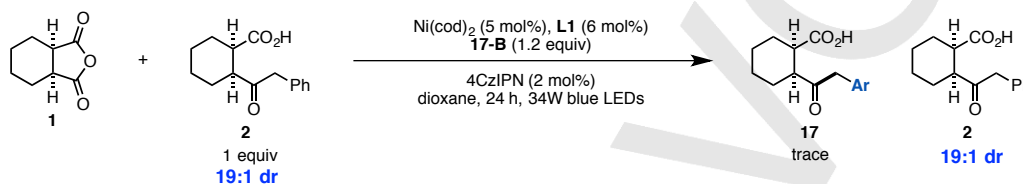


Figure S4. Isolated product was subjected to the reaction conditions with a different trifluoroborate. No epimerization of the product was observed. There was only trace product formation of **17**. This is consistent with earlier studies that the addition of exogenous carboxylic acid (benzoic acid) inhibits the reaction.

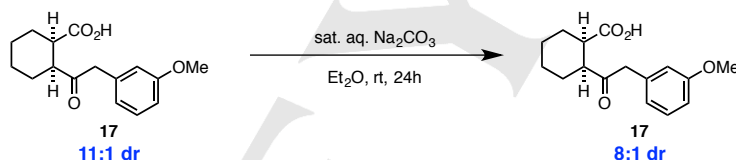


Figure S5. Isolated product was subjected to extended workup conditions to assess whether or not epimerization was occurring during the workup. Even after 24 h, only a small amount of epimerization was observed to the *trans* diastereomer.

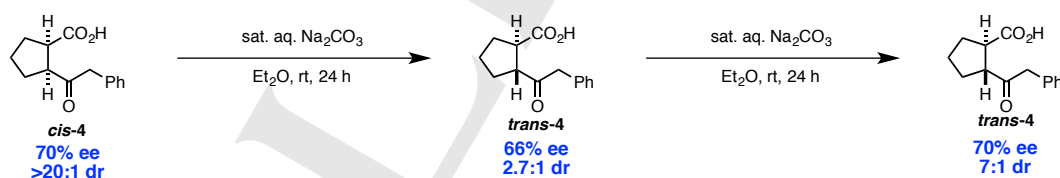


Figure S6. Some of the substrates were especially prone to epimerization in the workup. Special care was taken when isolating these substrates to minimize the amount of time spent under basic conditions. Cyclopentyl product **4** could be epimerized to favor the *trans* product 2.7:1 with nearly identical enantioselectivity. Subjecting that diastereomeric mixture to the same conditions epimerized the substrate even further, again with identical enantioselectivity. The same effect was observed for the cyclobutyl product **5**.

VI. Oxidative Addition Studies

Stoichiometric UV/Vis Studies of Oxidative Addition:

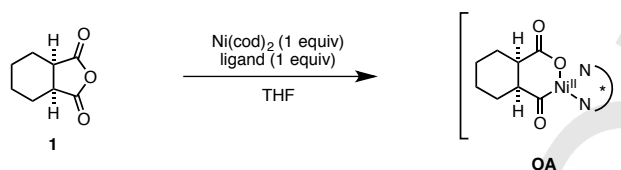


Figure S7. In an effort to detect the oxidative addition adduct, and assess the degree of reversibility, we conducted UV/Vis studies comparing different ligand classes. In addition, we conducted complementary stoichiometric competition studies to further assess the reversibility of oxidative addition.

General Procedure: All materials were prepared in an N₂-filled glovebox. Analyte solutions were dispensed into the cuvette, and the cuvette sealed with a Teflon septum and cap, then further sealed with electrical tape. All spectra were taken immediately following removal of the sample from the glovebox. The Ni(cod)₂ (6.68 × 10⁻⁵ M in THF) spectrum was taken from earlier work.⁷

Ligand solution (LS): A ligand stock solution was prepared as follows: ligand (0.018 mmol) was weighed into a 2-dram vial equipped with a Teflon coated stir bar, then 1.0 mL of THF was added. The stock solution was further diluted with THF to a final concentration of 3.6 × 10⁻⁴ M.

Nickel + ligand solution (CS): A catalyst stock solution was prepared as follows: Ni(cod)₂ (5.0 mg, 0.018 mmol) and ligand (1 equiv, 0.018 mmol) were weighed into a 2-dram vial equipped with a Teflon coated stir bar, then 1.0 mL of THF was added. The stock solution was stirred for ~10 min to ensure ligation, at which point any color change was noted. Then the stock solution was further diluted with THF to a final concentration of 3.6 × 10⁻⁴ M.

Anhydride solution (AS): A stock solution was prepared as follows: Anhydride **1** (5.6 mg, 0.036 mmol) was weighed into a 2-dram vial equipped with a Teflon coated stir bar, then dissolved in 1 mL THF. The stock solution was further diluted with THF to a final concentration of 3.6 × 10⁻⁴ M.

Nickel + Ligand + Anhydride solution: CS (0.2 mL) and AS (0.1 mL) were added to a 2-dram vial equipped with a Teflon coated stir bar and diluted to 0.5 mL with THF for a concentration of 7.3 × 10⁻³ M. The solution was allowed to stir for 10 min, at which point any color change was noted. The solution was then further diluted with THF to a final concentration of 3.6 × 10⁻⁴ M.

⁷ B. J. Shields, A. G. Doyle, *J. Am. Chem. Soc.* **2016**, *138*, 12719-12722.

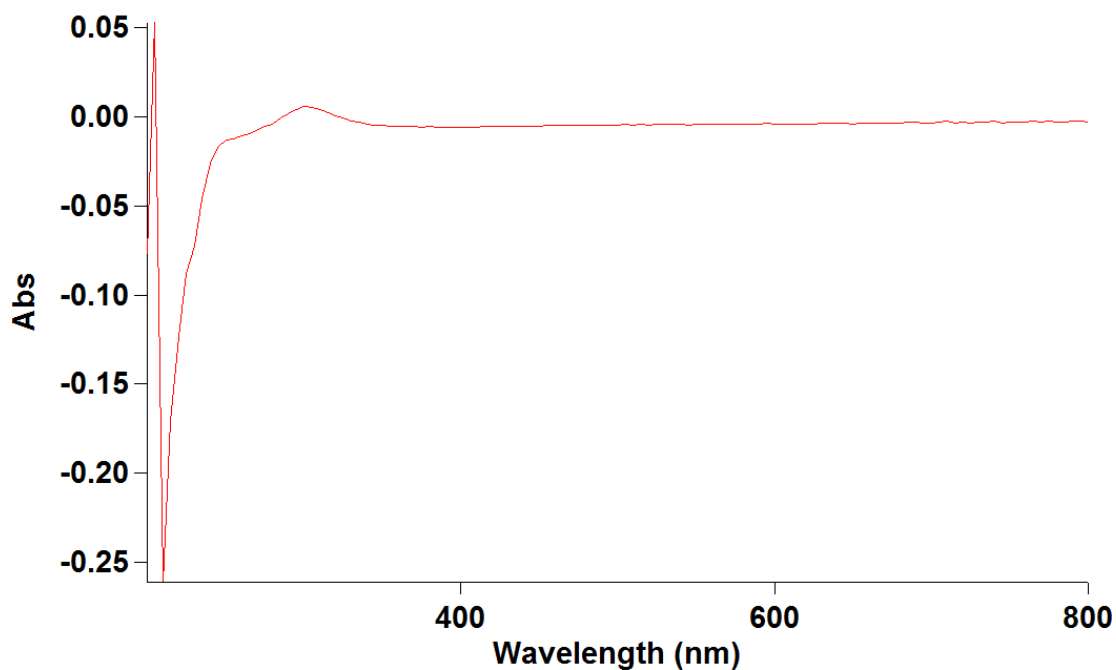


Figure S8. UV/Vis spectrum anhydride 1

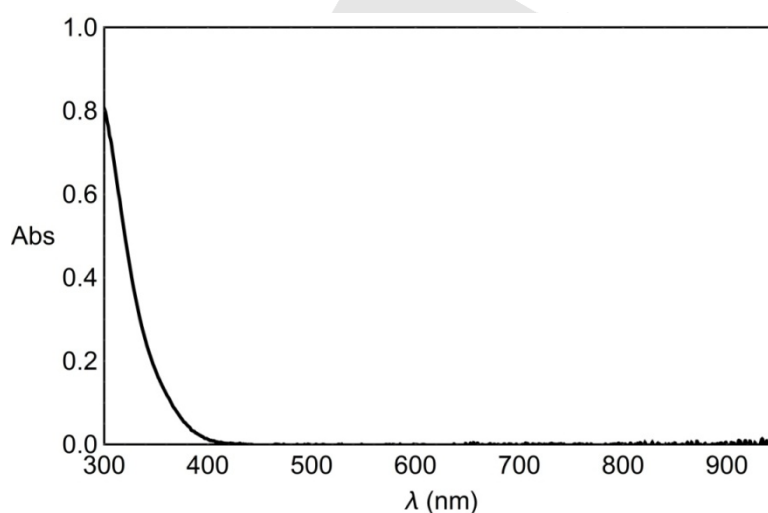


Figure S9. UV/Vis spectrum Ni(cod)₂

(S,S)-PhBox (L1):

The catalyst solution (CS) had no observable color change after mixing for 10 min. The mixed solution of CS and AS also had no observable color change after mixing for 10 min. To mimic the actual reaction conditions, an additional 19 equiv of anhydride was added to the previously stirring stock solution of CS and AS and stirred an additional 10 min (total stir time in excess of 30 min). A slight color change to orange was noted at the end of 10 min.

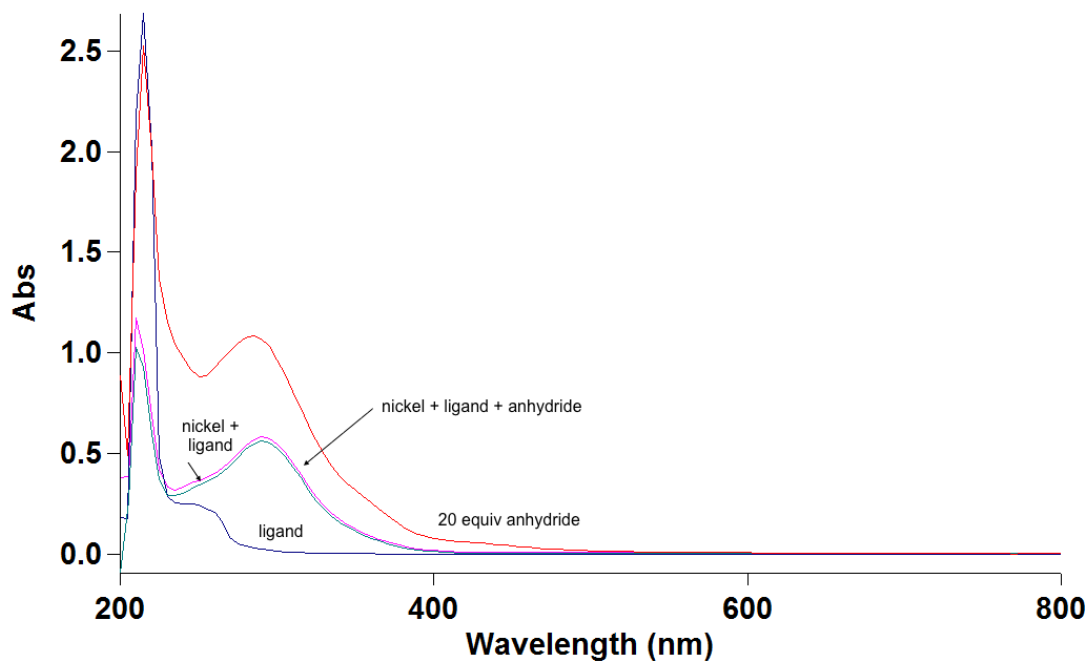


Figure S10. Anhydride and $\text{Ni}(\text{cod})_2$ spectra were omitted for clarity. The initial mixture of CS and AS shows no indication of oxidative addition, by color change or the development of changes in the visible region. However, after the addition of more anhydride and longer stir time, a slight change in color and change in spectrum were observed. These data suggest that oxidative addition, under stoichiometric conditions, is slow.

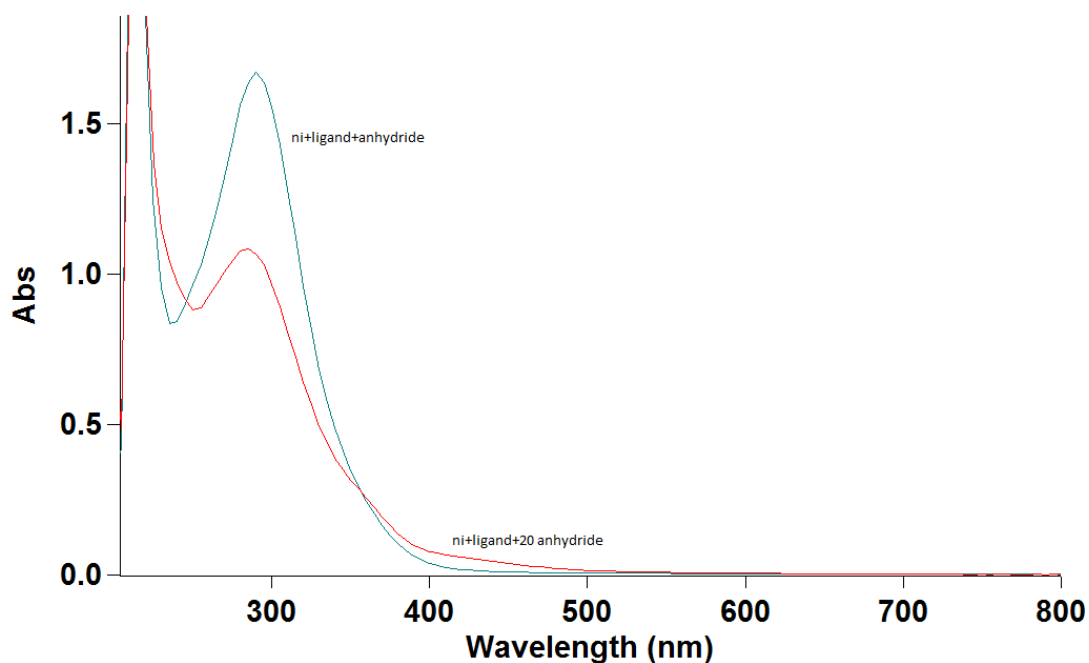


Figure S11. Anhydride, ligand, nickel + ligand and Ni(cod)₂ spectra were omitted for clarity. Anhydride **1** was used stoichiometrically and in excess (20 equiv). A stir time of 10 minutes was used for mixing **CS** and **AS** according to the general procedure. With an excess of anhydride, mimicking reaction conditions, oxidative addition is observed after only 10 min.

(S)-*t*BuPyrOx:

The catalyst solution (**CS**) formed a deep violet color after 10 min. The mixed solution of **CS** and **AS** formed a red color (within 1 min of mixing) and maintained the color after 10 min.

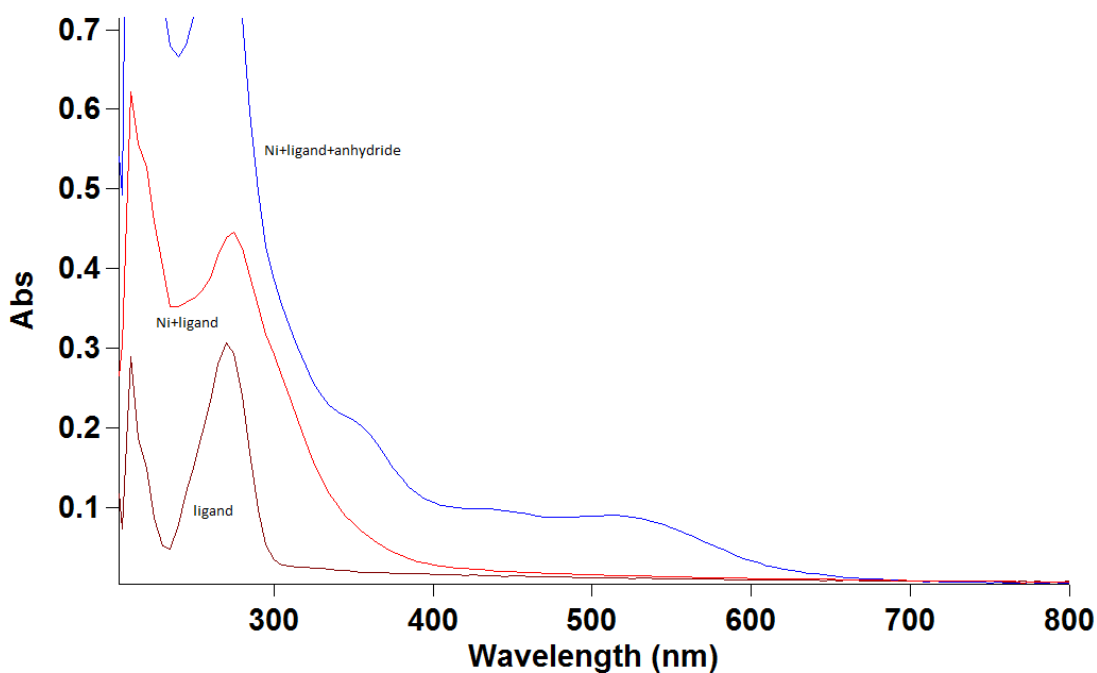


Figure S12. Anhydride and Ni(cod)₂ spectra were omitted for clarity. A significant change, consistent with the color change and probable oxidative addition, is observed in the spectrum, developing features in the 350-500 nm range. These data suggest that oxidative addition is occurring (within 10 min) under these catalyst conditions.

(S)-6-Me-*t*BuPyrOx (L4):

The catalyst solution (**CS**) formed a dark green color after 10 min. The mixed solution of **CS** and **AS** formed a red color (within 2 min of mixing) and maintained the color after 10 min.

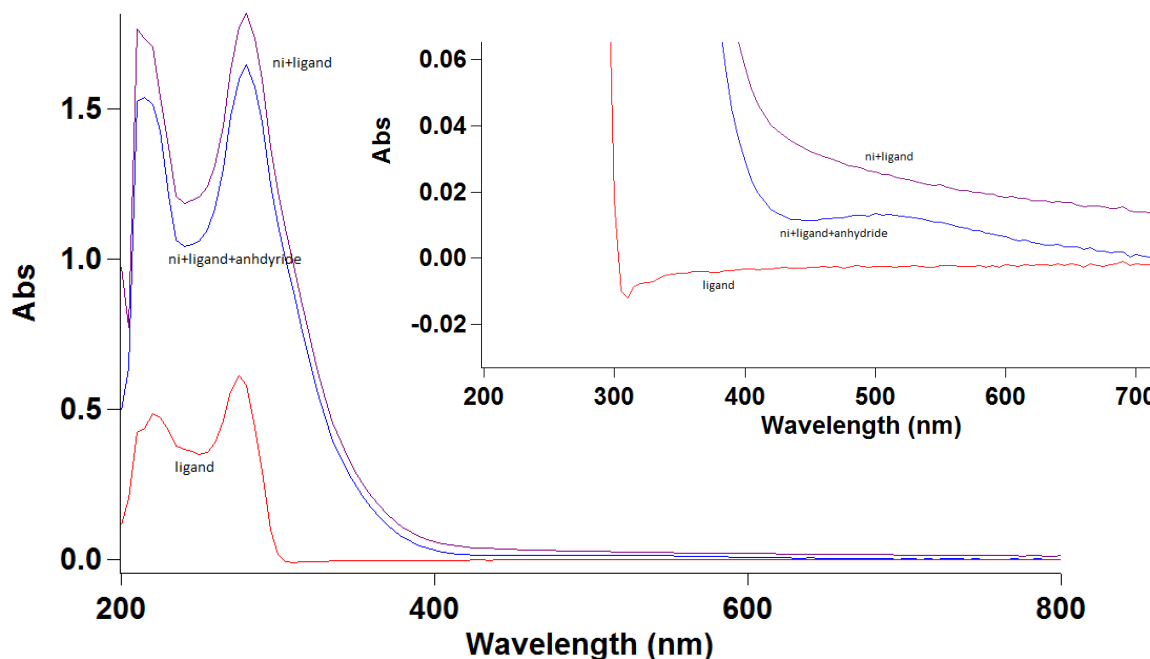


Figure S13. Anhydride and Ni(cod)₂ spectra were omitted for clarity. A small but significant change, consistent with the color change and probable oxidative addition, is observed in the spectrum, developing a feature at 500 nm. These data suggest that oxidative addition is occurring (within 10 min) under these catalyst conditions.

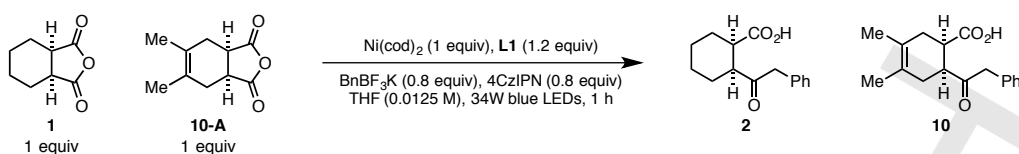
Stoichiometric competition studies to probe oxidative addition:

Procedure A: Cyclohexanecarboxylic anhydride **1** (1.9 mg, 0.013 mmol, 1 equiv) and benzyl trifluoroborate (2.0 mg, 0.01 mmol, 0.8 equiv) were weighed into a 1-dram vial equipped with a Teflon coated stirbar. The reaction tube was then brought into an N₂-filled glovebox. Then a pre-stirred dissolved solution of Ni(cod)₂ (3.4 mg, 0.013 mmol, 1 equiv) and (-)-2,2'-Isopropylidenebis-(4*S*)-4-phenyl-2-oxazoline (**L1**) (3.1 mg, 0.015 mmol, 1.2 equiv) in 0.9 mL of THF was added. The reaction was stirred for 10 min. After 10 min, a solution of anhydride **10-A** (2.3 mg, 0.013 mmol, 1 equiv) in 0.1 mL of THF was added, and the reaction stirred for an additional 10 min. 4CzIPN (7.9 mg, 0.01 mmol, 0.8 equiv) was added and the reaction vial sealed with a septa cap. The vial was wrapped with electrical tape, and then removed from the glovebox, where it was immediately irradiated with a 34W blue LED lamp, ~3 cm from the light source for 1 h. A fan was used to keep the reaction cool. After 1 h, the reaction was diluted with equal volumes Et₂O and 1 M HCl. The organic layer was dried over Na₂SO₄, filtered and concentrated and analyzed by ¹H NMR to determine the product ratio. The procedure was repeated using **10-A** initially, and then adding anhydride **1**.

Procedure B: Following procedure **A**, addition of anhydride **1** and anhydride **10-A** was reversed.

Procedure C: Following procedure **A**, upon addition of **10-A** no 10 min stir was performed.

Procedure D: Following procedure **A**, anhydrides **1**, and **10-A** were both added initially and stirred for 10 min with nickel and ligand.



entry	conditions	ratio 2:10
1	Procedure A	1.9:1
2	Procedure B	1.3:1
3	Procedure C	1.4:1
4	Procedure D	1.3:1

Table S4. Assessment of oxidative addition reversibility. This data suggests either that oxidative addition is fast and reversible, so an equilibrium mixture of product is obtained, or that oxidative addition is slow, and is not occurring fully until after irradiation with light. In accordance with the UV/Vis data, we attribute the equilibrium mixture of products to a slow oxidative addition, rather than a fast and reversible process.

VII. Evaluation of Racemic Background Reaction

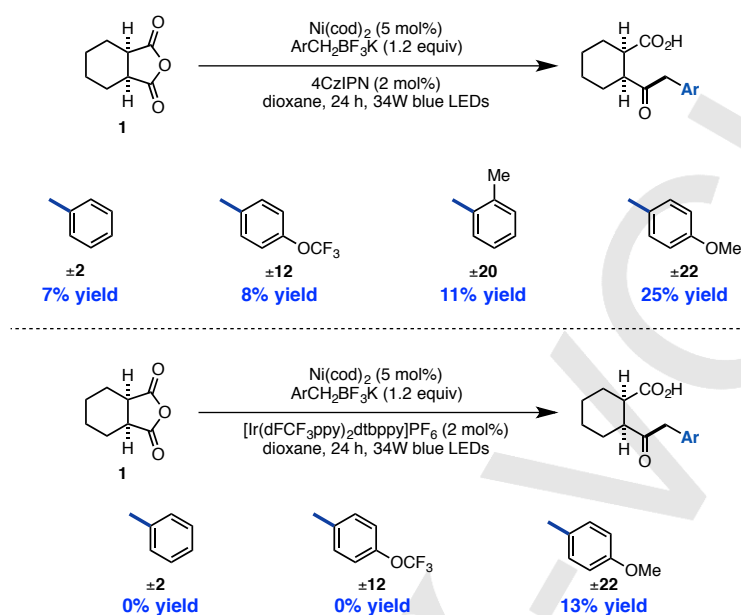


Figure S14. Evaluation of racemic background reaction. Control reactions following the screening general procedure were performed for a number of substrates where chiral ligand was omitted. For electron neutral or electron deficient trifluoroborates (BnBF_3K and **12-B**), a small, but significant amount of product was formed. For sterically hindered *ortho* substituted BF_3K 's (**20-B**), a slightly larger racemic background reaction was observed. With electron rich trifluoroborates, such as **22-B**, a much more significant racemic background was observed. The racemic background may be mediated by a $\text{Ni}(0/\text{I}/\text{III})$ pathway, where the benzylic radical adds to nickel first. Alternatively, the photocatalyst itself may be acting as a ligand for oxidative addition. In the case where $[\text{Ir}(\text{dFCF}_3\text{ppy})_2\text{dtbbpy}]\text{PF}_6$ was employed, a racemic background reaction was only observed for electron rich trifluoroborates, such as **20-B**. The existence of this background reaction likely plays a role in the changing enantioselectivity.

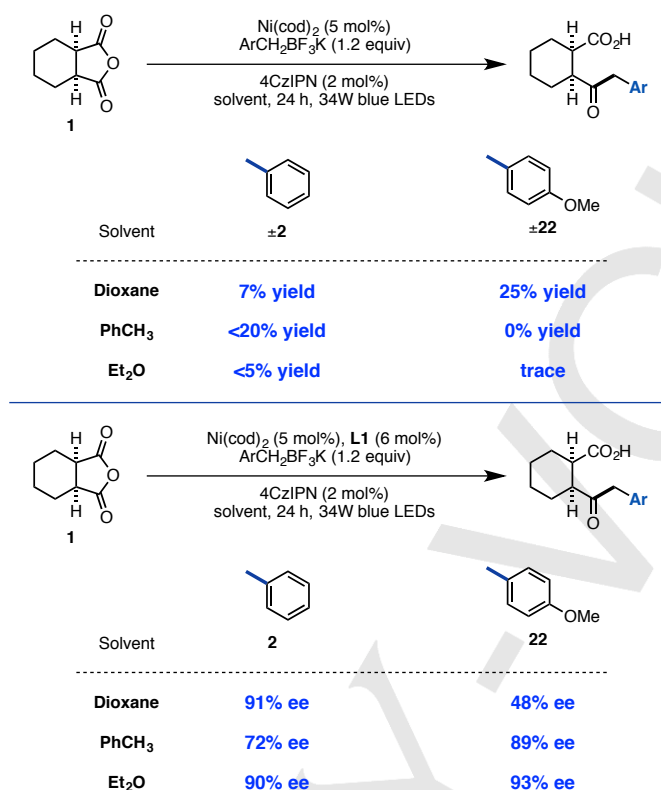


Figure S15. Evaluation and comparison of solvent effects on the racemic background reaction and enantioselectivity. Interestingly, in toluene, a significantly larger racemic background reaction is observed for product **2**, whereas no product **22** is detected under identical conditions. A correlation between racemic background and erosion of selectivity is observed for these two products.

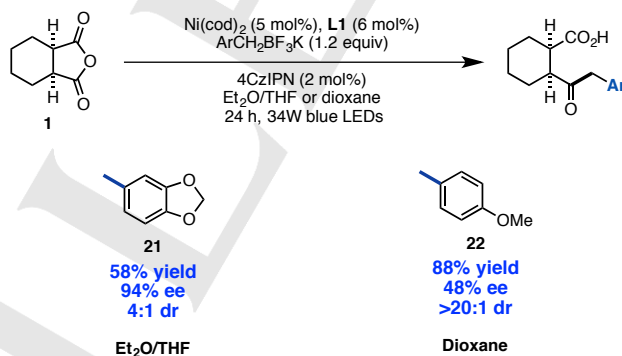


Figure S16. Additional isolations performed, according to general procedure **A** or **B**. Product **21** could be obtained in high enantioselectivity, albeit reduced yield and dr. Additionally, the enantioselectivity of **22** was significantly eroded under the optimized conditions, due to a more prolific racemic background.

Hammett analysis:

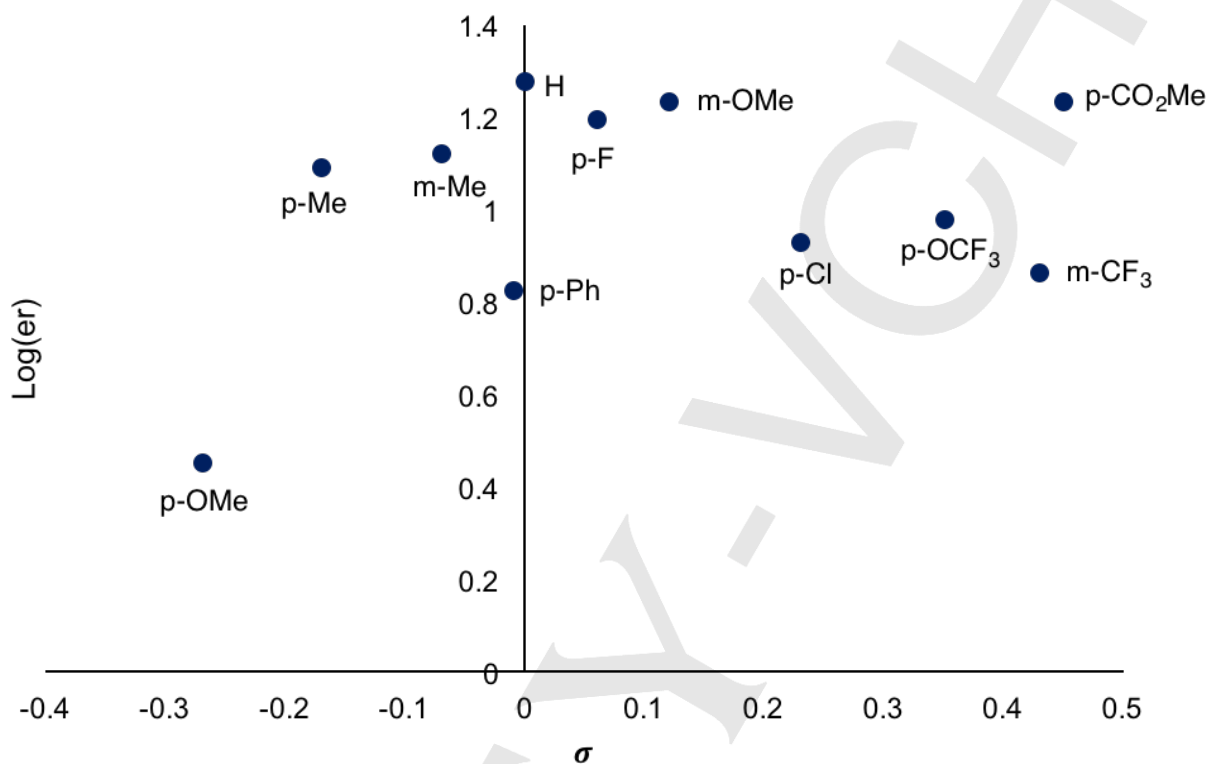


Figure S17. Enantiomeric ratio plotted v. σ^8 values under standard reaction conditions. There is no trend among changing electronics in trifluoroborate (and resultant benzylic radical) with product enantioselectivity. This suggests that the benzylic radical is not involved in the enantiodetermining step, and the mechanism is likely proceeding through a Ni(0/II/III) cycle.

⁸ C. Hansch, A. Leo, R. W. Taft, *Chem. Rev.* **1991**, *91*, 165-195.

VIII. Effect of Trifluoroborate Purity

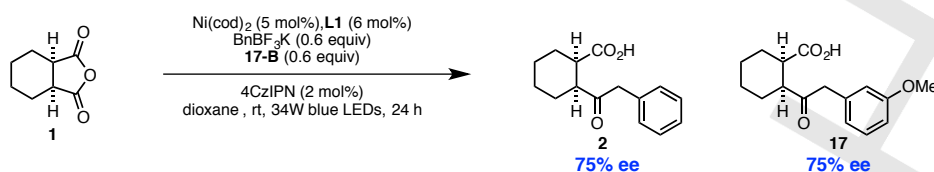


Figure S18. During early probes into substrate scope, it was noted that the enantioselectivity was changing drastically depending on trifluoroborate. We quickly ruled out a mechanistic change via Hammett analysis. In order to determine if an impurity was causing changes in selectivity, we ran a control experiment comparing synthetic material to commercially available trifluoroborate. The reaction was carried out according to the general procedure. The commercial benzyl trifluoroborate salt and unpurified synthetic **17-B** were used in a 1:1 ratio. The selectivity of product **2a** was eroded from 91% ee to 75% ee, identical to that of product **17**. This strongly suggests that the enantioselectivity was eroded due to an impurity in the synthetic material, and is not mechanistically relevant.

Reaction scheme showing the conversion of substrate **1** to product **Ar**. Reagents: $\text{Ni}(\text{cod})_2$ (5 mol%), **L1** (6 mol%), $\text{ArCH}_2\text{BF}_3\text{K}$ (1.2 equiv), **4CzIPN** (2 mol%), dioxane (0.05 M), 24 h, 34W blue LEDs.

Product	Crude BF_3K	Recrystallized BF_3K
16	59% yield 46% ee dr nd	84% yield 83% ee >20:1 dr
17	78% yield 71% ee 13:1 dr	86% yield 89% ee 11:1 dr
18	79% yield 63% ee dr nd	84% yield 86% ee dr nd
19	53% yield 75% ee 15:1 dr	77% yield 85% ee 8:1 dr
21	73% yield 29% ee >20:1 dr	89% yield 70% ee >20:1 dr
22	67% yield 41% ee >20:1 dr	88% yield 48% ee >20:1 dr

Figure S19. Comparison of product selectivity as a function of trifluoroborate purity. In some cases, dramatic changes in selectivity and yield were observed with unpurified synthetic trifluoroborates (see each preparation of trifluoroborate for purification details).

IX. Derivatization Studies

Scale up and purification:

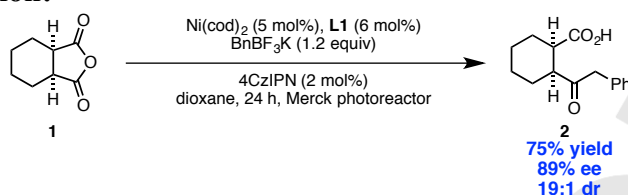


Figure S20. Scale-up reaction, 0.5 mmol. Procedure: Cyclohexanecarboxylic anhydride **1** (77.1 mg, 0.50 mmol) and benzyl trifluoroborate (119 mg, 0.60 mmol) were weighed into a 20 mL scintillation vial, equipped with a teflon coated stirbar. The reaction vessel was then brought into an N₂-filled glovebox. Ni(cod)₂ (6.9 mg, 0.025 mmol) and (-)-2,2'-Isopropylidenebis-(4*S*)-4-phenyl-2-oxazoline (**L1**) (10.0 mg, 0.030 mmol) were added to the vial, along with 10 mL dioxane. The mixture was allowed to stir for ~10 minutes at room temperature, at which point the reaction mixture became homogenous. 4CzIPN (7.9 mg, 0.010 mmol) was added and the reaction vessel sealed with a septa cap. The vial was removed from the glovebox, where it was immediately irradiated with the Merck photoreactor (450 nm light). A fan was used to keep the reaction cool. After 24 h, the reaction tube was removed from the light source, and the solvent was removed. The residue was dissolved in 1 M HCl (30 mL) and diethyl ether (30 mL). The aqueous layer was extracted once with additional diethyl ether (15 mL). The combined ether layers were then extracted with sat. aq. Na₂CO₃ (4 x 25 mL). The combined aqueous layers were acidified with conc. HCl until ~pH 2. The aqueous layer was extracted with diethyl ether (3 x 30 mL). The combined organic layers were washed with brine (30 mL) and then dried over Na₂SO₄, filtered and concentrated. The crude product was purified over silica gel using CH₂Cl₂ → 5% MeOH in CH₂Cl₂ to afford **2** (92.1 mg, 75% yield, 89% ee, 19:1 dr).

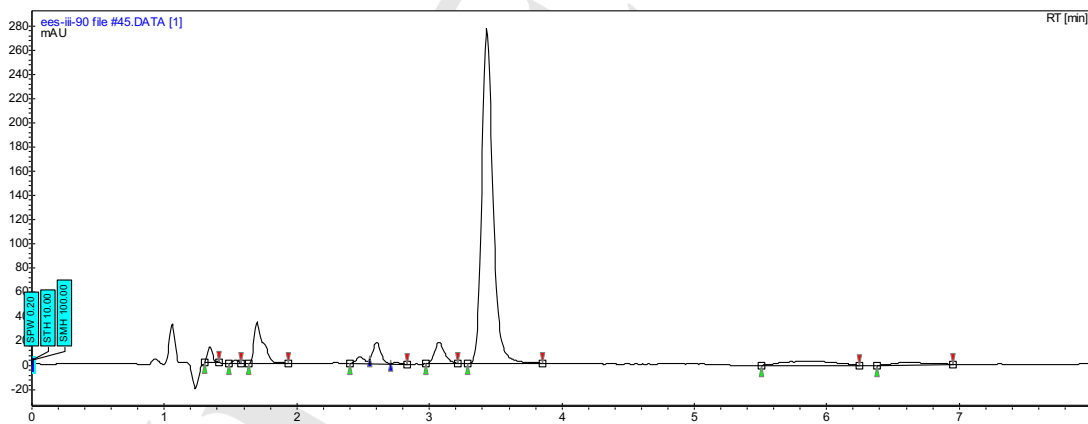


Figure S21. Diastereomers and enantiomers were separated using preparative HPLC analysis on a chiral stationary phase (AD-H 2 x 25 cm, 15% EtOH/CO₂, 100 bar, 70 mL/min, 220 nm). In the process, the minor enantiomer was also removed, leaving the product in excess of 99% ee.

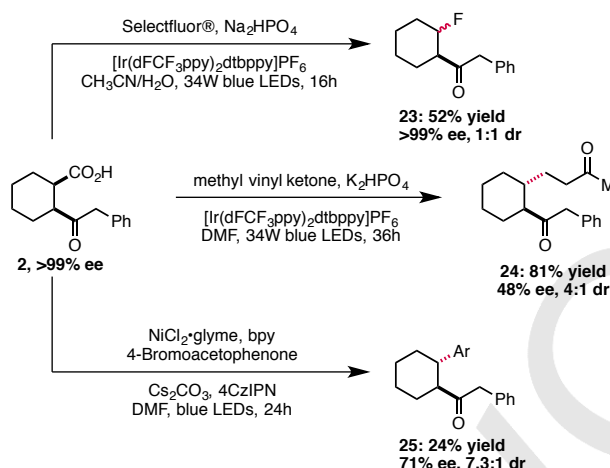
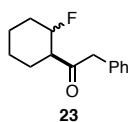


Figure S22. Derivatization reactions. The use of acyl electrophiles such as anhydrides in cross coupling has been investigated by a number of groups, but in the case of acyclic electrophiles, the acyl leaving group is lost as stoichiometric waste. In the case of meso cyclic anhydrides, the resultant product is a carboxylic acid, which can act as a traceless functional group for manipulation into further molecular complexity. For example, conversion of the carboxylic acid into the corresponding fluoride using Selectfluor® provides the fluorinated product in good yield with no erosion of enantioselectivity.⁹ Carbon-carbon bond formation via decarboxylative Michael addition is also possible in excellent yield, good diastereoselectivity.¹⁰ Interestingly, racemization of the ketone stereocenter was observed, eroding the enantioselectivity. Further, Ni/photoredox-catalyzed arylation of the keto-acid generates **25** in good diastereoselectivity albeit in low yield.¹¹ Again, racemization of the ketone stereocenter was observed, eroding the enantioselectivity. These examples highlight the power of photoredox catalysis combined with cross coupling catalysis to access complex products in modest to high enantioselectivity from simple symmetric starting materials in two steps.

Procedures and characterization data:



Procedure: Enantiopure keto acid **2** (80 mg, 0.325 mmol), Selectfluor® (345 mg, 0.974 mmol), Na₂HPO₄ (92 mg, 0.650 mmol), [Ir(dFCF₃ppy)₂dtbbpy]PF₆ (3.6 mg, 0.00325 mmol) were weighed into a 2-dram vial. CH₃CN/H₂O (1:1, 3.3 mL) was added, a stirbar added and the vial sealed with a teflon septum. The contents were degassed for 10 minutes with stirring with N₂ by sparging. The vial was then irradiated with two 34W blue LED lamps ~4cm from the vial, with a fan used for cooling for 17 h. Upon completion of the reaction, the reaction was extracted with diethyl ether (3 x 10 mL). The combined organic layers were dried over Na₂SO₄, filtered and

⁹ S. Ventre, F. R. Petronijevic, D. W. C. MacMillan, *J. Am. Chem. Soc.* **2015**, *137*, 5654-5657.

¹⁰ L. Chu, C. Ohta, Z. Zuo, D. W. C. MacMillan, *J. Am. Chem. Soc.* **2014**, *136*, 10886-10889.

¹¹ J. Luo, J. Zhang, *ACS Catal.* **2016**, *6*, 873-877.

concentrated. The crude oil **23** was purified over silica gel using hexanes → 15% EtOAc in hexanes to afford a yellow oil (37.2 mg, 52% yield, >99% ee, 1:1 dr).

¹H NMR (501 MHz, CDCl₃): Isolated as 1:1 mixture of diastereomers. See NMR spectra for details.

¹³C NMR (126 MHz, CDCl₃): δ Isolated as 1:1 mixture of diastereomers. See NMR spectra for details.

¹⁹F NMR (282 MHz, CDCl₃): δ -171.04 and -171.22.

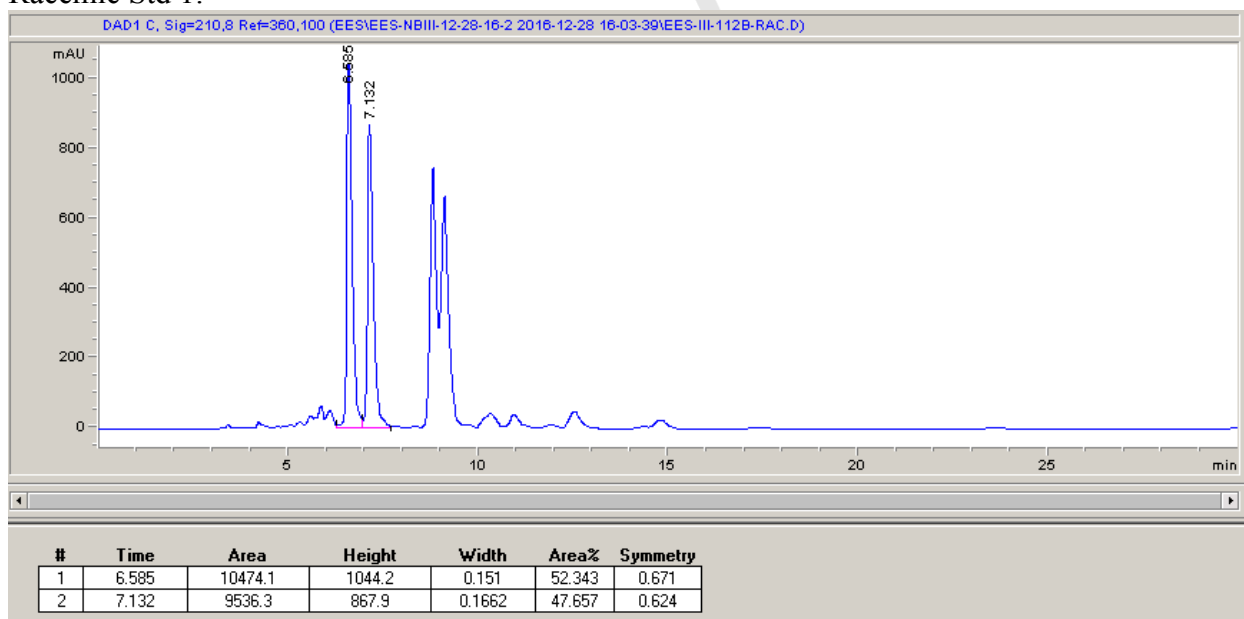
HRMS: (ESI-TOF) calculated for ([C₁₄H₁₇FO + Na]⁺): 243.1156, found 243.1160.

IR (ATR, cm⁻¹): 2939, 2865, 1711, 1497, 1452, 1327, 1119, 1030, 953, 806, 752, 703.

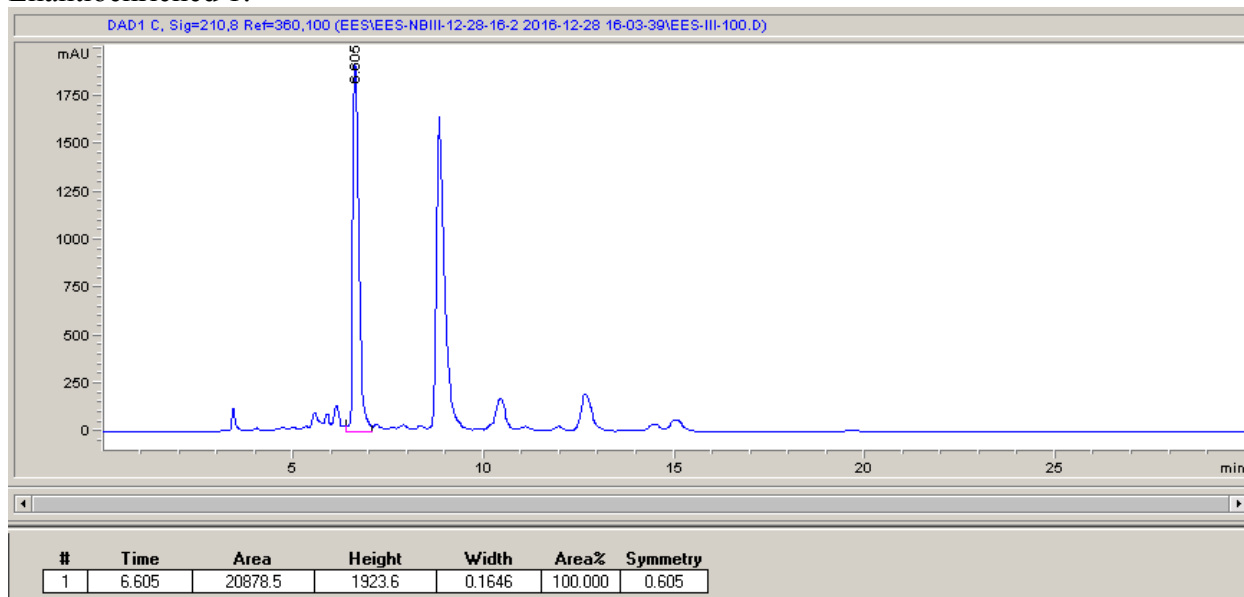
HPLC: Isomer 1: Chiralcel[®] OD-H, 5% IPA in Hexanes, 30 min run, 1 mL/min.

HPLC: Isomer 2: ChiralPak[®] AS-H, 5% IPA in Hexanes, 30 min run, 1 mL/min.

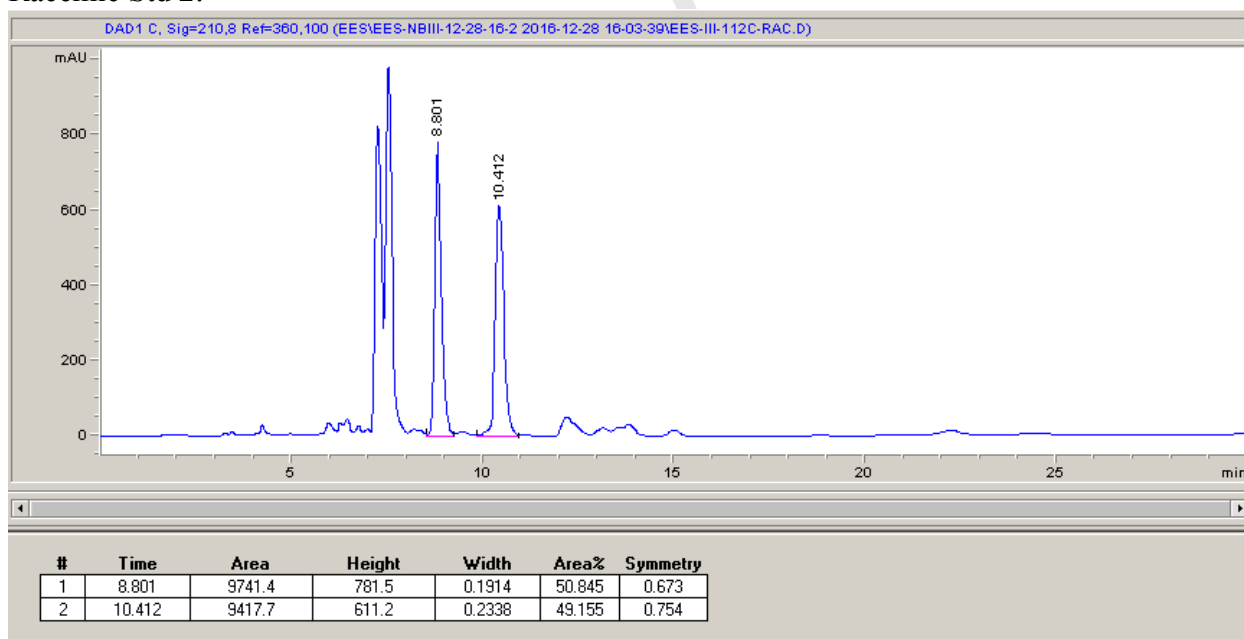
Racemic Std 1:



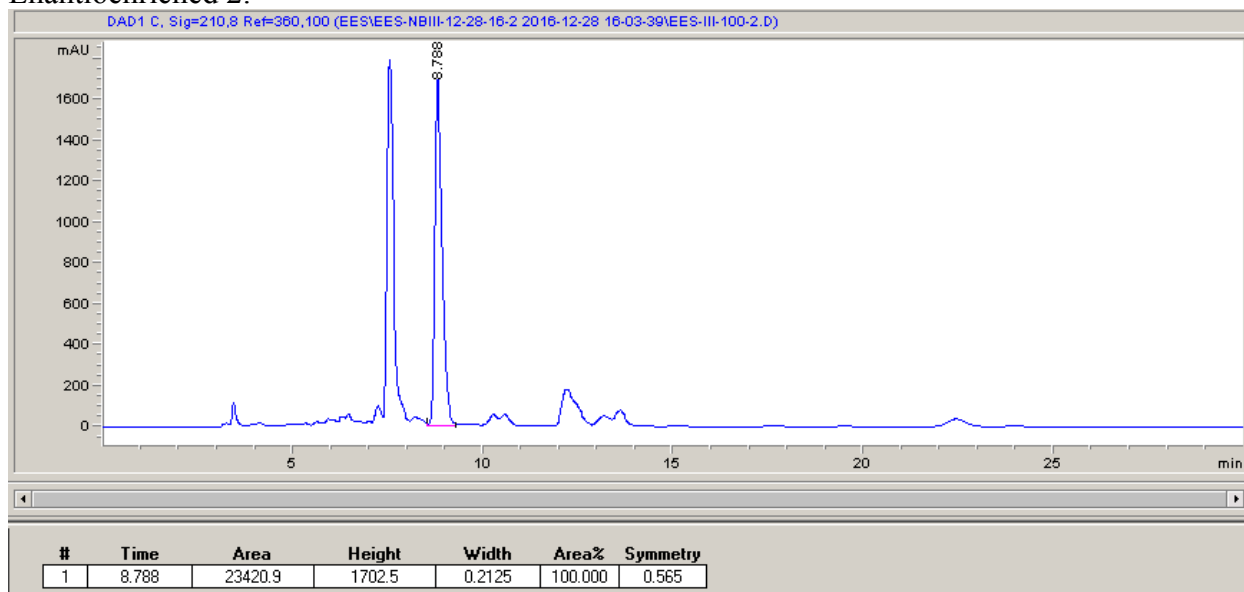
Enantioenriched 1:



Racemic Std 2:



Enantioenriched 2:



Confirmation of epimerization on ketone stereocenter:

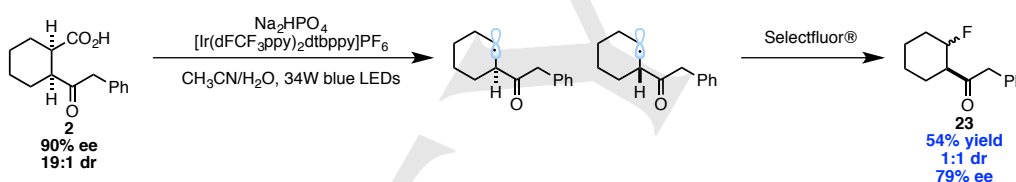
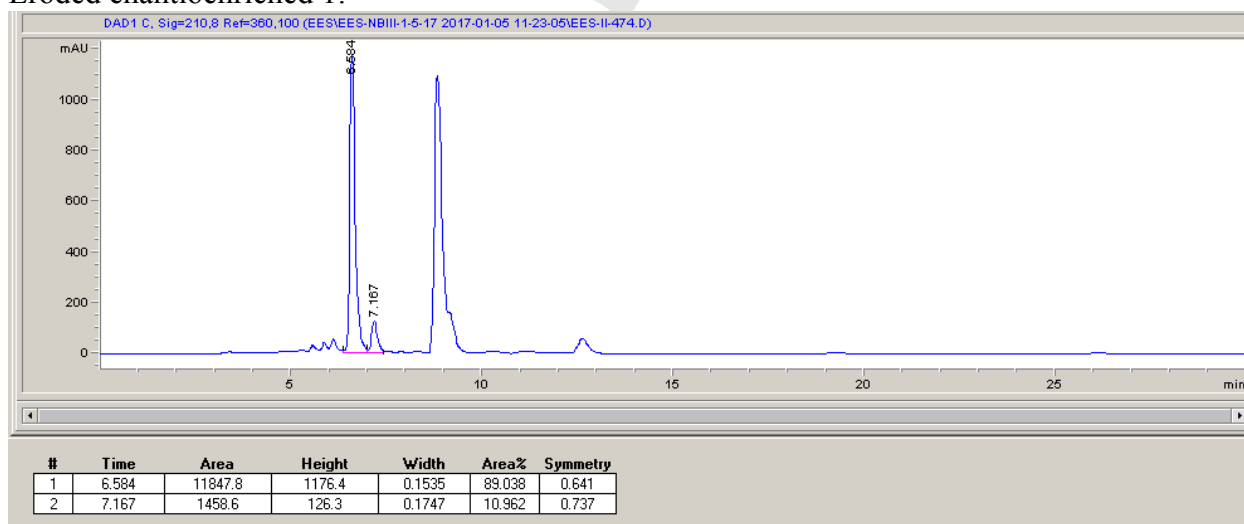
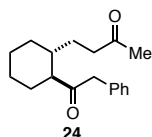
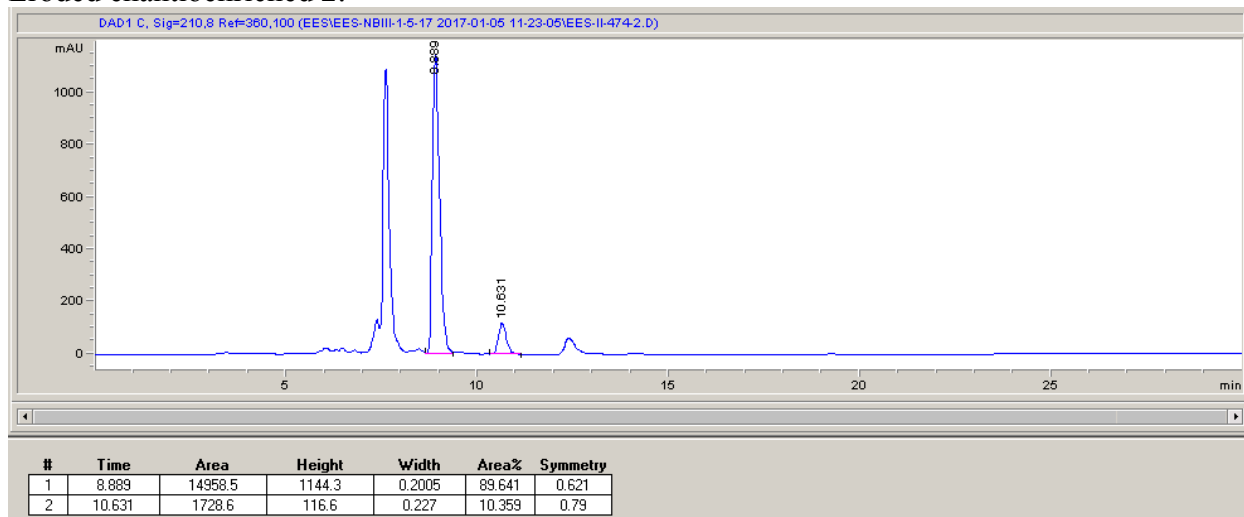


Figure S23. When a mixture of diastereomers *cis*-2 and *trans*-2 was employed in the fluorination reaction, an erosion of enantioselectivity was observed. This is attributed to the formation of enantiomers upon decarboxylation of 2.

Eroded enantioenriched 1:



Eroded enantioenriched 2:



Procedure: An 8 mL vial equipped with a stir bar was charged with enantiopure keto acid **2** (63.9 mg, 0.259 mmol, 1.0 equiv), $[\text{Ir}(\text{dFCF}_3\text{ppy})_2\text{dtbbpy}]\text{PF}_6$ (2.9 mg, 0.0026 mmol, 1.0 mol%), K_2HPO_4 (54 mg, 0.311 mmol, 1.2 equiv) and DMF (0.65 mL, 0.4 M). The mixture was sealed with a Teflon septum and the contents were degassed for 10 minutes with stirring with N_2 by sparging. At the same time, methyl vinyl ketone (used without purification) was sparged by N_2 . Under N_2 , methyl vinyl ketone (21.0 μL , 0.259 mmol, 1.0 equiv) was added to the reaction. The vial was sealed with electrical tape, then irradiated with a 34W blue LED lamp for 36 h, using a fan for cooling. Upon completion the reaction was diluted with sat. aq. NaHCO_3 and extracted with Et_2O (3x20mL). The combined organic layers were washed with water and brine, dried over Na_2SO_4 and concentrated. The crude oil **24** was purified over silica gel using hexanes \rightarrow 10% EtOAc in hexanes to afford a yellow oil (56.8 mg, 81% yield, 48% ee, 4:1 dr).¹²

^1H NMR (501 MHz, CDCl_3): δ 7.32 (dd, $J = 8.3, 6.6$ Hz, 2H), 7.28 – 7.24 (m, 1H), 7.23 – 7.18 (m, 2H), 3.79 – 3.66 (m, 2H), 2.37 – 2.25 (m, 3H), 2.05 (m, 3H), 1.83 – 1.66 (m, 4H), 1.49 – 1.39 (m, 1H), 1.31 – 1.11 (m, 4H).

^{13}C NMR (126 MHz, CDCl_3): δ 211.64, 209.06, 133.97, 129.76, 128.75, 127.09, 55.90, 49.74, 41.01, 37.54, 30.62, 30.24, 29.84, 28.54, 25.89, 25.67.

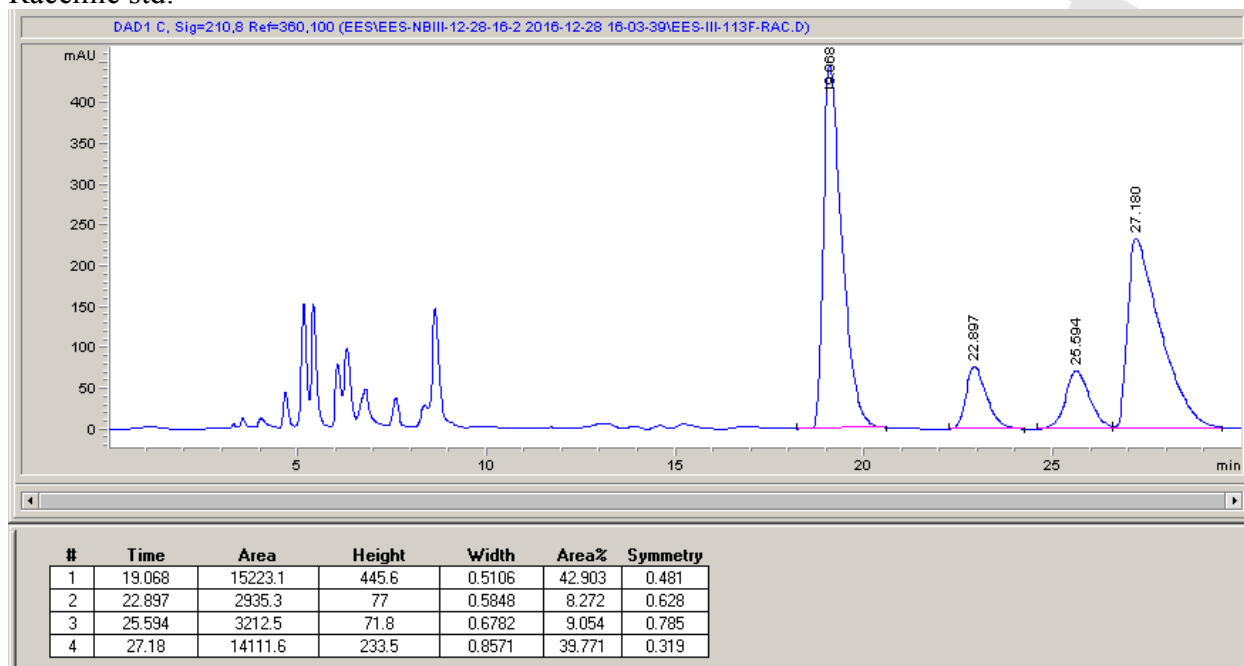
HRMS: (ESI-TOF) calculated for $([\text{C}_{18}\text{H}_{24}\text{O}_2 + \text{Na}]^+)$: 295.1669, found 295.1669.

IR (ATR, cm^{-1}): 2926, 2855, 1737, 1709, 1496, 1448, 1359, 1219, 1164, 1031, 704.

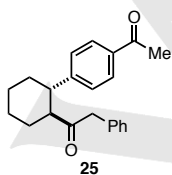
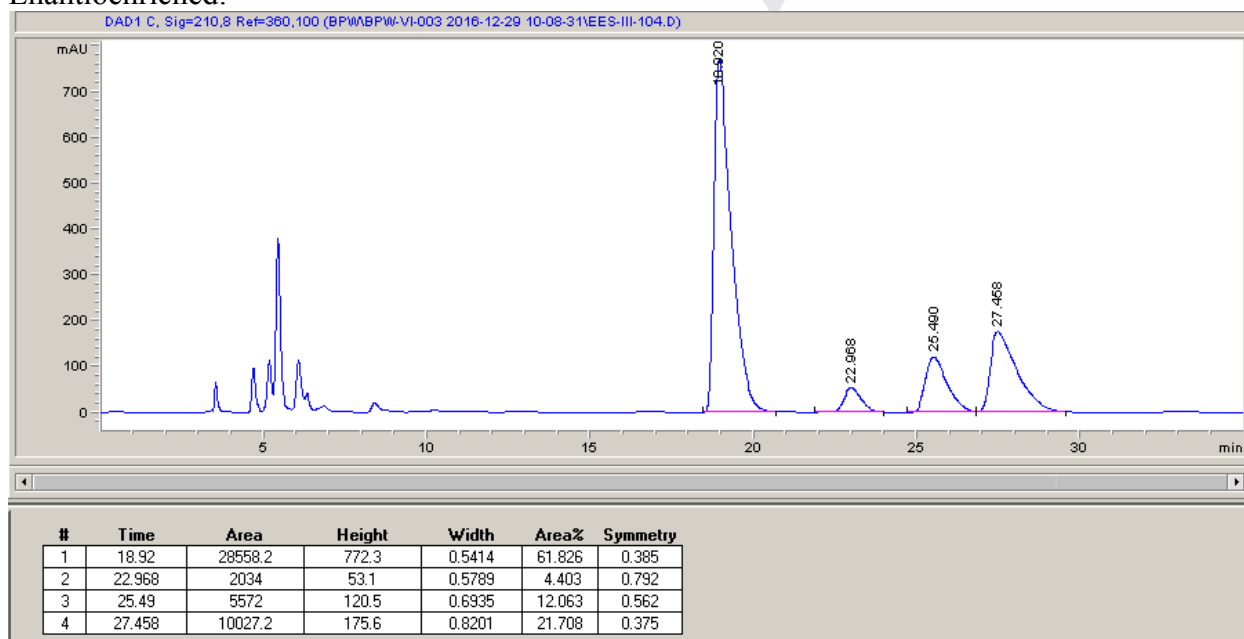
¹² L. Chu, C. Ohta, Z. Zuo, D. W. C. MacMillan, *J. Am. Chem. Soc.* **2014**, *136*, 10886-10889.

HPLC: Chiralcel® OJ-H, 5% IPA in Hexanes, 35 min run, 1 mL/min.

Racemic std:



Enantioenriched:



Procedure: A 20 mL vial equipped with a stir bar was charged with enantiopure keto acid **2** (104 mg, 0.422 mmol, 3.0 equiv), NiCl₂•glyme (3.1mg, 0.0141 mmol, 10 mol%), 2,2'-bipyridine (3.3 mg, 0.0212 mmol, 15 mol%), 4CzIPN (2.8 mg, 0.0034 mmol, 2.5 mol%), Cs₂CO₃ (137 mg, 0.422 mmol, 3.0 equiv), 4-bromoacetophenone (28 mg, 0.141mmol, 1.0 equiv) and DMF (7.1 mL, 0.02 M). The mixture was sealed with a Teflon septum and the contents were degassed for 10 minutes with stirring with N₂ by sparging. The vial was sealed with electrical tape, then irradiated in the Merck photobox at 450 nm for 24 h, using a fan for cooling. Upon completion the reaction was poured into 40mL water and extracted with EtOAc (3 x 20 mL). The combined organic layers were washed with brine, dried over Na₂SO₄ and concentrated. The crude oil **25** was purified over silica gel using hexanes → 15% EtOAc in hexanes to afford a yellow oil (10.9 mg, 24% yield, 71% ee, 7.3:1 dr).¹³

¹H NMR (501 MHz, CDCl₃): δ 7.78 (d, *J* = 7.9 Hz, 2H), 7.23 – 7.09 (m, 5H), 6.83 (dd, *J* = 6.8, 2.5 Hz, 2H), 3.40 – 3.29 (m, 2H), 2.94 – 2.81 (m, 2H), 2.57 (s, 3H), 1.97 – 1.76 (m, 4H), 1.53 – 1.11 (m, 4H).

¹³C NMR (126 MHz, CDCl₃): δ 210.14, 197.80, 150.46, 135.31, 133.28, 129.41, 128.57, 128.53, 127.63, 126.82, 55.16, 50.22, 46.00, 33.60, 29.91, 26.61, 25.94, 25.56.

HRMS: (ESI-TOF) calculated for ([C₂₂H₂₅O₂ + H]⁺): 321.1849, found 321.1850.

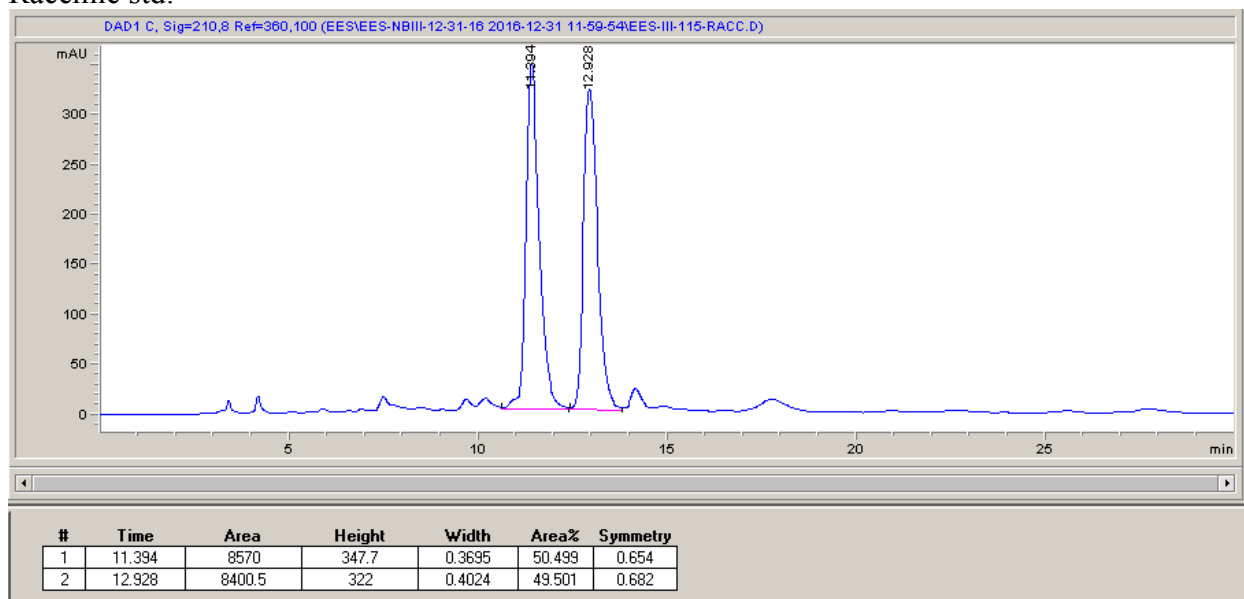
IR (ATR, cm⁻¹): 3019, 2926, 2855, 1735, 1708, 1681, 1495, 1447, 1267, 1216, 750, 703.

Optical Rotation: [α]_D²⁶ +7.3 (*c* 0.19, CHCl₃).

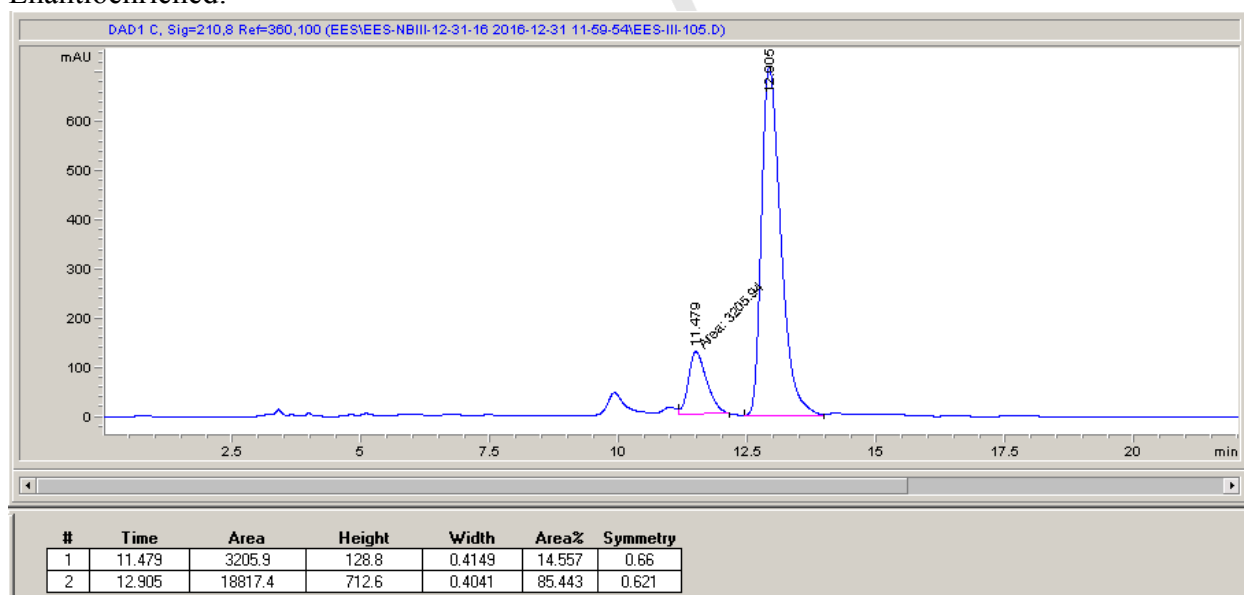
HPLC: Chiralcel[®] OD-H, 5% IPA in Hexanes, 30 min run, 1 mL/min.

¹³ J. Luo, J. Zhang, *ACS Catal.* **2016**, *6*, 873-877.

Racemic std:



Enantioenriched:



X. Determination of Absolute Stereochemistry

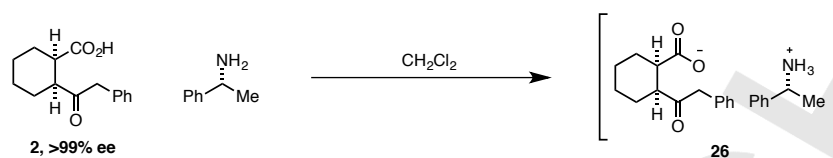


Figure S24. Enantiopure **2** was mixed in a 1:1 ratio with (R) -(+)- α -methylbenzylamine in CH_2Cl_2 at room temperature. After a few minutes of stirring, a precipitate began to form and afforded the ammonium salt. The salt was recrystallized by slow evaporation from Et_2O to afford an X-ray quality crystal, confirming the absolute stereochemistry.

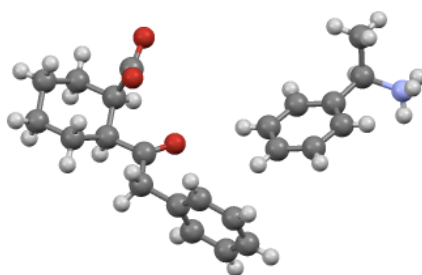
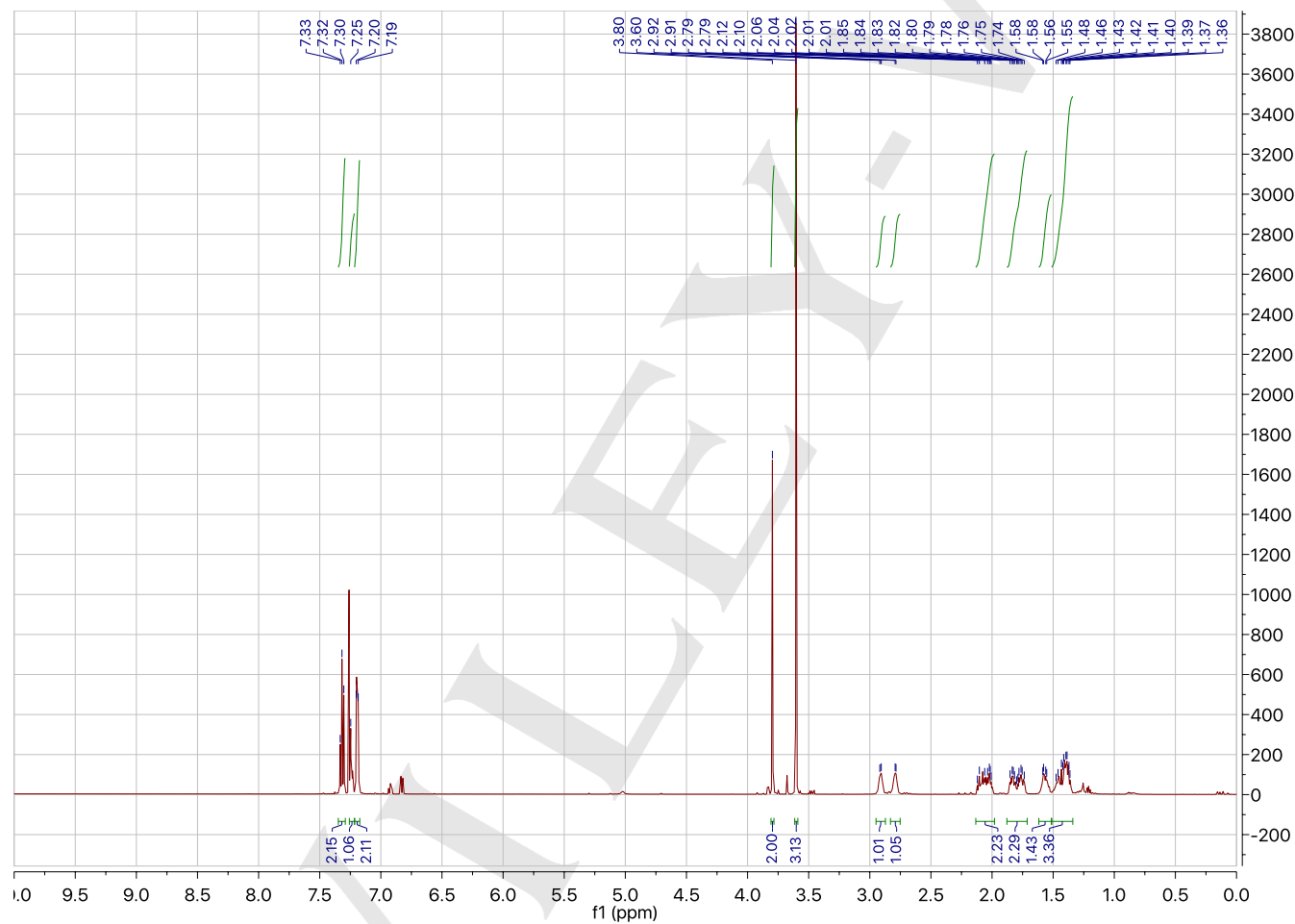
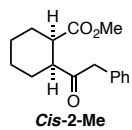
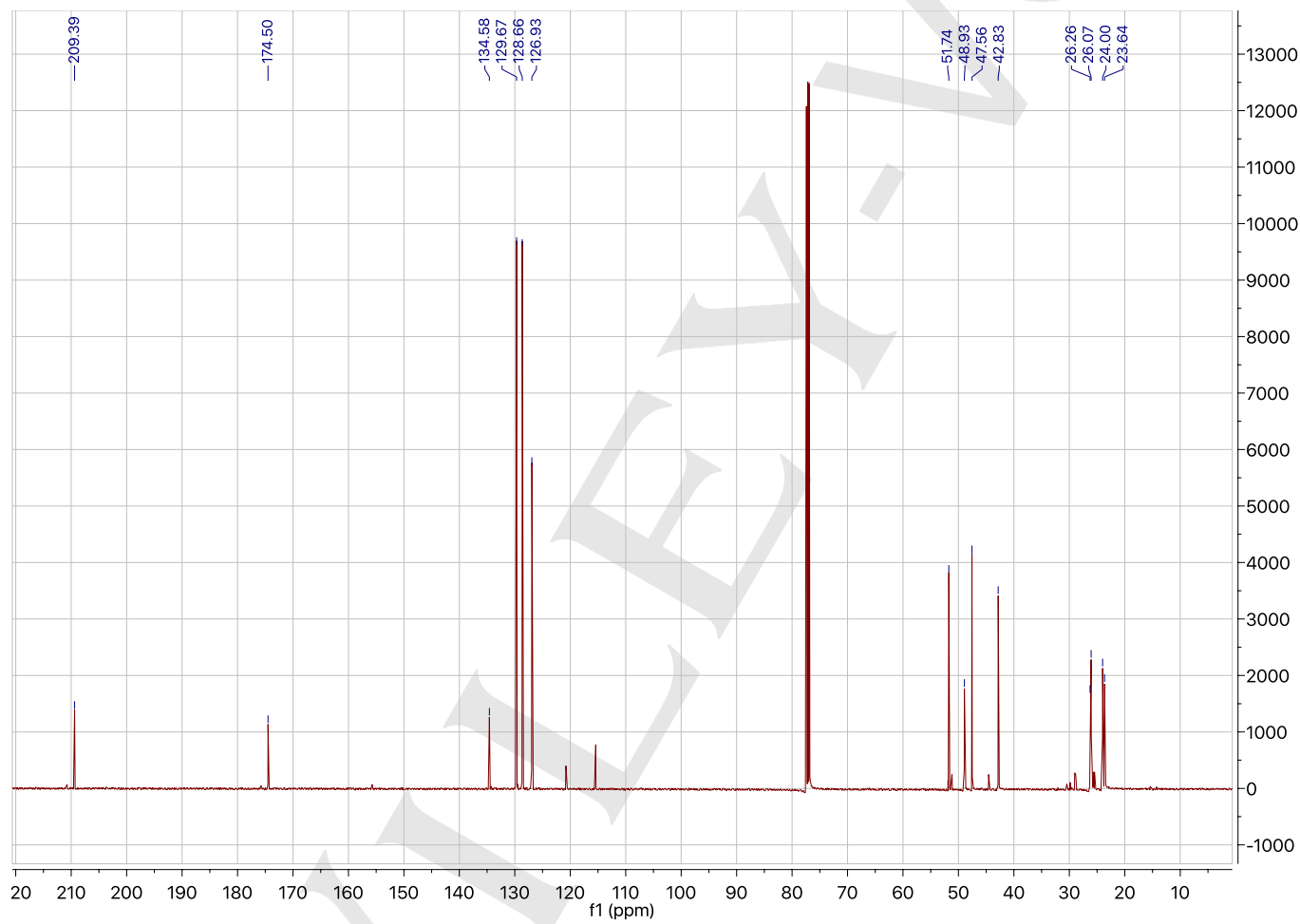
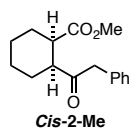


Figure S25. X-Ray structure of **26**. A thin rod-like specimen of $\text{C}_{23}\text{H}_{29}\text{NO}_3$, approximate dimensions 0.043 mm x 0.069 mm x 0.282 mm, was used for the X-ray crystallographic analysis. The X-ray intensity data were measured. See section **XII** for full crystallographic data (CCDC 1530628).

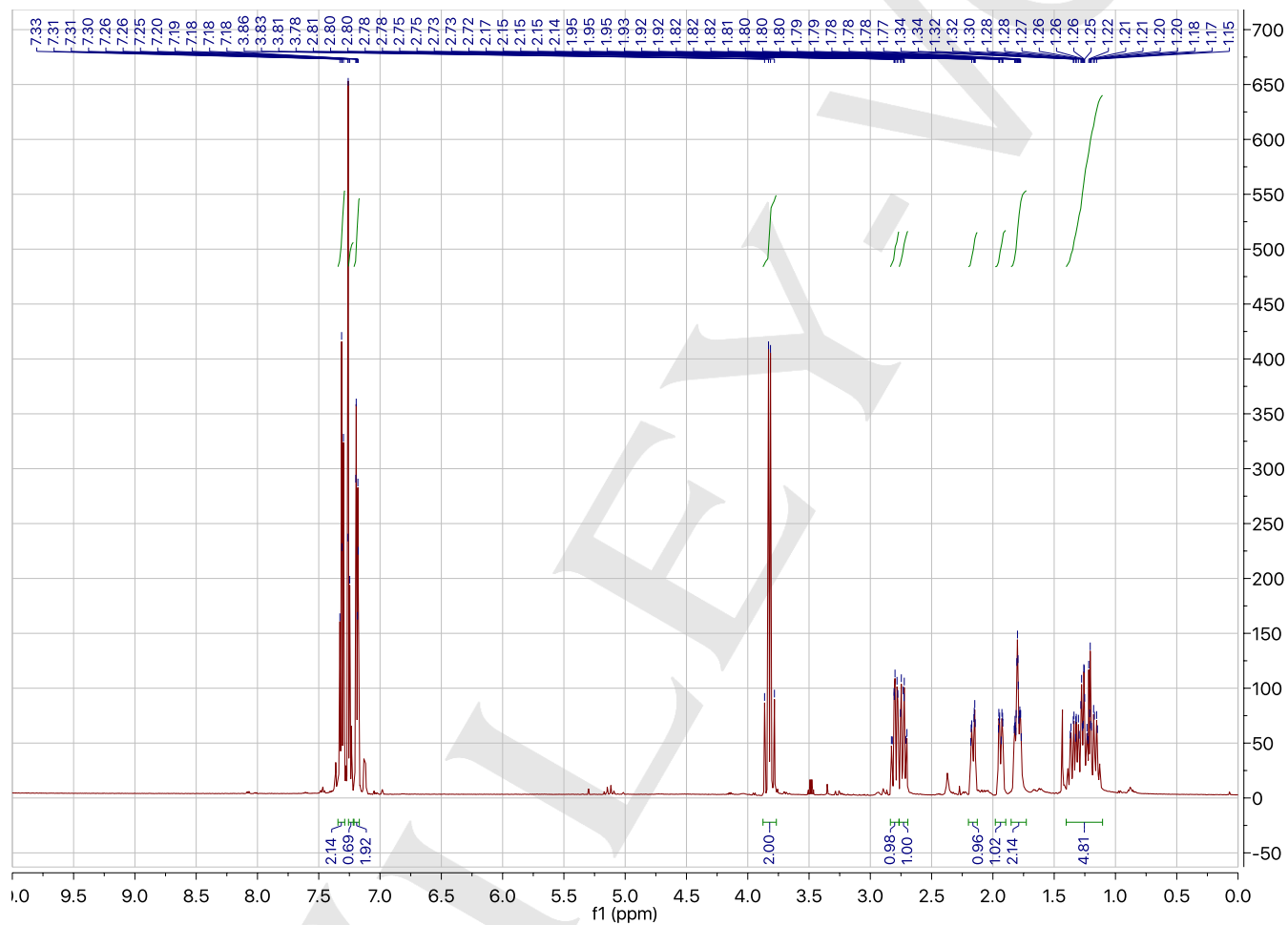
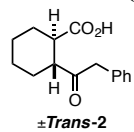
X. NMR Spectra

 ^1H NMR (501 MHz, CDCl_3): methyl (1*R*,2*S*)-2-(2-phenylacetyl)cyclohexane-1-carboxylate (*Cis*-2-Me)

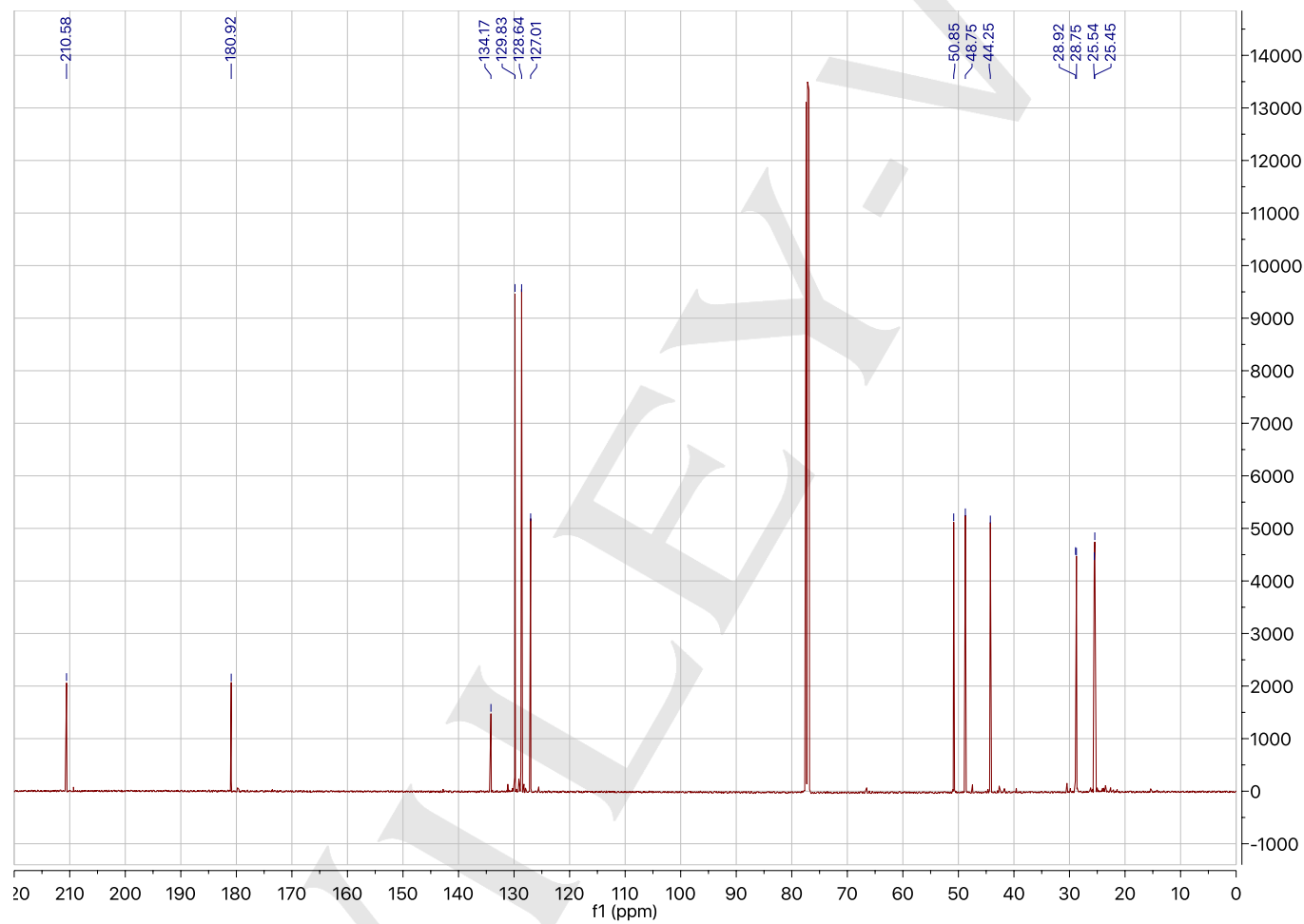
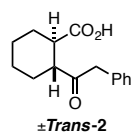
SUPPORTING INFORMATION

 ^{13}C NMR (126 MHz, CDCl_3): methyl (1*R*,2*S*)-2-(2-phenylacetyl)cyclohexane-1-carboxylate (*Cis*-2-Me)

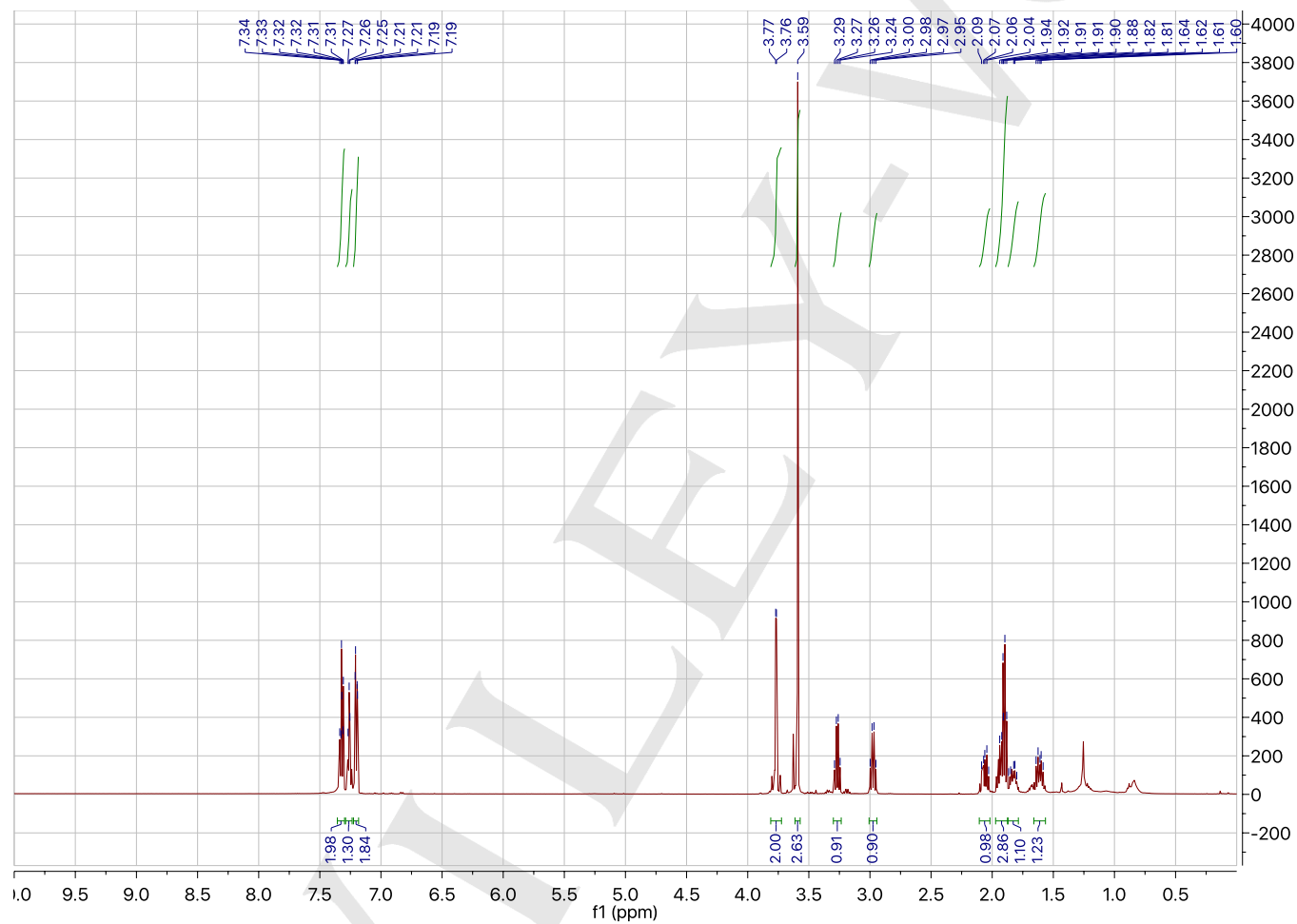
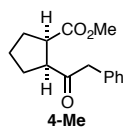
SUPPORTING INFORMATION

 ^1H NMR (501 MHz, CDCl_3): 2-(2-phenylacetyl)cyclohexane-1-carboxylic acid (*Trans*-2)

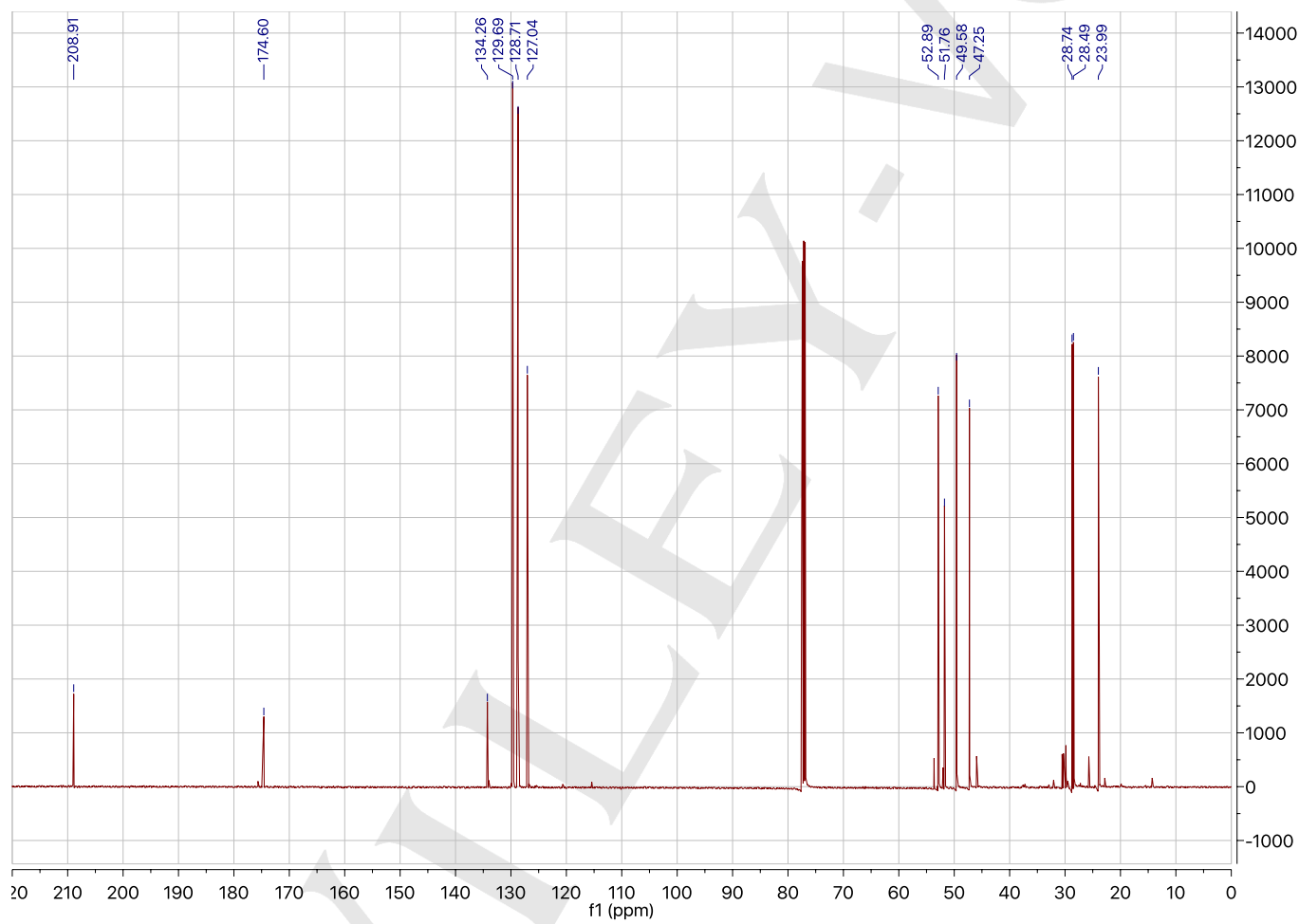
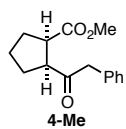
SUPPORTING INFORMATION

 ^{13}C NMR (126 MHz, CDCl_3): 2-(2-phenylacetyl)cyclohexane-1-carboxylic acid (*Trans*-2)

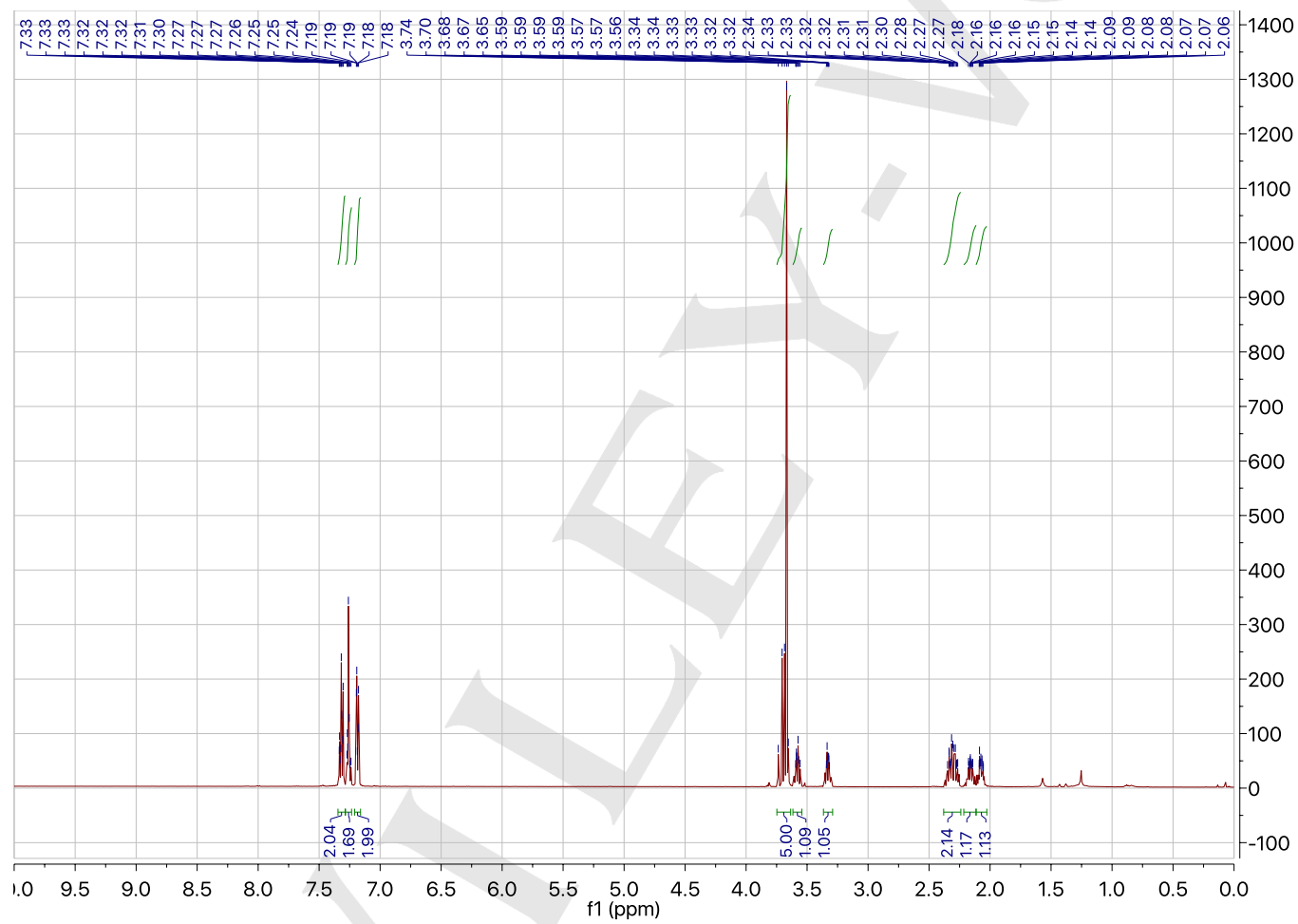
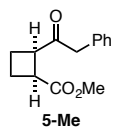
SUPPORTING INFORMATION

 ^1H NMR (501 MHz, CDCl_3): methyl (1*R*,2*S*)-2-(2-phenylacetyl)cyclopentane-1-carboxylate (4-Me)

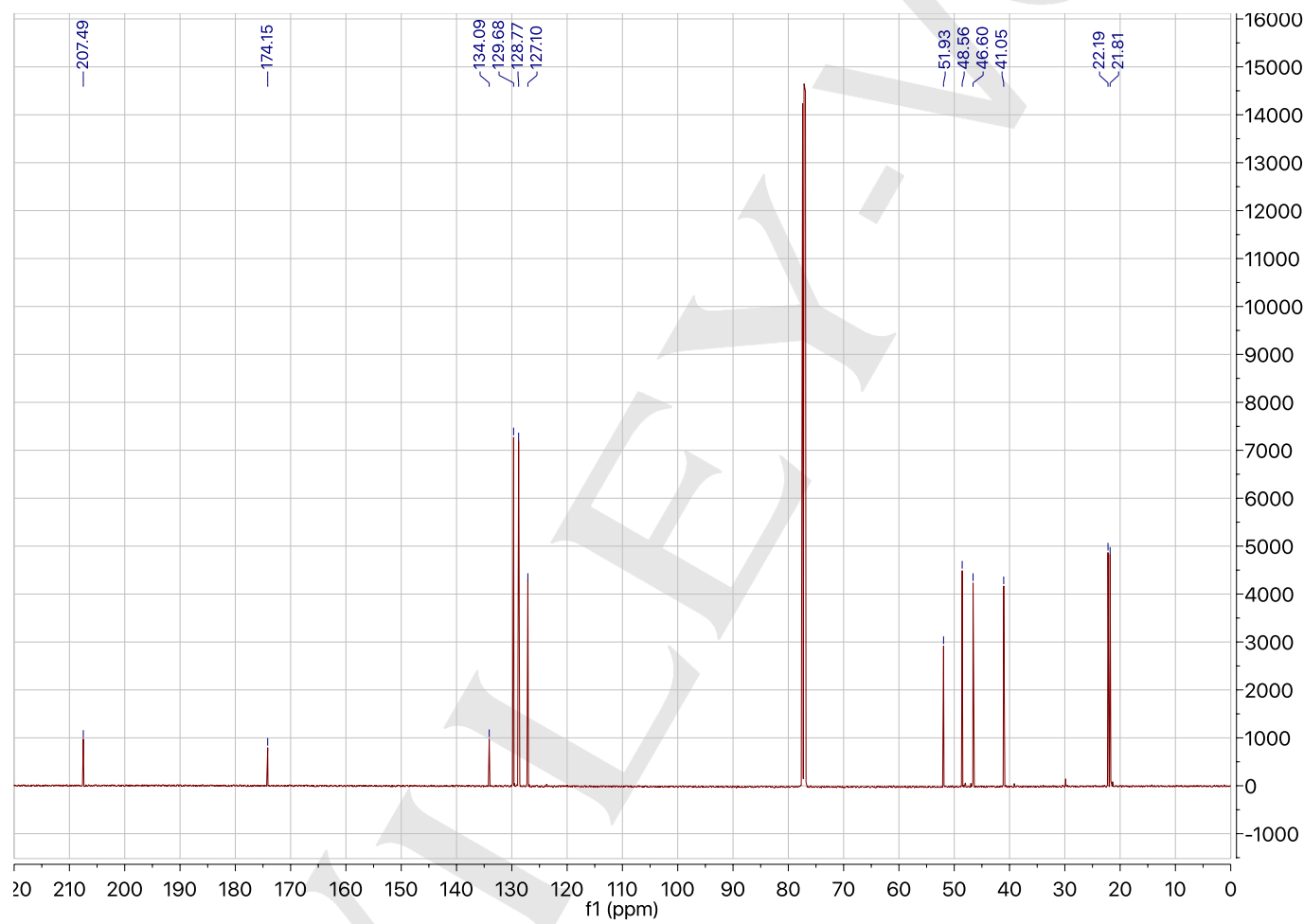
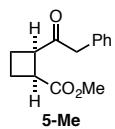
SUPPORTING INFORMATION

 ^{13}C NMR (126 MHz, CDCl_3): methyl (1*R*,2*S*)-2-(2-phenylacetyl)cyclopentane-1-carboxylate (4-Me)

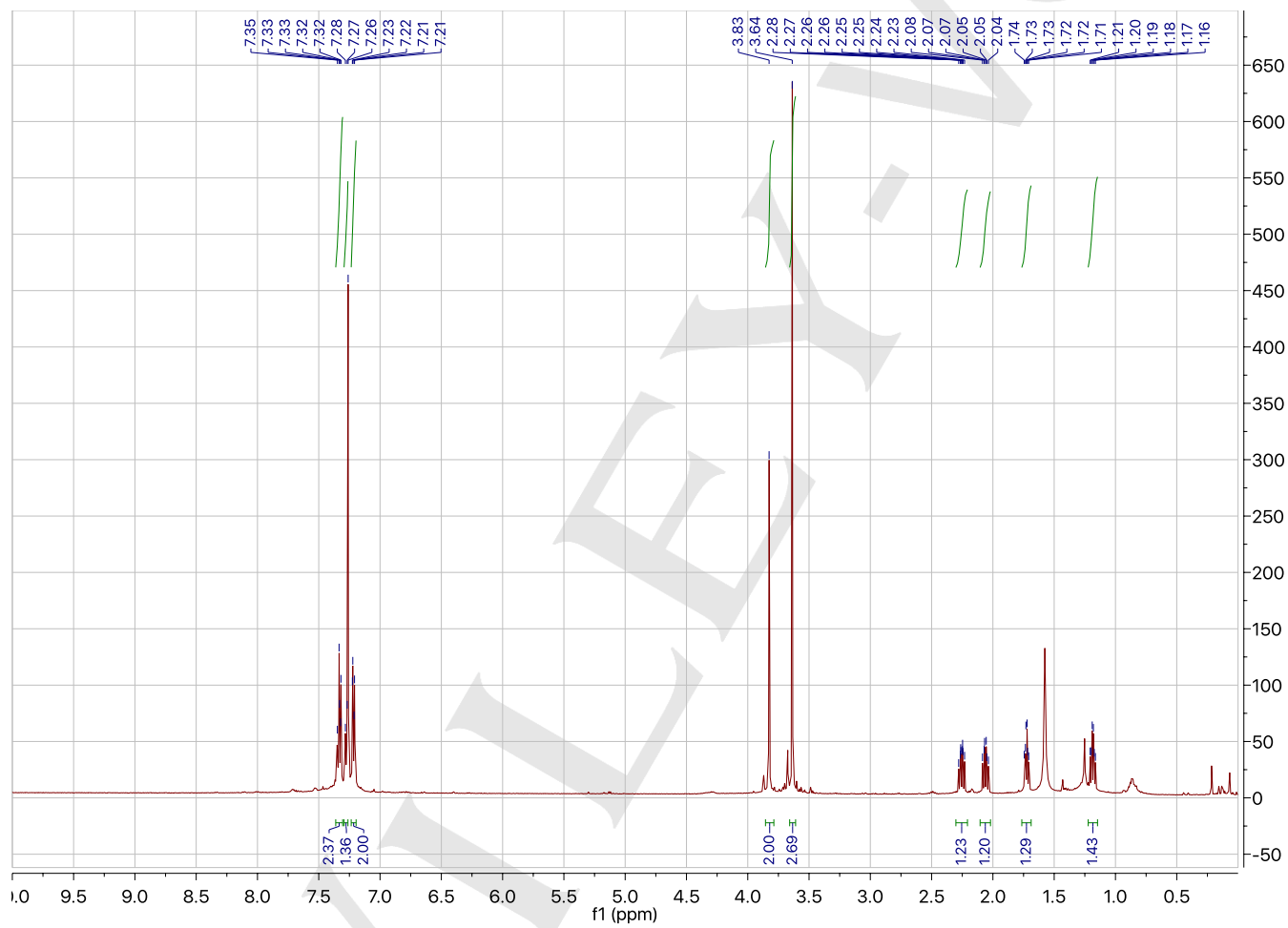
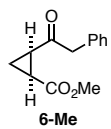
SUPPORTING INFORMATION

 ^1H NMR (501 MHz, CDCl_3): methyl (1*S*,2*R*)-2-(2-phenylacetyl)cyclobutane-1-carboxylate (5-Me)

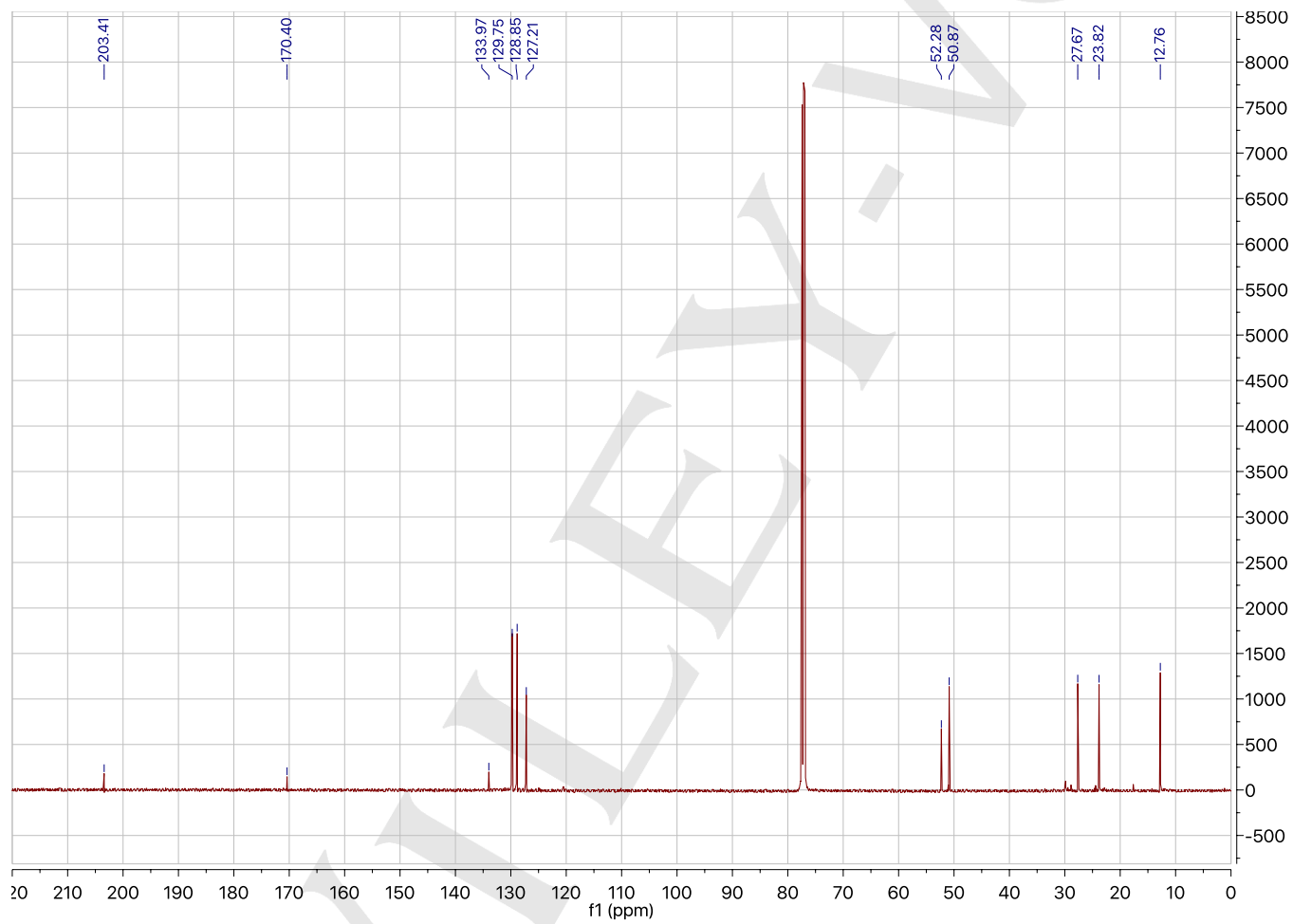
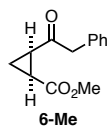
SUPPORTING INFORMATION

 ^{13}C NMR (126 MHz, CDCl_3): methyl (1*S*,2*R*)-2-(2-phenylacetyl)cyclobutane-1-carboxylate (5-Me)

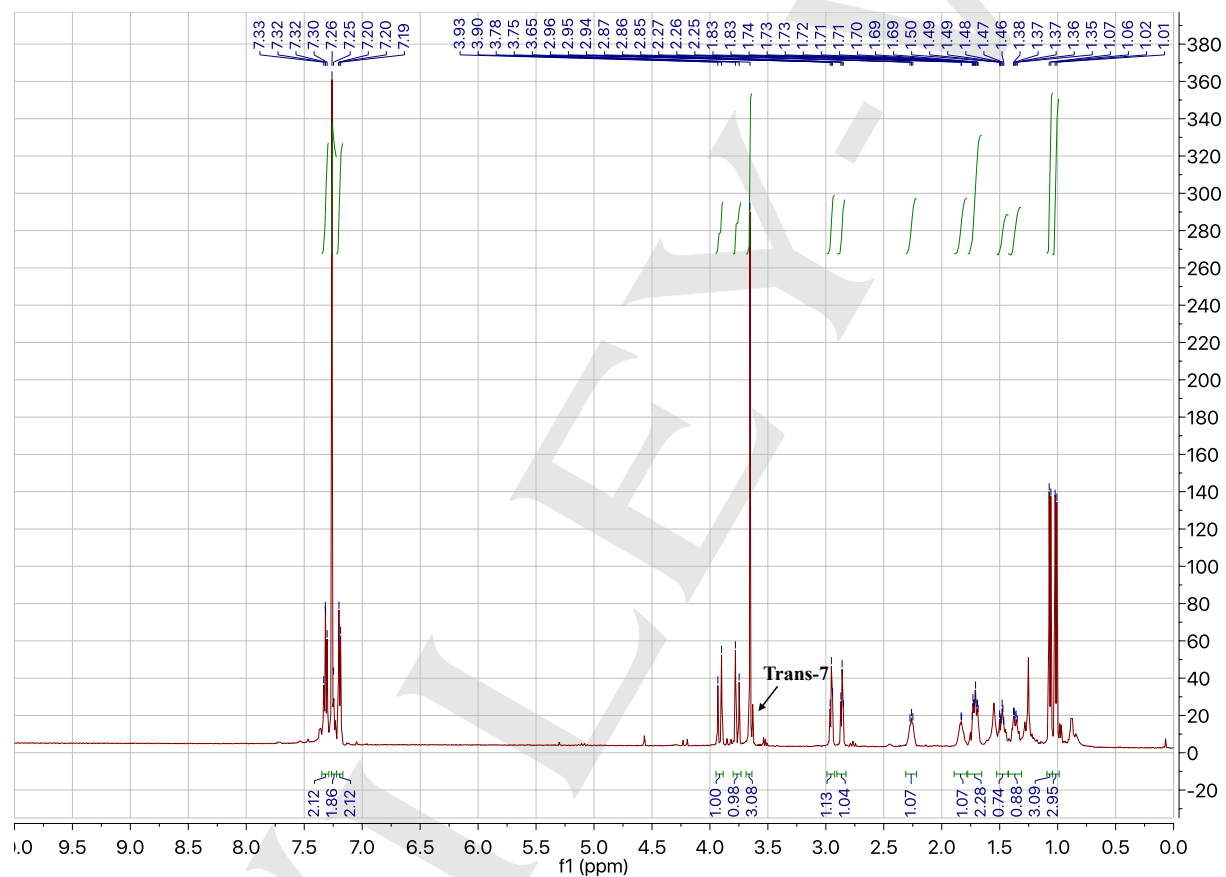
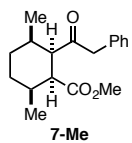
SUPPORTING INFORMATION

 ^1H NMR (501 MHz, CDCl_3): methyl (1*S*,2*R*)-2-(2-phenylacetyl)cyclopropane-1-carboxylate (6-Me)

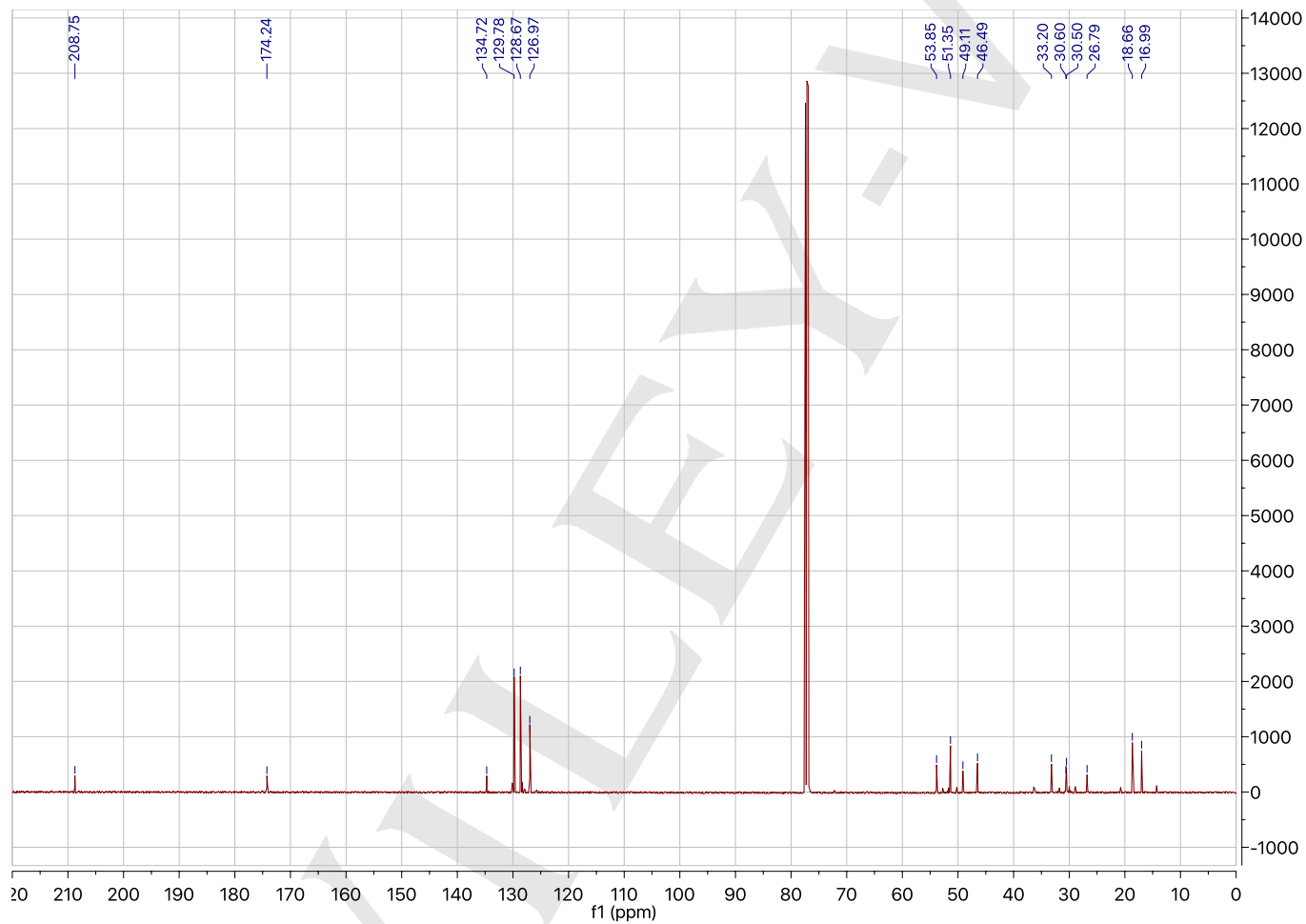
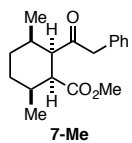
SUPPORTING INFORMATION

 ^{13}C NMR (126 MHz, CDCl_3): methyl (1*S*,2*R*)-2-(2-phenylacetyl)cyclopropane-1-carboxylate (6-Me)

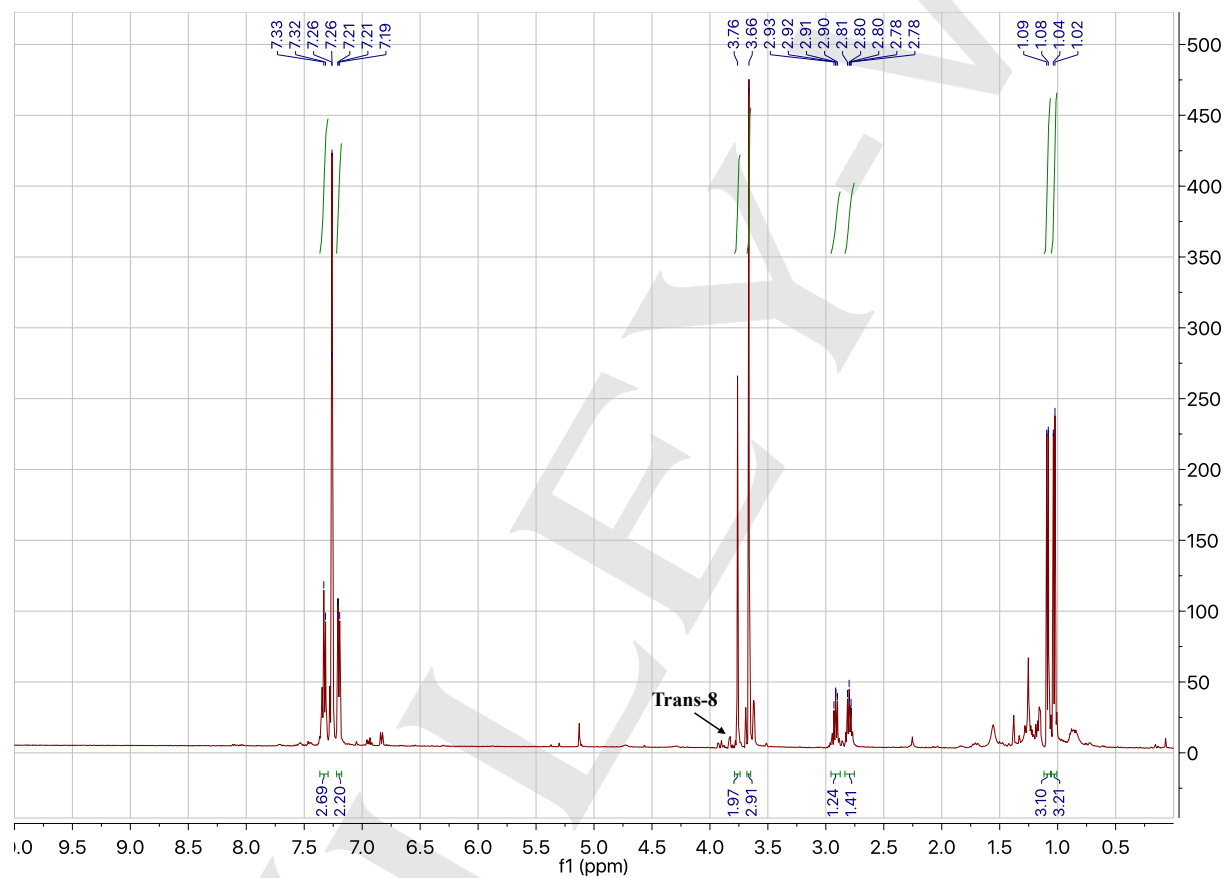
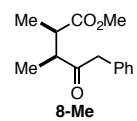
SUPPORTING INFORMATION

 ^1H NMR (501 MHz, CDCl_3): methyl (1*S*,2*R*,3*R*,6*S*)-3,6-dimethyl-2-(2-phenylacetyl)cyclohexane-1-carboxylate (7-Me)

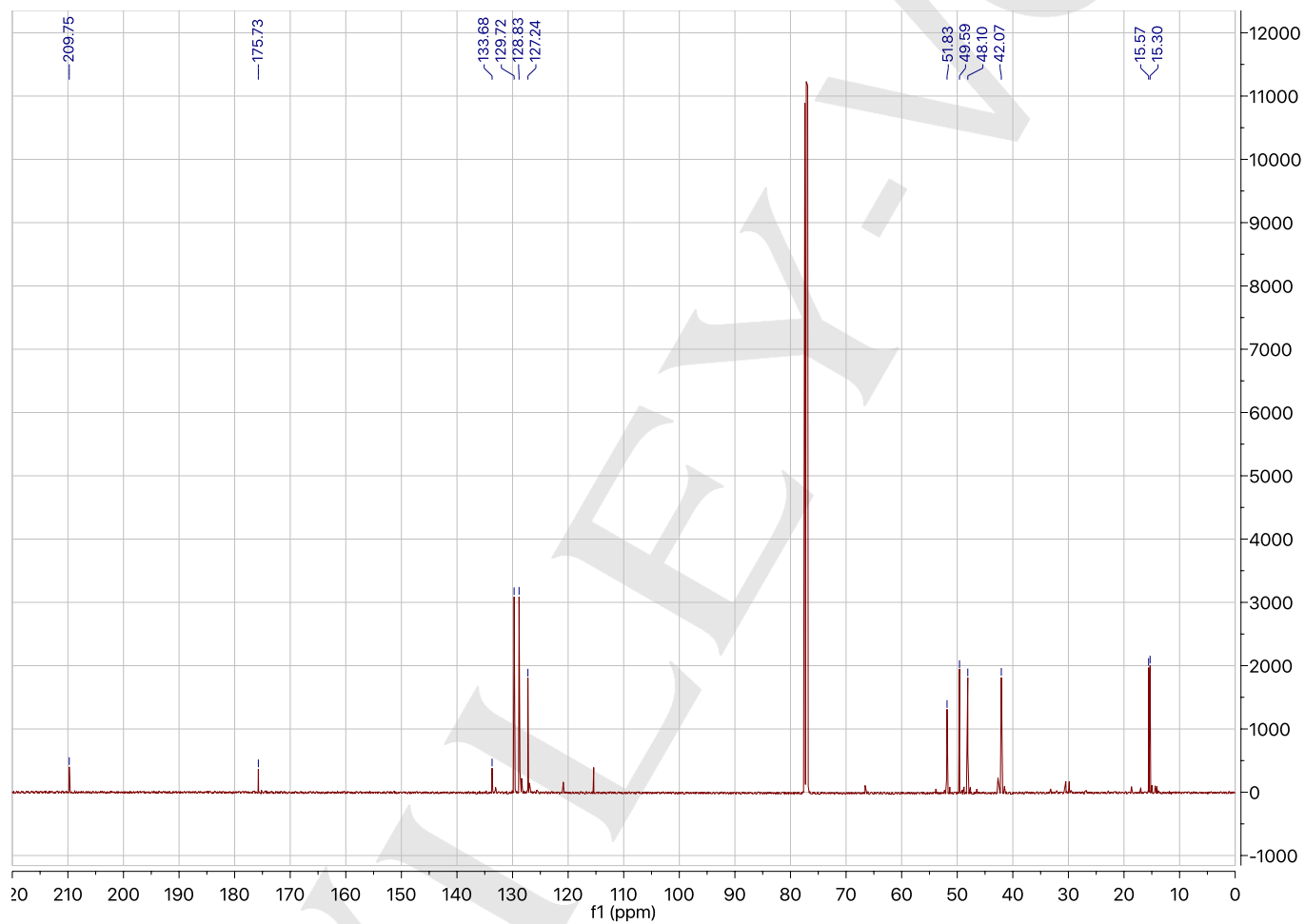
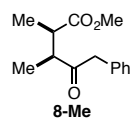
SUPPORTING INFORMATION

 ^{13}C NMR (126 MHz, CDCl_3): methyl (1*S*,2*R*,3*R*,6*S*)-3,6-dimethyl-2-(2-phenylacetyl)cyclohexane-1-carboxylate (7-Me)

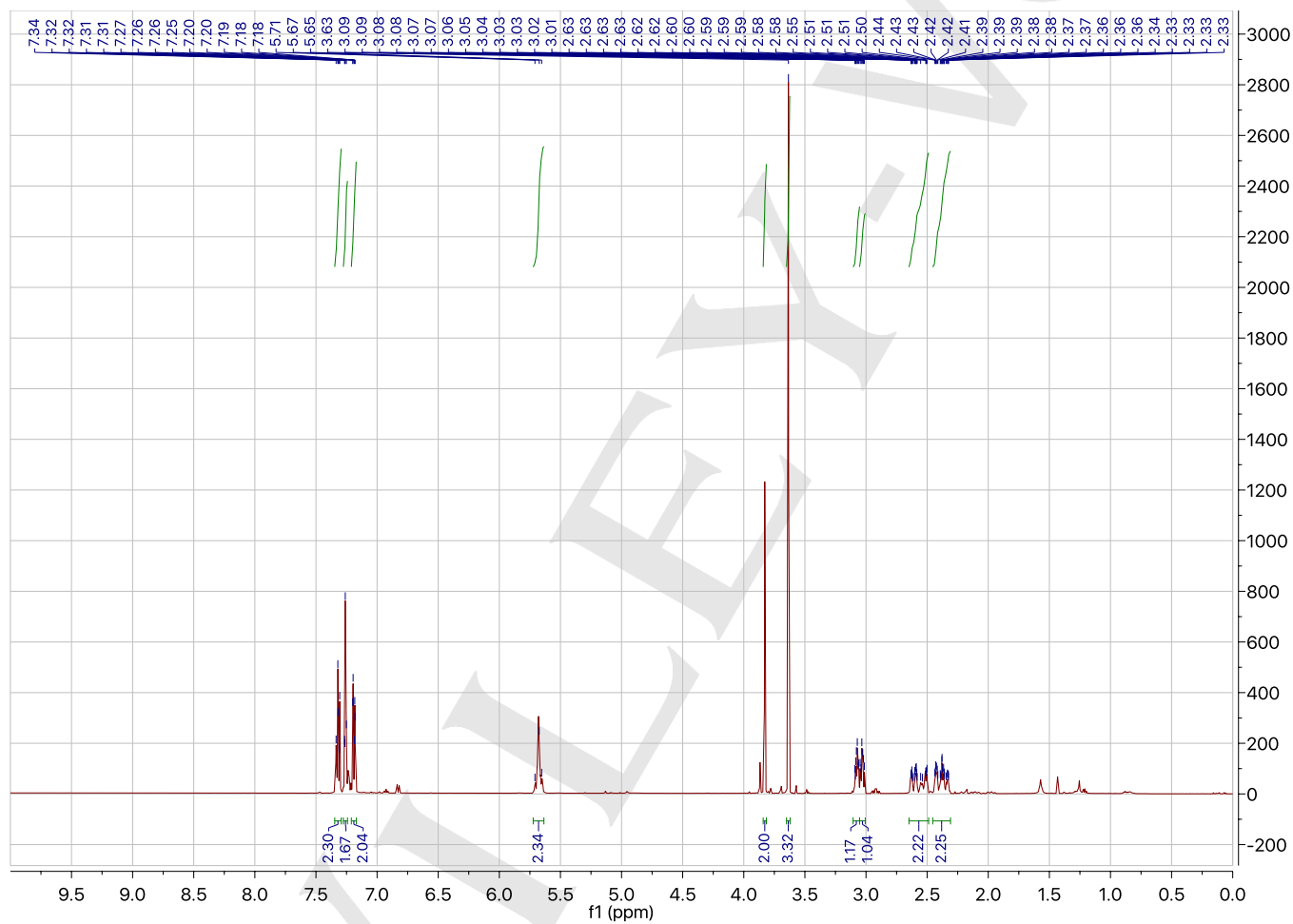
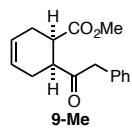
SUPPORTING INFORMATION

 ^1H NMR (501 MHz, CDCl_3): methyl (2*R*,3*S*)-2,3-dimethyl-4-oxo-5-phenylpentanoate (8-Me)

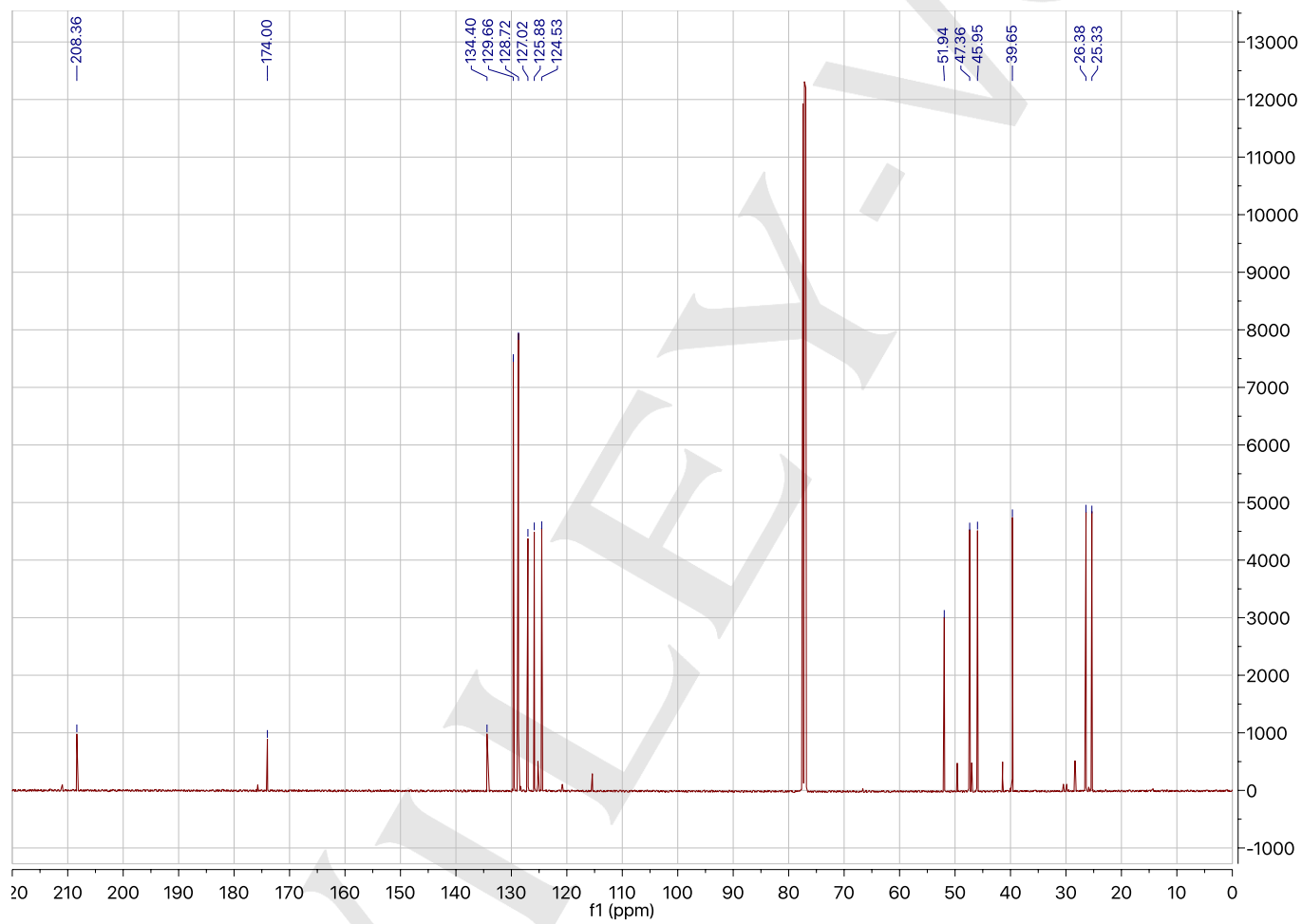
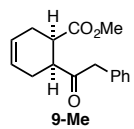
SUPPORTING INFORMATION

 ^{13}C NMR (126 MHz, CDCl_3): methyl (2*R*,3*S*)-2,3-dimethyl-4-oxo-5-phenylpentanoate (8-Me)

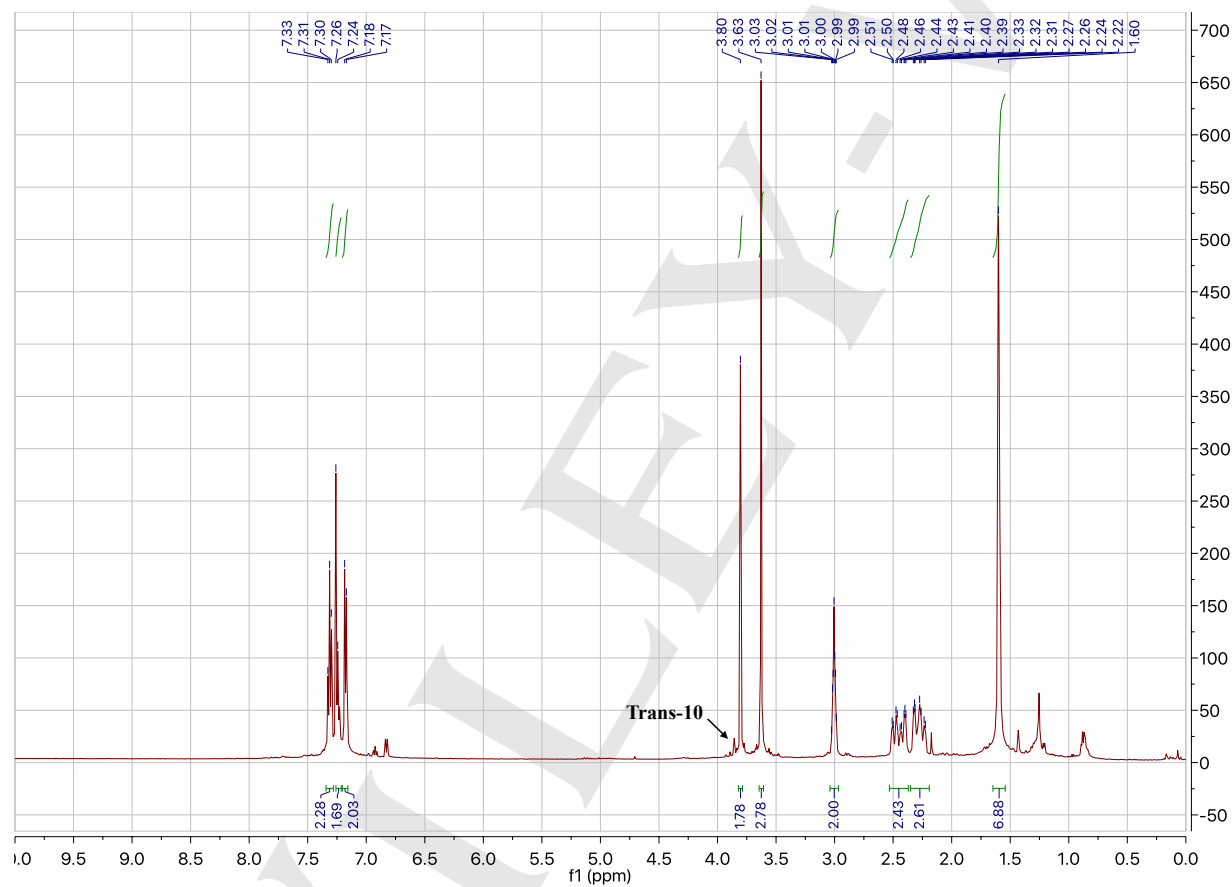
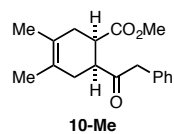
SUPPORTING INFORMATION

 ^1H NMR (501 MHz, CDCl_3): methyl (1*R*,6*S*)-6-(2-phenylacetyl)cyclohex-3-ene-1-carboxylate (9-Me)

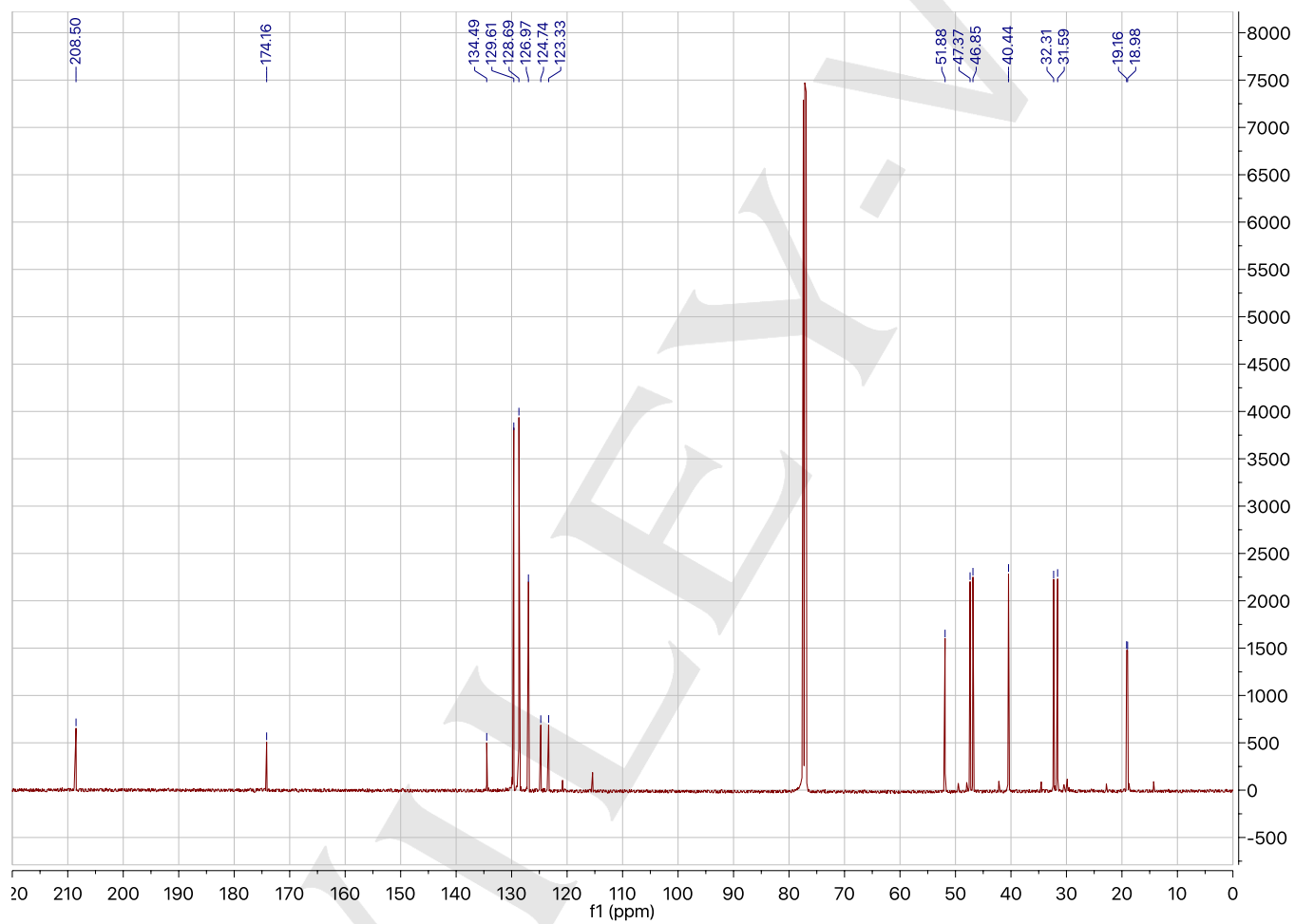
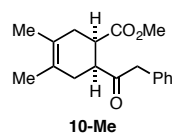
SUPPORTING INFORMATION

 ^{13}C NMR (126 MHz, CDCl_3): methyl (1*R*,6*S*)-6-(2-phenylacetyl)cyclohex-3-ene-1-carboxylate (9-Me)

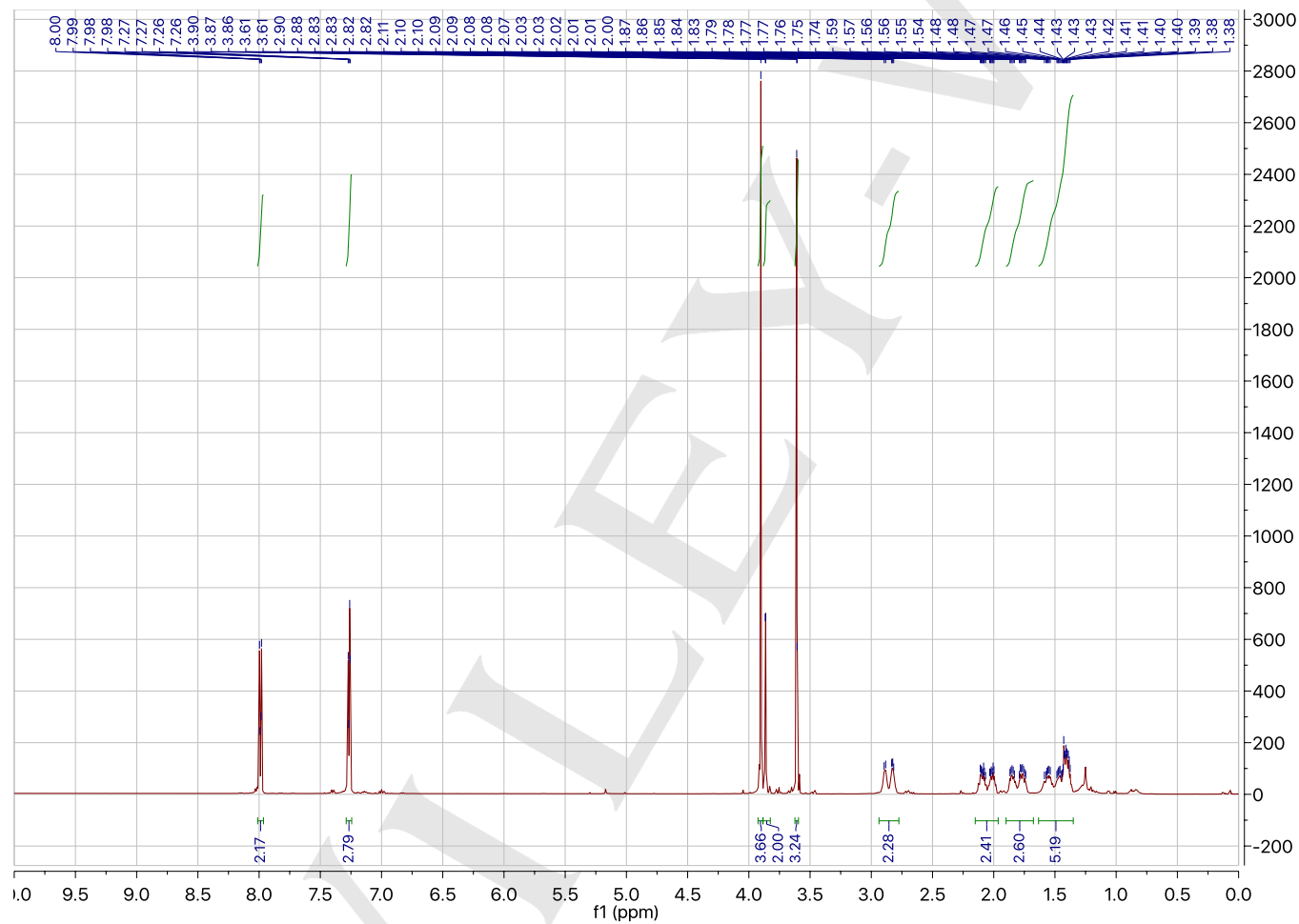
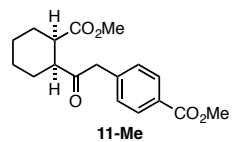
SUPPORTING INFORMATION

 ^1H NMR (501 MHz, CDCl_3): methyl (1*R*,6*S*)-3,4-dimethyl-6-(2-phenylacetyl)cyclohex-3-ene-1-carboxylate (10-Me)

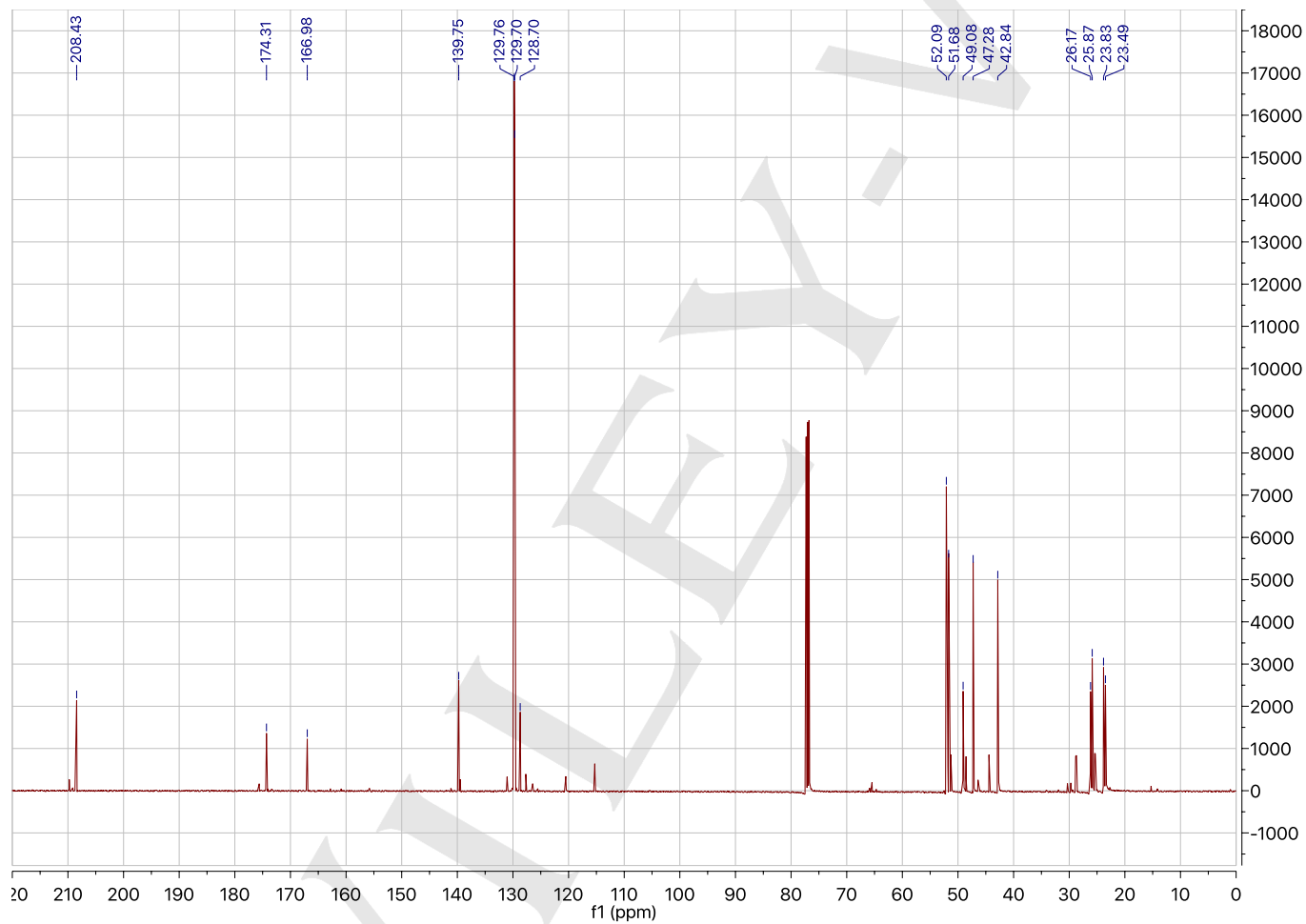
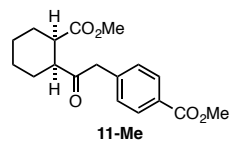
SUPPORTING INFORMATION

 ^{13}C NMR (126 MHz, CDCl_3): methyl (1*R*,6*S*)-3,4-dimethyl-6-(2-phenylacetyl)cyclohex-3-ene-1-carboxylate (10-Me)

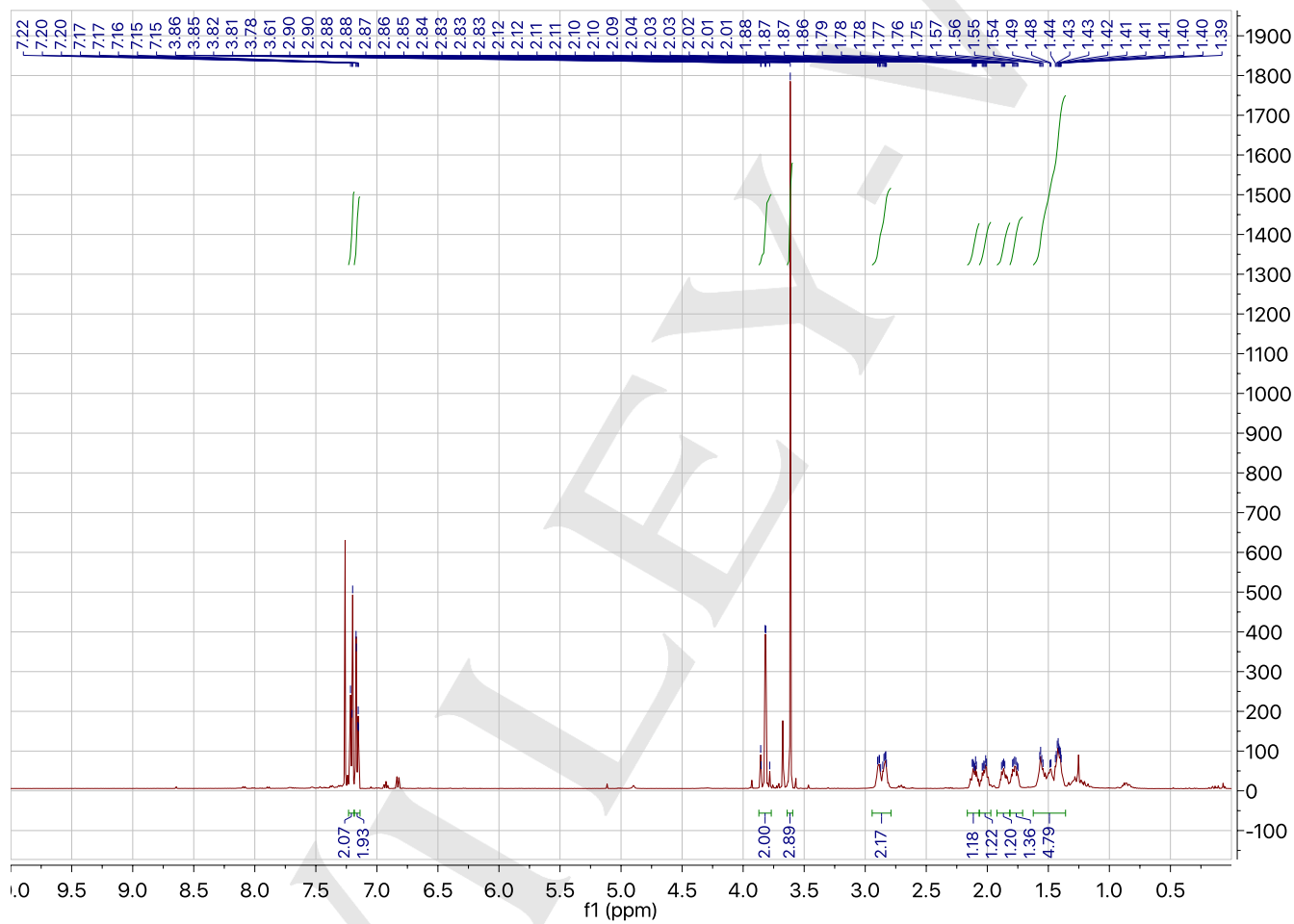
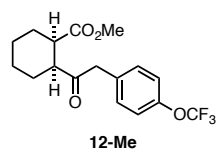
SUPPORTING INFORMATION

 ^1H NMR (501 MHz, CDCl_3): methyl 4-(2-((1*S*,2*R*)-2-(methoxycarbonyl)cyclohexyl)-2-oxoethyl)benzoate (11-Me)

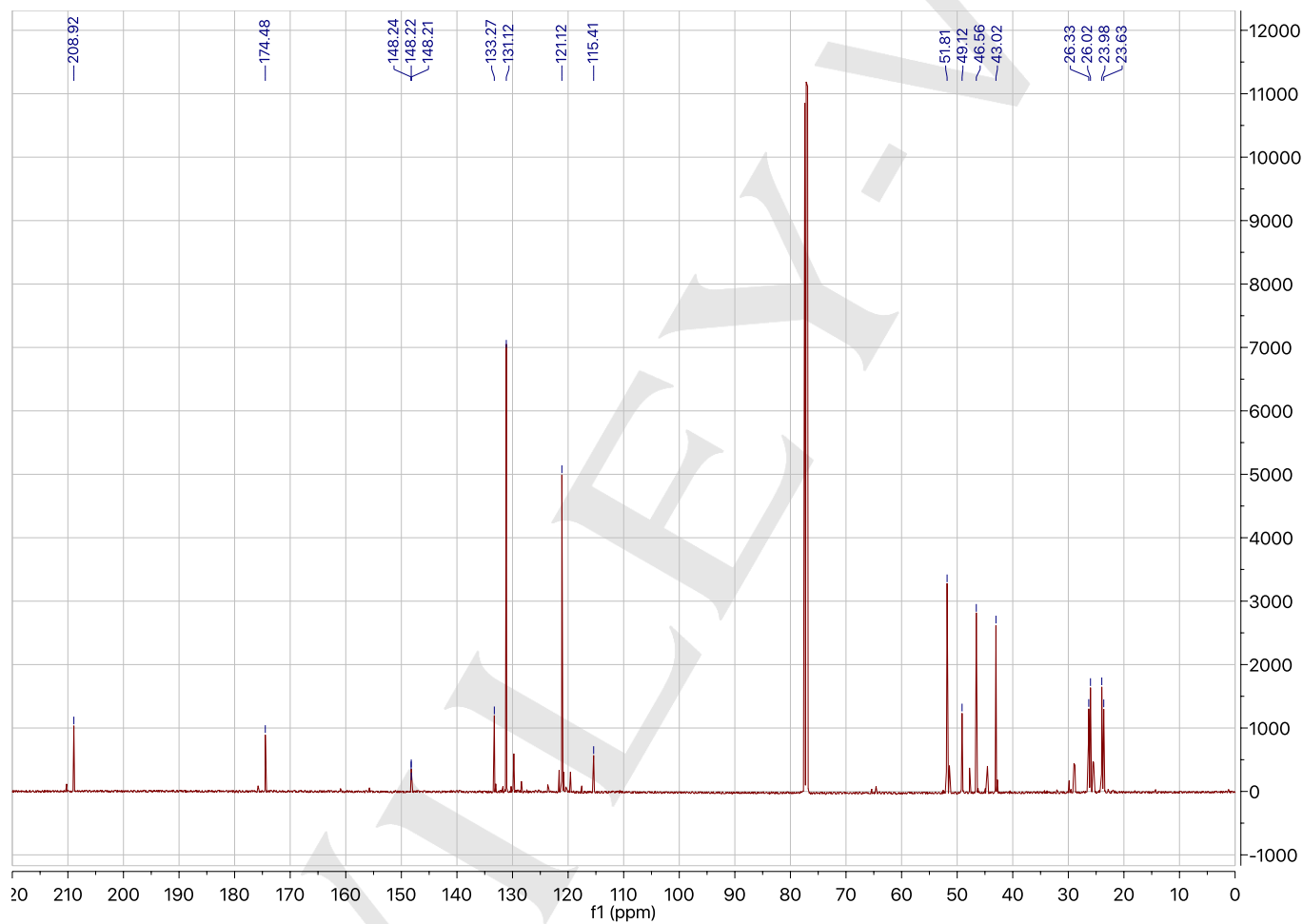
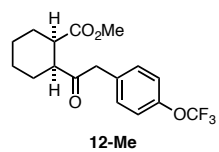
SUPPORTING INFORMATION

 ^{13}C NMR (126 MHz, CDCl_3): methyl 4-(2-((1*S*,2*R*)-2-(methoxycarbonyl)cyclohexyl)-2-oxoethyl)benzoate (11-Me)

SUPPORTING INFORMATION

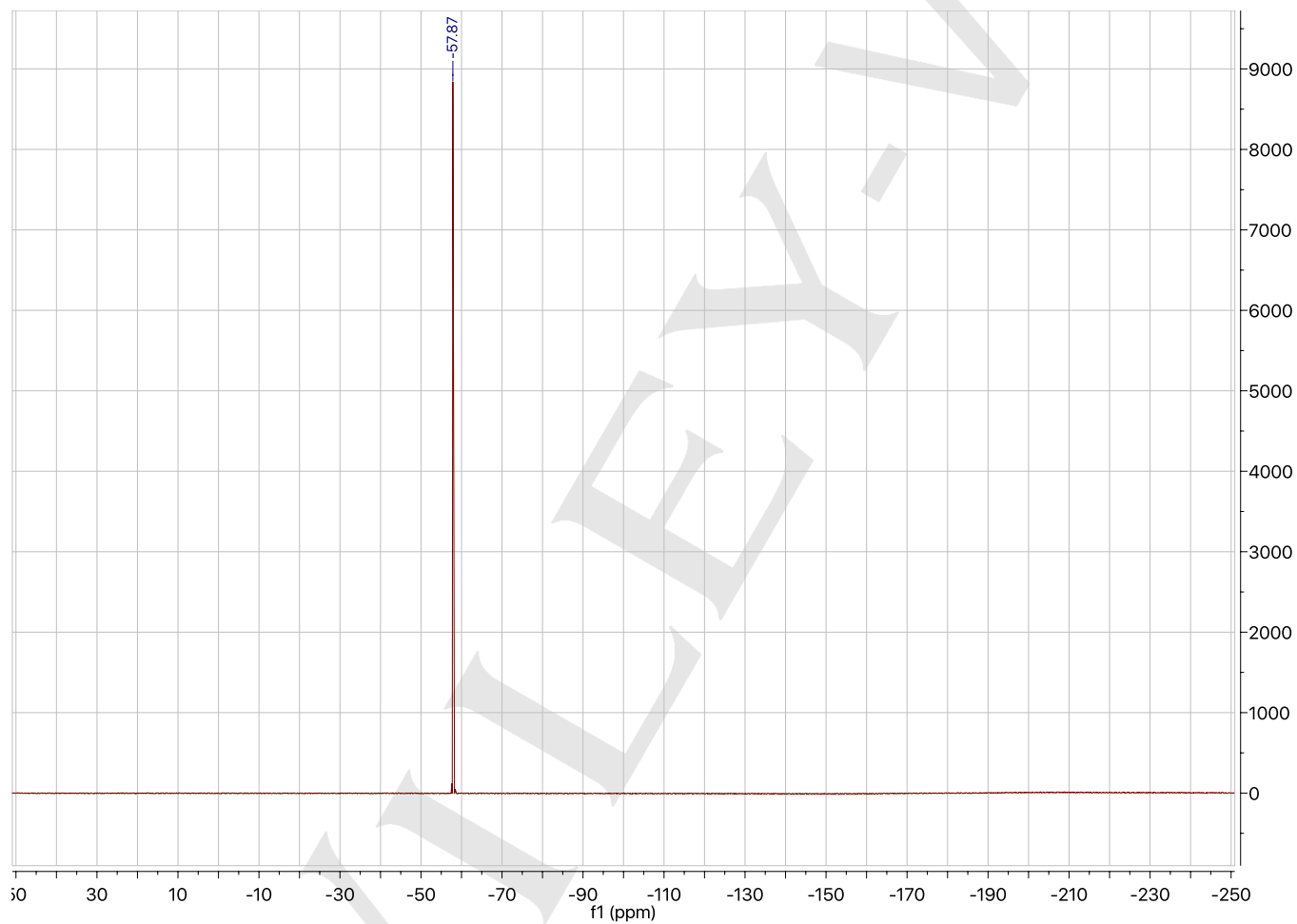
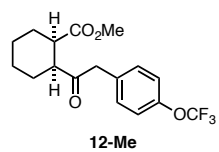
 ^1H NMR (501 MHz, CDCl_3): methyl (1*R*,2*S*)-2-(2-(4-(trifluoromethoxy)phenyl)acetyl)cyclohexane-1-carboxylate (12-Me)

SUPPORTING INFORMATION

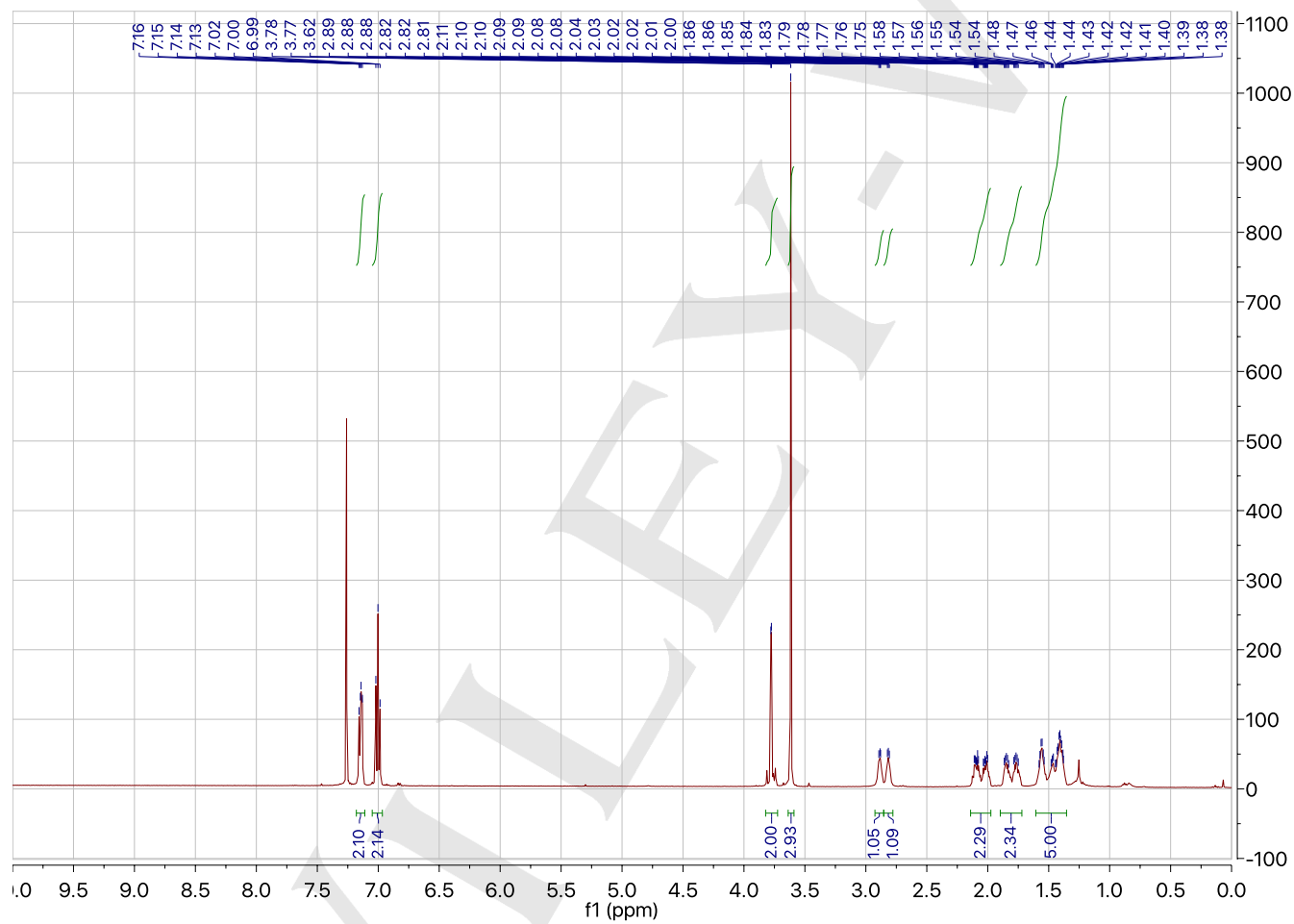
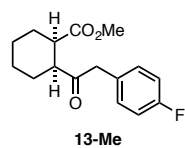
 ^{13}C NMR (126 MHz, CDCl_3): methyl (1*R*,2*S*)-2-(2-(4-(trifluoromethoxy)phenyl)acetyl)cyclohexane-1-carboxylate (12-Me)

SUPPORTING INFORMATION

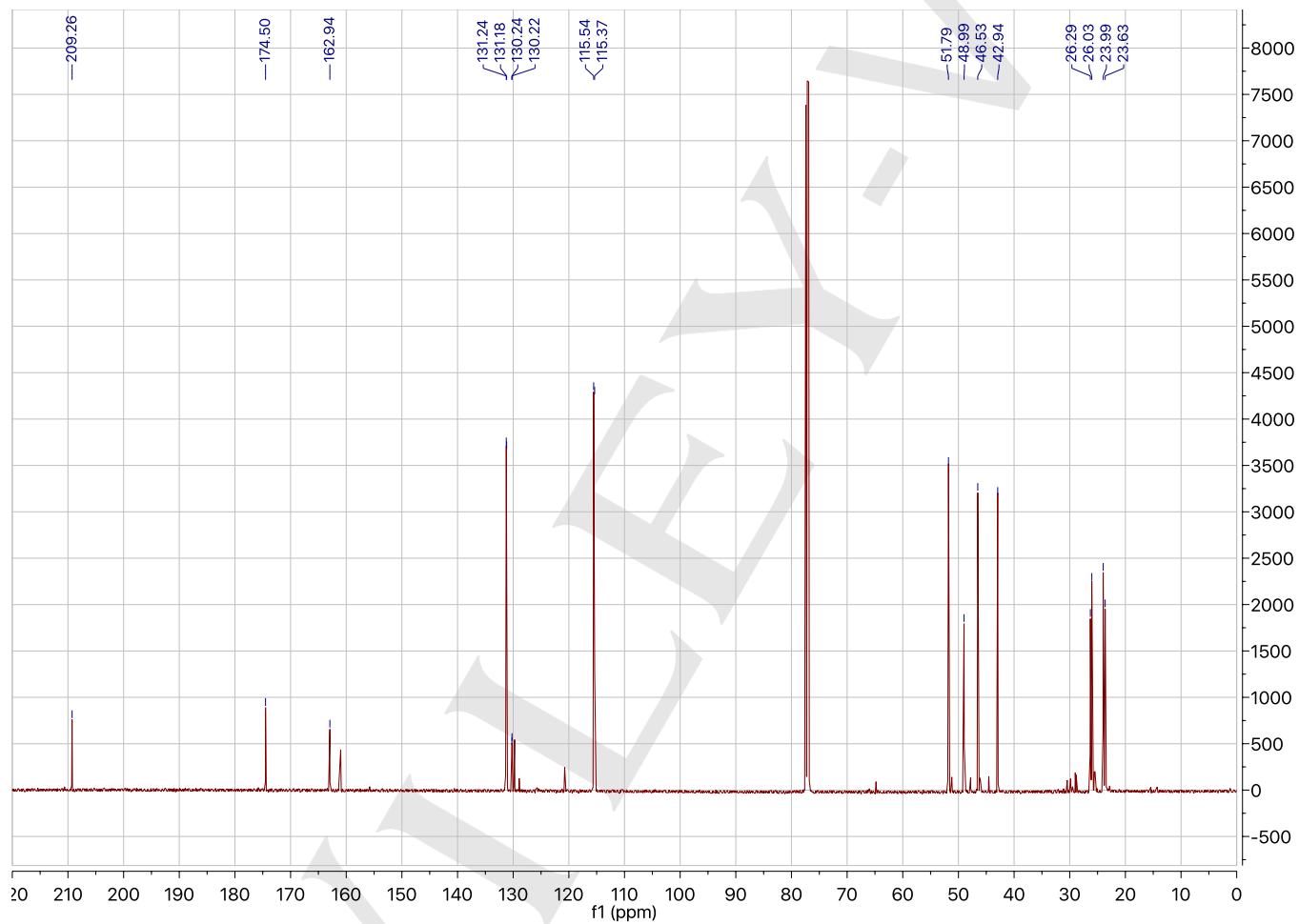
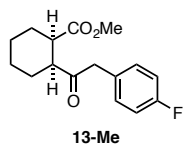
¹⁹F NMR (282 MHz, CDCl₃): methyl (1R,2S)-2-(2-(4-(trifluoromethoxy)phenyl)acetyl)cyclohexane-1-carboxylate (12-Me)



SUPPORTING INFORMATION

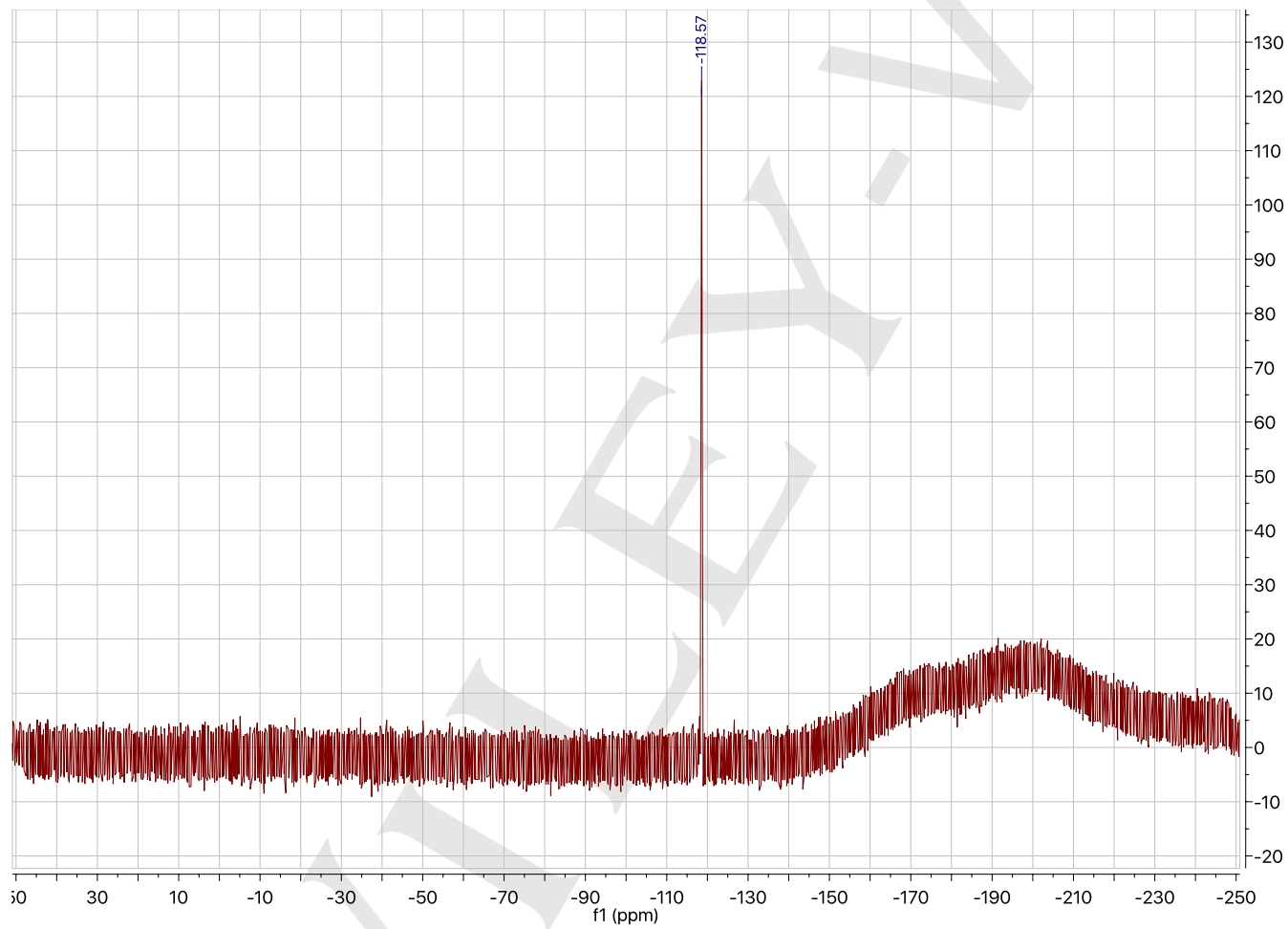
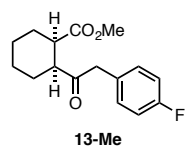
 ^1H NMR (501 MHz, CDCl_3): methyl (1*R*,2*S*)-2-(2-(4-fluorophenyl)acetyl)cyclohexane-1-carboxylate (13-Me)

SUPPORTING INFORMATION

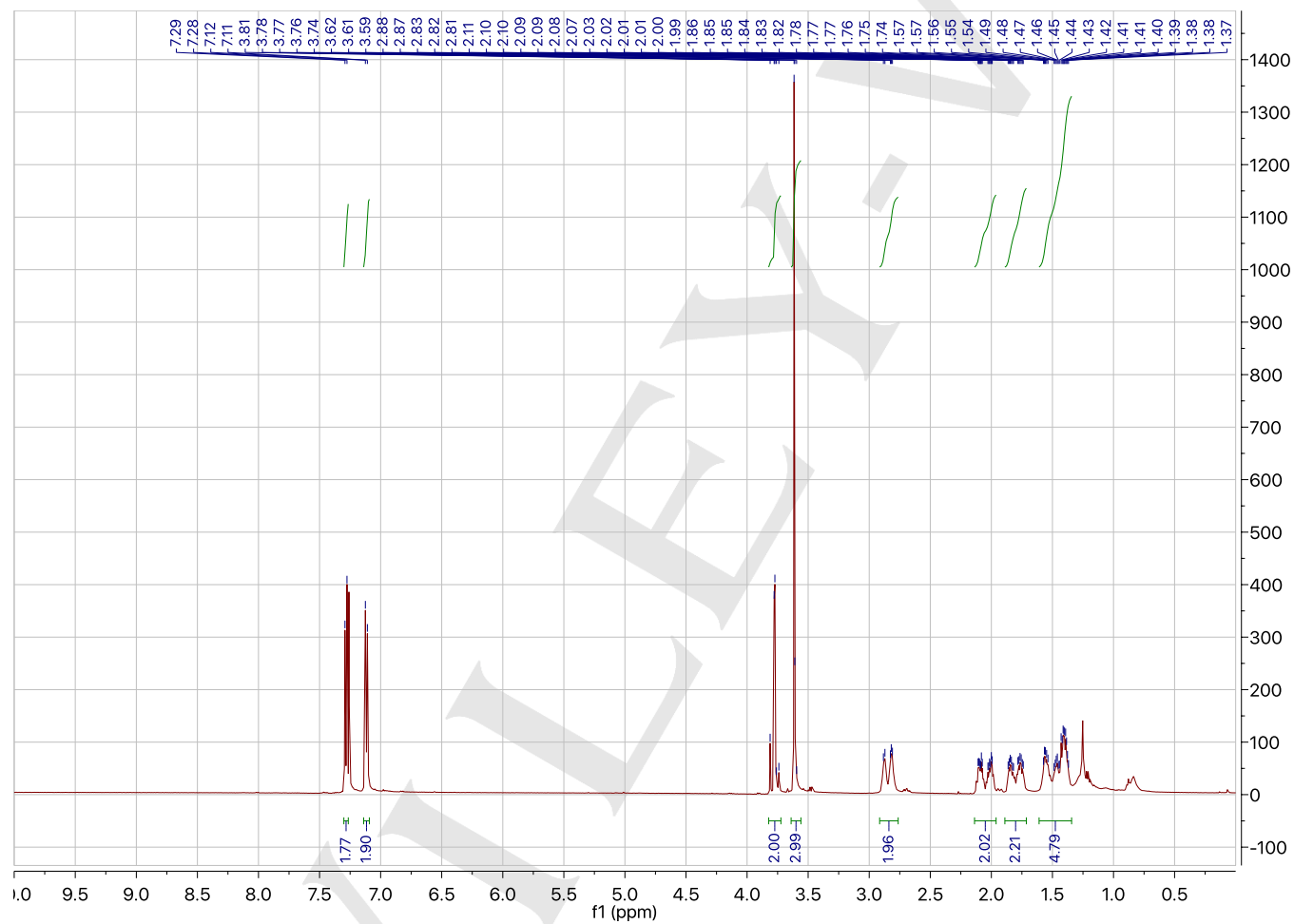
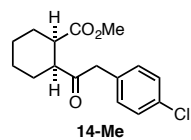
 ^{13}C NMR (126 MHz, CDCl_3): methyl (1*R*,2*S*)-2-(2-(4-fluorophenyl)acetyl)cyclohexane-1-carboxylate (13-Me)

SUPPORTING INFORMATION

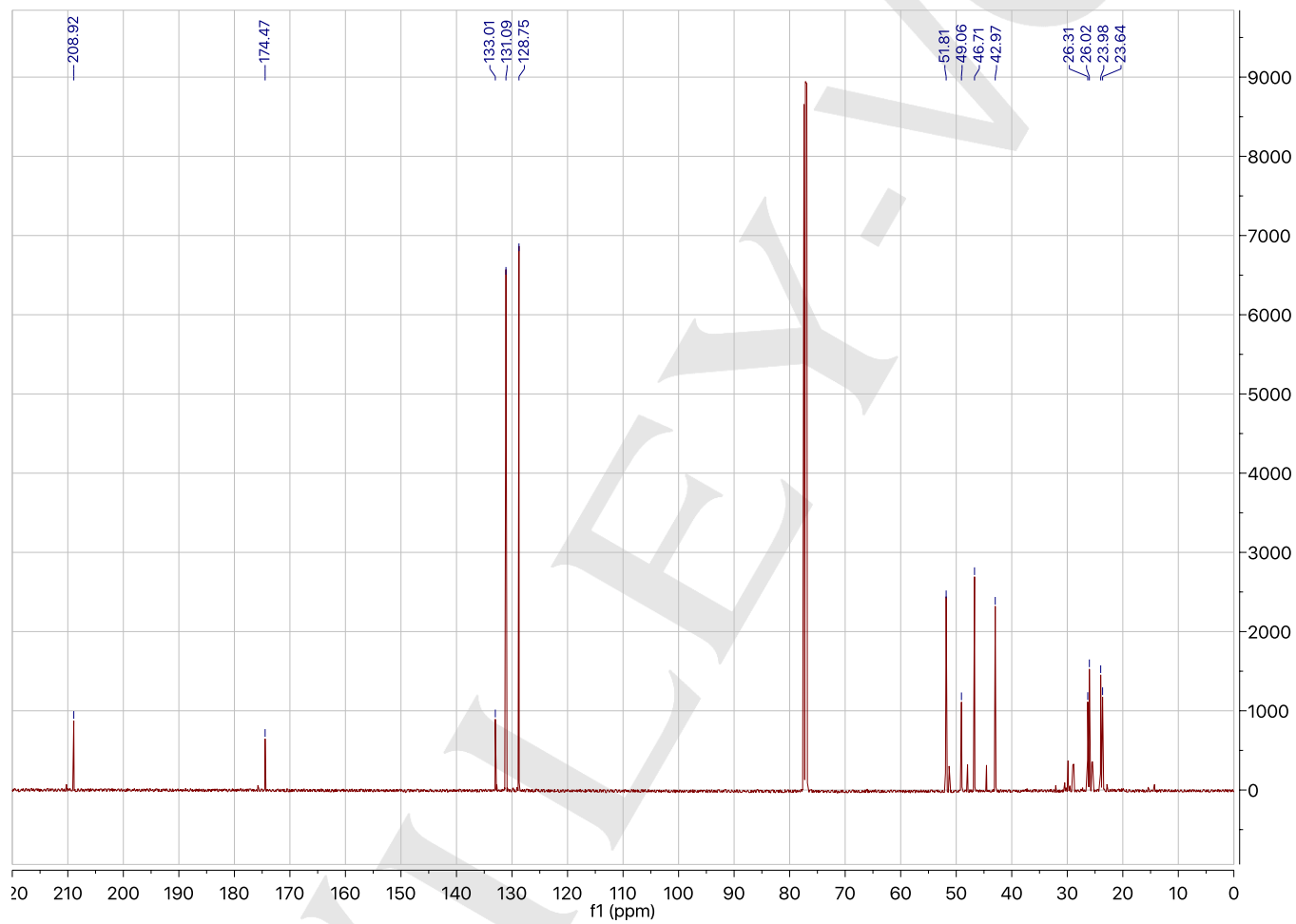
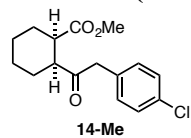
^{19}F NMR (282 MHz, CDCl_3): methyl (1*R*,2*S*)-2-(2-(4-fluorophenyl)acetyl)cyclohexane-1-carboxylate (13-Me)



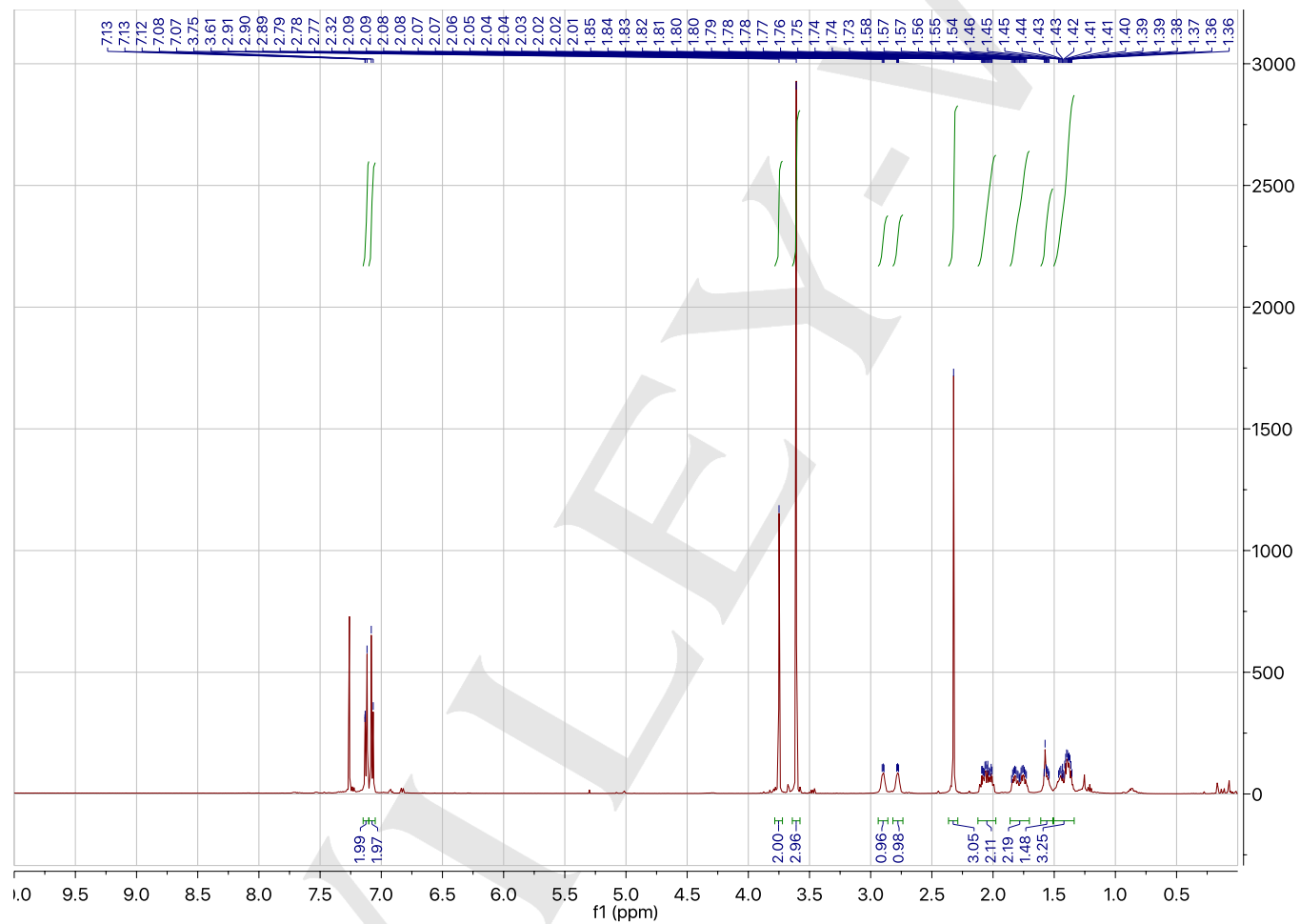
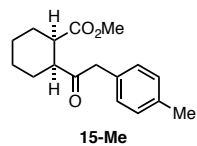
SUPPORTING INFORMATION

¹H NMR (501 MHz, CDCl₃): methyl (1*R*,2*S*)-2-(2-(4-chlorophenyl)acetyl)cyclohexane-1-carboxylate (14-Me)

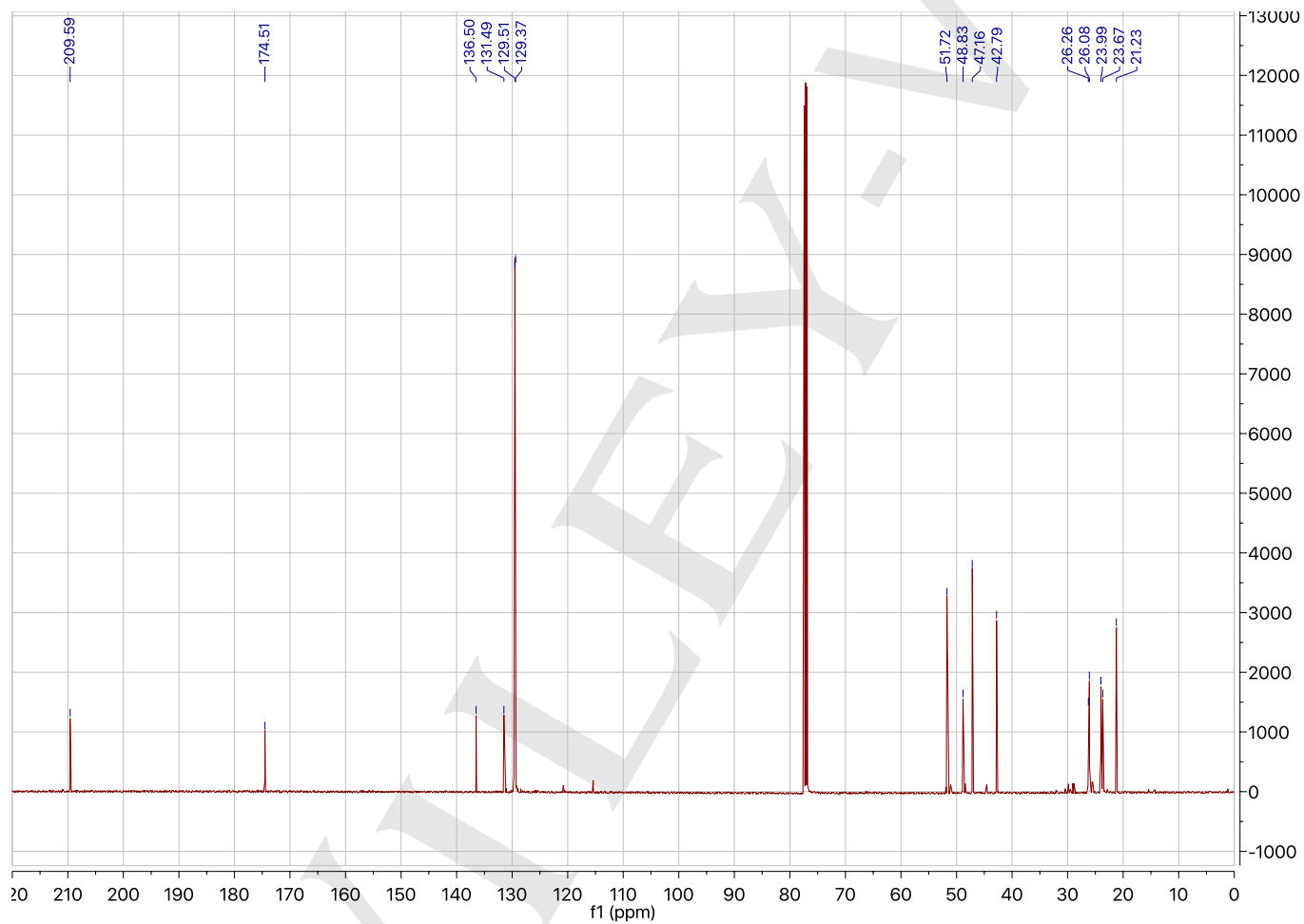
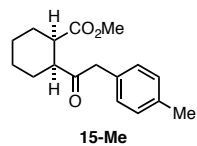
SUPPORTING INFORMATION

 ^{13}C NMR (126 MHz, CDCl_3): methyl (1*R*,2*S*)-2-(2-(4-chlorophenyl)acetyl)cyclohexane-1-carboxylate (14-Me)

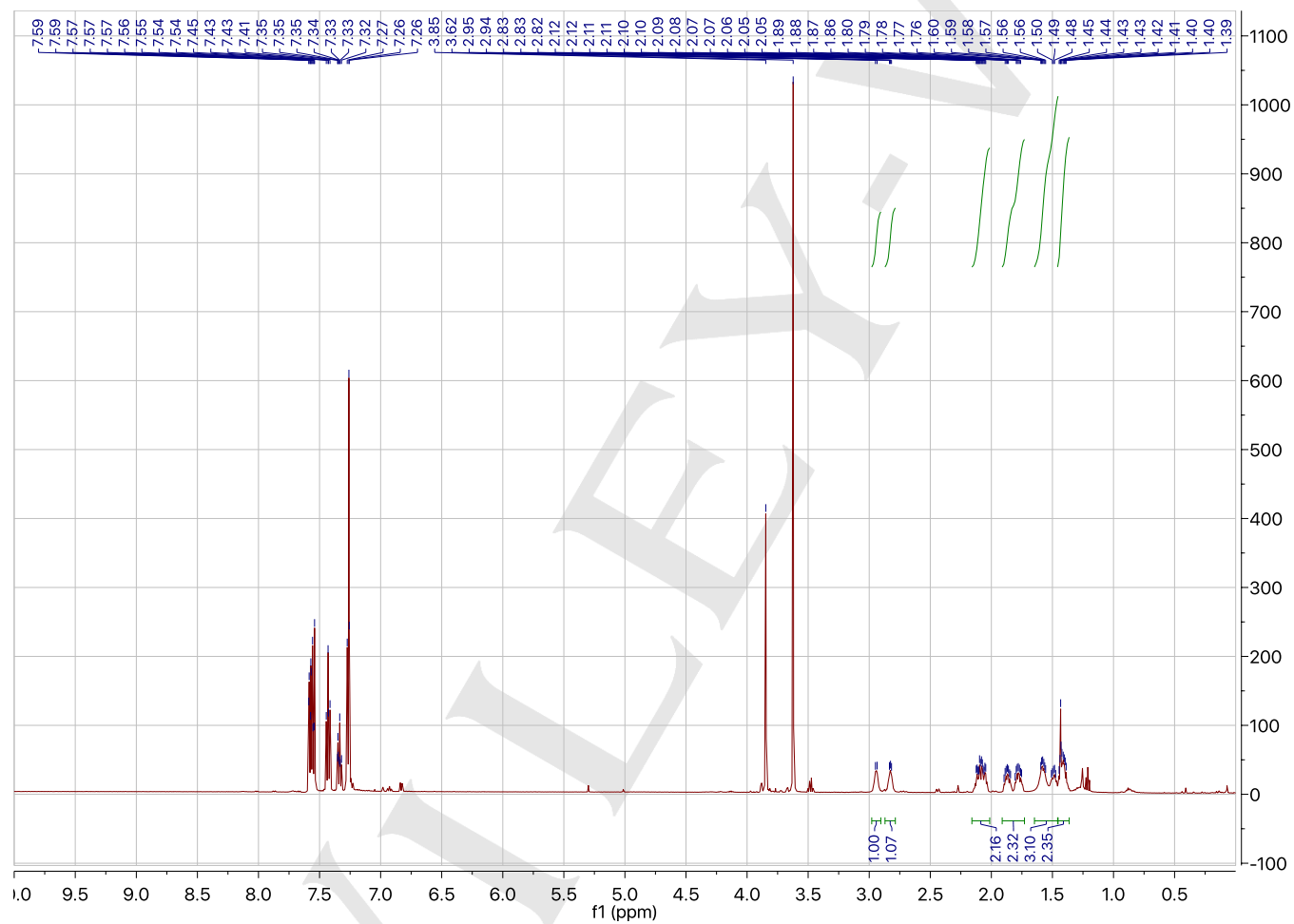
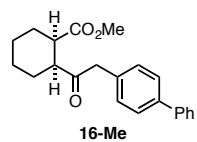
SUPPORTING INFORMATION

 ^1H NMR (501 MHz, CDCl_3): methyl (1*R*,2*S*)-2-(2-(*p*-tolyl)acetyl)cyclohexane-1-carboxylate (15-Me)

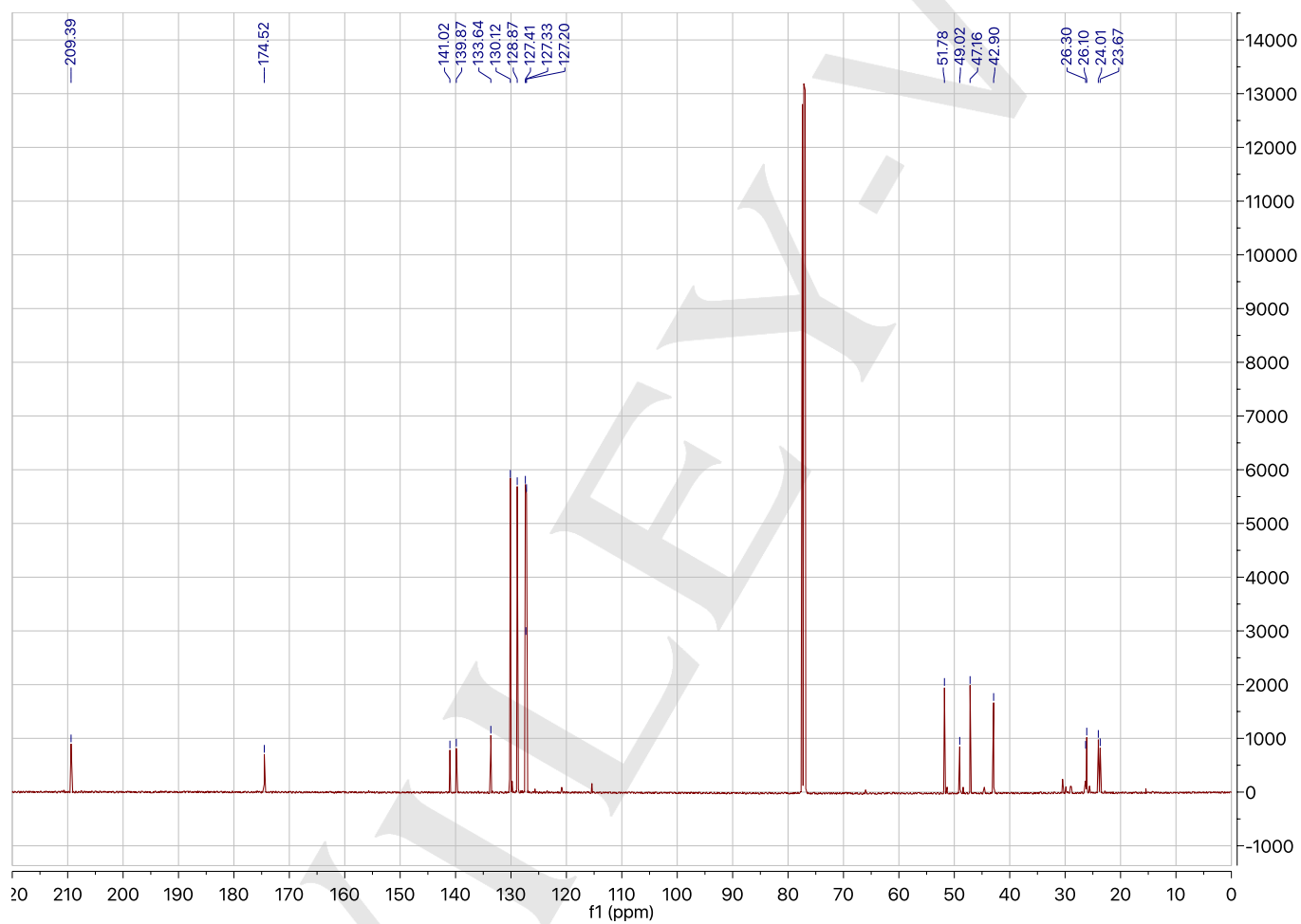
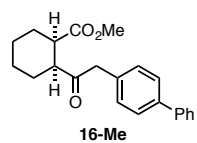
SUPPORTING INFORMATION

 ^{13}C NMR (126 MHz, CDCl_3): methyl (1*R*,2*S*)-2-(2-(*p*-tolyl)acetyl)cyclohexane-1-carboxylate (15-Me)

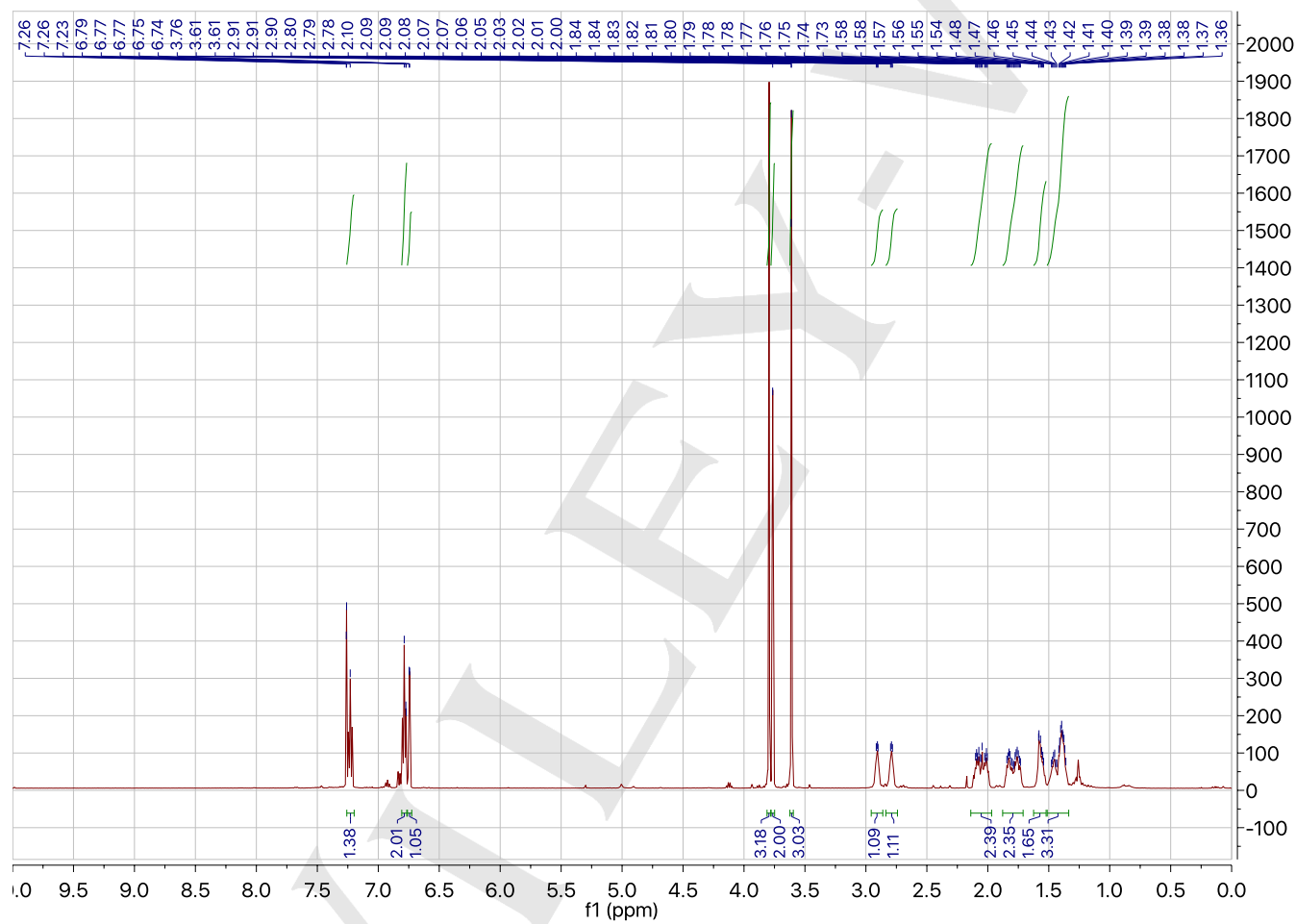
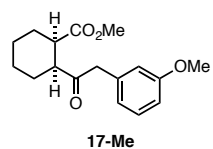
SUPPORTING INFORMATION

 ^1H NMR (501 MHz, CDCl_3): methyl (1*R*,2*S*)-2-(2-([1,1'-biphenyl]-4-yl)acetyl)cyclohexane-1-carboxylate (16-Me)

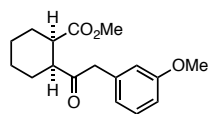
SUPPORTING INFORMATION

 ^{13}C NMR (126 MHz, CDCl_3): methyl (1*R*,2*S*)-2-(2-([1,1'-biphenyl]-4-yl)acetyl)cyclohexane-1-carboxylate (16-Me)

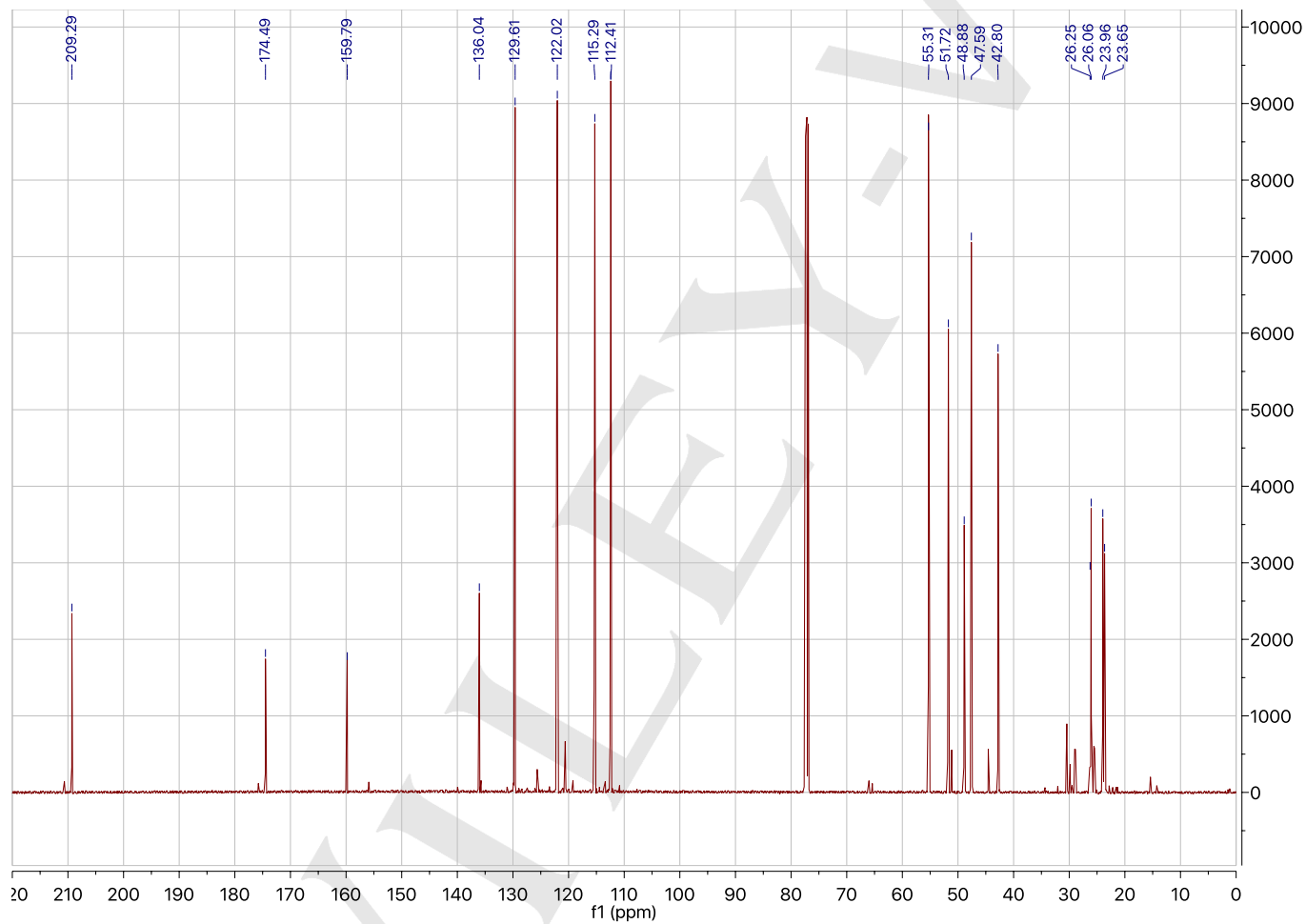
SUPPORTING INFORMATION

 ^1H NMR (501 MHz, CDCl_3): methyl (1*R*,2*S*)-2-(2-(3-methoxyphenyl)acetyl)cyclohexane-1-carboxylate (17-Me)

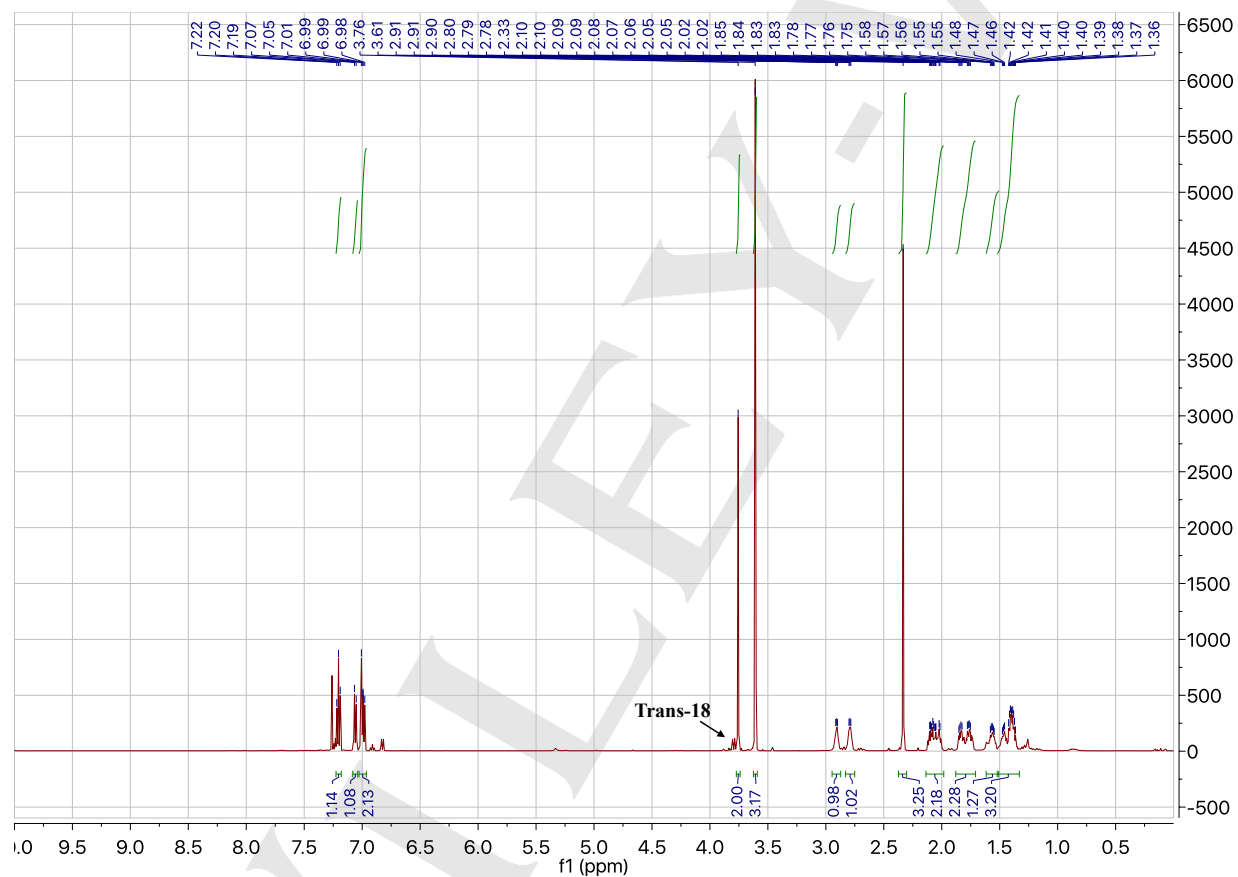
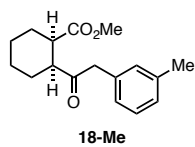
SUPPORTING INFORMATION

 ^{13}C NMR (126 MHz, CDCl_3): methyl (1*R*,2*S*)-2-(2-(3-methoxyphenyl)acetyl)cyclohexane-1-carboxylate (17-Me)

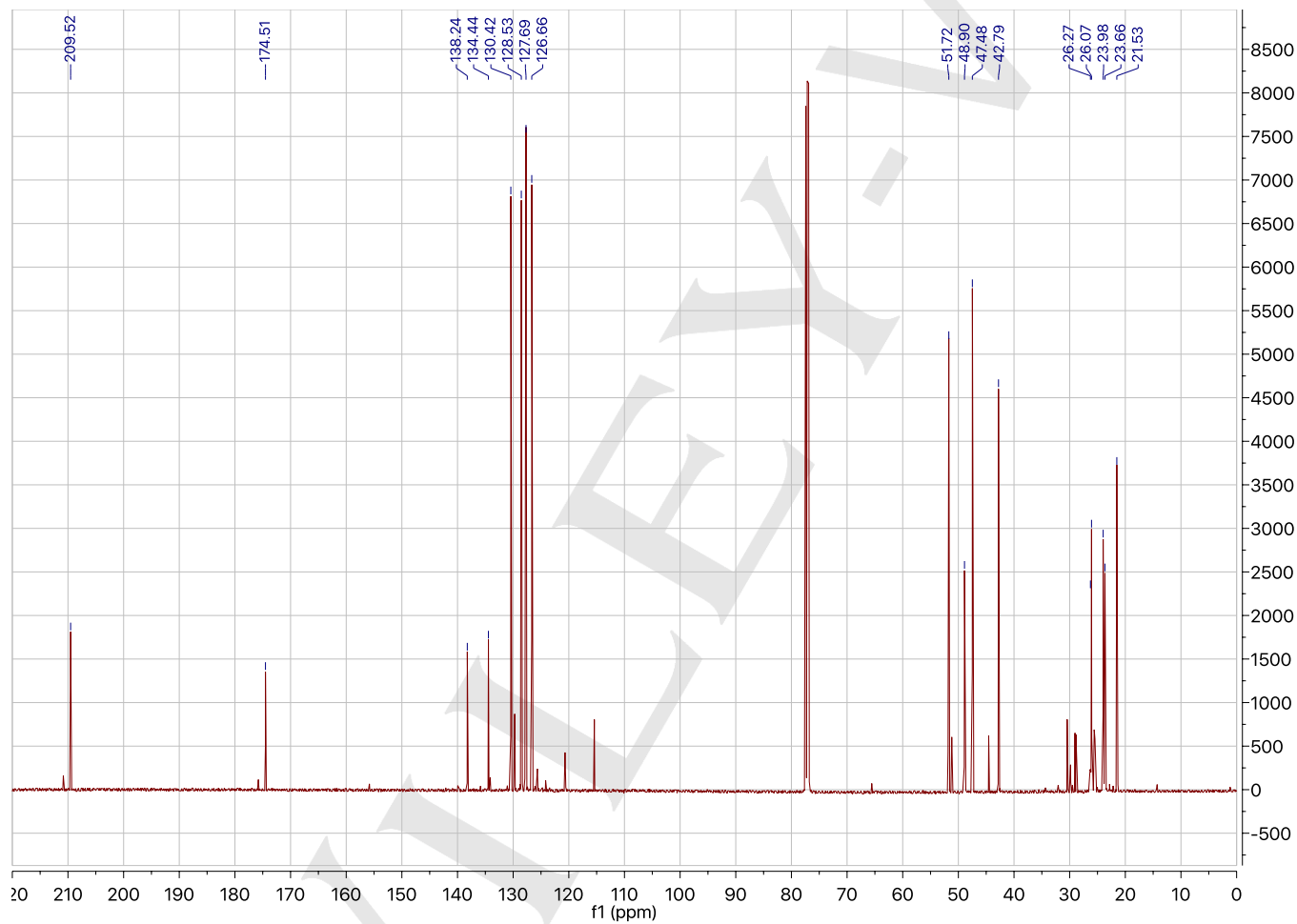
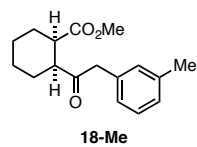
17-Me



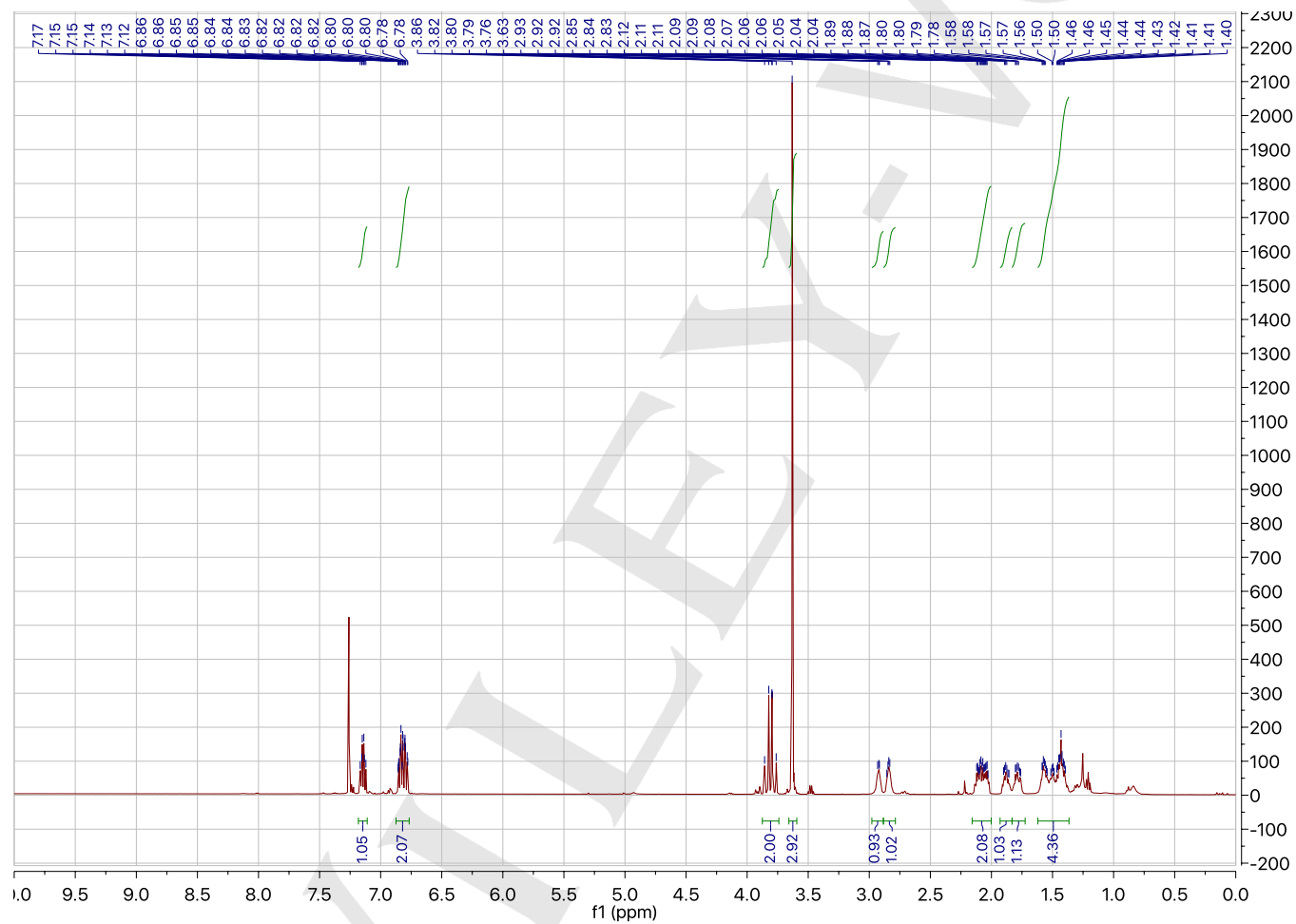
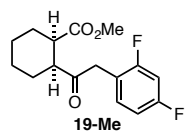
SUPPORTING INFORMATION

 ^1H NMR (501 MHz, CDCl_3): methyl (1*R*,2*S*)-2-(2-(*m*-tolyl)acetyl)cyclohexane-1-carboxylate (18-Me)

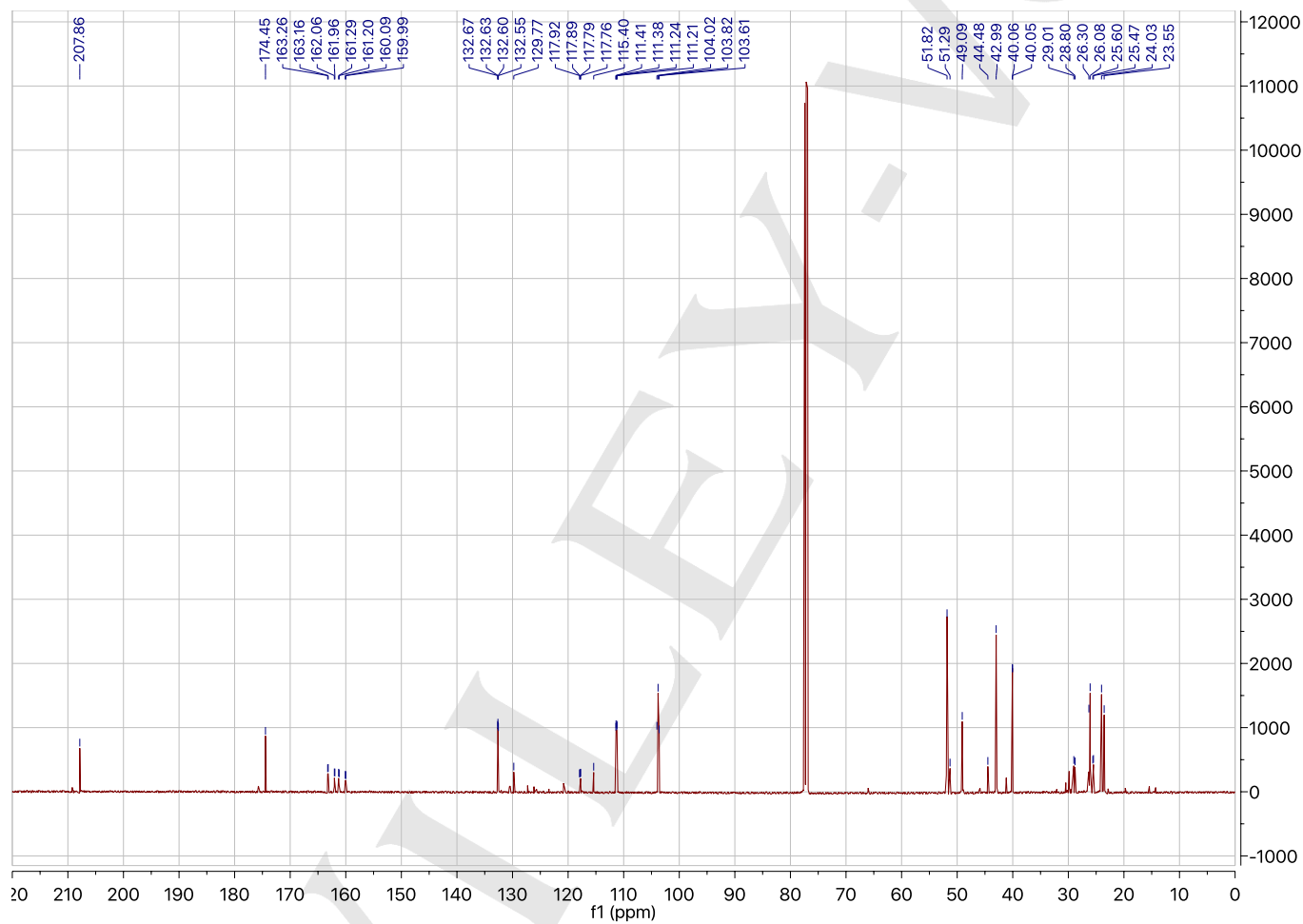
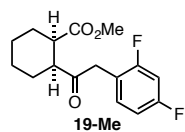
SUPPORTING INFORMATION

 ^{13}C NMR (126 MHz, CDCl_3): methyl (1*R*,2*S*)-2-(2-(*m*-tolyl)acetyl)cyclohexane-1-carboxylate (18-Me)

SUPPORTING INFORMATION

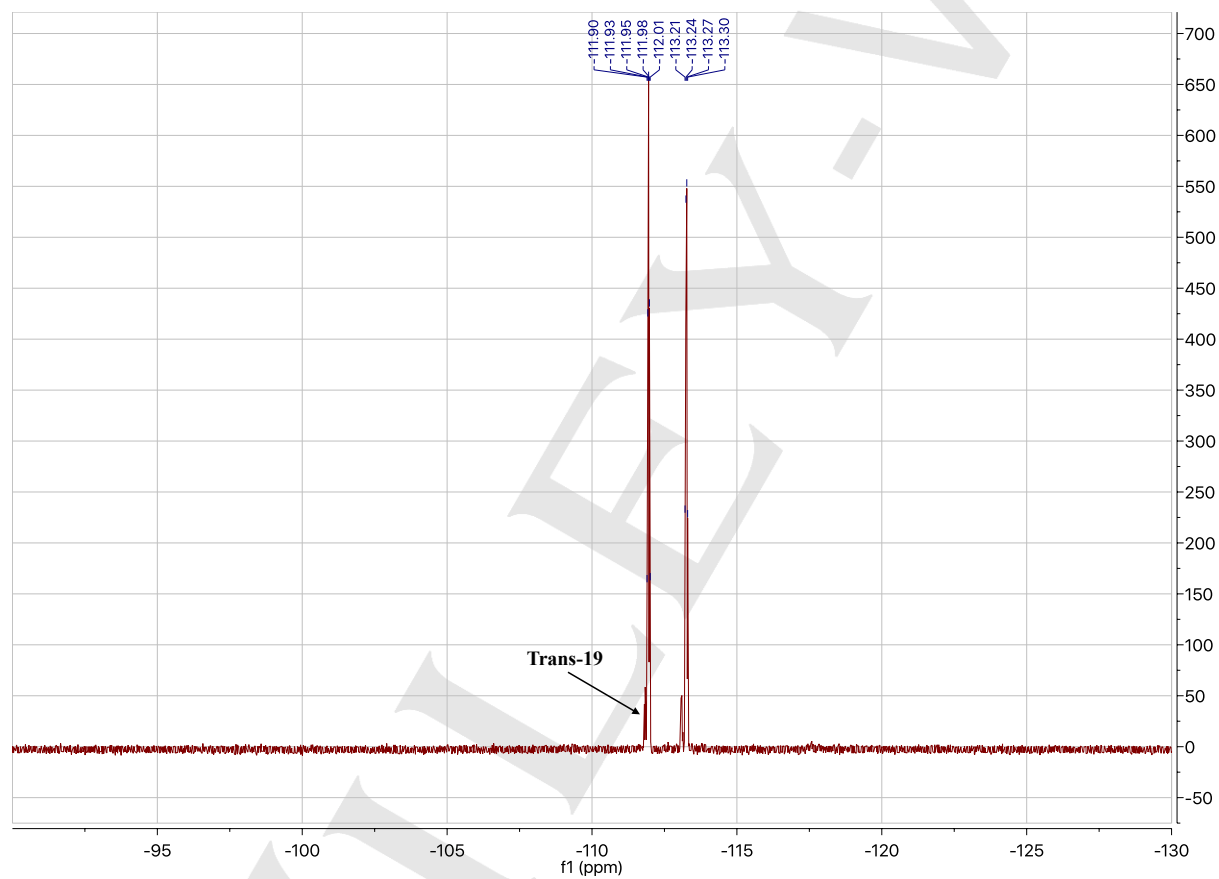
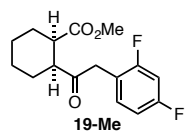
 ^1H NMR (501 MHz, CDCl_3): methyl (1*R*,2*S*)-2-(2-(2,4-difluorophenyl)acetyl)cyclohexane-1-carboxylate (19-Me)

SUPPORTING INFORMATION

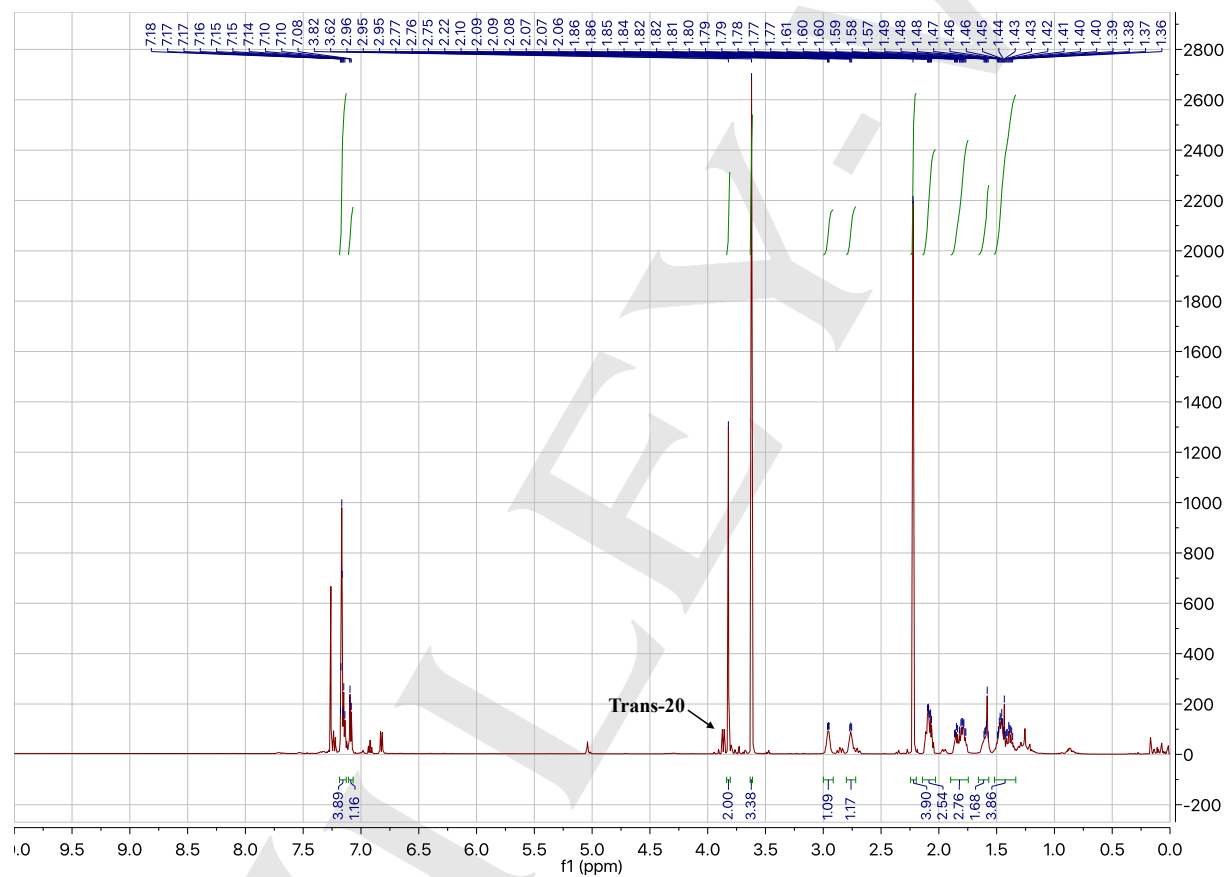
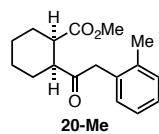
 ^{13}C NMR (126 MHz, CDCl_3): methyl (1*R*,2*S*)-2-(2-(2,4-difluorophenyl)acetyl)cyclohexane-1-carboxylate (19-Me)

SUPPORTING INFORMATION

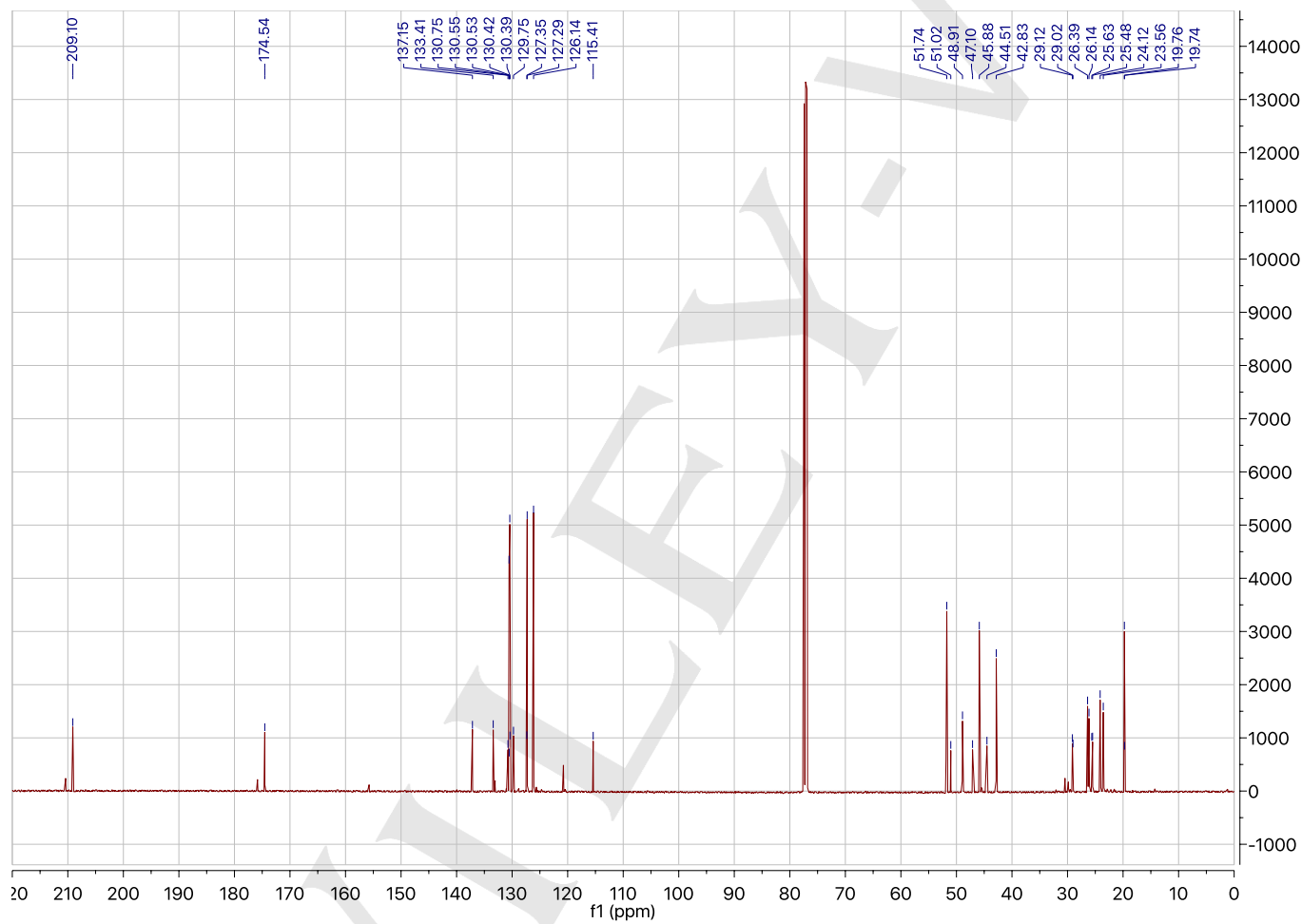
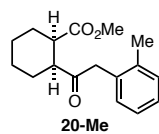
^{19}F NMR (282MHz, CDCl_3): methyl (1*R*,2*S*)-2-(2-(2,4-difluorophenyl)acetyl)cyclohexane-1-carboxylate (19-Me)



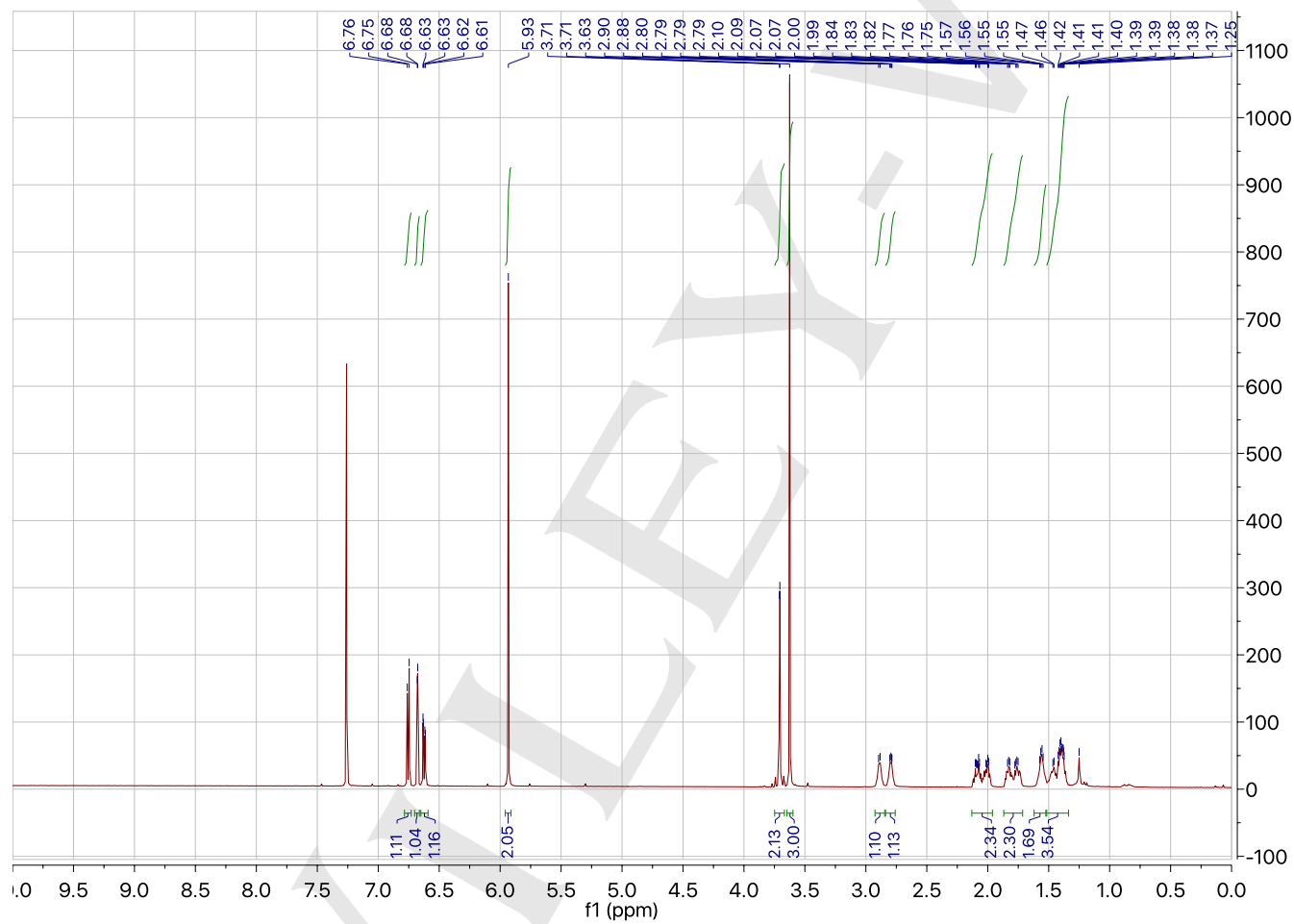
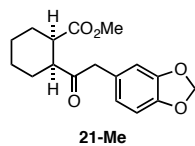
SUPPORTING INFORMATION

 ^1H NMR (501 MHz, CDCl_3): methyl (1*R*,2*S*)-2-(2-(*o*-tolyl)acetyl)cyclohexane-1-carboxylate (20-Me)

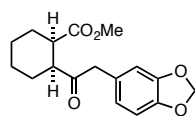
SUPPORTING INFORMATION

 ^{13}C NMR (126 MHz, CDCl_3): methyl (1*R*,2*S*)-2-(2-(*o*-tolyl)acetyl)cyclohexane-1-carboxylate (20-Me)

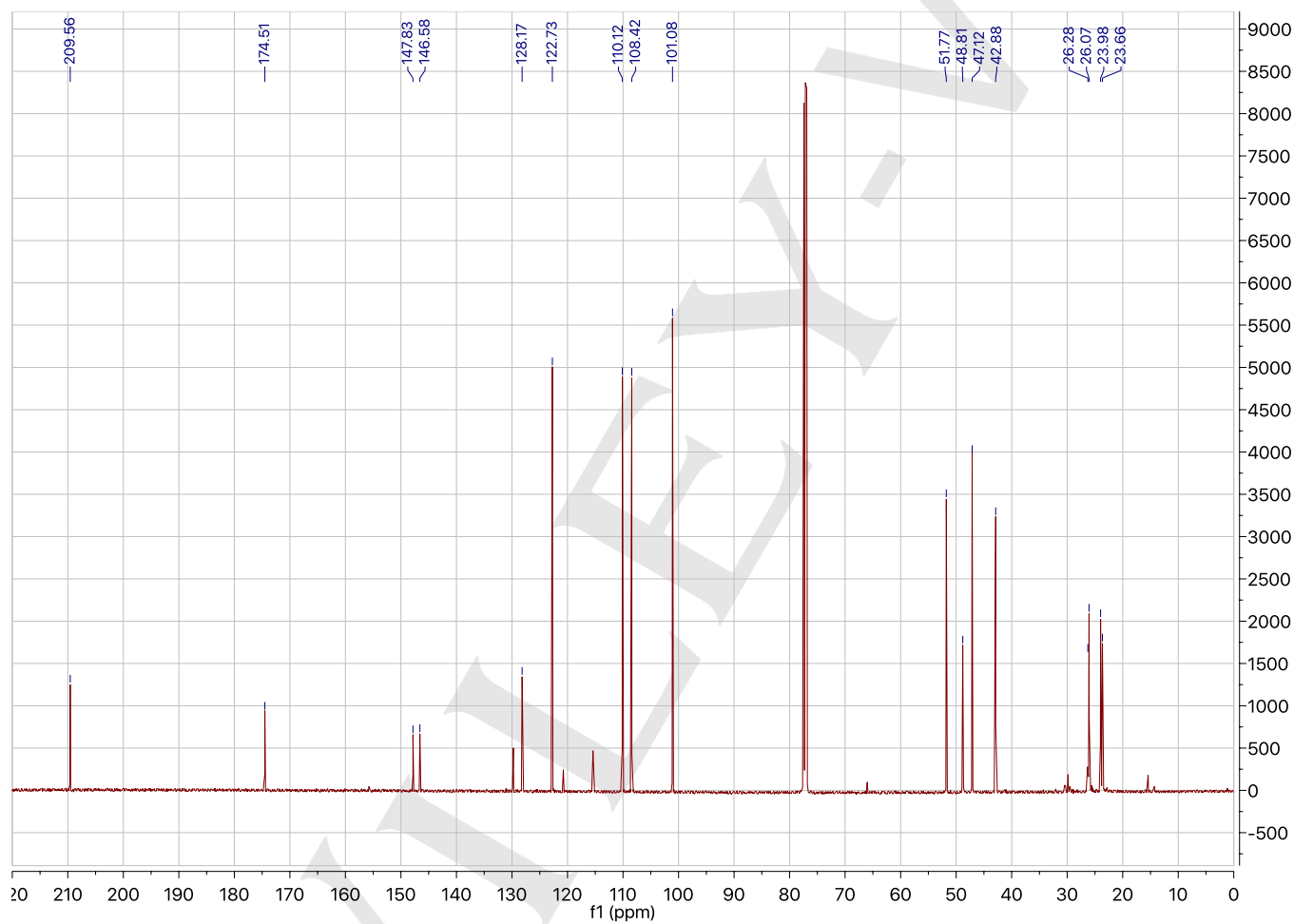
SUPPORTING INFORMATION

 ^1H NMR (501 MHz, CDCl_3): methyl (1*R*,2*S*)-2-(2-(benzo[*d*][1,3]dioxol-5-yl)acetyl)cyclohexane-1-carboxylate (21-Me)

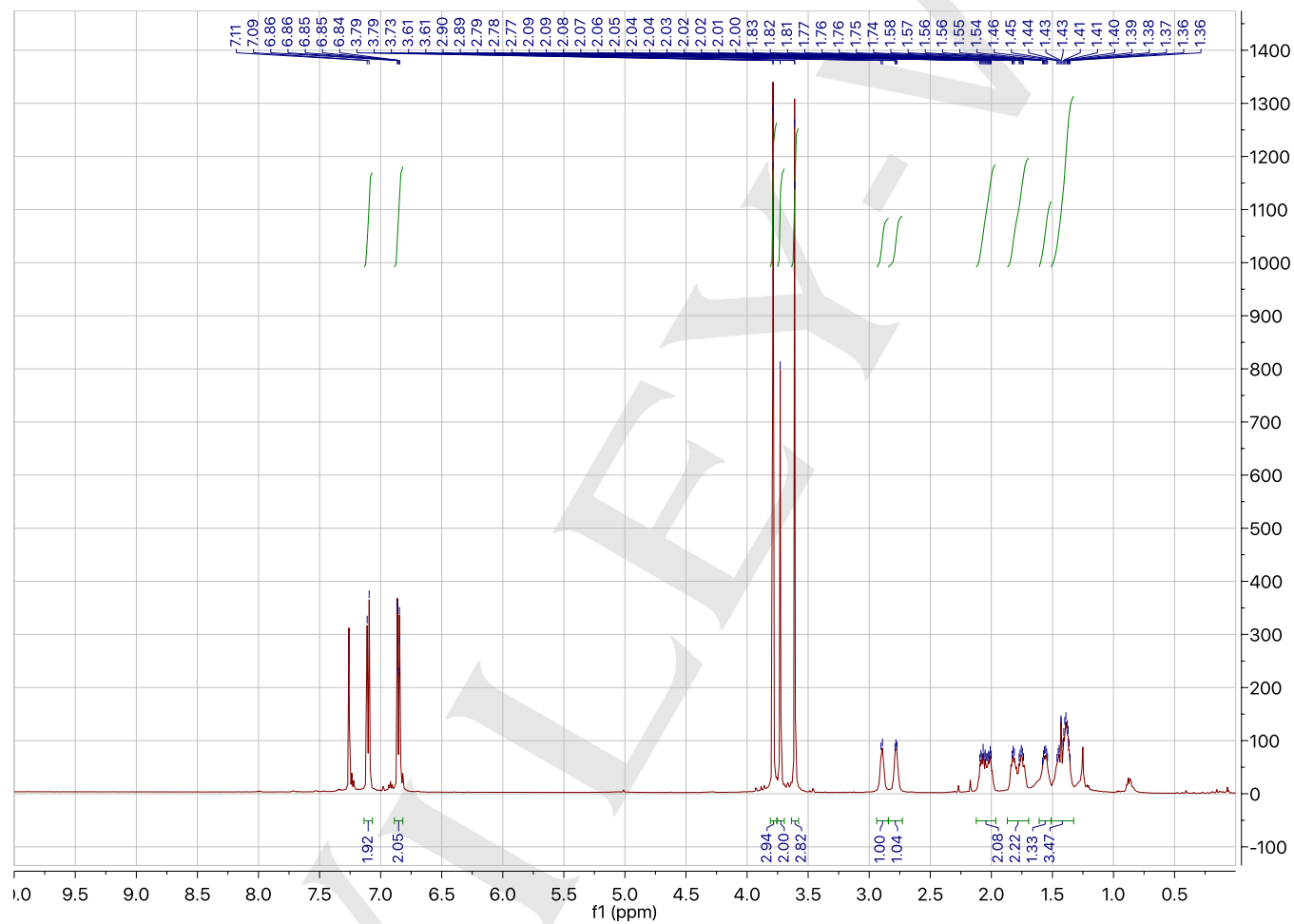
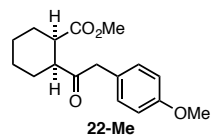
SUPPORTING INFORMATION

 ^{13}C NMR (126 MHz, CDCl_3): methyl (1*R*,2*S*)-2-(2-(benzo[*d*][1,3]dioxol-5-yl)acetyl)cyclohexane-1-carboxylate (21-Me)

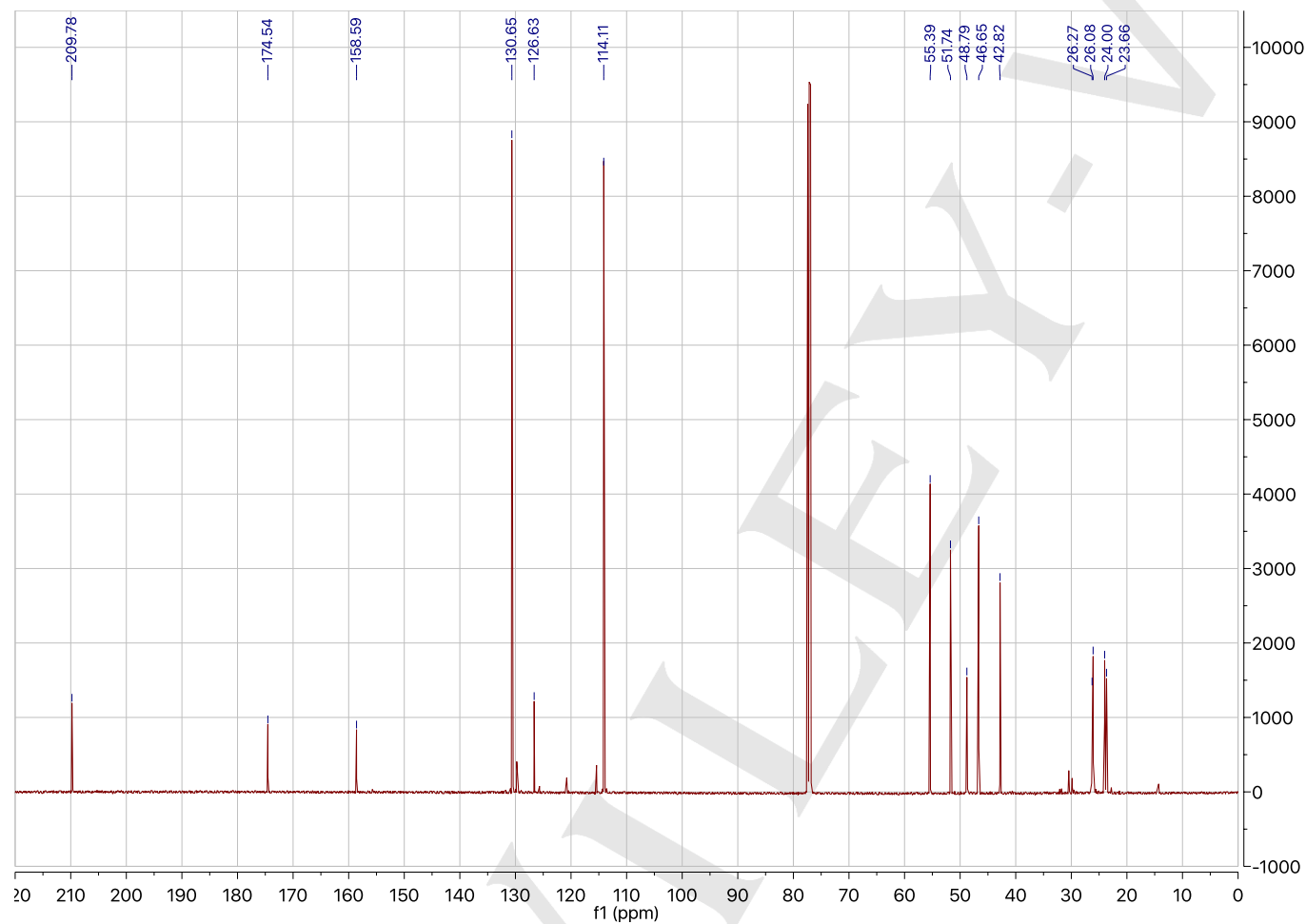
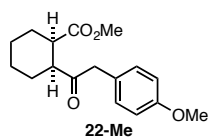
21-Me



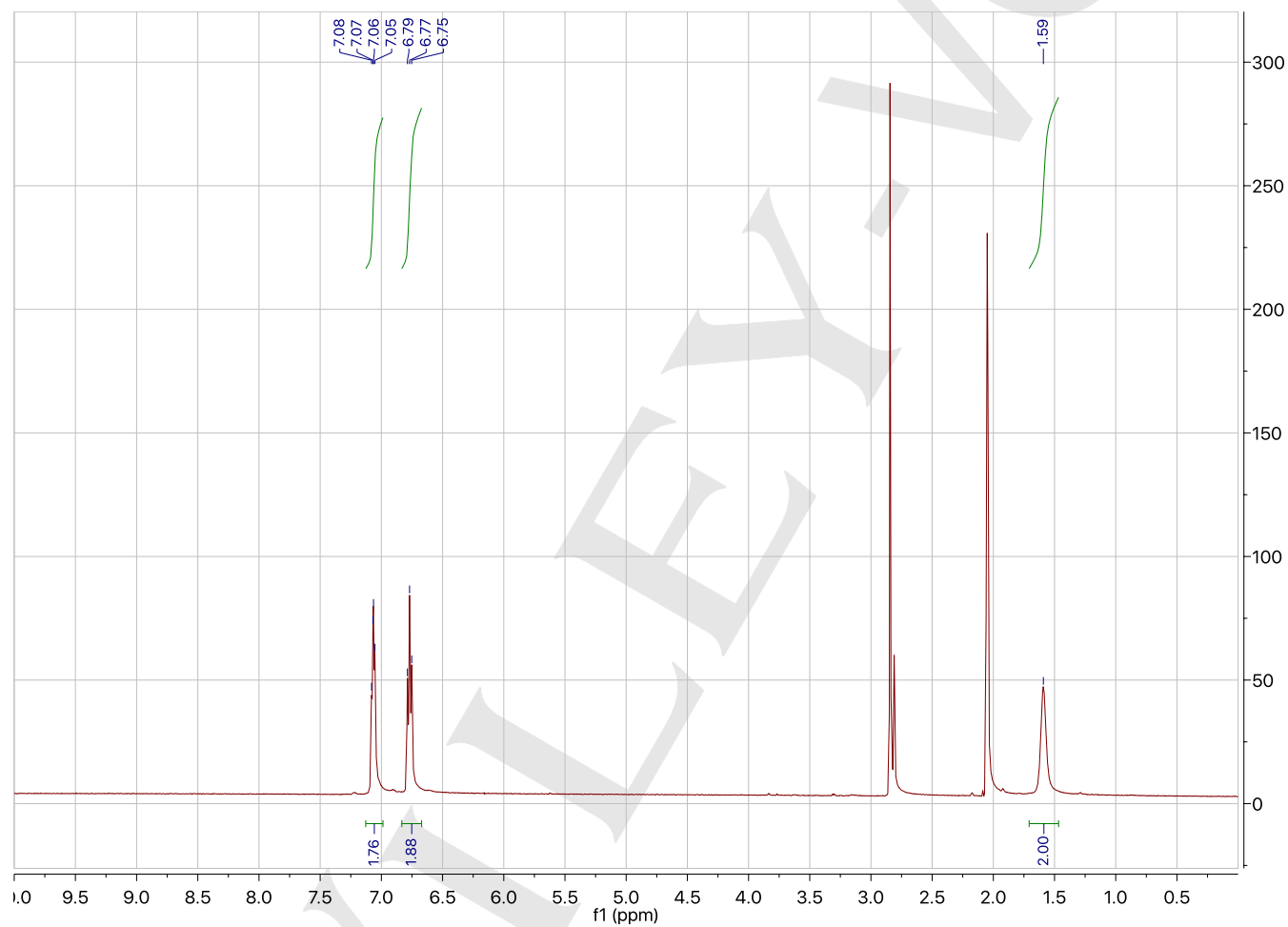
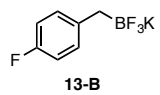
SUPPORTING INFORMATION

 ^1H NMR (501 MHz, CDCl_3): methyl (1*R*,2*S*)-2-(2-(4-methoxyphenyl)acetyl)cyclohexane-1-carboxylate (22-Me)

SUPPORTING INFORMATION

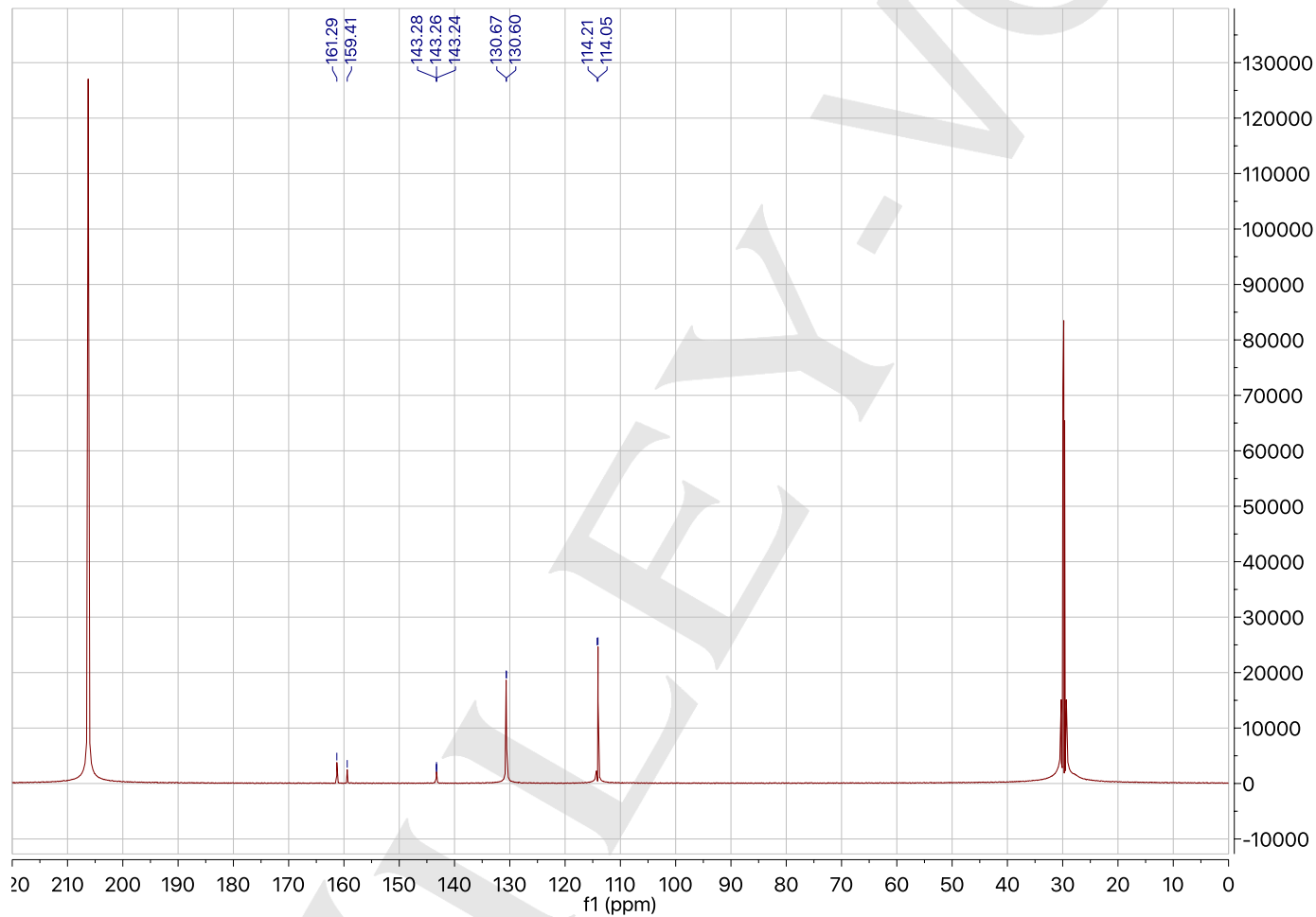
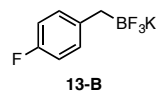
 ^{13}C NMR (126 MHz, CDCl_3): methyl (1*R*,2*S*)-2-(2-(4-methoxyphenyl)acetyl)cyclohexane-1-carboxylate (22-Me)

SUPPORTING INFORMATION

 ^1H NMR (501 MHz, acetone- d_6): trifluoro(4-fluorobenzyl)- λ^4 -borane, potassium salt (13-B)

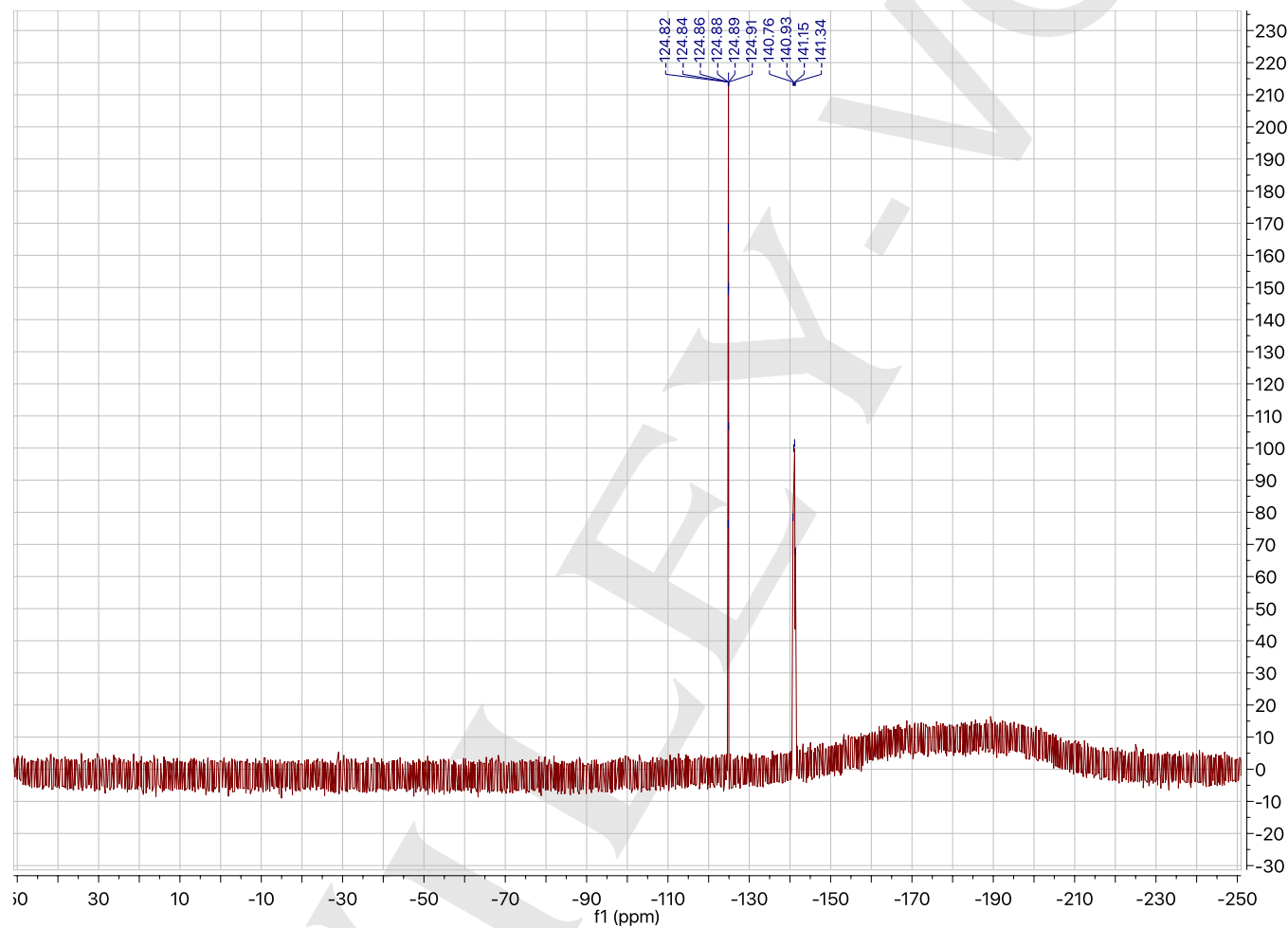
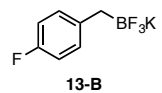
SUPPORTING INFORMATION

^{13}C NMR (126 MHz, acetone- d_6): trifluoro(4-fluorobenzyl)- λ^4 -borane, potassium salt (13-B)

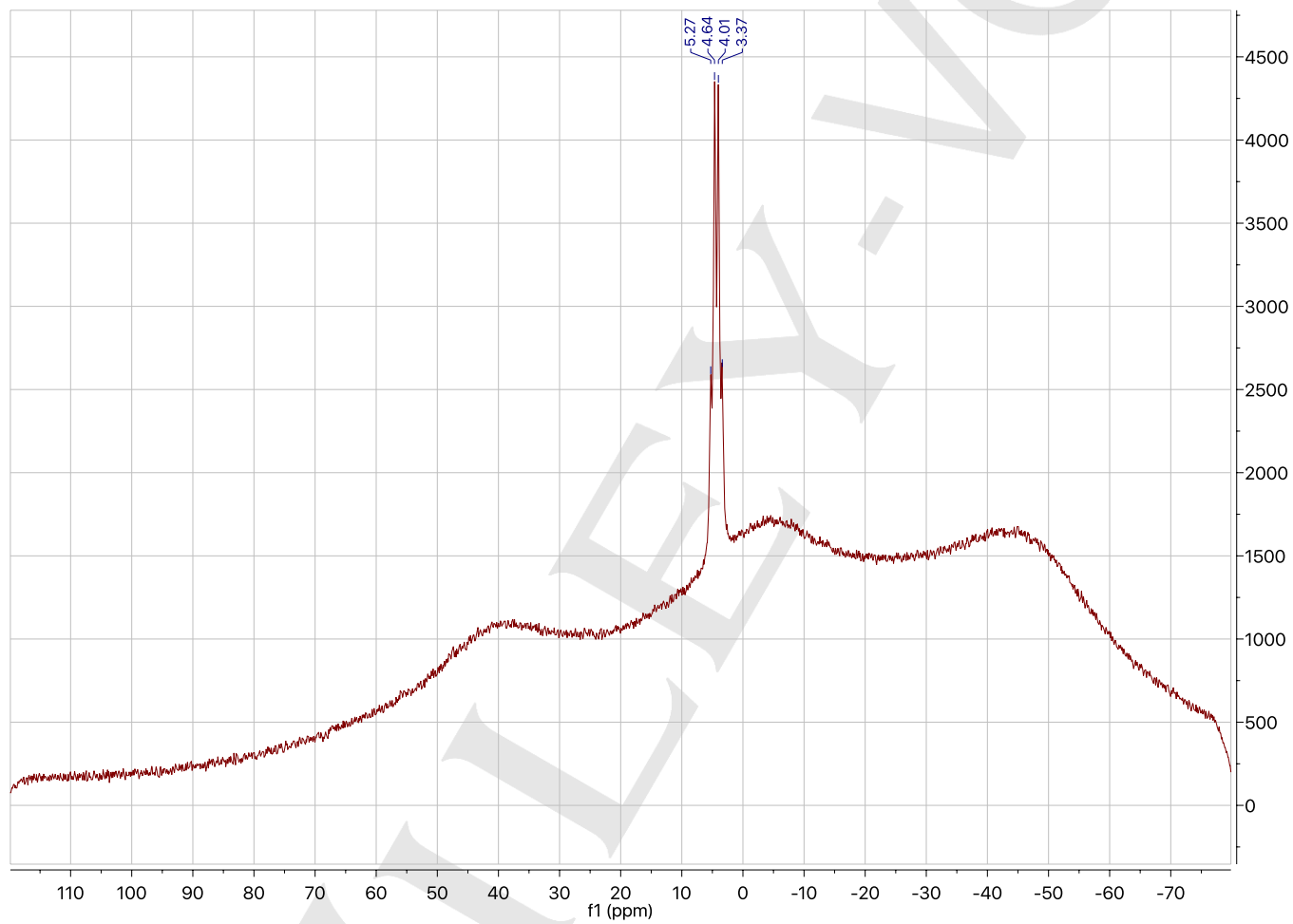
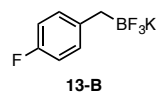


SUPPORTING INFORMATION

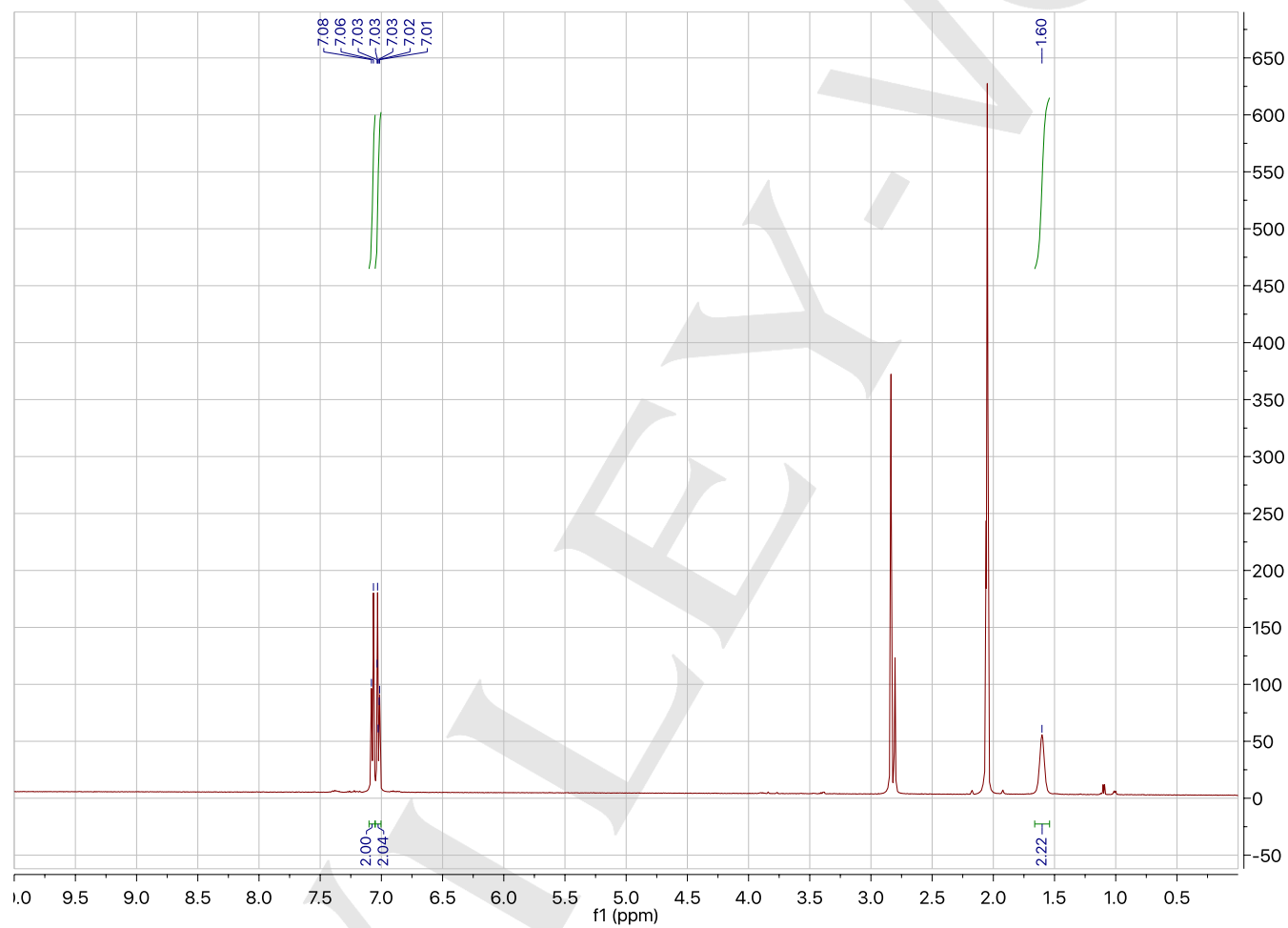
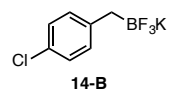
^{19}F NMR (282 MHz, acetone- d_6): trifluoro(4-fluorobenzyl)- λ^4 -borane, potassium salt (13-B)



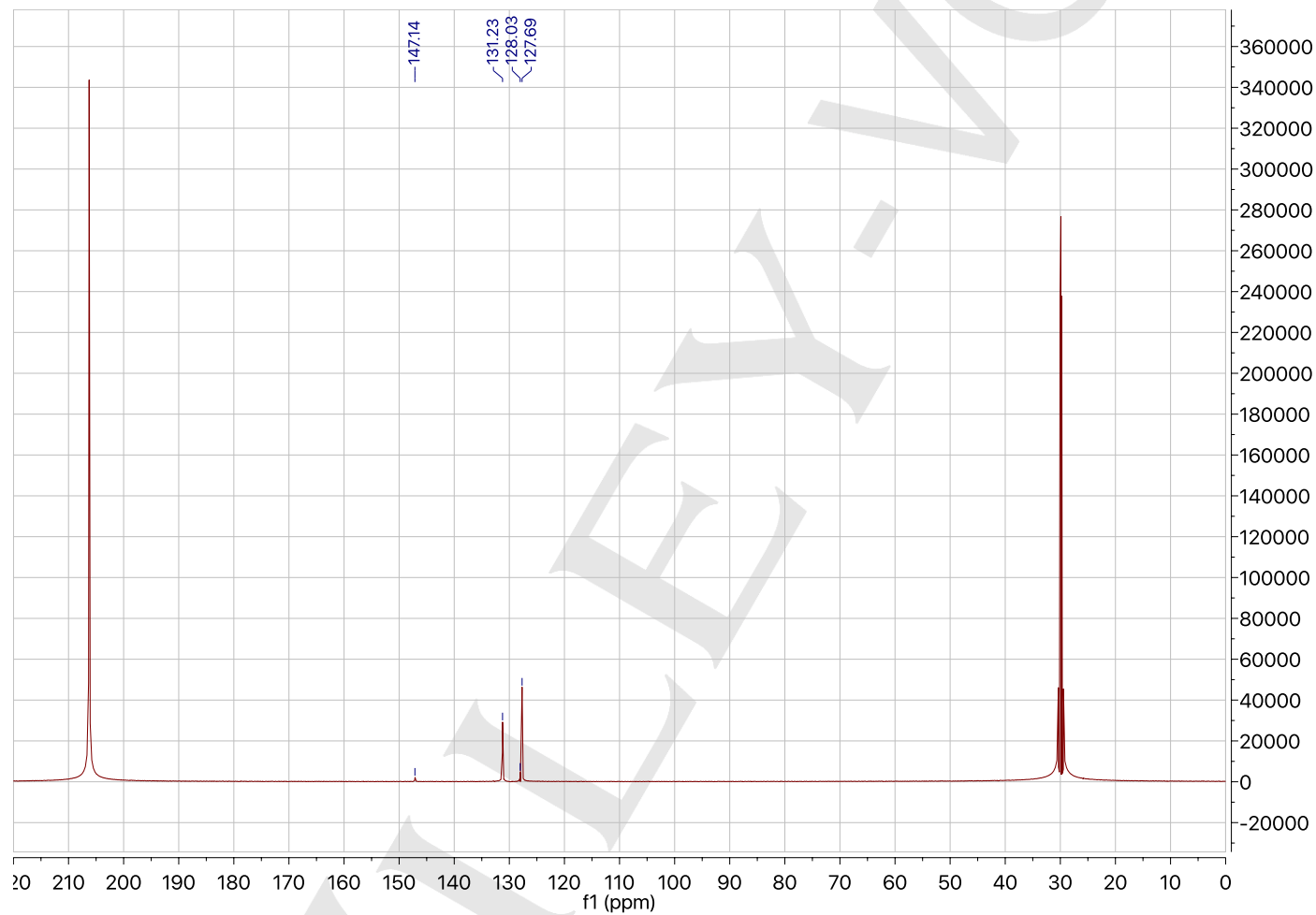
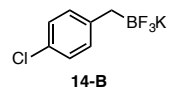
SUPPORTING INFORMATION

 ^{11}B NMR (96 MHz, acetone- d_6): trifluoro(4-fluorobenzyl)- λ^4 -borane, potassium salt (13-B)

SUPPORTING INFORMATION

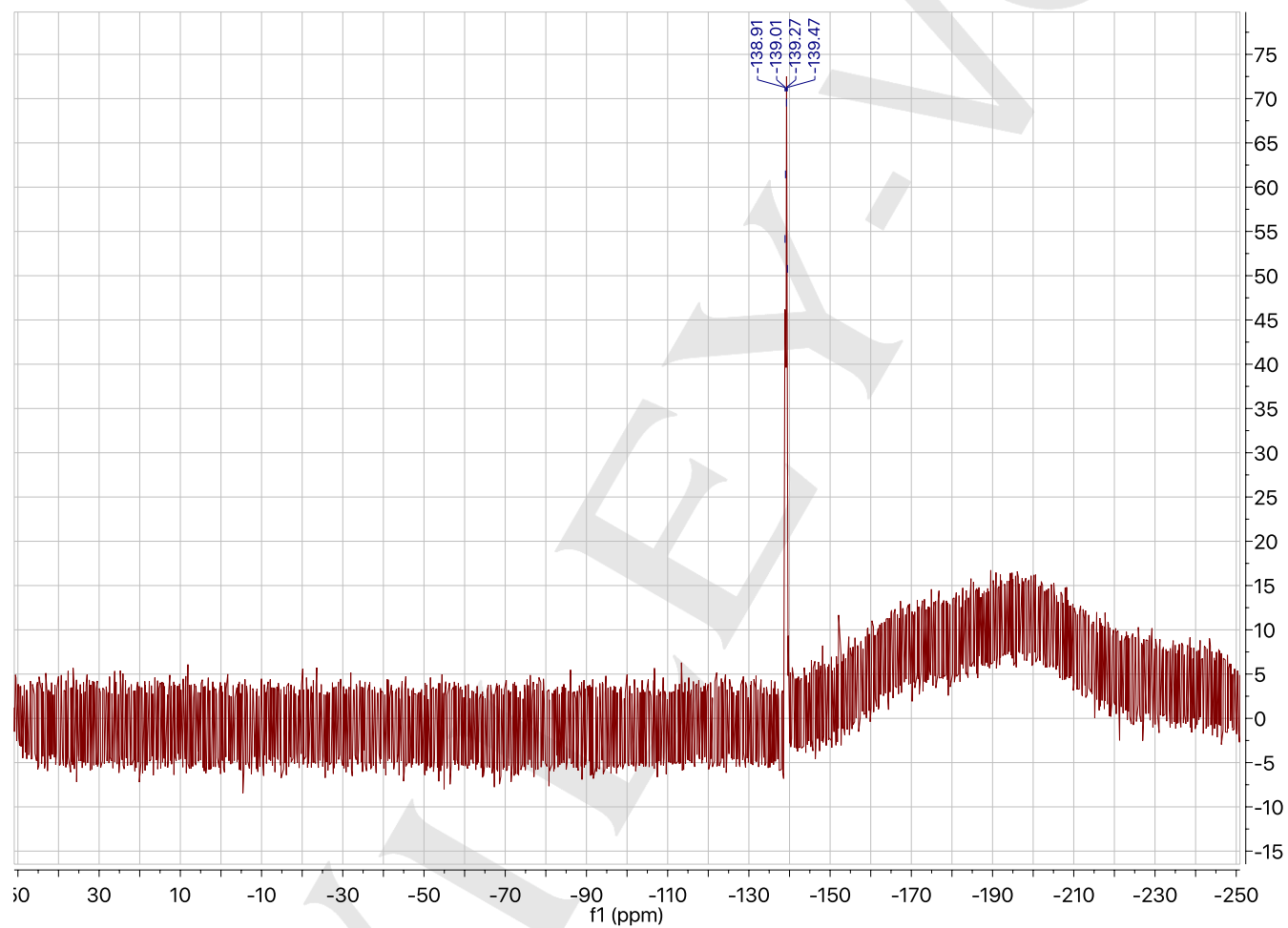
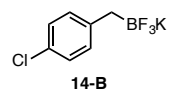
 ^1H NMR (501 MHz, acetone- d_6): (4-chlorobenzyl)trifluoro- λ^4 -borane, potassium salt (14-B)

SUPPORTING INFORMATION

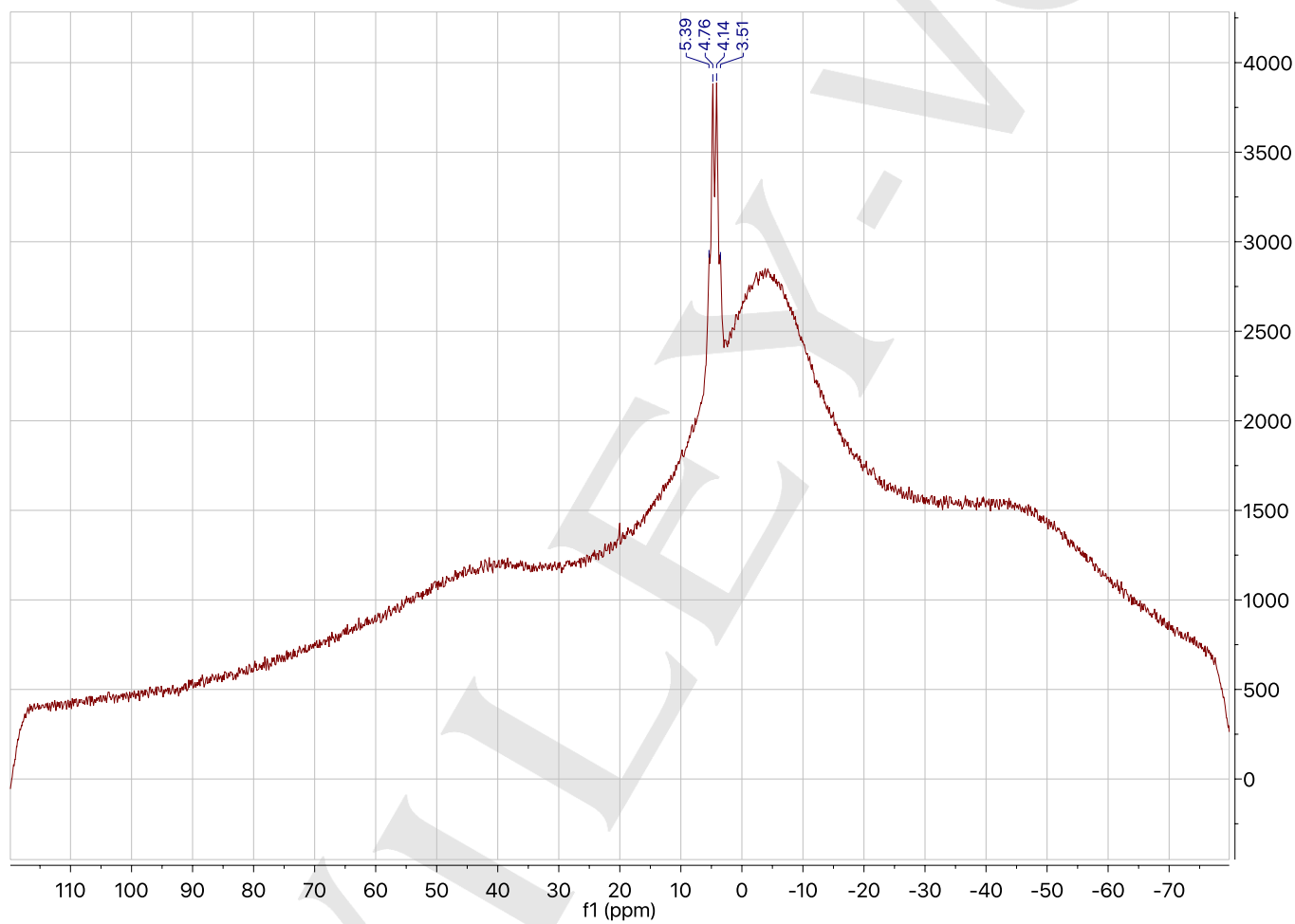
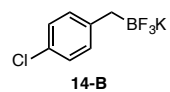
 ^{13}C NMR (126 MHz, acetone- d_6): (4-chlorobenzyl)trifluoro- λ^4 -borane, potassium salt (14-B)

SUPPORTING INFORMATION

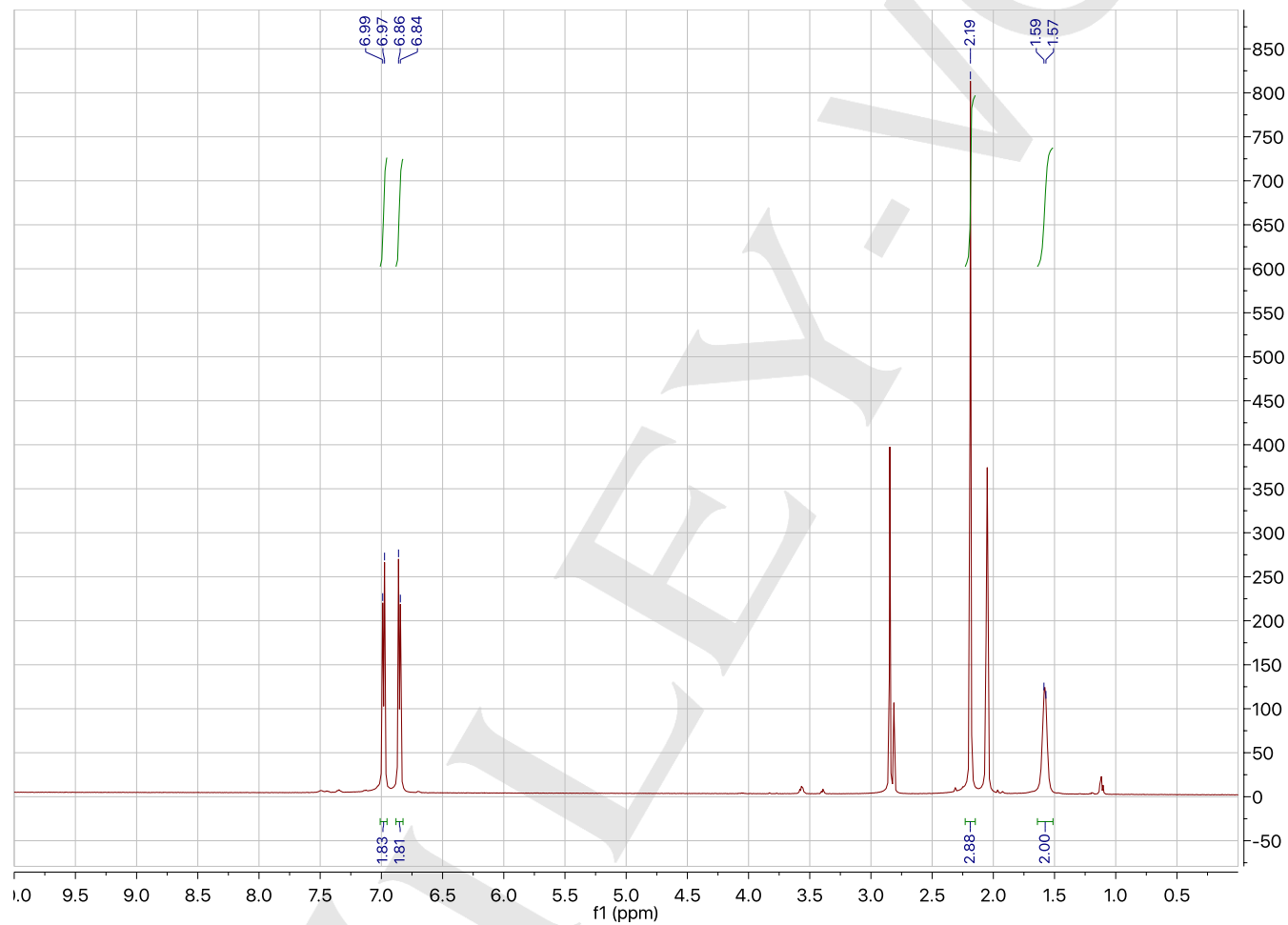
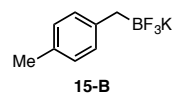
^{19}F NMR (282 MHz, acetone- d_6): (4-chlorobenzyl)trifluoro- λ^4 -borane, potassium salt (14-B)



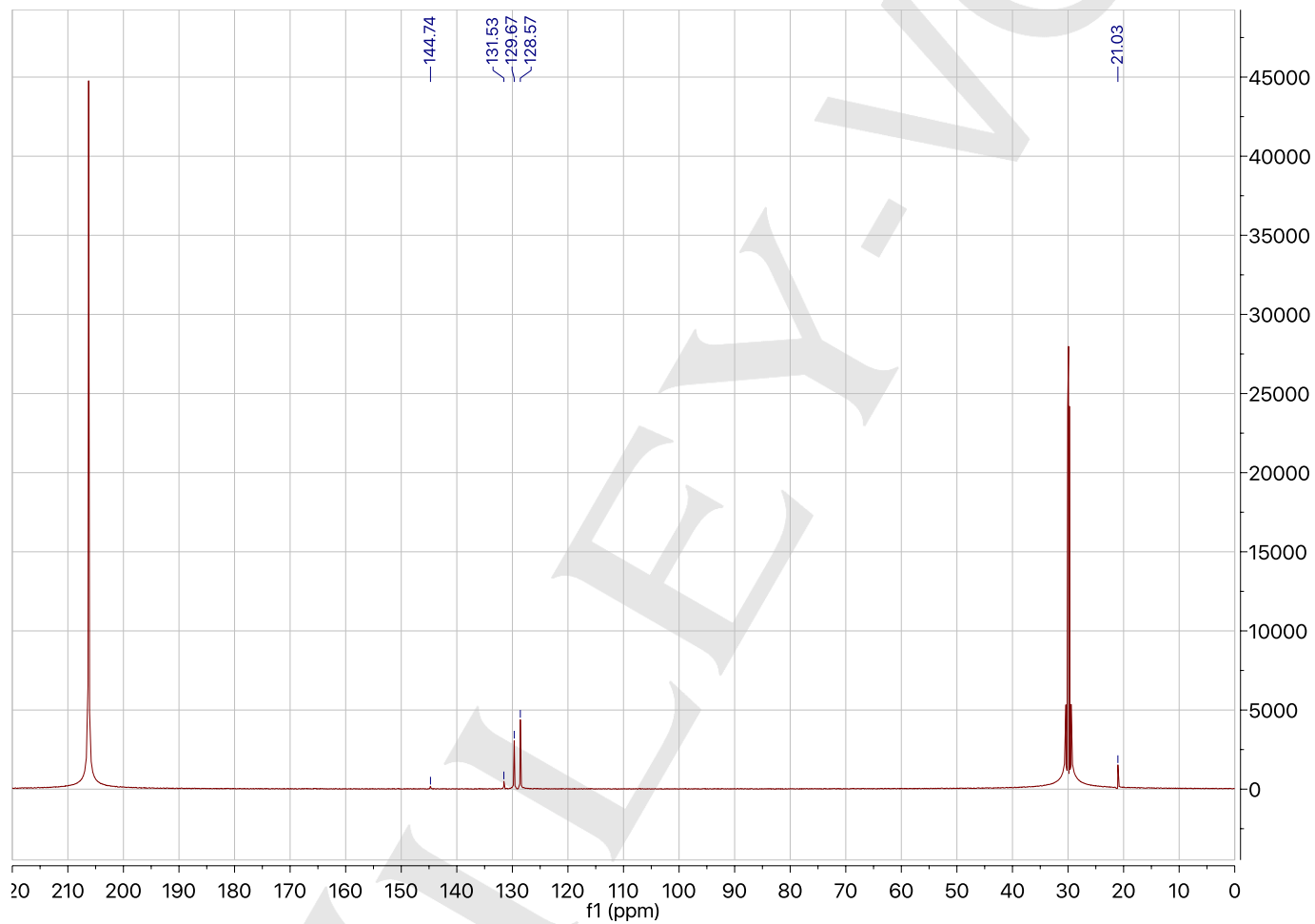
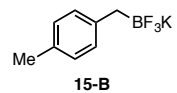
SUPPORTING INFORMATION

 ^{11}B NMR (96 MHz, acetone- d_6): (4-chlorobenzyl)trifluoro- λ^4 -borane, potassium salt (14-B)

SUPPORTING INFORMATION

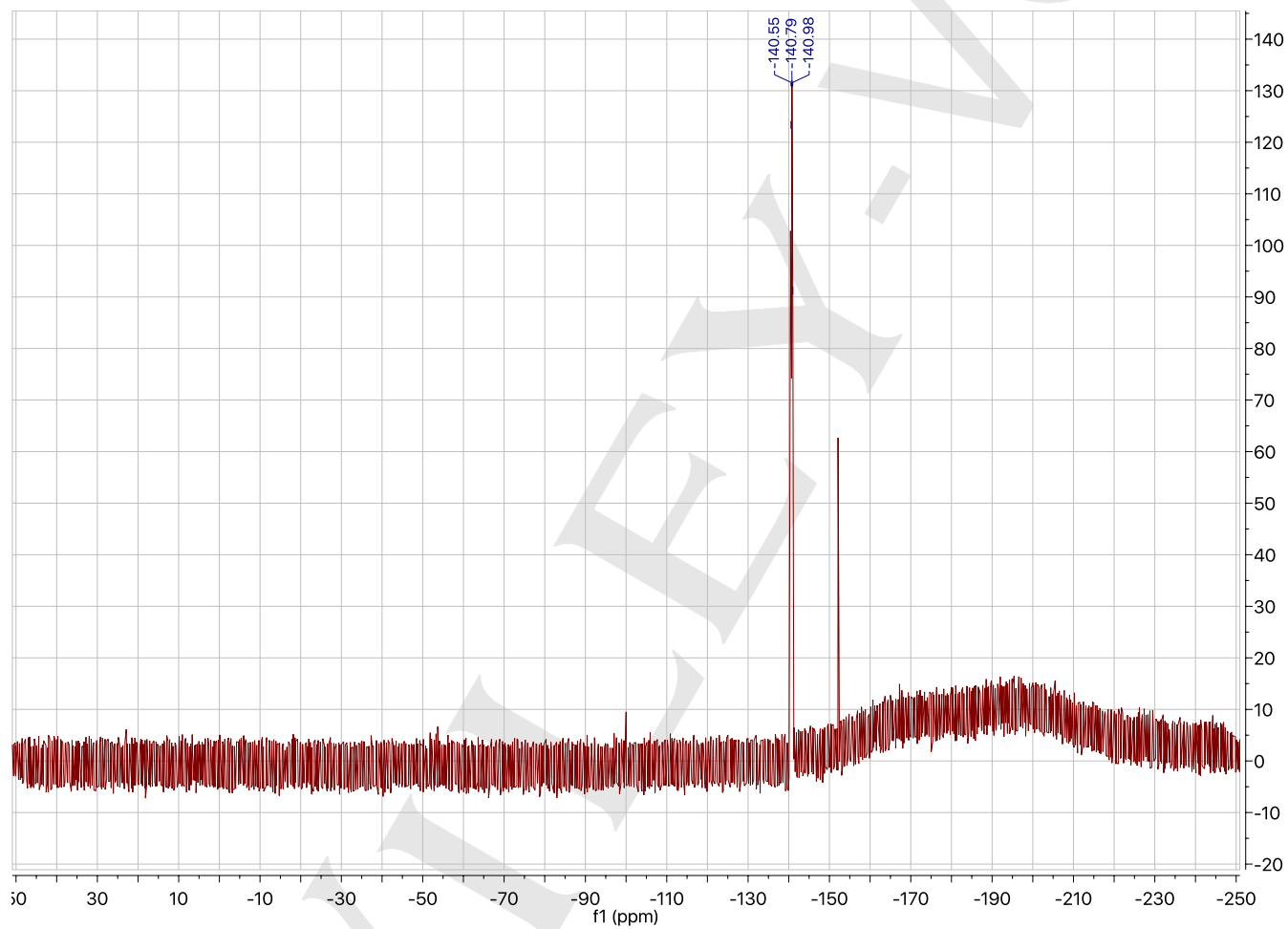
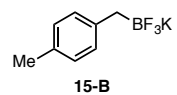
 ^1H NMR (501 MHz, acetone- d_6): trifluoro(4-methylbenzyl)- λ^4 -borane, potassium salt (15-B)

SUPPORTING INFORMATION

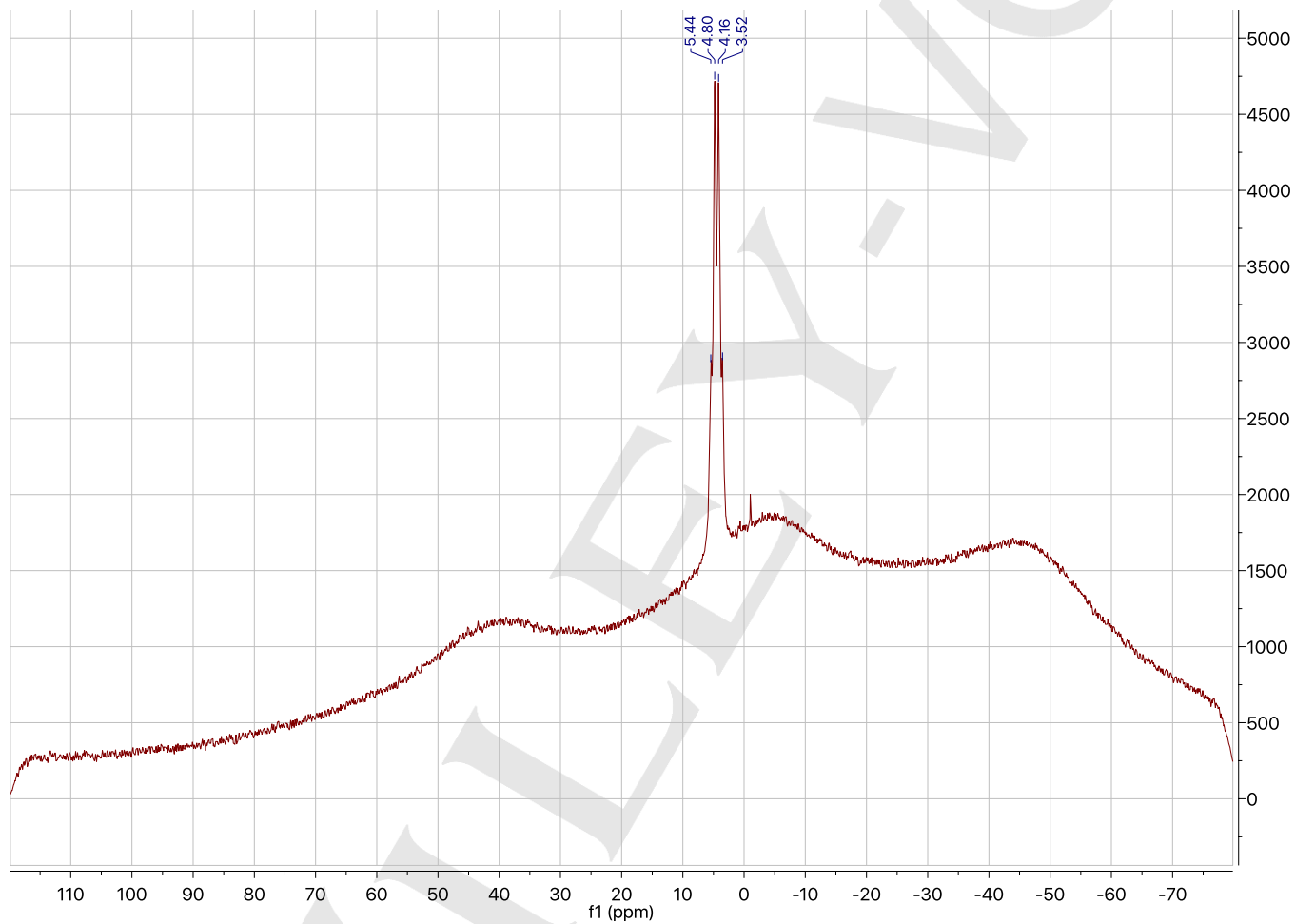
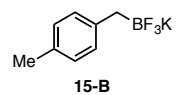
 ^{13}C NMR (126 MHz, acetone- d_6): trifluoro(4-methylbenzyl)- λ^4 -borane, potassium salt (15-B)

SUPPORTING INFORMATION

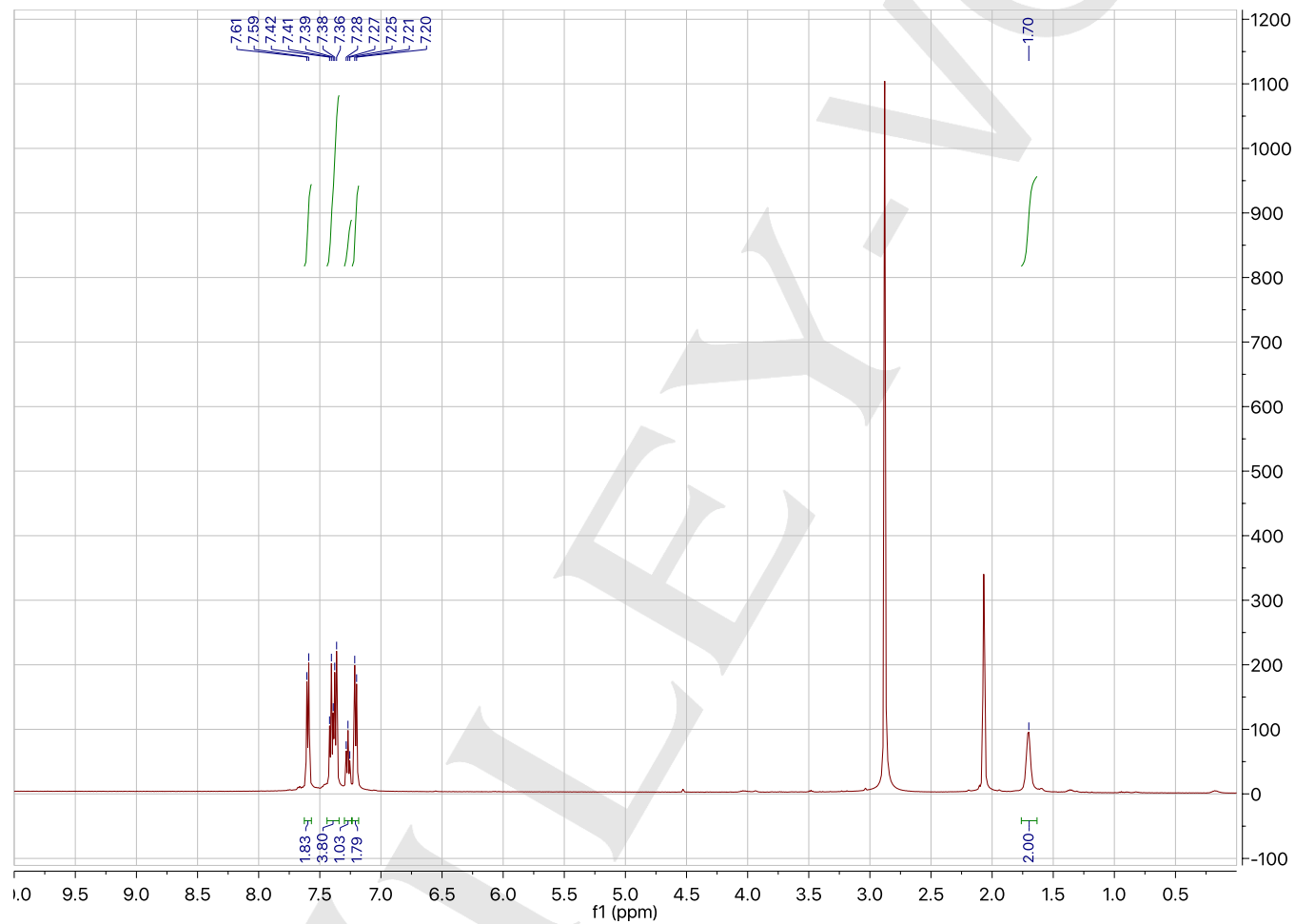
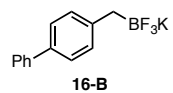
^{19}F NMR (282 MHz, acetone- d_6): trifluoro(4-methylbenzyl)- λ^4 -borane, potassium salt (15-B)



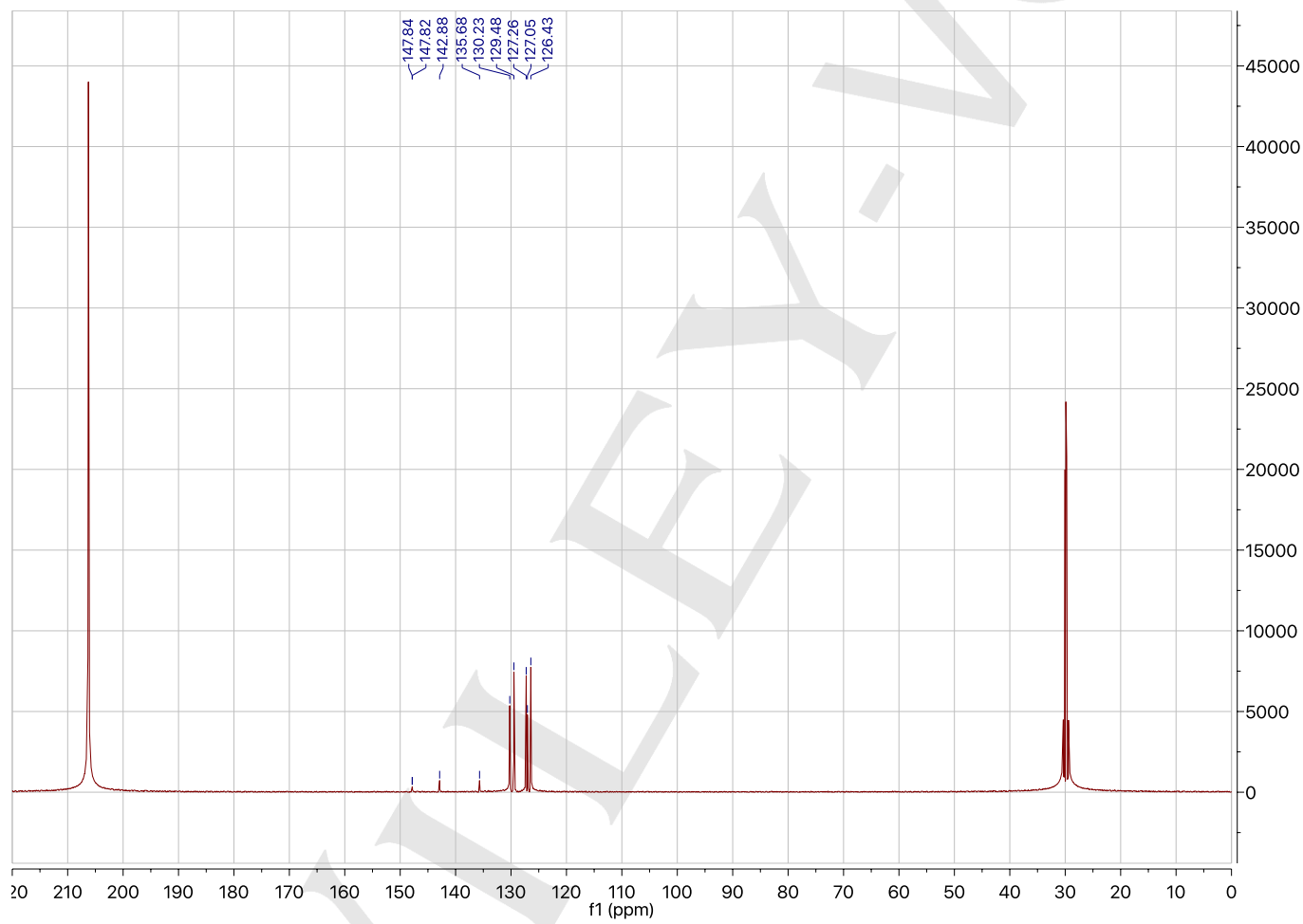
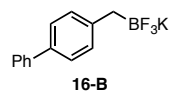
SUPPORTING INFORMATION

 ^{11}B NMR (96 MHz, acetone- d_6): trifluoro(4-methylbenzyl)- λ^4 -borane, potassium salt (15-B)

SUPPORTING INFORMATION

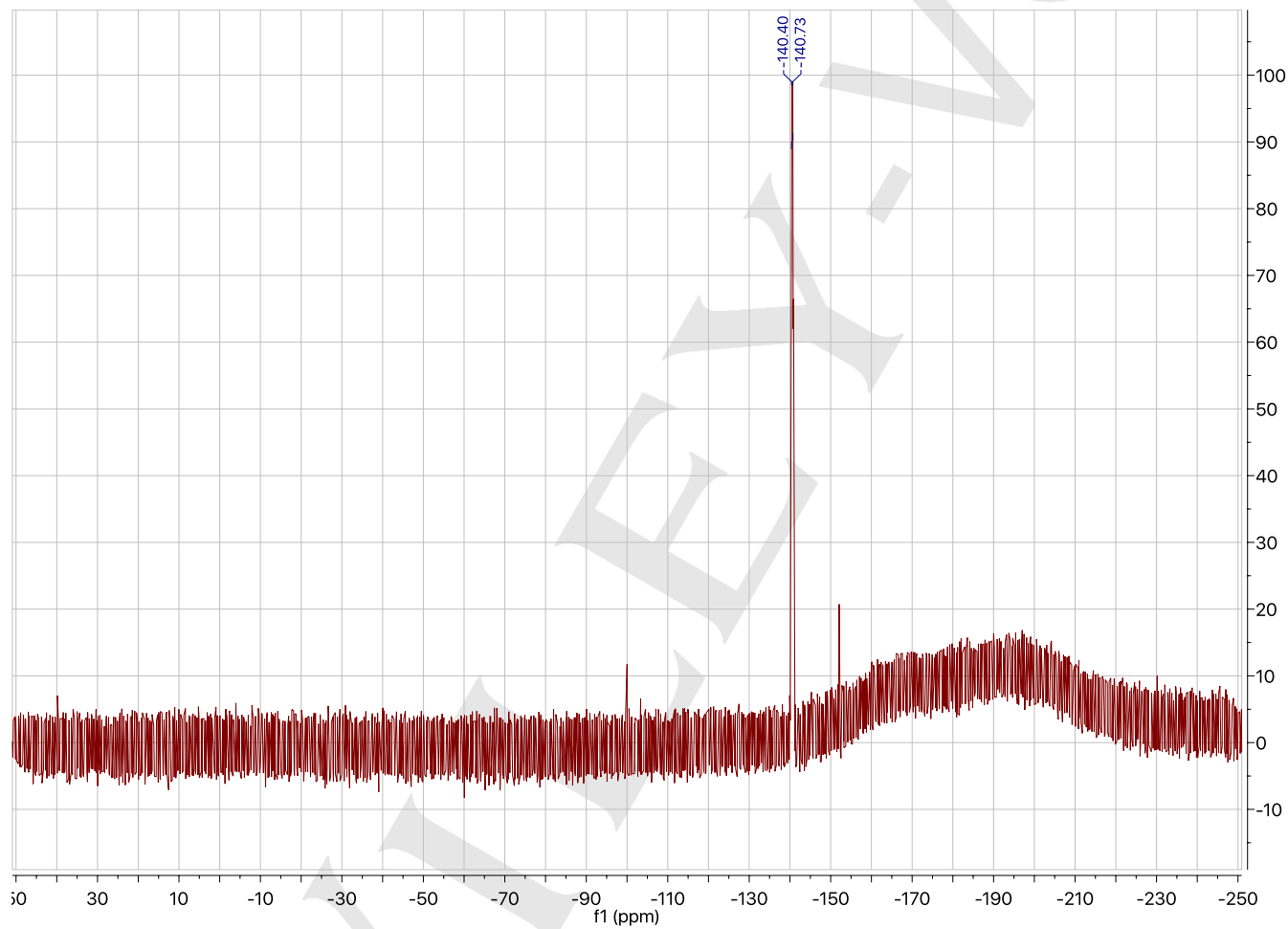
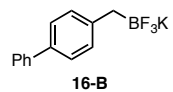
 ^1H NMR (501 MHz, acetone- d_6): ([1,1'-biphenyl]-4-ylmethyl)trifluoro- λ^4 -borane, potassium salt (16-B)

SUPPORTING INFORMATION

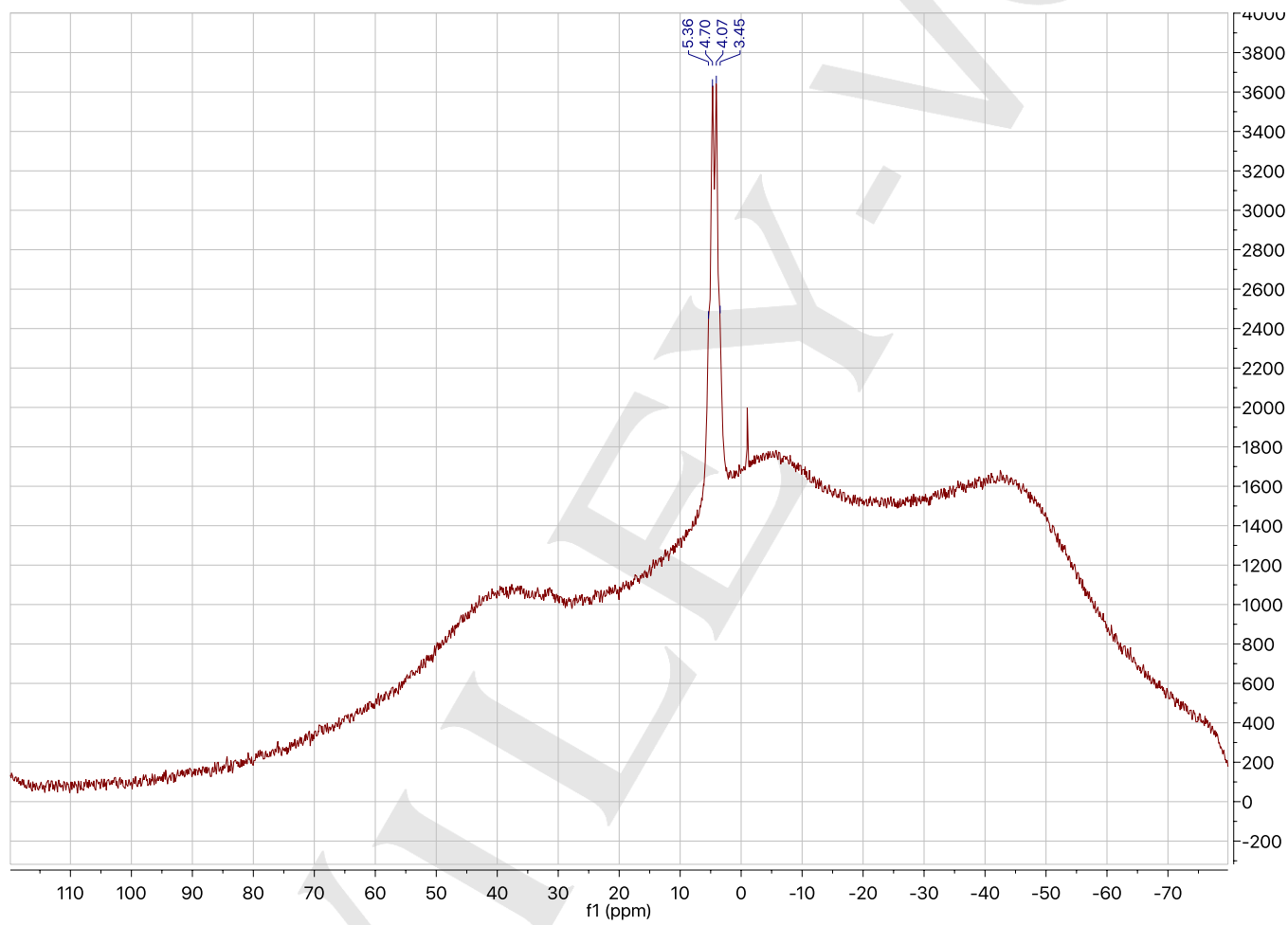
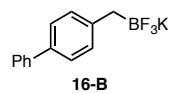
 ^{13}C NMR (126 MHz, acetone- d_6): ([1,1'-biphenyl]-4-ylmethyl)trifluoro- λ^4 -borane, potassium salt (16-B)

SUPPORTING INFORMATION

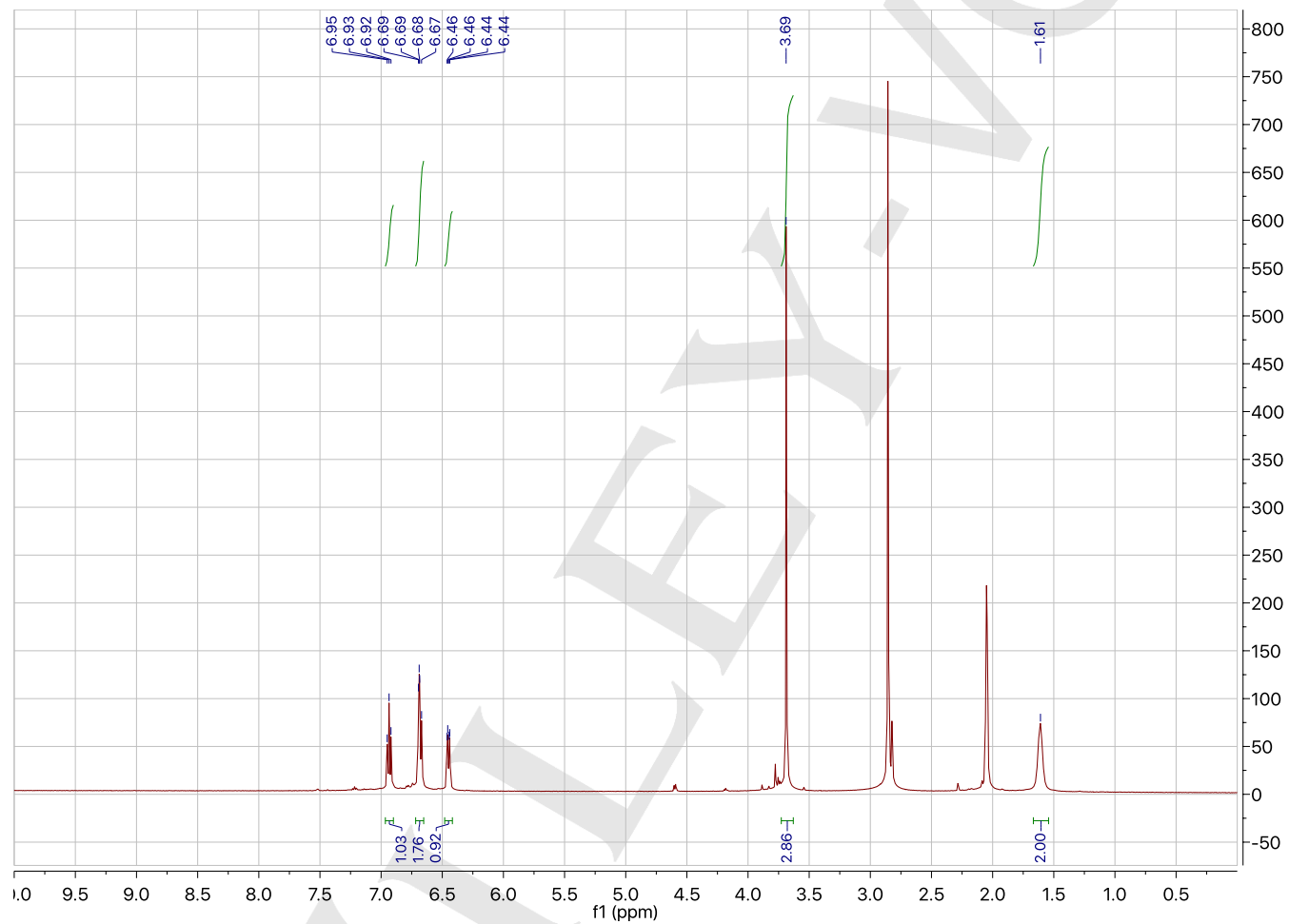
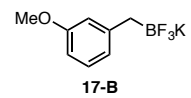
^{19}F NMR (282 MHz, acetone- d_6): ([1,1'-biphenyl]-4-ylmethyl)trifluoro- λ^4 -borane, potassium salt (16-B)



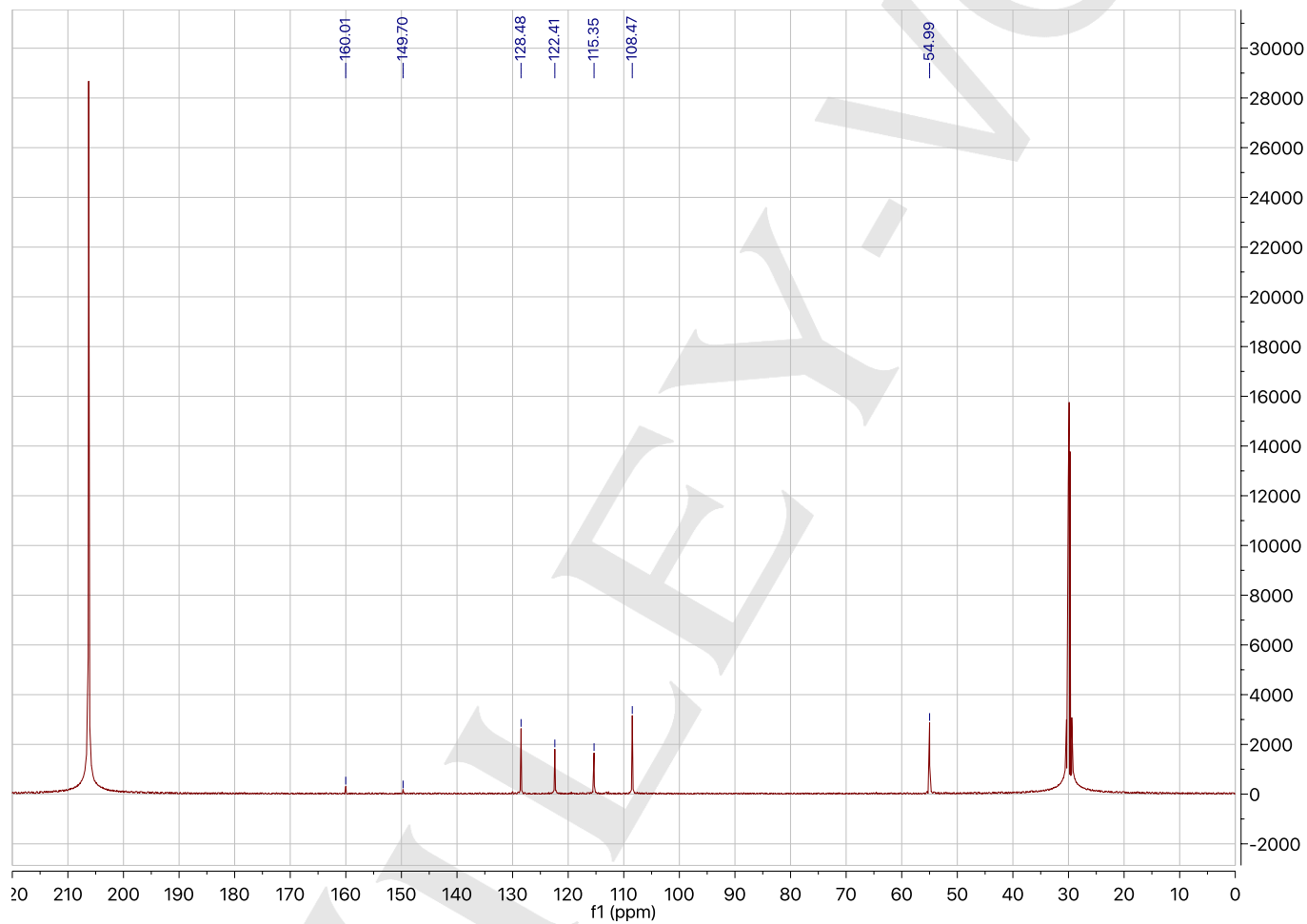
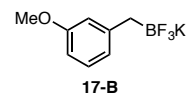
SUPPORTING INFORMATION

 ^{11}B NMR (96 MHz, acetone- d_6): ([1,1'-biphenyl]-4-ylmethyl)trifluoro- λ^4 -borane, potassium salt (16-B)

SUPPORTING INFORMATION

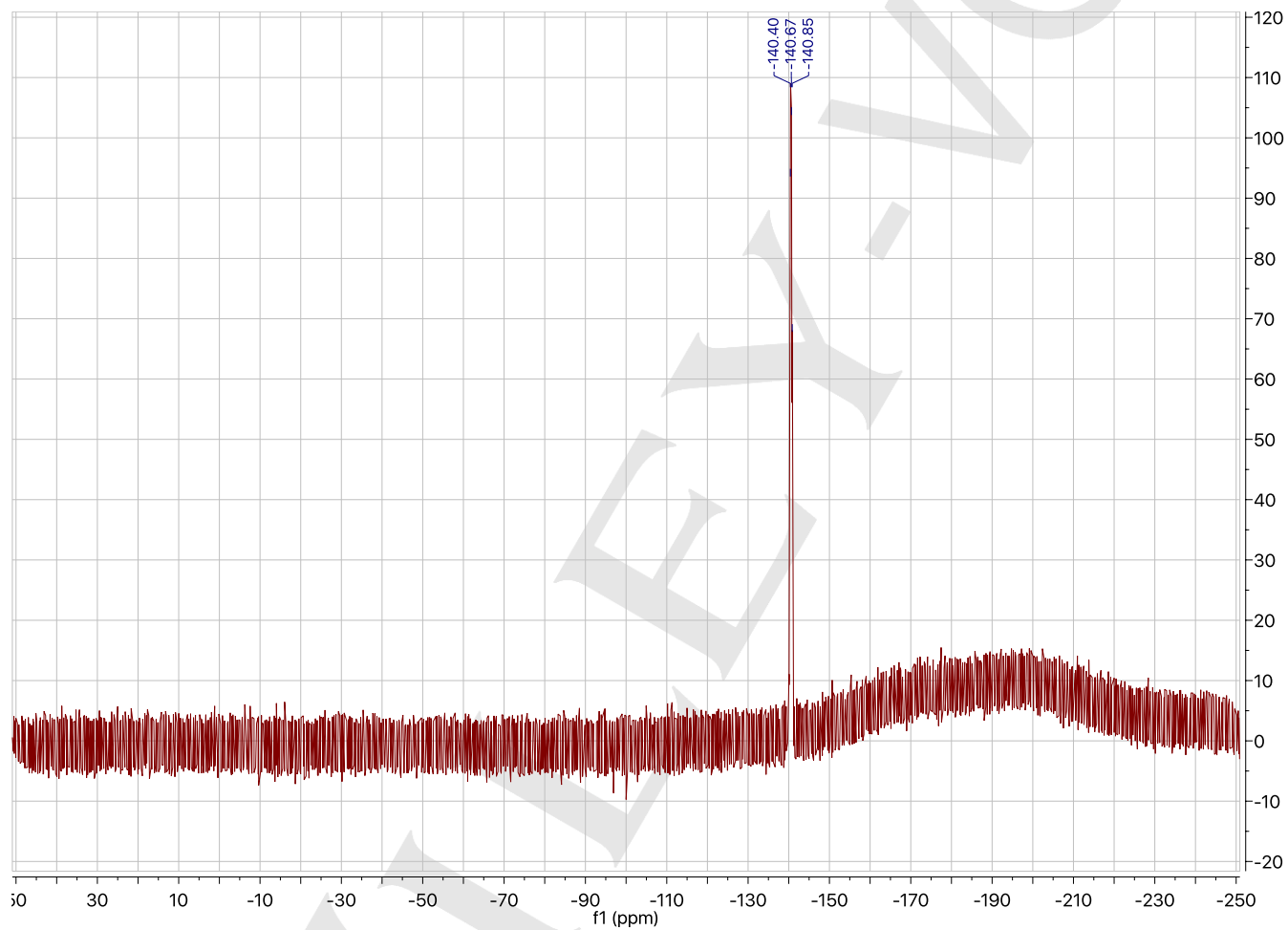
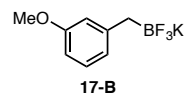
 ^1H NMR (501 MHz, acetone- d_6): trifluoro(3-methoxybenzyl)- λ^4 -borane, potassium salt (17-B)

SUPPORTING INFORMATION

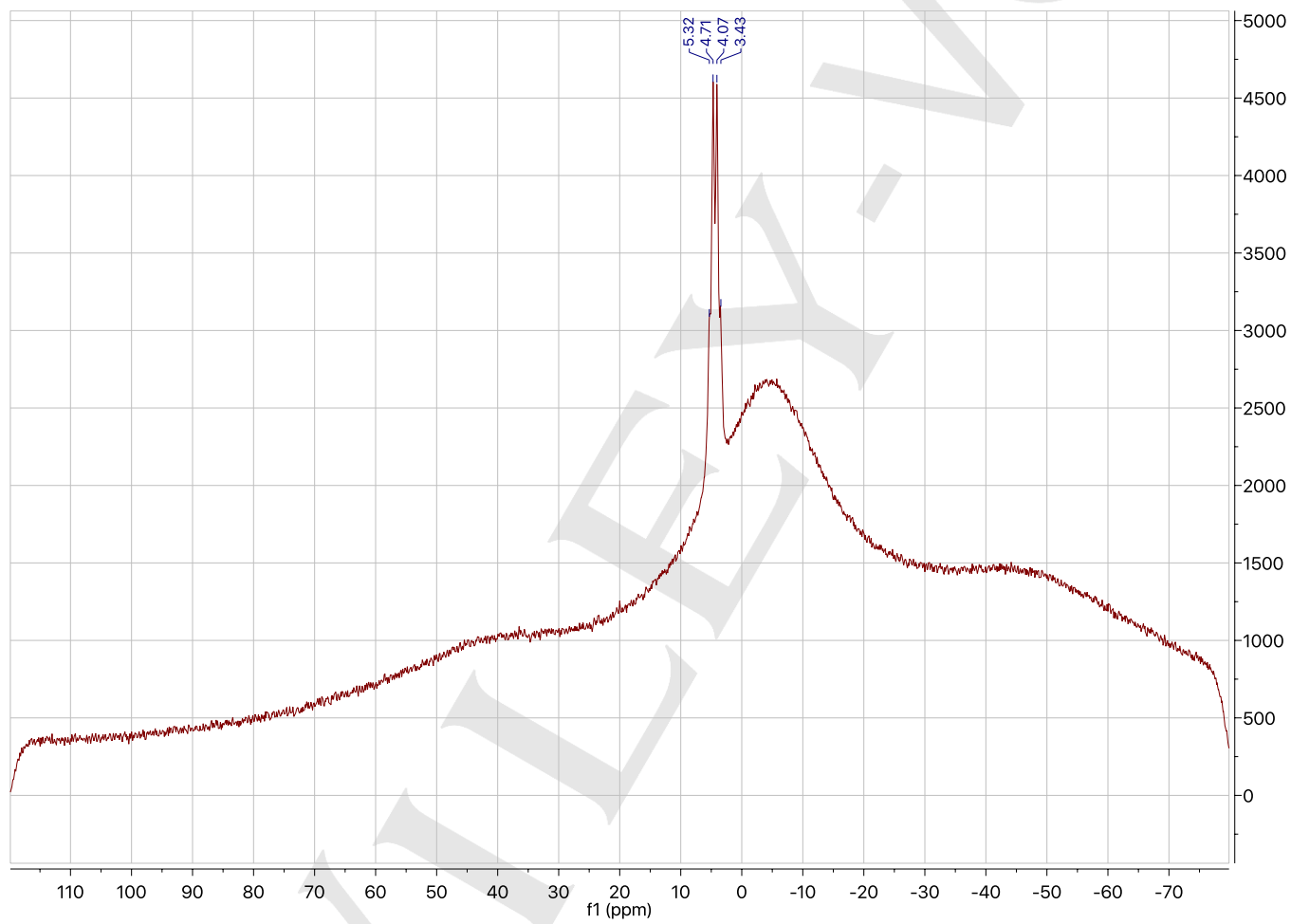
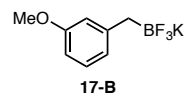
 ^{13}C NMR (126 MHz, acetone- d_6): trifluoro(3-methoxybenzyl)- λ^4 -borane, potassium salt (17-B)

SUPPORTING INFORMATION

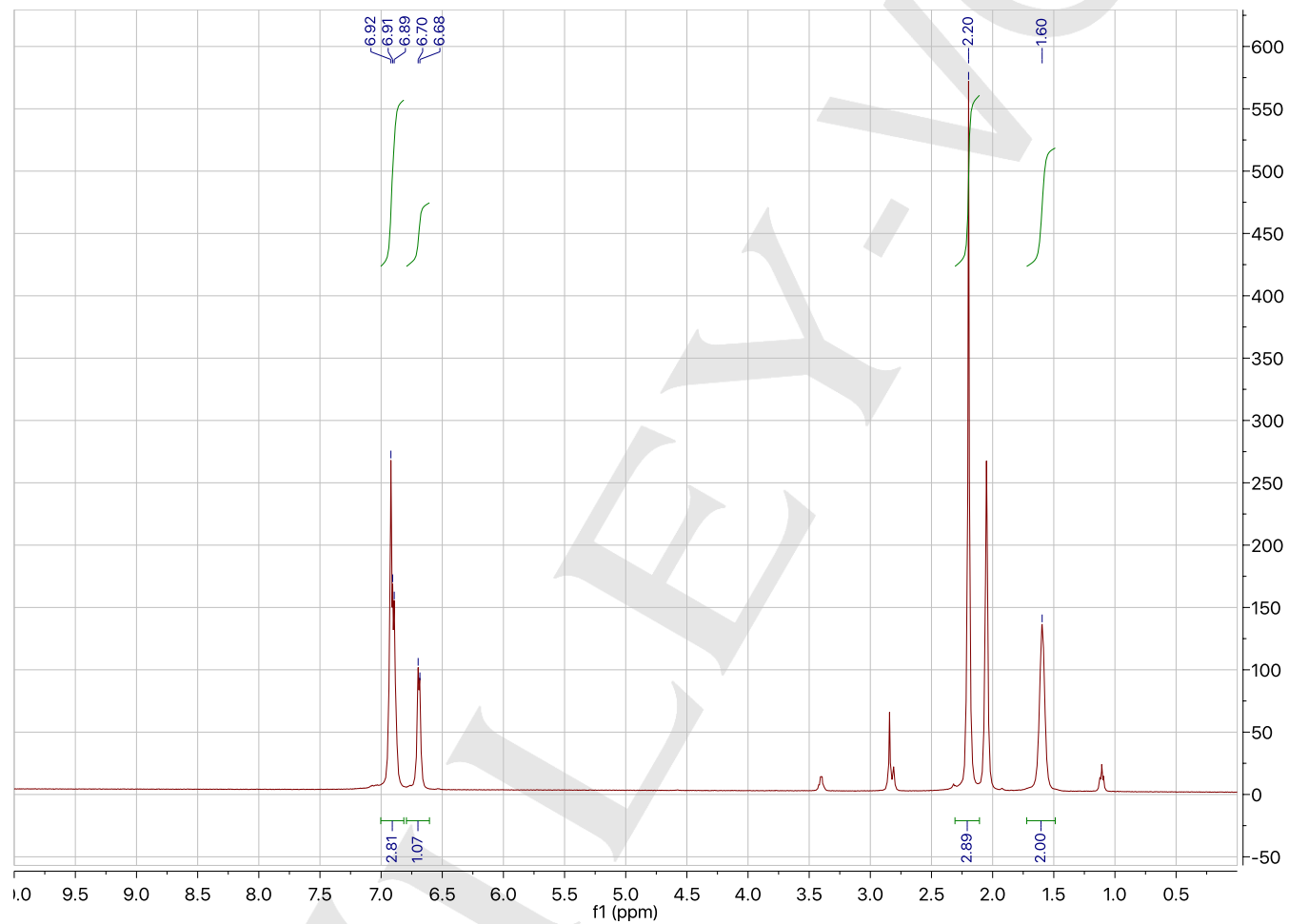
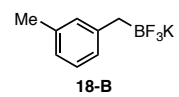
^{19}F NMR (282 MHz, acetone- d_6): trifluoro(3-methoxybenzyl)- λ^4 -borane, potassium salt (17-B)



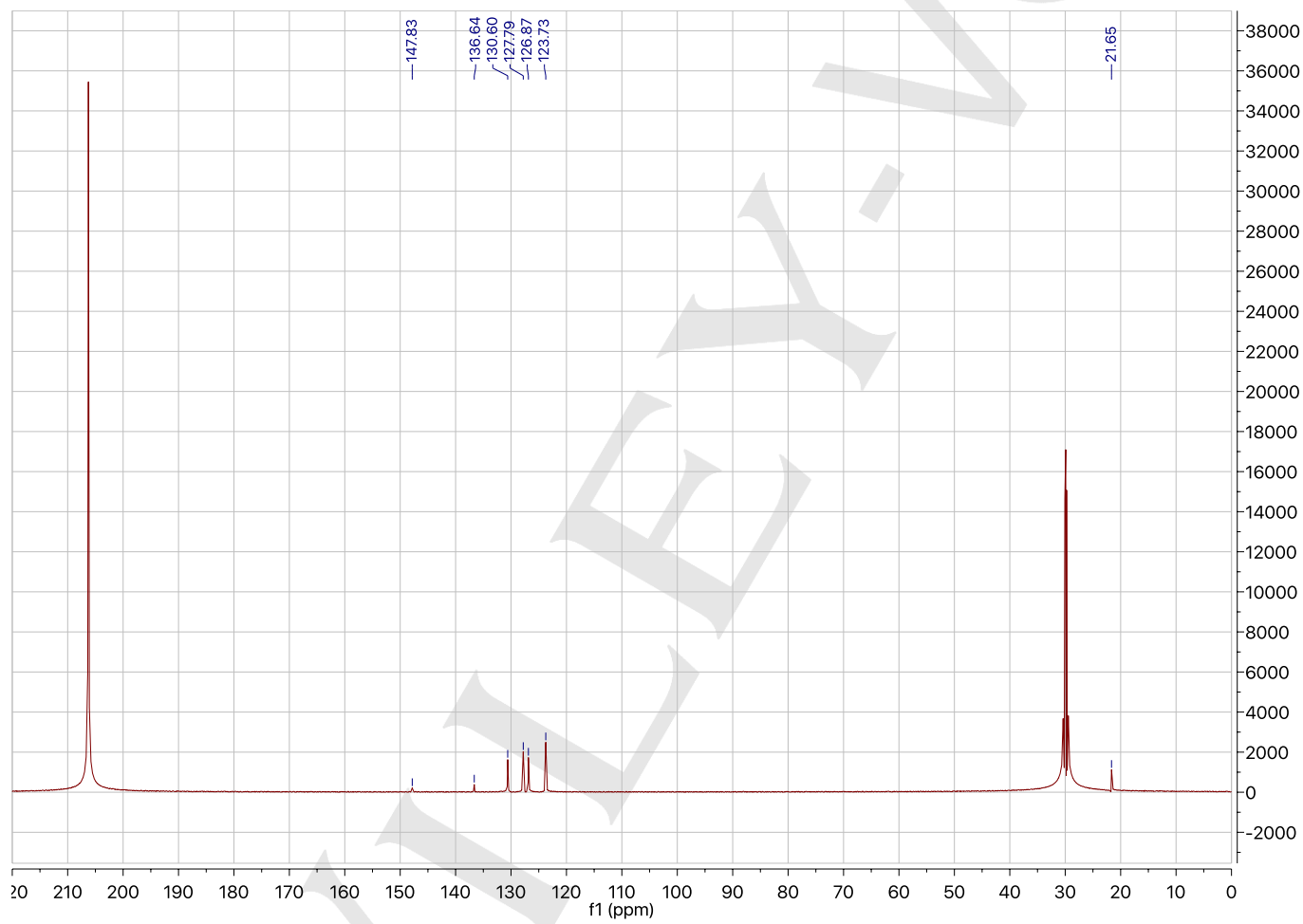
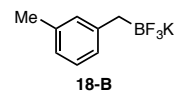
SUPPORTING INFORMATION

 ^{11}B NMR (96 MHz, acetone- d_6): trifluoro(3-methoxybenzyl)- λ^4 -borane, potassium salt (17-B)

SUPPORTING INFORMATION

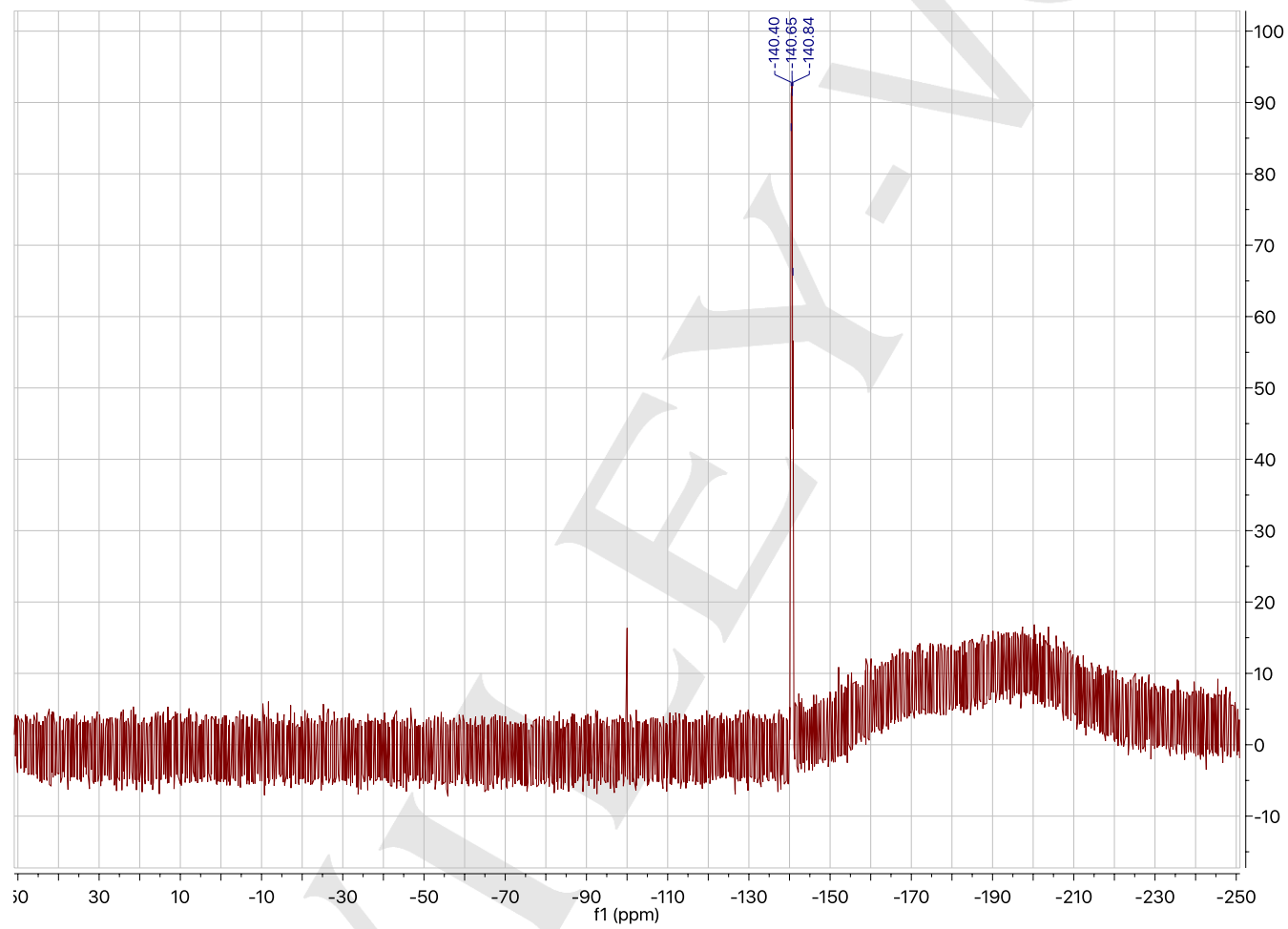
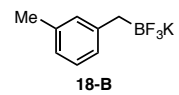
 ^1H NMR (501 MHz, acetone- d_6): trifluoro(3-methylbenzyl)- λ^4 -borane, potassium salt (18-B)

SUPPORTING INFORMATION

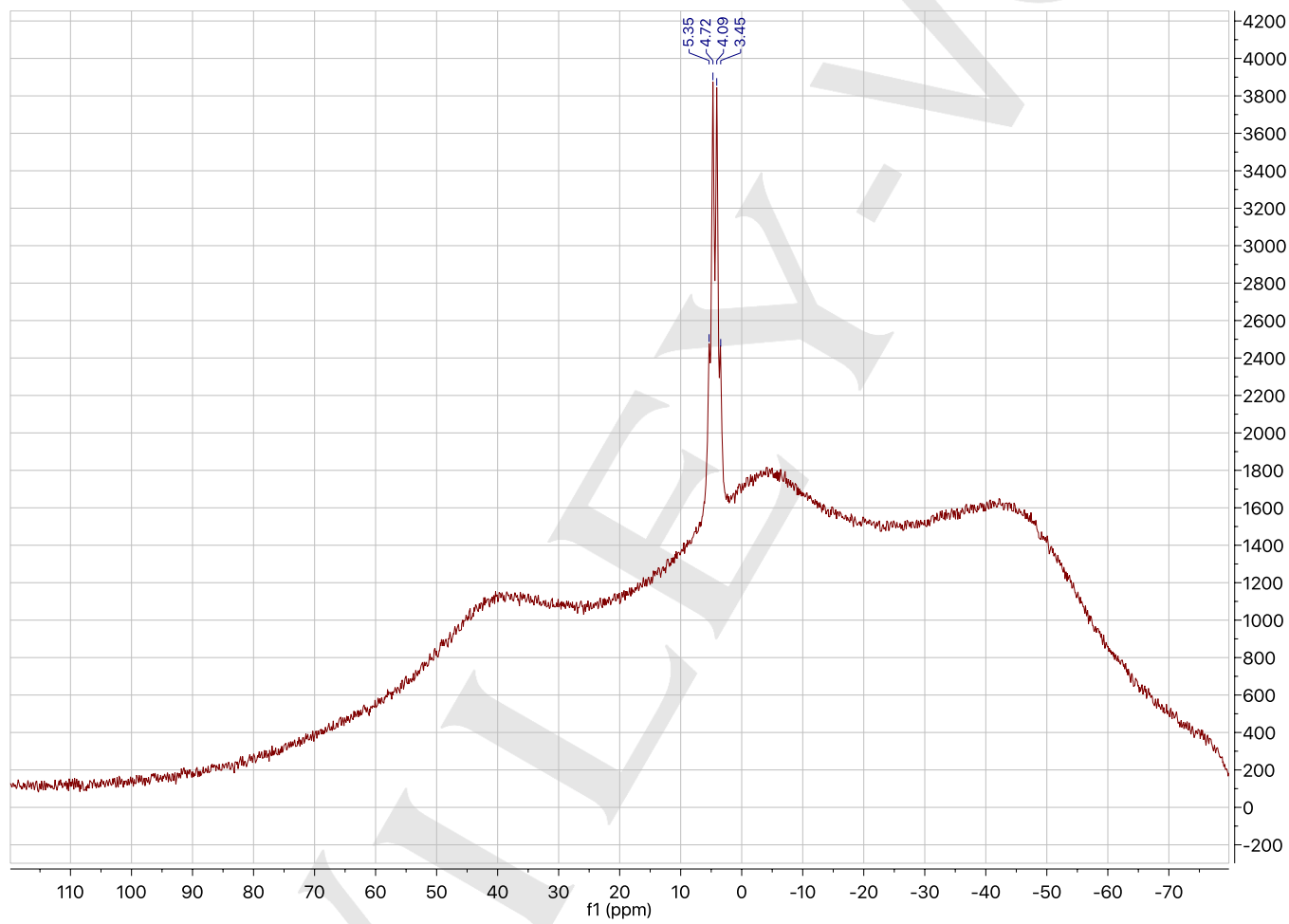
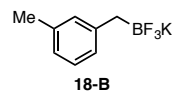
 ^{13}C NMR (126 MHz, acetone- d_6): trifluoro(3-methylbenzyl)- λ^4 -borane, potassium salt (18-B)

SUPPORTING INFORMATION

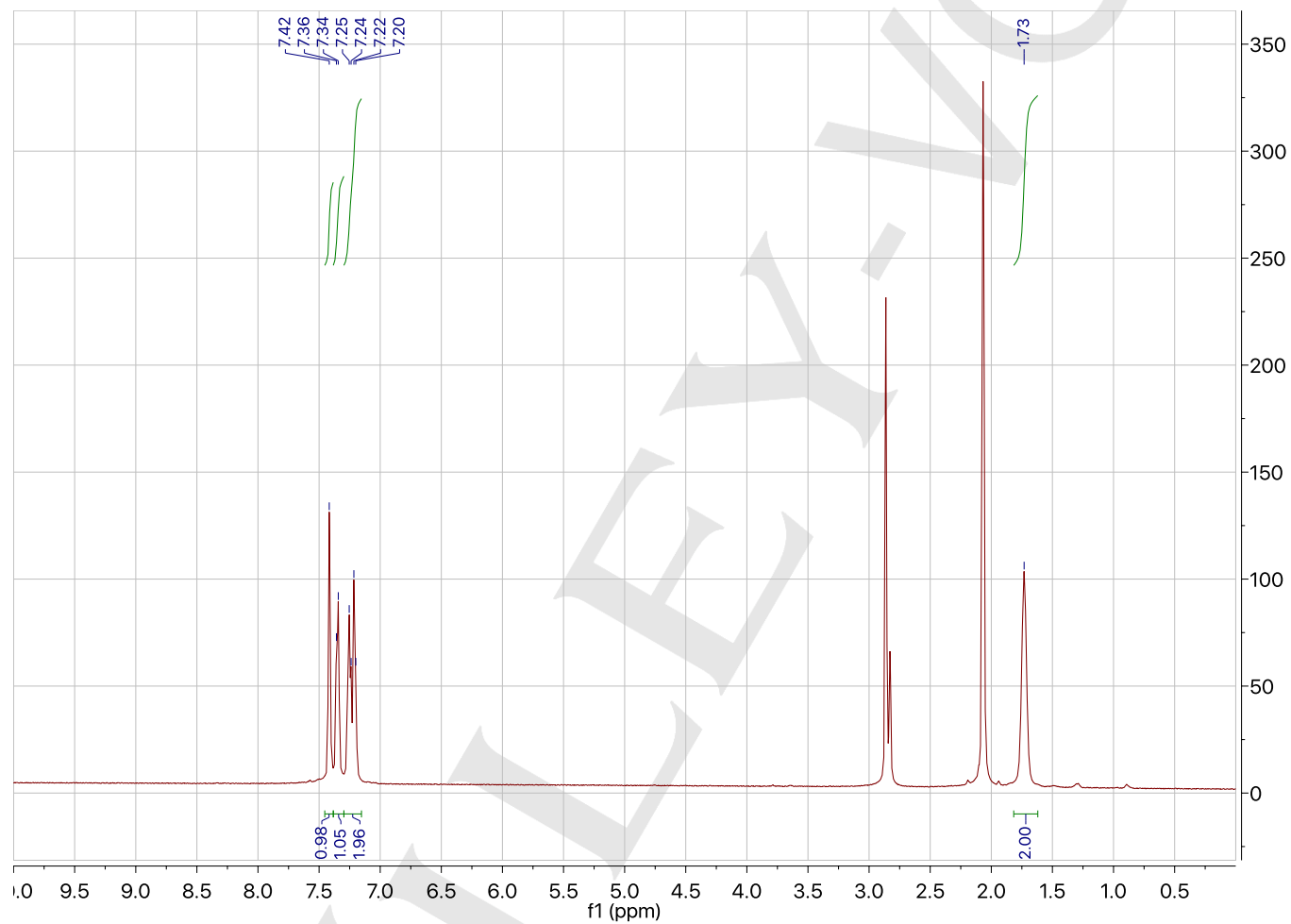
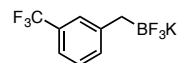
^{19}F NMR (282 MHz, acetone- d_6): trifluoro(3-methylbenzyl)- λ^4 -borane, potassium salt (18-B)



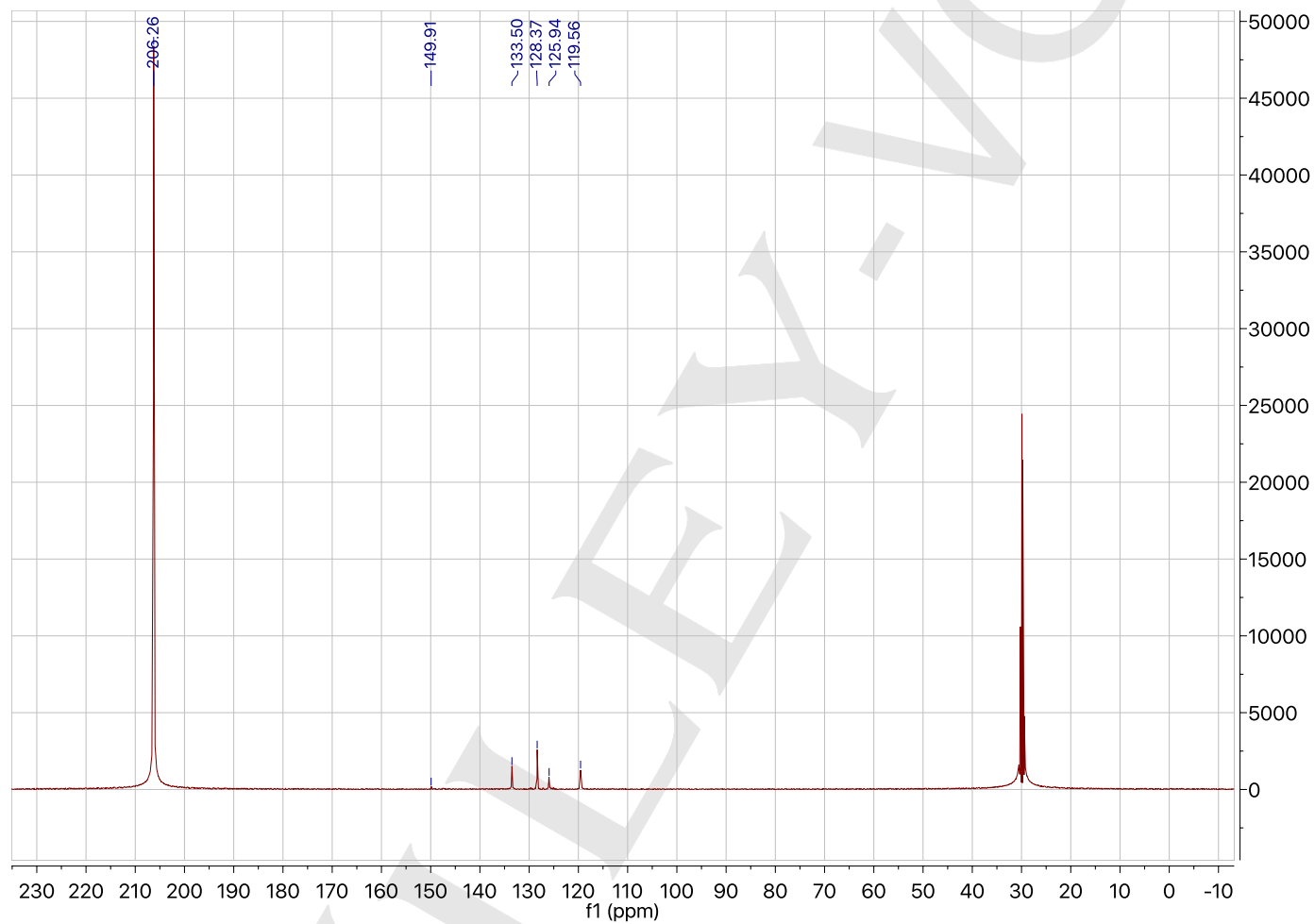
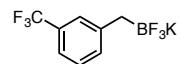
SUPPORTING INFORMATION

 ^{11}B NMR (96 MHz, acetone- d_6): trifluoro(3-methylbenzyl)- λ^4 -borane, potassium salt (18-B)

SUPPORTING INFORMATION

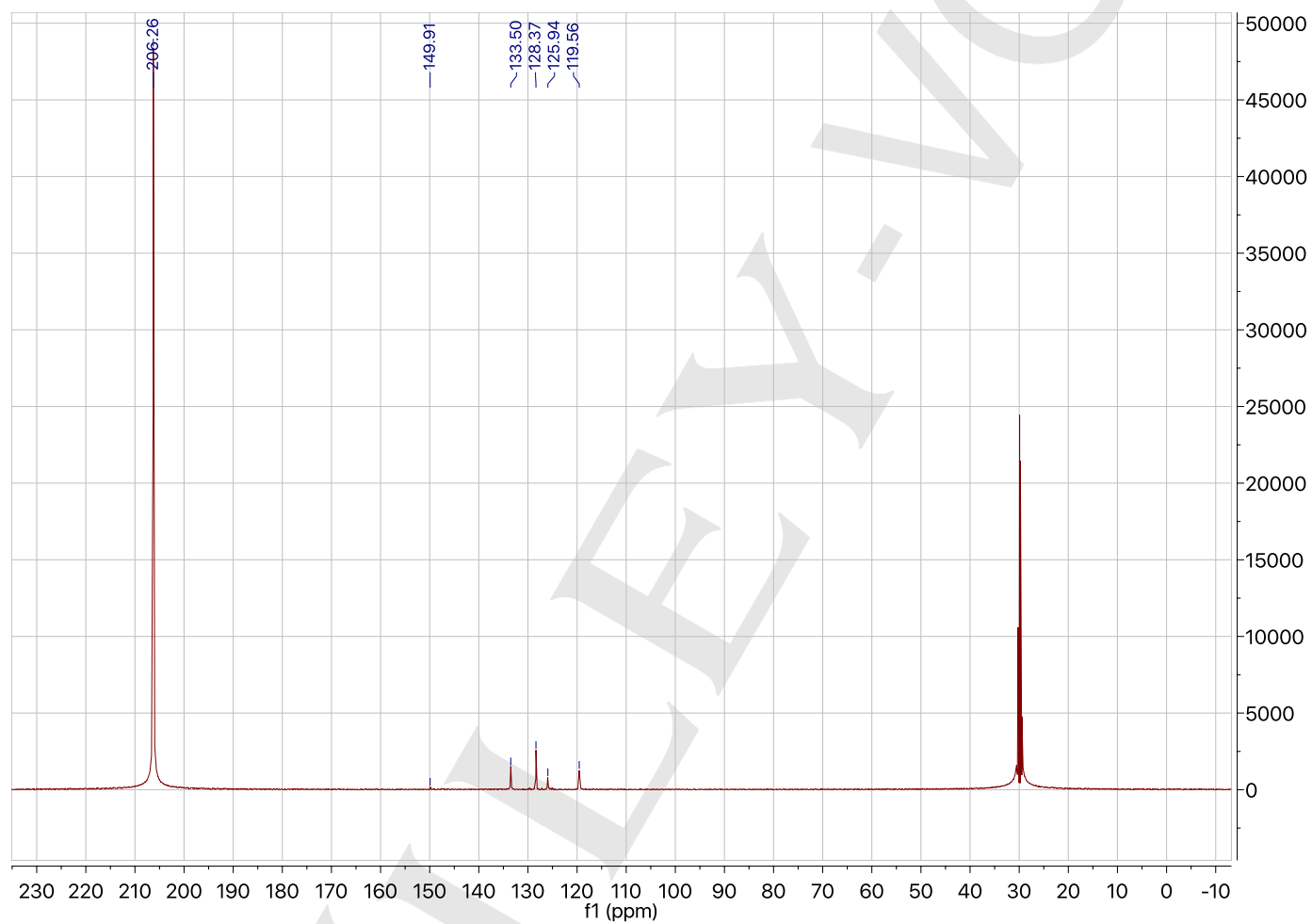
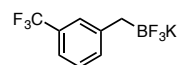
 ^1H NMR (501 MHz, acetone- d_6): trifluoro(3-(trifluoromethyl)benzyl)- λ^4 -borane, potassium salt

SUPPORTING INFORMATION

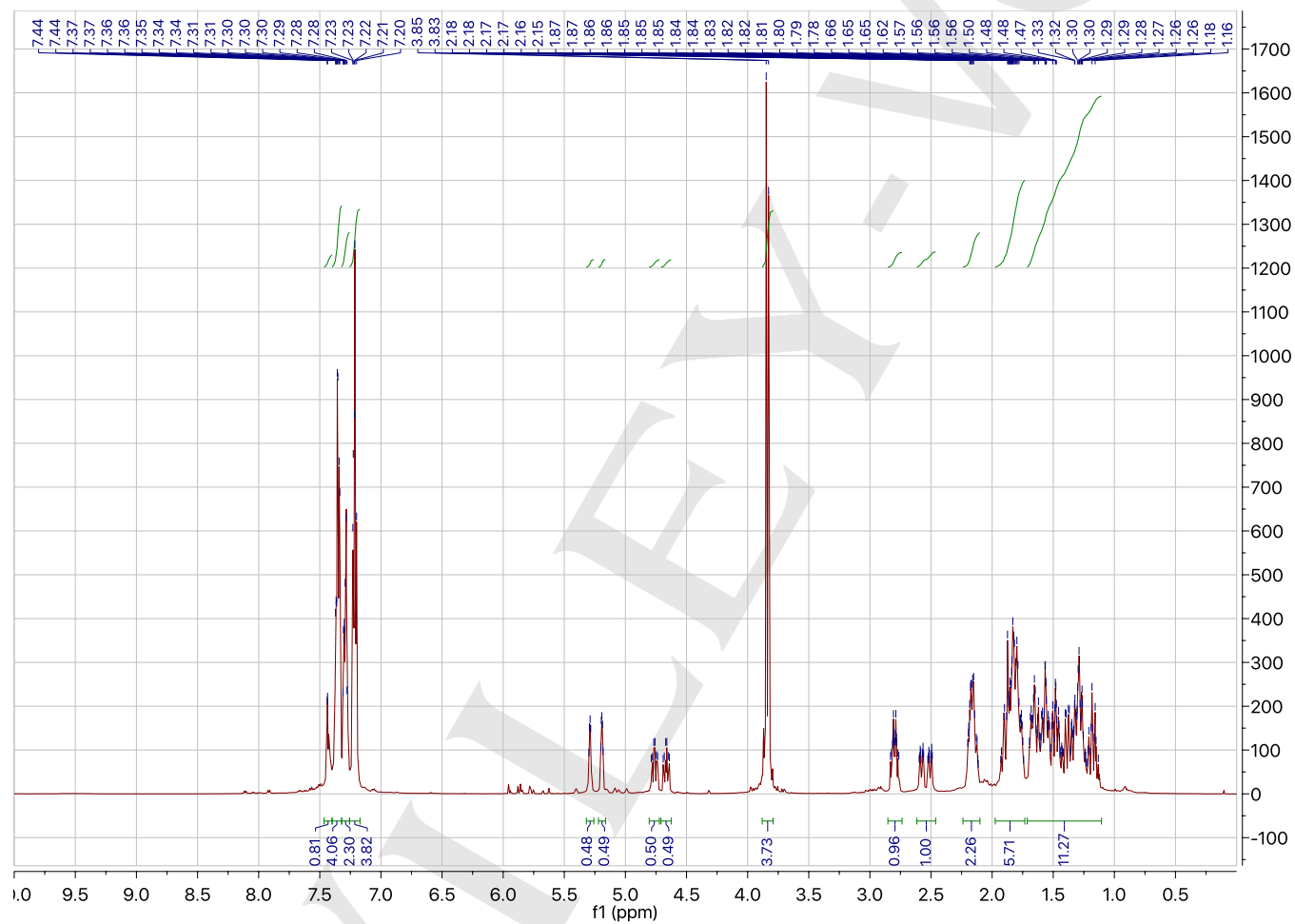
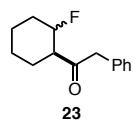
 ^{13}C NMR (126 MHz, acetone- d_6): trifluoro(3-(trifluoromethyl)benzyl)- λ^4 -borane, potassium salt

SUPPORTING INFORMATION

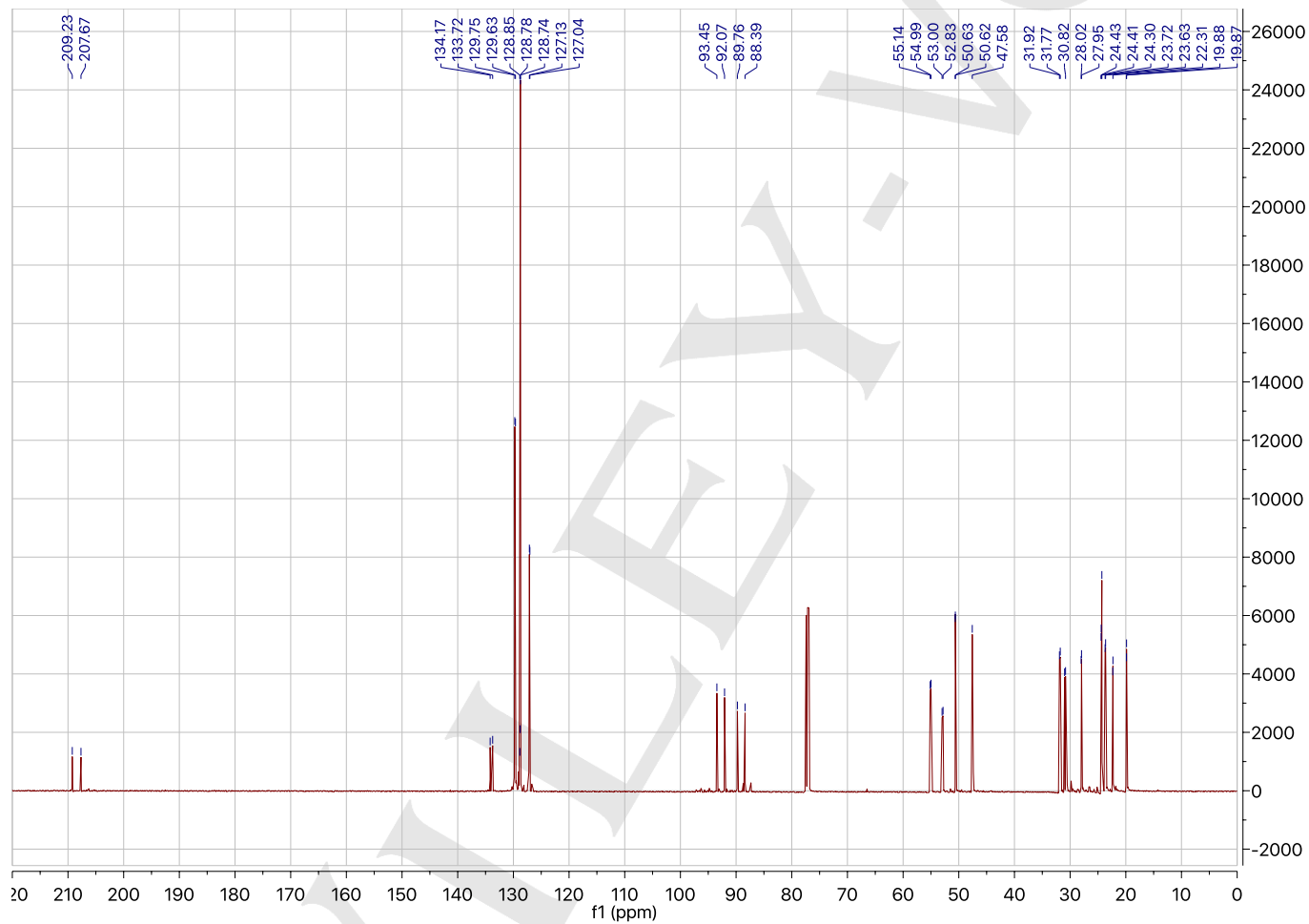
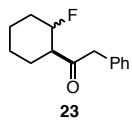
^{19}F NMR (282 MHz, acetone- d_6): trifluoro(3-(trifluoromethyl)benzyl)- λ^4 -borane, potassium salt



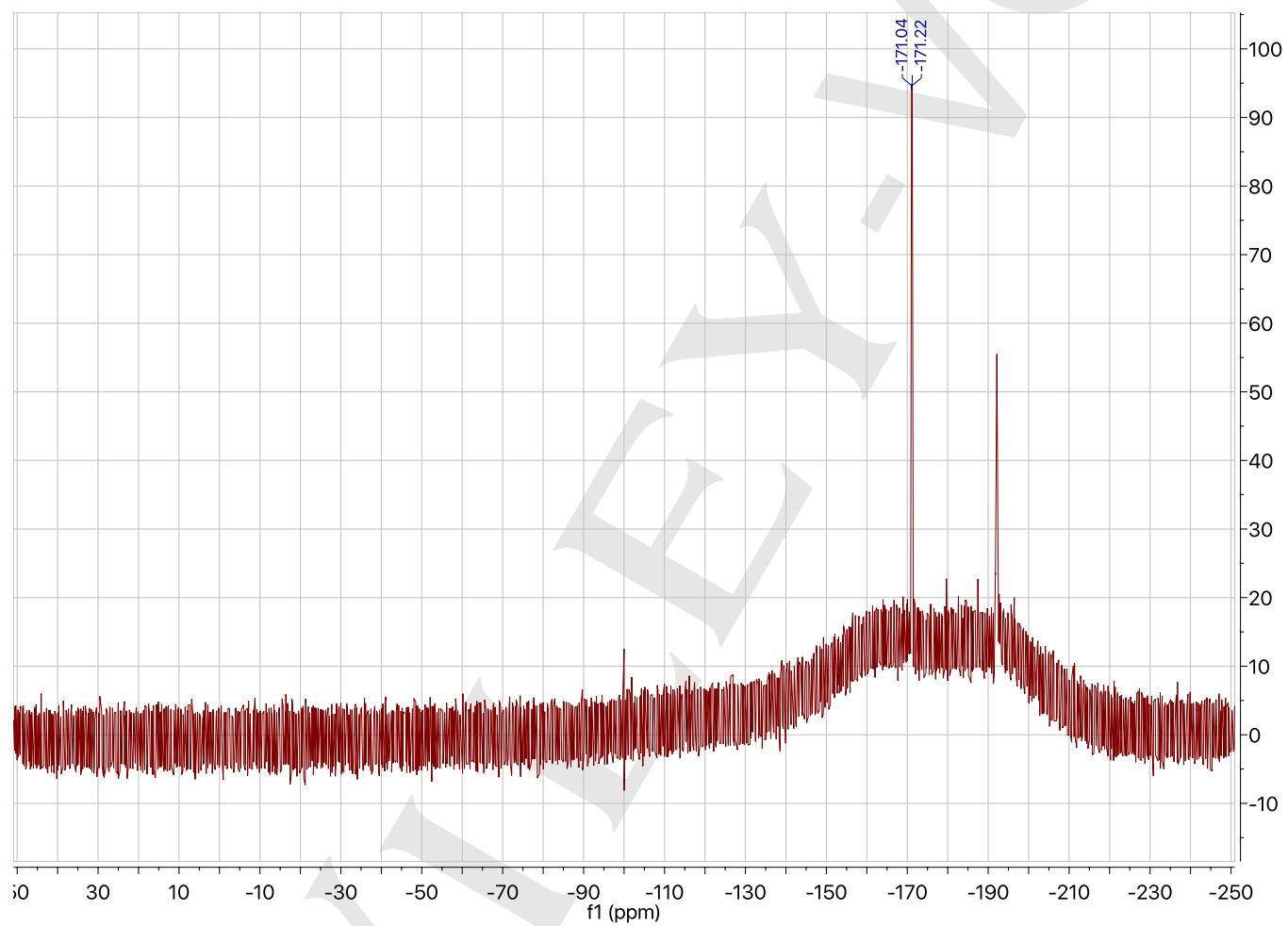
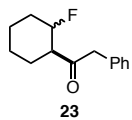
SUPPORTING INFORMATION

 ^1H NMR (501 MHz, CDCl_3): 1-((1R)-2-fluorocyclohexyl)-2-phenylethan-1-one (23)

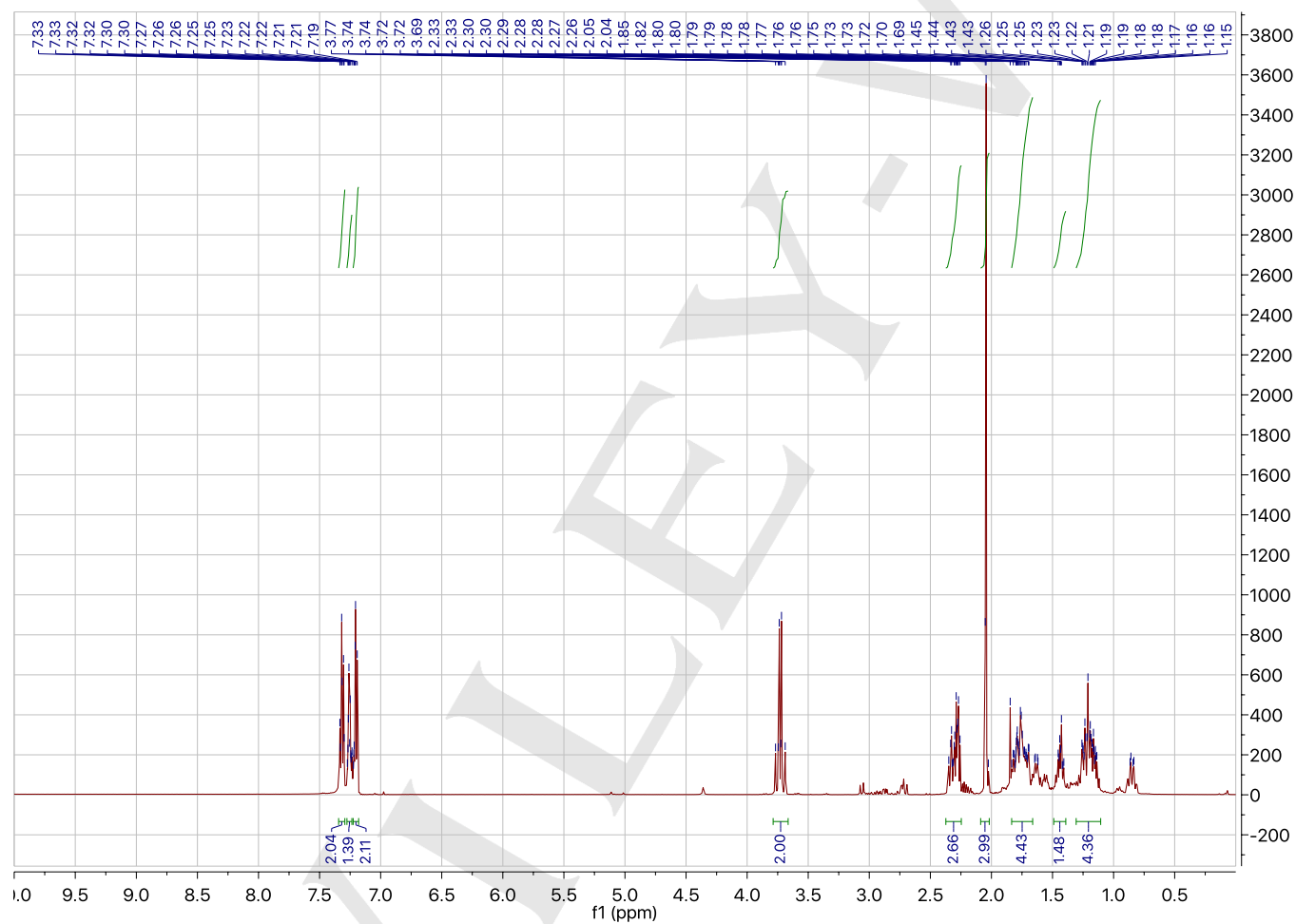
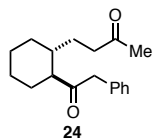
SUPPORTING INFORMATION

 ^{13}C NMR (126 MHz, CDCl_3): 1-((1*R*)-2-fluorocyclohexyl)-2-phenylethan-1-one (23)

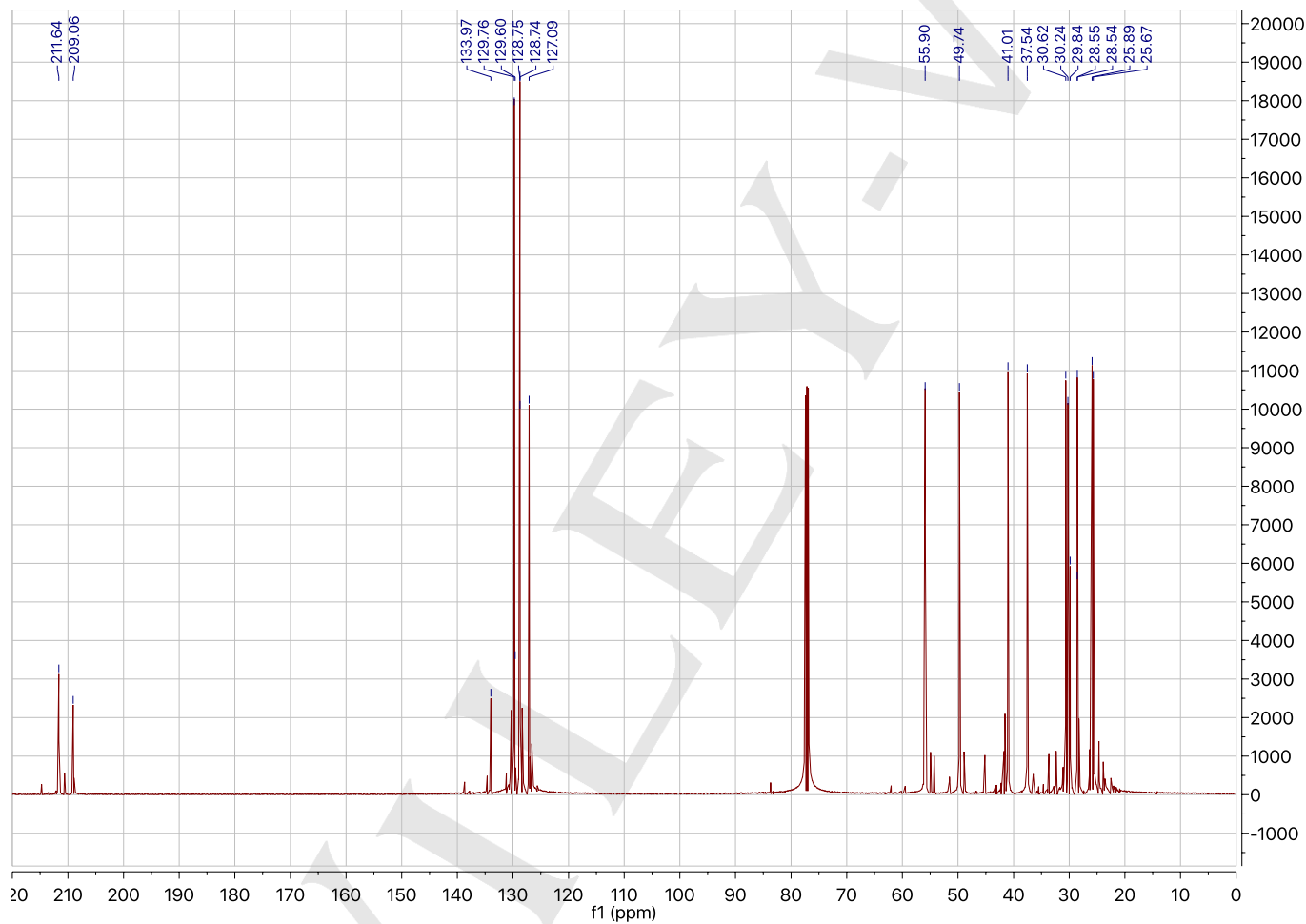
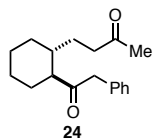
SUPPORTING INFORMATION

 ^{13}C NMR (126 MHz, CDCl_3): 1-((1*R*)-2-fluorocyclohexyl)-2-phenylethan-1-one (23)

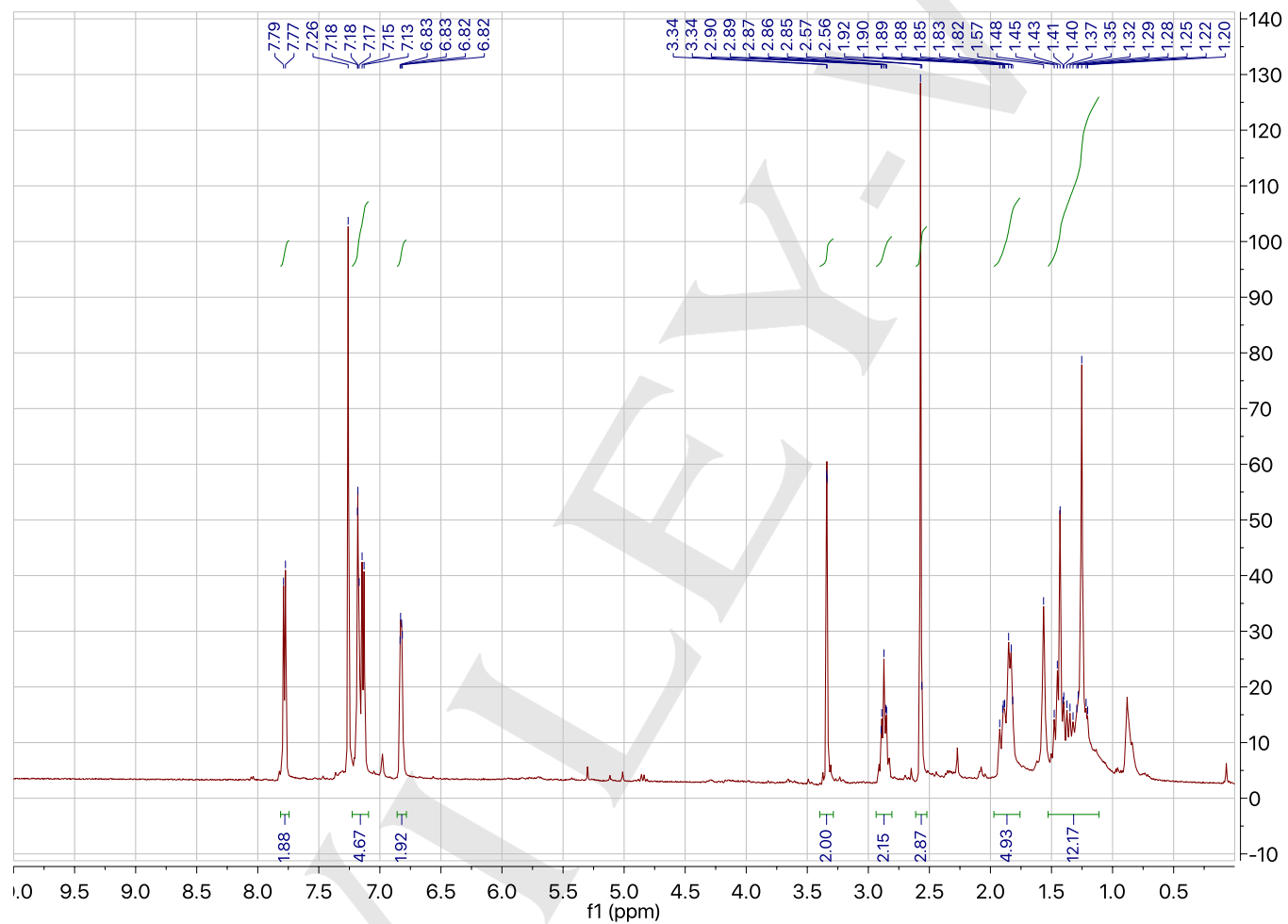
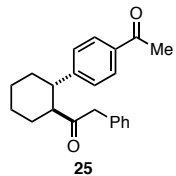
SUPPORTING INFORMATION

 ^1H NMR (501 MHz, CDCl_3): 4-((1*R*,2*S*)-2-(2-phenylacetyl)cyclohexyl)butan-2-one (24)

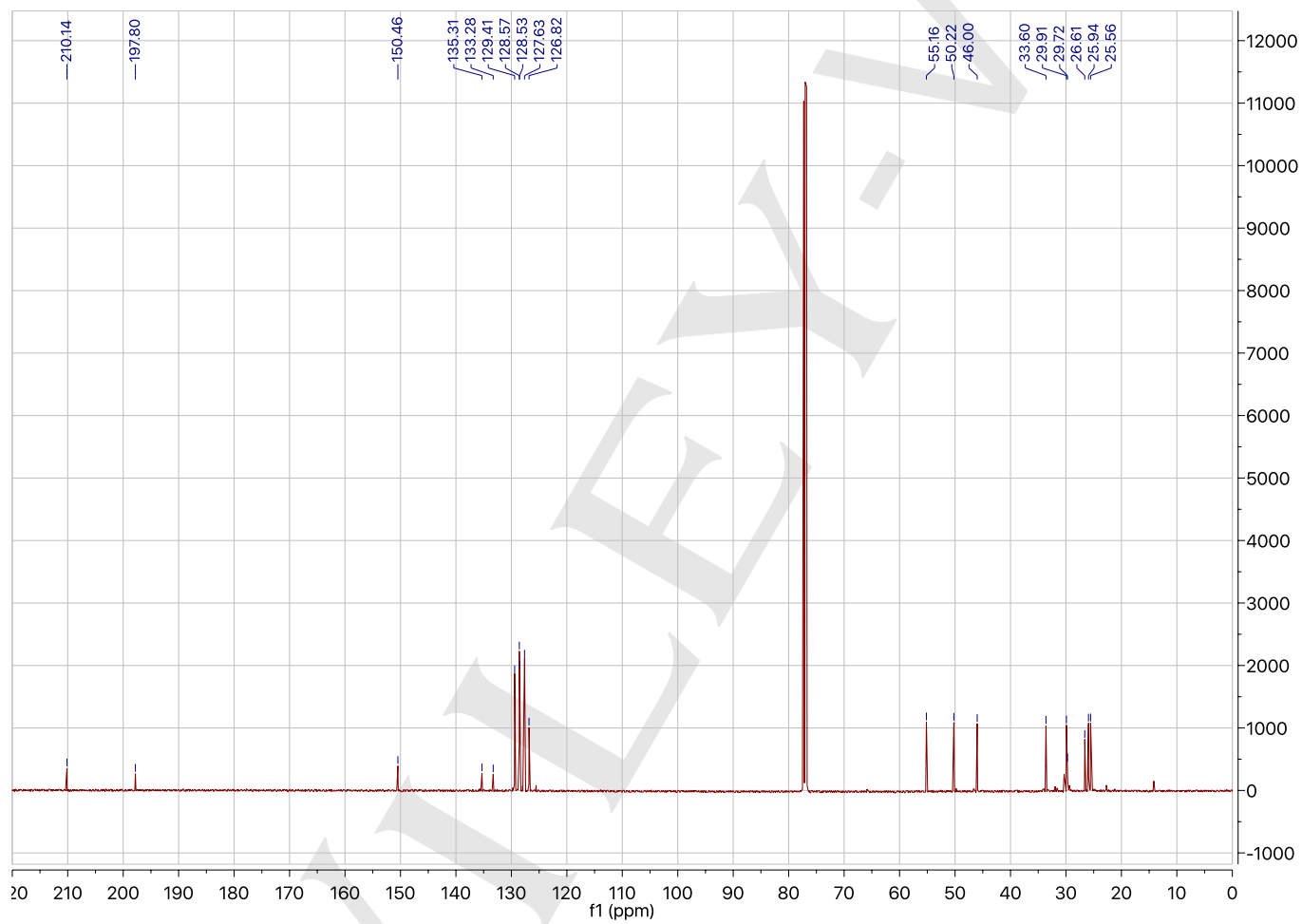
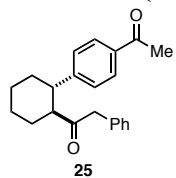
SUPPORTING INFORMATION

 ^{13}C NMR (126 MHz, CDCl_3): 4-((1*R*,2*S*)-2-(2-phenylacetyl)cyclohexyl)butan-2-one (24)

SUPPORTING INFORMATION

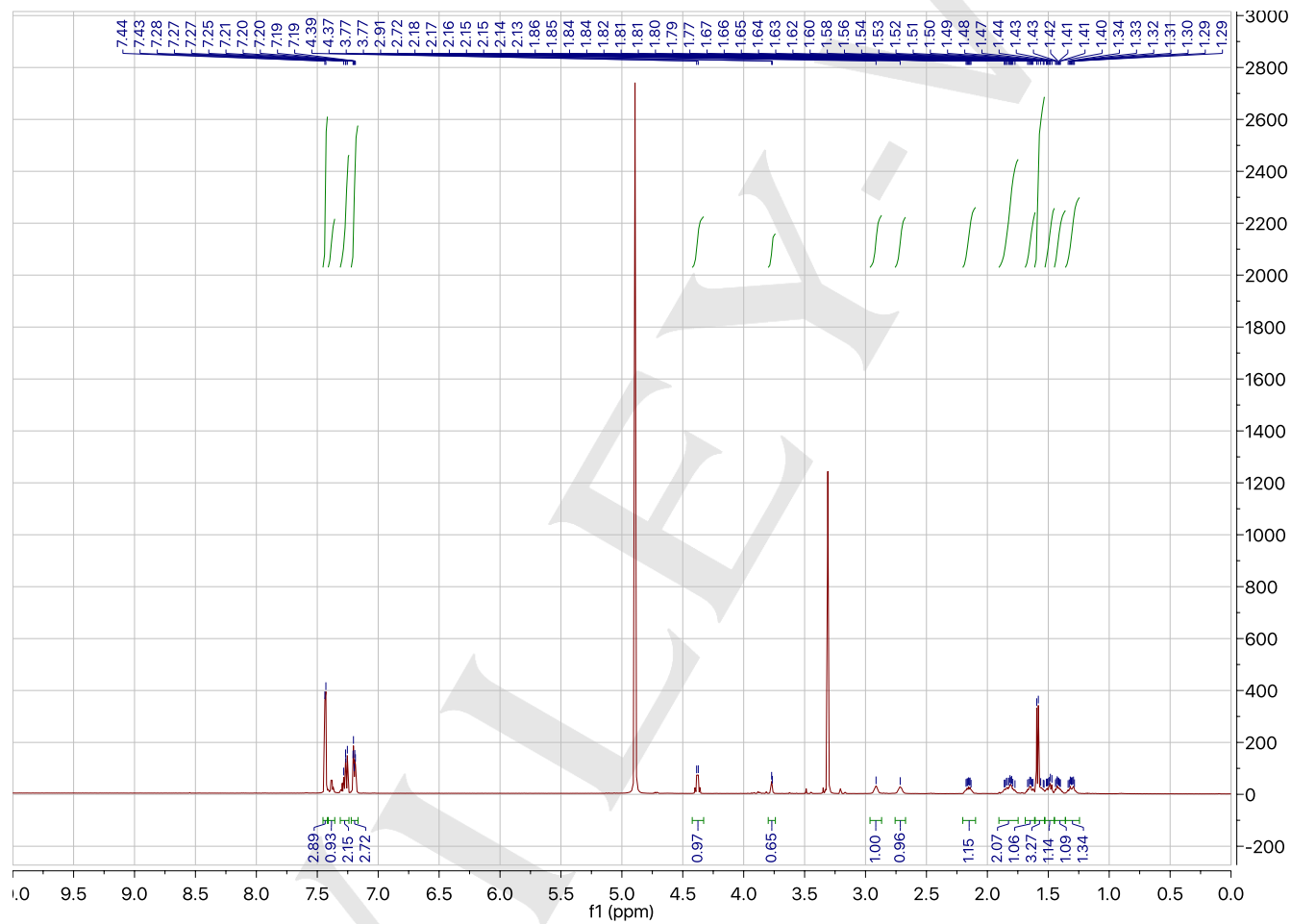
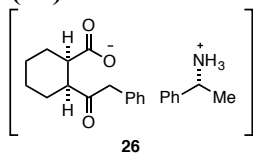
 ^1H NMR (501 MHz, CDCl_3): 1-((1*S*,2*S*)-2-(4-acetylphenyl)cyclohexyl)-2-phenylethan-1-one (25)

SUPPORTING INFORMATION

 ^{13}C NMR (126 MHz, CDCl_3): 1-((1*S*,2*S*)-2-(4-acetylphenyl)cyclohexyl)-2-phenylethan-1-one (25)

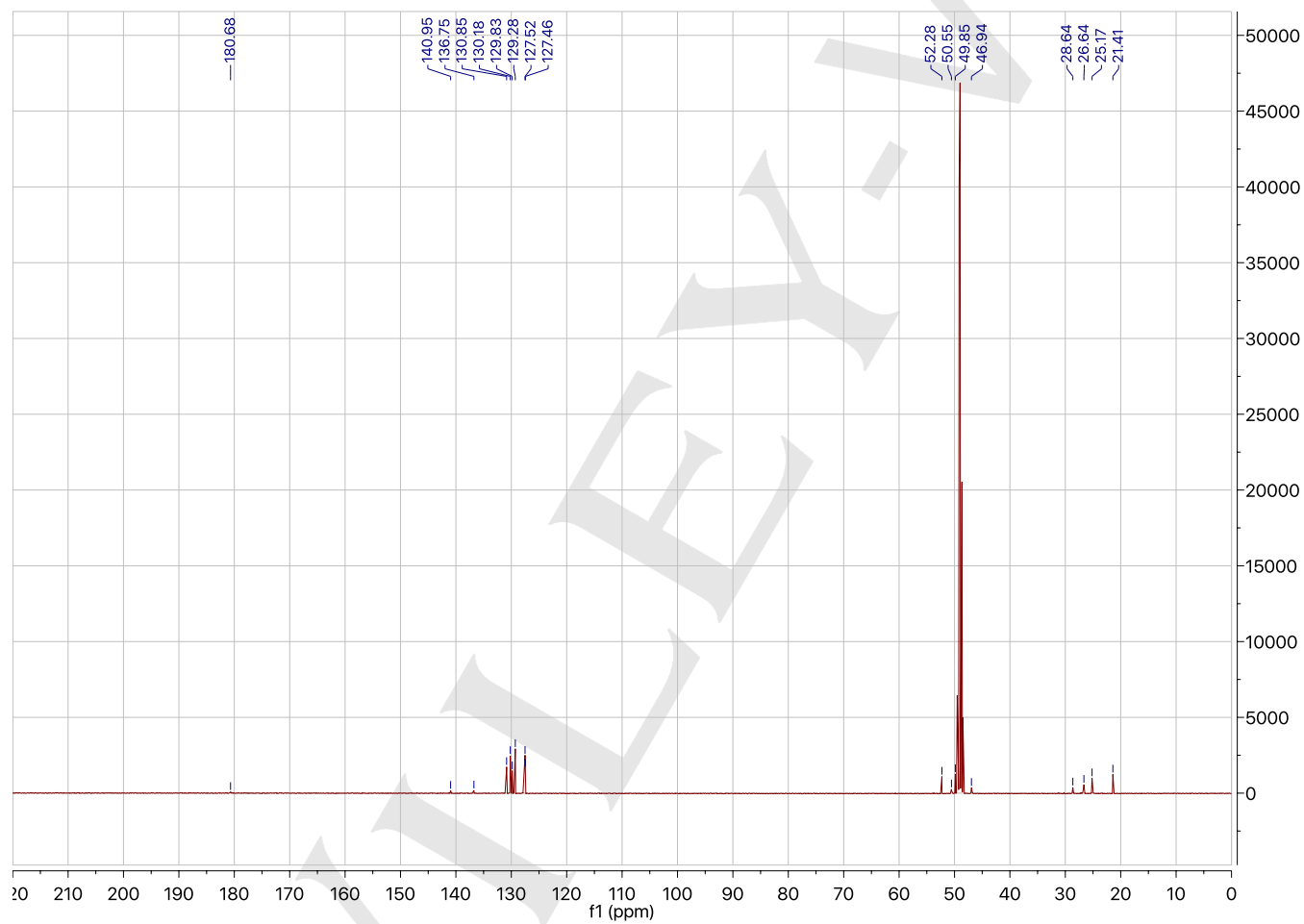
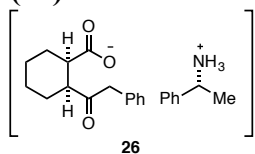
SUPPORTING INFORMATION

^1H NMR (501 MHz, CD_3OD): (*R*)-1-phenylethan-1-aminium (1*R*,2*S*)-2-(2-phenylacetyl)cyclohexane-1-carboxylate (26)



SUPPORTING INFORMATION

^{13}C NMR (126 MHz, CD_3OD): (*R*)-1-phenylethan-1-aminium (1*R*,2*S*)-2-(2-phenylacetyl)cyclohexane-1-carboxylate (26)



XII. Crystallographic Data

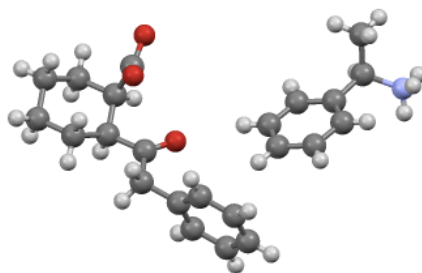


Table S5. A total of 5790 frames were collected. The total exposure time was 40.19 hours. The frames were integrated with the Bruker SAINT software package using a narrow-frame algorithm. The integration of the data using a **monoclinic** unit cell yielded a total of **15314** reflections to a maximum θ angle of **68.24°** (**0.83 Å** resolution), of which **3613** were independent (average redundancy **4.239**, completeness = **99.8%**, $R_{\text{int}} = 2.65\%$, $R_{\text{sig}} = 2.18\%$) and **3500** (**96.87%**) were greater than $2\sigma(F^2)$. The final cell constants of $a = 10.8239(7)$ Å, $b = 6.0156(4)$ Å, $c = 15.9544(10)$ Å, $\beta = 104.142(2)^\circ$, volume = **1007.34(11) Å³**, are based upon the refinement of the XYZ-centroids of **9869** reflections above $20\sigma(I)$ with $5.712^\circ < 2\theta < 140.2^\circ$. Data were corrected for absorption effects using the multi-scan method (SADABS). The ratio of minimum to maximum apparent transmission was **0.927**. The calculated minimum and maximum transmission coefficients (based on crystal size) are **0.8420** and **0.9730**.

The structure was solved and refined using the Bruker SHELXTL Software Package, using the space group **P 1 2 1 1**, with $Z = 2$ for the formula unit, **C₂₃H₂₉NO₃**. The final anisotropic full-matrix least-squares refinement on F^2 with **255** variables converged at $R1 = 2.52\%$, for the observed data and $wR2 = 5.98\%$ for all data. The goodness-of-fit was **1.042**. The largest peak in the final difference electron density synthesis was **0.171 e⁻/Å³** and the largest hole was **-0.133 e⁻/Å³** with an RMS deviation of **0.027 e⁻/Å³**. On the basis of the final model, the calculated density was **1.212 g/cm³** and $F(000)$, **396 e⁻**.

	dx/mm	2 θ /°	ω /°	φ /°	χ /°	Width /°	Frame s	Time /s	Wave-length/ Å	Voltage/k V	Current /mA	Temp/K
Omega	33.908	-52.54	-216.79	-105.00	54.74	0.50	297	30.00	1.54184	50	1.0	100
Omega	33.908	-52.54	-216.79	0.00	54.74	0.50	297	30.00	1.54184	50	1.0	100
Omega	33.908	88.89	-77.11	270.00	54.74	0.50	304	30.00	1.54184	50	1.0	100
Omega	33.908	88.89	-77.11	180.00	54.74	0.50	304	30.00	1.54184	50	1.0	100
Phi	33.908	74.19	-92.00	0.00	54.74	0.50	720	30.00	1.54184	50	1.0	100
Omega	33.908	103.89	-61.12	45.00	54.74	0.50	300	30.00	1.54184	50	1.0	100
Omega	33.908	-4.10	-169.10	0.00	54.74	0.50	300	15.00	1.54184	50	1.0	100
Omega	33.908	103.89	-61.12	-45.00	54.74	0.50	300	30.00	1.54184	50	1.0	100
Phi	33.908	104.19	-62.00	0.00	54.74	0.50	720	25.00	1.54184	50	1.0	100
Omega	33.908	-43.88	-209.88	0.00	54.74	0.50	304	15.00	1.54184	50	1.0	100
Omega	33.908	103.89	-61.12	0.00	54.74	0.50	300	25.00	1.54184	50	1.0	100
Omega	33.908	-58.88	-224.88	0.00	54.74	0.50	304	15.00	1.54184	50	1.0	100
Omega	33.908	103.89	-61.12	90.00	54.74	0.50	300	25.00	1.54184	50	1.0	100
Phi	33.908	-59.19	-73.00	0.00	54.74	0.50	720	20.00	1.54184	50	1.0	100
Phi	33.908	89.19	-77.00	0.00	54.74	0.50	320	25.00	1.54184	50	1.0	100

SUPPORTING INFORMATION

Table S6. Sample and crystal data for **26**.

Identification code	26	
Chemical formula	$C_{23}H_{29}NO_3$	
Formula weight	367.47 g/mol	
Temperature	100(2) K	
Wavelength	1.54178 Å	
Crystal size	0.043 x 0.069 x 0.282 mm	
Crystal system	monoclinic	
Space group	P 1 21 1	
Unit cell dimensions	a = 10.8239(7) Å	$\alpha = 90^\circ$
	b = 6.0156(4) Å	$\beta = 104.142(2)^\circ$
	c = 15.9544(10) Å	$\gamma = 90^\circ$
Volume	1007.34(11) Å ³	
Z	2	
Density (calculated)	1.212 g/cm ³	
Absorption coefficient	0.630 mm ⁻¹	
F(000)	396	

SUPPORTING INFORMATION

Table S7. Data collection and structure refinement for **26**.

Theta range for data collection	2.86 to 68.24°	
Index ranges	-13<=h<=12, -7<=k<=6, -19<=l<=19	
Reflections collected	15314	
Independent reflections	3613 [R(int) = 0.0265]	
Coverage of independent reflections	99.8%	
Absorption correction	multi-scan	
Max. and min. transmission	0.9730 and 0.8420	
Structure solution technique	direct methods	
Structure solution program	SHELXT (Sheldrick, 2016)	
Refinement method	Full-matrix least-squares on F ²	
Refinement program	SHELXL-2014/7 (Sheldrick, 2014)	
Function minimized	$\Sigma w(F_o^2 - F_c^2)^2$	
Data / restraints / parameters	3613 / 4 / 255	
Goodness-of-fit on F ²	1.042	
Final R indices	3500 data; I>2σ(I)	R1 = 0.0252, wR2 = 0.0591
	all data	R1 = 0.0266, wR2 = 0.0598
Weighting scheme	w=1/[σ ² (F _o ²)+(0.0227P) ² +0.2180P] where P=(F _o ² +2F _c ²)/3	
Absolute structure parameter	-0.01(6)	
Largest diff. peak and hole	0.171 and -0.133 eÅ ⁻³	
R.M.S. deviation from mean	0.027 eÅ ⁻³	

SUPPORTING INFORMATION

Table S8. Atomic coordinates and equivalent isotropic atomic displacement parameters (\AA^2) for **26**.

$U(\text{eq})$ is defined as one third of the trace of the orthogonalized U_{ij} tensor.

	x/a	y/b	z/c	$U(\text{eq})$
O1	0.91501(11)	0.1636(2)	0.41199(7)	0.0212(3)
N1	0.12993(13)	0.2258(2)	0.54822(9)	0.0174(3)
C1	0.88831(14)	0.2476(3)	0.33658(10)	0.0170(3)
O2	0.88524(11)	0.4513(2)	0.32107(8)	0.0220(3)
C2	0.85891(16)	0.0831(3)	0.26061(10)	0.0174(3)
O3	0.61851(11)	0.2709(2)	0.22461(8)	0.0255(3)
C3	0.97763(17)	0.9453(3)	0.25809(12)	0.0223(4)
C4	0.07671(17)	0.0833(3)	0.22785(11)	0.0235(4)
C5	0.01981(17)	0.1833(3)	0.13924(11)	0.0242(4)
C6	0.90437(16)	0.3287(3)	0.14030(11)	0.0209(4)
C7	0.80412(15)	0.1975(3)	0.17355(10)	0.0180(3)
C8	0.68318(16)	0.3245(3)	0.17599(10)	0.0184(4)
C9	0.64234(17)	0.5125(3)	0.11135(12)	0.0241(4)
C10	0.50849(16)	0.5927(3)	0.10493(11)	0.0207(4)
C11	0.48410(18)	0.7951(3)	0.13970(11)	0.0241(4)
C12	0.35990(19)	0.8644(3)	0.13339(12)	0.0289(4)
C13	0.25863(18)	0.7323(4)	0.09260(11)	0.0302(4)
C14	0.28191(18)	0.5300(3)	0.05744(12)	0.0283(4)
C15	0.40562(17)	0.4613(3)	0.06356(11)	0.0237(4)
C16	0.35619(16)	0.2514(4)	0.62033(11)	0.0263(4)
C17	0.26076(16)	0.1717(3)	0.53907(11)	0.0199(4)
C18	0.28794(15)	0.2688(3)	0.45802(10)	0.0192(4)
C19	0.37227(16)	0.1558(3)	0.41939(11)	0.0234(4)
C20	0.40537(17)	0.2427(3)	0.34743(11)	0.0266(4)
C21	0.35454(17)	0.4424(4)	0.31253(12)	0.0255(4)
C22	0.27145(17)	0.5564(3)	0.35056(12)	0.0256(4)
C23	0.23863(17)	0.4705(3)	0.42336(11)	0.0232(4)

SUPPORTING INFORMATION

Table S9. Bond lengths (Å) for 26.

O1-C1	1.271(2)	N1-C17	1.494(2)
N1-H1A	0.907(19)	N1-H1B	0.889(19)
N1-H1C	0.92(2)	C1-O2	1.249(2)
C1-C2	1.537(2)	C2-C7	1.534(2)
C2-C3	1.538(2)	C2-H2	1.0
O3-C8	1.209(2)	C3-C4	1.525(2)
C3-H3A	0.99	C3-H3B	0.99
C4-C5	1.521(3)	C4-H4A	0.99
C4-H4B	0.99	C5-C6	1.529(2)
C5-H5A	0.99	C5-H5B	0.99
C6-C7	1.537(2)	C6-H6A	0.99
C6-H6B	0.99	C7-C8	1.525(2)
C7-H7	1.0	C8-C9	1.521(2)
C9-C10	1.507(2)	C9-H9A	0.99
C9-H9B	0.99	C10-C11	1.390(3)
C10-C15	1.393(3)	C11-C12	1.388(3)
C11-H11	0.95	C12-C13	1.382(3)
C12-H12	0.95	C13-C14	1.388(3)
C13-H13	0.95	C14-C15	1.382(3)
C14-H14	0.95	C15-H15	0.95
C16-C17	1.524(2)	C16-H16A	0.98
C16-H16B	0.98	C16-H16C	0.98
C17-C18	1.512(2)	C17-H17	1.0
C18-C23	1.385(3)	C18-C19	1.396(2)
C19-C20	1.386(3)	C19-H19	0.95
C20-C21	1.381(3)	C20-H20	0.95
C21-C22	1.383(3)	C21-H21	0.95
C22-C23	1.394(2)	C22-H22	0.95
C23-H23	0.95		

SUPPORTING INFORMATION

Table S10. Bond angles (°) for 26.

C17-N1-H1A	109.8(13)	C17-N1-H1B	110.8(13)
H1A-N1-H1B	107.8(19)	C17-N1-H1C	112.9(13)
H1A-N1-H1C	105.5(19)	H1B-N1-H1C	109.8(19)
O2-C1-O1	124.49(15)	O2-C1-C2	119.03(14)
O1-C1-C2	116.48(15)	C7-C2-C1	112.66(14)
C7-C2-C3	111.02(13)	C1-C2-C3	110.76(14)
C7-C2-H2	107.4	C1-C2-H2	107.4
C3-C2-H2	107.4	C4-C3-C2	111.82(15)
C4-C3-H3A	109.3	C2-C3-H3A	109.3
C4-C3-H3B	109.3	C2-C3-H3B	109.3
H3A-C3-H3B	107.9	C5-C4-C3	110.67(14)
C5-C4-H4A	109.5	C3-C4-H4A	109.5
C5-C4-H4B	109.5	C3-C4-H4B	109.5
H4A-C4-H4B	108.1	C4-C5-C6	111.25(14)
C4-C5-H5A	109.4	C6-C5-H5A	109.4
C4-C5-H5B	109.4	C6-C5-H5B	109.4
H5A-C5-H5B	108.0	C5-C6-C7	110.97(15)
C5-C6-H6A	109.4	C7-C6-H6A	109.4
C5-C6-H6B	109.4	C7-C6-H6B	109.4
H6A-C6-H6B	108.0	C8-C7-C2	110.26(13)
C8-C7-C6	115.75(15)	C2-C7-C6	113.17(14)
C8-C7-H7	105.6	C2-C7-H7	105.6
C6-C7-H7	105.6	O3-C8-C9	121.03(15)
O3-C8-C7	121.20(15)	C9-C8-C7	117.67(14)
C10-C9-C8	113.54(14)	C10-C9-H9A	108.9
C8-C9-H9A	108.9	C10-C9-H9B	108.9
C8-C9-H9B	108.9	H9A-C9-H9B	107.7
C11-C10-C15	118.58(16)	C11-C10-C9	121.78(17)
C15-C10-C9	119.64(16)	C12-C11-C10	120.63(18)
C12-C11-H11	119.7	C10-C11-H11	119.7
C13-C12-C11	120.29(19)	C13-C12-H12	119.9
C11-C12-H12	119.9	C12-C13-C14	119.55(17)
C12-C13-H13	120.2	C14-C13-H13	120.2
C15-C14-C13	120.13(18)	C15-C14-H14	119.9
C13-C14-H14	119.9	C14-C15-C10	120.82(18)
C14-C15-H15	119.6	C10-C15-H15	119.6
C17-C16-H16A	109.5	C17-C16-H16B	109.5
H16A-C16-H16B	109.5	C17-C16-H16C	109.5
H16A-C16-H16C	109.5	H16B-C16-H16C	109.5
N1-C17-C18	112.73(14)	N1-C17-C16	108.04(13)
C18-C17-C16	111.89(14)	N1-C17-H17	108.0
C18-C17-H17	108.0	C16-C17-H17	108.0
C23-C18-C19	118.68(16)	C23-C18-C17	122.92(15)

SUPPORTING INFORMATION

C19-C18-C17	118.30(16)	C20-C19-C18	120.76(17)
C20-C19-H19	119.6	C18-C19-H19	119.6
C21-C20-C19	120.26(17)	C21-C20-H20	119.9
C19-C20-H20	119.9	C20-C21-C22	119.47(17)
C20-C21-H21	120.3	C22-C21-H21	120.3
C21-C22-C23	120.48(17)	C21-C22-H22	119.8
C23-C22-H22	119.8	C18-C23-C22	120.35(17)
C18-C23-H23	119.8	C22-C23-H23	119.8

SUPPORTING INFORMATION

Table S11. Anisotropic atomic displacement parameters (\AA^2) for **26**.

	U_{11}	U_{22}	U_{33}	U_{23}	U_{13}	U_{12}
O1	0.0224(6)	0.0234(7)	0.0161(6)	0.0024(5)	0.0016(5)	-0.0029(5)
N1	0.0185(7)	0.0184(8)	0.0152(7)	0.0000(6)	0.0041(6)	-0.0015(6)
C1	0.0125(8)	0.0203(9)	0.0189(8)	-0.0002(7)	0.0052(6)	-0.0014(6)
O2	0.0298(7)	0.0176(7)	0.0200(6)	-0.0022(5)	0.0087(5)	-0.0003(5)
C2	0.0189(8)	0.0164(8)	0.0173(8)	0.0004(7)	0.0054(6)	-0.0007(7)
O3	0.0227(6)	0.0320(7)	0.0237(6)	0.0064(5)	0.0094(5)	0.0026(5)
C3	0.0255(9)	0.0185(9)	0.0239(9)	-0.0010(7)	0.0080(7)	0.0024(7)
C4	0.0200(9)	0.0264(10)	0.0259(9)	-0.0015(8)	0.0089(7)	0.0031(7)
C5	0.0237(9)	0.0275(10)	0.0239(9)	-0.0007(8)	0.0105(7)	-0.0008(8)
C6	0.0226(9)	0.0226(10)	0.0188(8)	0.0007(7)	0.0075(7)	-0.0005(7)
C7	0.0201(8)	0.0185(9)	0.0159(8)	-0.0038(6)	0.0049(6)	-0.0021(7)
C8	0.0187(8)	0.0206(9)	0.0151(8)	-0.0027(7)	0.0027(7)	-0.0025(7)
C9	0.0232(9)	0.0258(10)	0.0250(10)	0.0049(7)	0.0091(7)	0.0024(7)
C10	0.0238(9)	0.0232(9)	0.0163(8)	0.0056(7)	0.0073(7)	0.0021(7)
C11	0.0297(10)	0.0239(10)	0.0191(9)	0.0033(7)	0.0067(7)	-0.0012(7)
C12	0.0406(12)	0.0254(10)	0.0236(10)	0.0056(8)	0.0134(9)	0.0126(8)
C13	0.0251(9)	0.0442(13)	0.0234(9)	0.0113(9)	0.0098(7)	0.0133(9)
C14	0.0241(10)	0.0418(12)	0.0184(9)	0.0037(8)	0.0043(7)	-0.0032(8)
C15	0.0296(10)	0.0240(10)	0.0186(9)	-0.0007(7)	0.0077(7)	0.0012(8)
C16	0.0190(9)	0.0369(11)	0.0224(9)	0.0054(8)	0.0040(7)	0.0026(8)
C17	0.0208(9)	0.0185(9)	0.0220(9)	0.0014(7)	0.0080(7)	0.0034(7)
C18	0.0171(8)	0.0207(9)	0.0192(8)	-0.0008(7)	0.0032(6)	-0.0025(7)
C19	0.0232(9)	0.0221(9)	0.0254(9)	0.0024(7)	0.0070(7)	0.0034(7)
C20	0.0221(9)	0.0348(11)	0.0251(9)	-0.0015(8)	0.0101(7)	0.0023(8)
C21	0.0235(9)	0.0336(10)	0.0195(9)	0.0027(8)	0.0056(7)	-0.0084(8)
C22	0.0264(10)	0.0227(10)	0.0267(10)	0.0081(7)	0.0044(7)	-0.0013(7)
C23	0.0226(9)	0.0224(10)	0.0259(10)	0.0004(8)	0.0081(7)	0.0016(7)

SUPPORTING INFORMATION

Table S12. Hydrogen atomic coordinates and isotropic atomic displacement parameters (\AA^2) for **26**.

	x/a	y/b	z/c	U(eq)
H1A	0.1111(19)	0.140(4)	0.5903(12)	0.026
H1B	0.0721(18)	0.198(4)	0.4993(12)	0.026
H1C	0.1223(19)	0.370(3)	0.5650(13)	0.026
H2	0.7927	-0.0224	0.2708	0.021
H3A	1.0159	-0.1141	0.3165	0.027
H3B	0.9520	-0.1825	0.2185	0.027
H4A	1.1079	0.2039	0.2699	0.028
H4B	1.1502	-0.0120	0.2250	0.028
H5A	0.9937	0.0623	0.0965	0.029
H5B	1.0852	0.2740	0.1212	0.029
H6A	0.8660	0.3833	0.0811	0.025
H6B	0.9321	0.4592	0.1780	0.025
H7	0.7761	0.0744	0.1310	0.022
H9A	0.7018	0.6388	0.1283	0.029
H9B	0.6489	0.4611	0.0537	0.029
H11	0.5531	0.8869	0.1680	0.029
H12	0.3444	1.0034	0.1572	0.035
H13	0.1736	0.7795	0.0886	0.036
H14	0.2127	0.4386	0.0291	0.034
H15	0.4207	0.3228	0.0392	0.028
H16A	0.3394	0.1767	0.6710	0.039
H16B	0.3477	0.4125	0.6263	0.039
H16C	0.4428	0.2164	0.6160	0.039
H17	0.2680	0.0063	0.5360	0.024
H19	0.4074	0.0179	0.4427	0.028
H20	0.4632	0.1644	0.3220	0.032
H21	0.3765	0.5011	0.2628	0.031
H22	0.2365	0.6941	0.3269	0.031
H23	0.1822	0.5508	0.4493	0.028

SUPPORTING INFORMATION

Table S13. Hydrogen bond distances (Å) and angles (°) for **26**.

	Donor-H	Acceptor-H	Donor-Acceptor	Angle
N1-H1A[⋯]O2	0.907(19)	1.81(2)	2.6961(19)	165.7(19)
N1-H1B[⋯]O1	0.889(19)	1.928(19)	2.7937(18)	164.2(18)
N1-H1C[⋯]O1	0.92(2)	1.87(2)	2.7800(19)	172.1(19)